



AMERICAN UNIVERSITY OF BEIRUT

PALEOENVIRONMENTAL RECONSTRUCTION OF THE  
BARREMIAN/LOWER APTIAN DEPOSITS OF LEBANON:  
SEDIMENTOLOGY AND MICROPALAEONTOLOGY

by  
SAMAR ELIAS GHADBAN

A thesis  
submitted in partial fulfillment of the requirements  
for the degree of Master of Science  
to the Department of Geology  
of the Faculty of Arts and Sciences  
at the American University of Beirut

Beirut, Lebanon  
December 2019

AMERICAN UNIVERSITY OF BEIRUT

PALEOENVIRONMENTAL RECONSTRUCTION OF THE  
BARREMIAN/LOWER APTIAN DEPOSITS OF LEBANON:  
SEDIMENTOLOGY AND MICROPALAEONTOLOGY

by  
SAMAR ELIAS GHADBAN

Approved by:

---

Dr. Josep Sanjuan Girbau, Assistant Professor  
Department of Geology,  
American University of Beirut

Advisor



---

Dr. Mohamed Salah, Chairperson & Associate Professor  
Department of Geology,  
American University of Beirut

Member of Committee



---

Dr. Joanna Doummar, Assistant Professor  
Department of Geology,  
American University of Beirut

~~Member of Committee~~



---

Dr. Sibelle Maksoud, Professor  
Department of Life and Earth Sciences,  
Lebanese University

Member of Committee



Date of thesis defense: December 20, 2019

# AMERICAN UNIVERSITY OF BEIRUT

## THESIS, DISSERTATION, PROJECT RELEASE FORM

Student Name:

Chadban                      Samar                      Elias  
Last                              First                              Middle

Master's Thesis                       Master's Project                       Doctoral Dissertation

I authorize the American University of Beirut to: (a) reproduce hard or electronic copies of my thesis, dissertation, or project; (b) include such copies in the archives and digital repositories of the University; and (c) make freely available such copies to third parties for research or educational purposes.

I authorize the American University of Beirut, to: (a) reproduce hard or electronic copies of it; (b) include such copies in the archives and digital repositories of the University; and (c) make freely available such copies to third parties for research or educational purposes

after: **One** --- year from the date of submission of my thesis, dissertation, or project.

**Two** --- years from the date of submission of my thesis, dissertation, or project.

**Three** --- years from the date of submission of my thesis, dissertation, or project.

Samar  
Signature

21 Jan. 2020  
Date



## ACKNOWLEDGEMENTS

First of all, I would like to express my deepest gratitude to my thesis advisor Dr. Josep Sanjuan Girbau at the American University of Beirut / Department of Geology for his continuous support, for his patience and encouragement throughout the two years of this research work. His feedback and supervision were essential for the accomplishment of this project.

I am grateful also to my committee members: Dr. Joanna Doummar, Dr. Mohamed Salah, and Dr. Sibelle Maksoud for their time in examining my work and their valuable comments and corrections.

Thanks are also extended to Dr. Khaled Trabelsi from Sfax University in Tunisia for his help in the preliminary classification of the ostracods, Dr. Pedro Mocho from Lisboa Univeristy in Portugal for his help in identifying probable reptilian/dinosaurs remains and Dr. Georges Kachacha from the Lebanese University for his help in the preliminary classification of some teeth remains.

Furthermore, I would like to thank all my colleagues who have assisted me during my field work and laboratory study namely Beshar Al Amine, Georges Wanna, Nabih Kazzi, Catherina Khairallah, Céline Eid, Reenal Faysal, Mohammed Al Mosaad and Ali Monzer. In addition to Mr. Maroun Ijreiss and Mr. Ahmad Azhari for their technical support in thin sections preparation and to Mrs. Rania Chatila of the Central Research Science Laboratory (CRSL) at the American University of Beirut, for granting me the possibility to use the SEM facility.

This work was funded by the URB project of the American University of Beirut entitled: "Fossil Charophytes from Lebanon" (Project number AUB-23936).

Finally, I must express my sincere gratitude to my parents for their continuous encouragement throughout my years of study.

## AN ABSTRACT OF THE THESIS OF

Samar Elias Ghadban for Master of Science  
Major: Geology

Title: Paleoenvironmental Reconstruction of the Barremian/Lower Aptian Deposits of Lebanon: Sedimentology and Micropaleontology

Lower Cretaceous rocks of the Abeih Formation in the sense of Walley (1983)/upper part of the “Grès de Base” of Maksoud et al. (2014) are here studied from the sedimentological and micropaleontological viewpoints. Nine stratigraphic sections were raised and systematically sampled for microfossils in the central area of Mount Lebanon (Qehmez, Ain Dara, Azzouniye, Barouk and Jezzine). Five depositional sedimentary environments have been identified based on facies and microfacies analyses: 1) fluvial, 2) coastal freshwater lakes, 3) estuarine (intertidal and subtidal), 4) shallow marine and 5) carbonate sand shoal. These deposits provided a diverse microfossil association composed of 7 species of charophytes, 7 species of ostracods as well as foraminifera, dasyclad algal thalli, echinoid remains, mollusk shells and vertebrate fragments. The ostracod fauna is reported here for the first time including a new species. All recovered microfossils are here described and illustrated providing new insights about their paleoecology, paleobiogeography and biostratigraphy.

Three microfossil assemblages can be distinguished in agreement with the facies succession and taphonomical aspects: 1) Coastal lake; 2) Estuary; 3) Shallow marine.

The paleobiogeographical analysis of the charophyte and ostracod assemblages indicates an opposite distributional pattern within the Peri-Tethyan realm. On the one hand, ostracods display a cosmopolitan distribution occurring in both northwest and southeast margins of the Tethys. On the other hand, charophytes show a regional distributional pattern within the Middle East and northeastern Africa representing a separate bioprovince.

Based on the biostratigraphic range of some of the microfossils recovered, the proposed age of the upper boundary of the studied lithologic units (in the proximity of the Banc de Mrejjat) is late Barremian to early Aptian.

**Keywords:** Mount Lebanon, charophyte, ostracod, late Barremian, early Aptian, paleoecology, paleobiogeography, biostratigraphy.

# CONTENTS

ACKNOWLEDGEMENTS .....	v
ABSTRACT .....	vi
LIST OF ILLUSTRATIONS .....	xii
LIST OF PLATES .....	xx
LIST OF TABLES .....	xxii

## Chapter

1. INTRODUCTION .....	1
1.1. Thesis Aims .....	1
1.2. Early Cretaceous in the Levant area: An Overview .....	2
1.3. Geomorphology and structures of Lebanon .....	7
1.4. Stratigraphy of Lower Cretaceous units: Previous studies .....	10
1.5. Micropaleontology .....	17
1.5.1. Charophytes .....	17
1.5.2. Ostracods .....	23
1.5.3. Foraminifera .....	27
1.5.4. Dasycladales algae .....	29
1.6. Study area .....	30
2. METHODOLOGY .....	32

2.1. Field work.....	32
2.1.1. Planning .....	32
2.1.2. Field techniques and equipments.....	32
2.2. Laboratory work .....	35
2.2.1. Soft samples treatment.....	35
2.2.2. Sieving process .....	35
2.2.3. Microfossil extraction.....	36
2.2.4. Scanning electron microscope .....	37
2.2.5. Thin sections preparation.....	39
<b>3. SEDIMENTOLOGY.....</b>	<b>40</b>
3.1. Qehmez section 1 .....	41
3.2. Qehmez section 2.....	43
3.3. Ain Dara section .....	43
3.4. Azzouniye section 1 .....	45
3.5. Azzouniye section 2.....	46
3.6. Barouk section 1 .....	48
3.7. Barouk section 2 .....	51
3.8. Jezzine section 1 .....	52
3.9. Jezzine section 2 .....	56
<b>4. FACIES ASSEMBLAGES AND INTERPRETATION.....</b>	<b>57</b>
4.1. Fluvial .....	57

4.1.1. Channel fill.....	57
4.1.2. Floodplain .....	58
4.2. Coastal freshwater lakes .....	58
4.3. Estuary .....	59
4.3.1. Intertidal zone .....	59
4.3.1.1. Intertidal Channels.....	60
4.3.1.2. Intertidal burrowed mud flats/lagoon .....	60
4.3.1.3. Oyster Reefs.....	62
4.3.2. Subtidal zone.....	62
4.4. Shallow marine .....	63
4.5. Carbonate sand shoal .....	64
<b>5. MICROPALAEONTOLOGY .....</b>	<b>66</b>
5.1. Charophytes .....	67
5.2. Ostracods .....	86
5.3. Foraminifera.....	105
5.4. Other micro and macrofossils .....	108
5.4.1. Dasycladal thalli .....	108
5.4.2. Gastropods .....	109
5.4.3. Echinoid remains .....	109
5.4.4. Vertebrate remains .....	109
5.4.4.1. Teeth .....	109
5.4.4.2. Bones .....	112
5.4.5. Vegetal remains .....	113

<b>6. DISCUSSION &amp; CONCLUSION</b> .....	115
6.1. Microfossil taphonomy and paleoecology .....	115
6.2. Biostratigraphy.....	119
6.3. Paleobiogeography.....	120
6.3.1. Charophytes .....	121
6.3.2. Ostracods .....	124
6.4. Conclusion .....	125
<b>REFERENCES</b> .....	128
Appendix	
<b>A. STRATIGRAPHIC LOGS DESCRIPTION</b> .....	144
A.1. Description of Qehmez section 1 .....	145
A.2. Description of Qehmez section 2.....	150
A.3. Description of Ain Dara section .....	153
A.4. Description of Azzouniye section 1 .....	157
A.5. Description of Azzouniye section 2.....	160
A.6. Description of Barouk section 1 .....	170
A.7. Description of Barouk section 2 .....	175
A.8. Description of Jezzine section 1 .....	177

A.9. Description of Jezzine section 2 .....205

## ILLUSTRATIONS

Figure	Page
1. Simplified map showing the regional tectonic setting East of the Mediterranean Sea (modified from Walley, 1998).....	3
2. Tectonic map showing the Syrian Arc Fold Belt and the Dead Sea Transform Fault (DST) (taken from Jaradat et al., 2008). Lebanon is highlighted in red. ....	6
3. Simplified map of Lebanon showing main geostructures (modified from Walley, 1997). Mount Hermon (2814 m) and Qornet es Saouda (3087 m) are shown. ....	8
4. Simplified map showing the main faults in Lebanon. HF: Hasbaya fault; RcF: Rachaya fault; RF: Roum fault; SF: Serghaya fault; YF: Yammouneh fault. Modified from Nemer et al., (2008). ....	9
5. Simplified lithostratigraphic section of Lebanon (modified after Walley, 1997 and new data from Maksoud et al., 2014). Studied lithologic unit is highlighted in red. ..	16
6. Charophyte plant of <i>Lychnothamnus barbatus</i> (taken from Karol et al., 2017).....	18
7. Vegetative and reproductive structure of extant Characeae. <b>A:</b> General structure of thallus. r, rhizoids; b, starch bulbils; i, internodes; n, nodes; w, whorls of branchlets. <b>B:</b> Structure of fructification of a monoecious species. ic, internodal cell; ct, cortical cell; co, coronula; o, oogonium; br, bract-cell ; a, antheridium. <b>C:</b> Internal structure of the oogonium after fertilization. co, coronula; ow, oospore wall; sp, spiral cell (partly calcified); os, oospore nucleus; p, pedicel; so, sister cell of oospore; st, storage material (taken from Martín-Closas, 2000). ....	19
8. Female reproductive organs of a charophyte (40 X magnifications) 1) organic Oospore, 2a) Outer morphology of a calcified oospore (gyrogonite), 2b) Longitudinal section of a gyrogonite showing its internal structure; dotted lines represent the uncalcified parts of spiral and coronular cells that do not calcify (taken from Feist et al., 2005). ....	20
9. Draw of the longitudinal section of <i>Globator maillardii</i> fructification. This draw represents a reconstruction of the living fructification considering the organic and inorganic parts. ap, apical cells; an, apical neck; u, utricle; csh, calcitic shell; os, oospore nucleus; so, sister cell of oospore; p, pedicel; ow, oospore wall; sp, spiral cell; st, storage material. Note that only the calcitic shell (csh) is preserved in the fossil record (taken from Martín-Closas et al., 1999).....	21
10. Morphology of an ostracod carapace (Cronin, 2009). A: Right empty valve/internal view, B: Left outer valve showing the appendixes of the animal.....	24



11. Sketch of the inner ostracod valve. Note the terminology of the different muscle scars (Haq & Boersma, 1998).....	26
12. Growth form and internal structure of Dasycladaceae (taken from Wray, 1977, in Haq & Boersma, 1998).....	30
13. Geographic map of Lebanon showing the studied area in central Mount Lebanon. Studied outcrops are located near the villages of Qehmez, Ain Dara, Azzouniye, Barouk, and Jezzine. ....	31
14. Jacob staff used to measure the thickness of beds (Barouk section). ....	33
15. Field photo from the top of the Barouk section. About 2 kg of sediments were extracted for the sample B7. ....	34
16. Hard limestone sample collected from Jezzine section 2. ....	34
17. Sample preparation A: Chemicals used during the soft sample treatment (hydrogen peroxide and sodium carbonate), B: solution of the sample soaked with water and chemicals. ....	35
18. Sieving process of the soft rock samples for microfossil extraction. This process was performed in the thin section lab (Geology Department, AUB).....	36
19. Binocular microscope, light, picking tray, brush, and microfossil cells used to store and study the microfossils.....	37
20. Material used during the SEM sessions (stubs and adhesive tape). Note the fossil ostracod shells orderly glued on the tape.....	38
21. Sputter coater machine (Quorum Q150T). ....	38
22. SEM MIRA 3LMU located in the Central Research Science Laboratory (CRSL) of AUB. ....	39
23. Geologic map of the Qehmez area showing the location of the two stratigraphic sections. Modified from Dubertret (1955).....	41
24. Stratigraphic log of the Qehmez section 1.....	42
25. Stratigraphic log of the Qehmez section 2.....	43
26. Geologic map of the areas of Ain Dara and Azzouniye showing the location of the three studied sections. Modified after Dubertret (1955).....	44
27. Stratigraphic log for Ain Dara section.....	45

28. Stratigraphic log of the Azzouniye section 1.....	46
29. Stratigraphic log of the Azzouniye section 2.....	47
30. Geologic map of the area of Barouk showing the location of the two studied sections. Modified after Dubertret (1955). .....	48
31. Stratigraphic log of the Barouk section 1 (base).....	49
32. Stratigraphic log of Barouk section 1 (top). .....	50
33. Stratigraphic log of Barouk section 2. ....	51
34. Geologic map of Jezzine area showing the location of the two stratigraphic sections. Modified from Dubertret (1955).....	52
35. Legend for the Jezzine section 1 stratigraphic log.....	53
36. Stratigraphic log of Jezzine section 1 (base). ....	54
37. Stratigraphic log of Jezzine section 1 (top). ....	55
38. Stratigraphic log showing the Jezzine section 2. ....	56
39. Structure of <i>Atopochara trivolvis</i> utricle opened out on a basal plane (Martín-Closas & Wang, 2008). ....	70
40. A graph showing the variation of Width vs. Height of <i>Clavator</i> utricles recovered from sample B5 (Barouk section 1) in lateral and lateral anterior view.....	75
41. SEM photo of the <i>Charaxis</i> sp. recovered from J15. ....	85
42. Illustration of the terminology used to describe the carapace of the genus <i>Cypridea</i> . ACA: Anterior Cardinal Angle. AVR: Anteroventral rostrum. PCA: Posterior Cardinal Angle. PVR: Posteroventral region (Sames, 2011). ....	88
43. Illustration showing some external morphological terms used in the description of the <i>Cypridea</i> carapaces (Byung-Do et al., 2017).....	88
44. Dispersion graphic showing the relation between the carapace length and height in lateral view (n=14).....	95
45. SEM photo of the reptilian tooth recovered from Jezzine section (J12). ....	112
46. Bone fragments recovered from the Jezzine section 1. ....	113

47. A) Field photo of a large conifer trunk located at the base of the Jezzine section 1. B) Amber fragment recovered from an organic-matter rich interval at the base of the Jezzine section 1, scale bar 1mm. ....	114
48. Detailed photo of a conifer wood fragment recovered at the base of the Jezzine section 1. ....	114
49. Paleoecological model showing a transgression hemicycle in the Abeih Fm at Jezzine (J), Azzouniye (Az) and Barouk (B). Note the distribution of facies belts as well as the microfossil assemblages.....	118
50. Lower Cretaceous chronostratigraphy. Suggested age of the upper boundary of the studied lithologic unit (shadow rectangle) according to the microfossil assemblage.	120
51. Paleogeographic map of mesogea during the Lower Cretaceous (Barremian-Aptian) showing the distribution of the dominant charophyte species recovered in the Abeih Fm./“Grès de Base”. <i>Clavator ampullaceus</i> , <i>Asciidiella reticulata</i> and <i>Sphaerochara asema</i> . Capital letters represent the position of the 5 main localities from where these species were found. The dashed ellipse indicates the possible bioprovince where this assemblage thrived. <b>S</b> = Somalia, <b>Pa</b> =Palestine, <b>L</b> =Lebanon, <b>P</b> = Portugal, <b>R</b> = Romania. Note the latitudinal position of Lebanon (in the Equator) during the Early Cretaceous. Paleogeographic map modified from Decourt et al. (1993).....	122
52. Biogeographic distribution of <i>Atopochara trivolvis</i> var. <i>trivolvis</i> on a paleogeographic map of the world at 120 Ma. Black dots represent the reported geographic location of this species in the Mesogea. The red star represents the occurrence of this species in Lebanon (extracted from Martín-Closas & Wang 2008).....	123
53. Paleogeographic map of Mesogea during the Lower Cretaceous (Barremian-Aptian) showing the distribution of the dominant <i>Cypridea</i> ostracod species recovered in the Abeih Fm./“Grès de Base”. Capital letters represent the position of the 3 main localities from where these species were found. The dotted circle indicates the possible bioprovince where this assemblage thrived in the Tethys realm. <b>UK</b> = United Kingdom, <b>S</b> =Spain and <b>L</b> =Lebanon. Paleogeographic map modified from Decourt et al. (1993).....	125
54. A: field photo showing the cross-bedded sandstone beds (SS) intercalated with thin lignite bands (L) at the base of Qehmez section 1, B: note the arrangement of lignite layers among the foresets.....	146
55. Filed photo showing a reddish hard interval of ferruginous concretions (along the dotted white line) in Qehmez section 1. ....	146
56. Field photo showing the contact between silty marl and sandstone intervals showing balls and pillows structures, Qehmez section 1. ....	147

57. Thin section photo of the sample Q* (mudstone rich in quartz grains).....	148
58. Detailed photo of the upper part of the beige silty marl interval showing vertical branching burrows. The sample Q4 has been extracted from this interval.....	150
59. Detailed photo of the fossil-rich marl interval (coquina). .....	151
60. Field photo showing the alternating succession of bioclastic limestone and marl intervals.....	152
61. Microfacies of sample AD.1. A, B & C: wackestone of charophyte thalli. Note the several sections of <i>Charaxis martinclosasi</i> (C.M.T= transverse section; C.M.L = longitudinal section) and <i>Munieria</i> (M). Note that the C.M.T. is located at the node where 8 nodal cells can be counted. D: wackestone showing a transverse section of a gastropod shell. ....	154
62. Field photo showing the location of samples AD.2 (dark grey marl) and AD.3 (grey limestone).....	155
63. Microfacies (wackestone/packstone of charophytes) obtained from the sample AD.3. A: tangential section of a utricle (U) probably <i>Clavator ampullaceus</i> . B & C: several sections of charophyte thalli <i>Charaxis martinclosasi</i> (C.M) and charophyte bract cells (B.C). D: detail of an equatorial section of a utricle (U). ....	156
64. Detail field photo showing a vertical trace fossil in a silty marl interval located at the base of Azzouniye 1 section. ....	158
65. Field photo showing the position of the sample AZ.2 and the pisolitic conglomerate interval (marked between dotted lines) located at the top of the Azzouniye section 1.	159
66. Field photo of the marl interval with pisoids and microfossils burrowed by large vertical bioturbations at the top of Azzouniye section 1. ....	160
67. Detailed field photo showing the basal quartz arenite alternated with lignite lenses.	161
68. Detailed field photo showing quartz arenite interval with trough cross-stratification.	162
69. Detailed field photo showing the normal grading. ....	162
70. Detailed field photo of the pisolitic conglomerate. Note the large size of some pisoids.	163
71. Detailed field photo showing the quartz arenite with lignite lenses. ....	164
72. Detailed field photo showing carbonized wood remains.....	165
73. Detailed photo showing the pisolitic conglomerate interval. Note the decreasing size of pisoids upwards. ....	166

74. Detailed field photo of the pisolitic conglomerate. Pisoids are more concentrated (clast supported) at the base of the interval becoming more dispersed (matrix supported) at its top.....	167
75. General field photo of silty marl intervals rich in pisoids and the thin limestone layer studied for microfacies (sample AZ.5). .....	168
76. Microfacies from the sample AZ. 5. Grainstone of micritized ooids and intraclasts. (M.S=mollusk shell, I=intraclast, M.O=micritized ooid, Q=quartz).....	169
77. General field photo showing the sandstone intervals at the base of the Barouk section. Red arrows indicate the presence of two indurated beds.....	171
78. Field photo showing the quartz arenite beds with tabular cross-bedding. Red arrows mark the location of the hard concretions.....	172
79. Detailed photo of a sandstone bed showing tabular cross-bedding. ....	173
80. Field photo of the grey marl interval from which sample B7 was collected. ....	176
81. Field image showing the alteration of silty marl (SM) and sandstone (SS) beds at the top of the Barouk section 2. ....	177
82. Field photo showing the ferruginous sandstone bed (SS) with iron nodules (red) topped with grey clays (Cl) from which J1 is extracted. ....	179
83. Detailed photo of a large carbonized wood located at the base of sandstone interval.	180
84. Detailed photo of the dark grey clays rich in plant debris and amber. ....	181
85. Detailed photo of the silty marl interval with vertical burrows (outlined with dotted lines).....	182
86. Field image of the pisolitic conglomerate interval. ....	183
87. Detailed photo showing a cross-section of a pisoid.....	183
88. Field image showing the silty marl (SM) interval topped by a medium to coarse sandstone (SS) bed displaying an erosive base (marked with a dotted line). ....	184
89. Field photo showing the upper part of the oyster bank. Note that oyster shells are arranged in living position forming a reef. ....	186
90. Field image of the burrowed marly limestone (ML) interval. Note the vertical change of facies from soft marls (M) at the base of the section to hard limestone (L) at its top. Note also the presence of vertical burrows cutting the horizontal strata (dotted red	

line). Samples J6, J7, and J8 were collected respectively from the base, middle, and upper part. B: Detailed photo of a vertical burrow cast.....	187
91. Detail images of the facies located at the top of the marly limestone interval. A: Gastropod casts; B: Weathered surface of the limestone interval (wackestone/packstone facies) with mollusk shells.....	188
92. Detail images of the facies (rudstone of oncoids) located at the top of hard limestone interval (L). .....	188
93. Wackestone microfacies from sample J6. A: oblique equatorial section of foraminifera ( <i>Choffatella</i> ) shell (Ch); B: oblique axial section of a foraminifera ( <i>Textularia</i> ) shell (Tx); C: rounded quartz grains (Q) of different sizes; D: oyster shell (O.S) showing its internal structure or lamellae. ....	189
94. Wackestone/packstone microfacies from sample J7. Note the abundance of gastropod shell fragments (G), quartz grains (Q), and ostracod shells (O). Few miliolid shell (MI), and mollusk shells (M.S) are also observed. ....	190
95. Wackestone/packstone microfacies from sample J8. ( <i>Munieria</i> =M; <i>Charaxis martinclasi</i> =C.M; Charophyte utricle=U; <i>Salpingoporella dinarica</i> =S.d; Mollusk shell=M.S). Note the transverse section in C showing the inner micritic wall (M.W) and the radial calcitic structure (R.C) of <i>Salpingoporella dinarica</i> . ....	191
96. Detailed field photo of the ferruginous crust. ....	192
97. Detailed field photo showing the upper part of the marl interval. Note the increase of pisoids concentrated on top.....	193
98. Detailed image of the facies at the base of the marl interval from where the sample J10 was recovered. Note the presence of carbonized wood fragments. ....	193
99. Detailed facies showing imbricated pisoids.....	194
100. Field photo of a bone fragment in silty marl interval (below J12). ....	195
101. Detailed facies photo of the burrowed siltstone bed with horizontal burrows. ....	196
102. Detailed image of a sandstone bed with broken oyster and gastropod shells. ....	197
103. Field image of the white silty marl interval from which sample J14 was extracted..	198
104. Field photo of the sandstone interval with tabular cross-bedding. ....	200
105. Detailed photo of the foresets showing normal grading. ....	200

106. General field photo of the facies located at the top of the section Jezzine 1. Note the vertical succession of deposits; M=marl; SM=Silty marl; SS=sandstone. The silty marl interval is rich in oysters in between the dotted line. ....203
107. Detailed field photo of the contact between two sandstone intervals showing the opposite foreset dipping directions related to herringbone structures. Black lines represent the dipping direction of the foresets. ....204
108. Bioclastic packstone microfacies of sample J18. Note: A) zoom of a bivalve shell (Bv.); B) several sections of bioclasts (D=dasycladal oblique view; Ch=subaxial view of a *Choffatella* shell, M.S=Mollusk shell, Miliolid shells=MI; C) Equatorial and subaxial view of a *Choffatella* shell. Note the location of the proloculus in the equatorial section; D) several bioclasts. Note the transverse cross-section of skeletal tubular structures related to serpulid worm tubes (SE).....205
109. Packstone microfacies from sample J19. Note the abundance of mollusk shell fragments. A) Several bioclasts (Gastropod = G and Mollusk shell = M.S). B) Packstone of mollusk shells, gastropod shell (G), and *Choffatella* (Ch) in subaxial view. C) *Choffatella* in subaxial view and Dasycladal thalli (D) in equatorial view. D) Fragments of mollusk shells and echinoid spine (E.S).....206
110. Wackestone/packstone microfacies from sample J21. A) Abundance of bivalve shells (Bv.) and mollusk fragments; B & E) *Choffatella* in subaxial view; C) ostracod shells (O) and miliolid shells (MI); D) Several bioclast (*Choffatella* and micritized bivalve fragments); F) Few gastropod shells (G). ....208
111. Grainstone microfacies of sample J22. A) The nucleus of the some ooids is composed of gastropod shells; B) Ooids and few bioclasts (mollusk shells); C & D) Ooids with large intraclast. (Ooid = Oo, Intraclast = I, Gastropod shell = G, Mollusk shell = M.S). ....209

## PLATES

Plate	Page
1. A & C ( <i>Atopochara trivolvris trivolvris</i> , lateral view, AD.2), B ( <i>Atopochara trivolvris trivolvris</i> , basal view, AD.2), D ( <i>Atopochara trivolvris trivolvris</i> , apical view, J20), E ( <i>Ascidiella reticulata</i> , basal view, AD.2), F ( <i>Ascidiella reticulata</i> , apical view, J15), G & H ( <i>Ascidiella reticulata</i> , lateral view, AD.2), I ( <i>Ascidiella reticulata</i> , lateral view, B5). Red arrows in G-I point to the lateral pores.....	73
2. <i>Clavator ampullaceus</i> . A & B (apical view, AD.2), C (basal view, AD.2), D (basal view, J15), E (basal view, AD.2), F (lateral view, AD.2), G (detail of the utricle's basal pore in D, AD.2).....	77
3. <i>Clavator ampullaceus</i> . A (lateral anterior view, AD.0), B (lateral posterior view, AD.2), C (basal view, AZ.3), D (lateral view, AD.0), E (lateral anterior view, J15), F (lateral posterior view, AD.2), G (apical view, J15), H (detail of the apical pore showing a flower-like shape, J15), I ( <i>Ascidiella reticulata</i> , nodular layer covering the gyrogonite, apical view, J15).....	78
4. A ( <i>Sphaerochara asema</i> , basal view, J15), B ( <i>Sphaerochara asema</i> , basal view, B5), C ( <i>Sphaerochara asema</i> , lateral view, AD.2), D ( <i>Sphaerochara asema</i> , apical view, B5), E & F ( <i>Mesochara</i> cf. <i>harrisii</i> , lateral view, B5), G ( <i>Charaxis martinclosasi</i> , lateral view, AZ.3), H ( <i>Charaxis martinclosasi</i> , lateral view, AD.0), I ( <i>Charaxis martinclosasi</i> , internode, AD.0).....	82
5. <i>Cypridea tuberculata</i> . A (lateral view, AD.2), 1 (detailed anterior view), 2 (detailed centrodosral view), 3 (detailed posterior view), B (ventral view, AZ.2), C (dorsal view, AZ.2), D (lateral view, AD.2), E (lateral view, B5).....	90
6. A ( <i>Cypridea piedmonti</i> adult, right lateral view, AD.2), B ( <i>Cypridea piedmonti</i> juvenile, right lateral view, AD.0), C ( <i>Cypridea piedmonti</i> , right lateral view, B5), D ( <i>Cypridea piedmonti</i> , right lateral view, J10), E, F, & I ( <i>Cypridea piedmonti</i> , right lateral view, B5), G & H ( <i>Cypridea piedmonti</i> , left lateral view, B5), J ( <i>Cypridea</i> sp 1., B5), K ( <i>Cypridea piedmonti</i> , ventral view, B5), L ( <i>Cypridea piedmonti</i> , dorsal view, B5).....	93
7. <i>Cypridea</i> sp. A (lateral view, B5), 1 (detailed anterior view), 2 (detailed posterior view), B (lateral view, B5), C & D (detailed ornamentation structures, B5).....	96
8. <i>Cypridea</i> sp. A (right lateral valve, B5), B (left lateral valve, B5).....	97



9. <i>Cypridea</i> sp. A (dorsal view, B5), B (ventral view, B5).....	98
10. <i>Perissocytheridea</i> sp. A (right lateral view, J13), B (ventral view, J20), C (dorsal view, J20), D (lateral view, J20), E (lateral view, J20), F & G (lateral view, Q4), H (lateral view, J13).....	101
11. ( <i>Meta</i> ) <i>cytheropteron</i> sp. A & C (dorsal view, J5), B & D (lateral view, J5), E (ventral view, J13).....	103
12. A ( <i>Ovocytheridea</i> sp., right lateral valve, AZ.2), B ( <i>Ovocytheridea</i> sp., right lateral valve, AZ.3), C ( <i>Ovocytheridea</i> sp., right lateral valve, J5), D ( <i>Dolocytheridea</i> sp., B5), E ( <i>Dolocytheridea</i> sp., J20), F & G ( <i>Salpingoporella dinarica</i> , AZ.2).....	104
13. A, B, & C ( <i>Choffatella</i> cf. <i>decipiens</i> , B5), D ( <i>Choffatella</i> cf. <i>decipiens</i> , Q4), E (Potamididae, B5), F & G (Potamididae, AZ.1), H (basal part of an echinoid spine).....	107
14. Assemblage of teeth. A & B (from AZ.2), C (from J12), D (from AD.0), E & F (from J15).....	111

## TABLES

Table	Page
1. List showing the elevations above sea level (asl), GPS coordinates at the base and top and thicknesses of the studied sections.....	40
2. A summary of the facies description and their associated environment.....	65
3. List of microfossils and their relative abundance based on semi-quantitative visual estimation. All samples were collected in soft rocks (marls and silty marls) from the Abeih Formation (Walley, 1983) or Grès de Base (Maksoud et al., 2014). .....	67

# CHAPTER 1

## INTRODUCTION

### 1.1. Thesis Aims

The main objective of this study is to perform a paleoenvironmental reconstruction of the Early Cretaceous (Barremian) non-marine and transitional deposits of the Abeih Formation (Walley, 1983) which represents the upper part of the “Grès de Base” recently defined by Maksoud et al. (2014). These studies have been performed in the central area of Lebanon, from North to South, near the villages of Qehmez, Ain Dara, Azzouniye, Barouk and Jezzine (Mount Lebanon, Lebanon). This rock formation is here studied in detail taking into account the stratigraphical and sedimentological features, the microfacies type and the microfossil content. Results obtained from this study help in the characterization of the Lower Cretaceous basin evolution in a context of a local marine transgression.

Five secondary aims have been covered in this research work:

- Stratigraphic study and facies analysis of the Lower Cretaceous deposits of the Abeih Formation (Walley, 1983) or the upper part of the Grès de Base (Maksoud et al., 2014).
- Taxonomic classification of the microfossil assemblage recovered from the Lower Cretaceous deposits in central Lebanon.
- Estimation of the the relative ages of the Abeih Formation.

- Reconstruction of the paleoenvironment that prevailed during the Early Cretaceous in Lebanon.
- Paleobiogeographical and paleoecological implications on the basis of the microfossil assemblage.

## **1.2. Early Cretaceous in the Levant area: An Overview**

The geology of Lebanon is composed mainly of sedimentary rocks representing part of the Palmyride and Levant basins (Fig. 1). The Levant Basin occupies the Eastern Mediterranean area which represents a complex tectonic region where the Arabian, African, and Eurasian plates interact (Homberg et al., 2009; Hawie et al., 2013). The extension of the Palmyride Basin is wide from the Mediterranean Sea (in the proximity of Cyprus) until the Nile Delta of Egypt. A major deformation phase of the Levant Basin started during the Late Paleozoic until the Early Mesozoic due to breakup of Pangea. The latter event resulted in the development of the Eastern Mediterranean basin (opening of the Tethys Ocean) by rifting and the onset of passive margins during the Early Cretaceous (Garfunkel, 1998; Ghalayini et al., 2014).

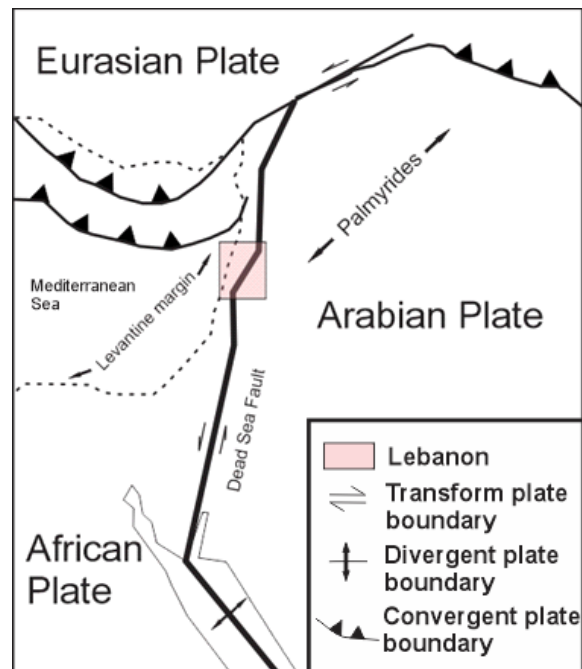


Figure 1: Simplified map showing the regional tectonic setting East of the Mediterranean Sea (modified from Walley, 1998).

The absence of Upper Jurassic to Lower Cretaceous sedimentary rocks in Syria and northern parts of Lebanon suggests that a general tectonic uplift of the Palmyride basin occurred during the Late Jurassic (Kimmeridgian stage) exposing the Lower Mesozoic deposits (Dubertret, 1955; Walley, 2001; Nader, 2011). Thus, an erosional phase prevailed until the Early Cretaceous with possible reactivation of previous faults due to volcanic activity (Brew et al., 2001; Nader, 2011). A sedimentary hiatus of about 25 million years (My) has been detected before the deposition of Lower Cretaceous fluvio-deltaic sandstone, coastal marls and shallow marine shales in Lebanon, Syria and Jordan which are the object of this study. Source rocks of these fluvio-deltaic deposits have been related to older exposed Paleozoic sandstones and vanished uplifted basements located in the Arabian plate

such as the Rutbah high in southern Syria and the Afro-Arabian Shield (Dubertret, 1975; Nader, 2011; Hawie et al., 2013).

The tectonic evolution of Lebanon can be summarized in two main phases. The first phase is related to the aforementioned tectonic history and occurred during the Late Permian extending until the Early Cretaceous. It consisted of an extensional phase related to the opening of the NeoTethys (Walley, 1998). The first rifting pulse extended from the Late Permian to the Early Triassic. This extension phase was associated with the NE-SW trending of the Palmyride rift (Garfunkel & Derin, 1984; Gardoch et al., 2010). Later, from the Late Triassic to Jurassic the seafloor spreading occurred along the Levantine margin (Garfunkel, 1989). A possible second rifting phase occurred during the Early Jurassic until the development of a passive margin during the Late Jurassic (Druckman, 1977; Hirsch et al., 1998; Gardosh, 2002; Roberts & Peace, 2007).

Later, from Late Cretaceous to Early Miocene, a regional compressional phase (Syrian arc deformation) progressively closed the Neotethys Ocean creating a general uplift and a complex folding system in the area. This fold system is known as the Syrian arc fold belt extending from Egypt through Sinai Peninsula reaching the Palmyrides in Syria following a NE-SW trend passing through Lebanon in a NNE-SSW direction (Fig. 2). The Syrian arc deformation started in the Late Cretaceous probably during the collision between the Eurasian and the Afro-Arabian plates. During the Neogene, tectonic compressive movements changed towards a transform-fault system located along the Dead Sea fault (Walley, 1998).

However, the evolution of the geologic structures in Lebanon has been a matter of debate for many geologists. Many authors; namely Ponikarov (1967), Dubertret (1975), Hancock and Atiya (1979) suggest that the Lebanese geologic structures represent a part of the Syrian arc fold belt, first defined by Krenkel (1924). The main geologic structures of Lebanon follow the same trend of the Syrian arc fold belt (Fig. 2). The first deformation phase caused the emergence of gentle anticlinal structures in the Palmyride basin. Later, the second deformation phase of the Syrian arc belt (Late Eocene to the Late Oligocene and possibly Early Miocene) caused a major uplift of the Lebanese mountain ranges (Krenkel, 1924; Walley, 1998; Walley, 2001).

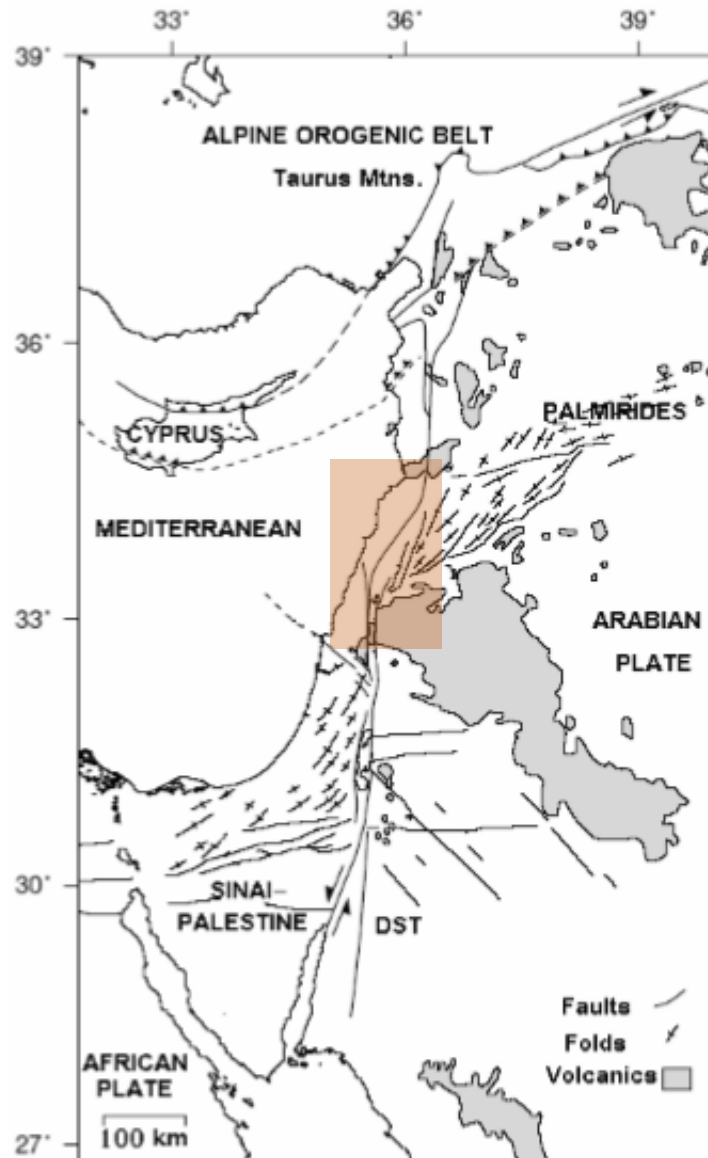


Figure 2: Tectonic map showing the Syrian Arc Fold Belt and the Dead Sea Transform Fault (DST) (taken from Jaradat et al., 2008). Lebanon is highlighted in red.

Mesozoic sedimentary rocks in Lebanon show a characteristic thickening toward the southwest directions (Saint-Marc, 1974; Dubertret, 1955; Walley, 1997). Homberg et al. (2009) justified this variation in thickness examining most of the Lebanese faults. These authors realized that most of the Middle Jurassic to Upper Lower Cretaceous faults are dip-slip normal growth faults resulting from



extensional stresses with a WNW-ESE direction. According to Homberg et al. (2009) these extensional fault systems possibly originated during the very Early Cretaceous (Valanginian) being active until the end of the Early Cretaceous (beginning of Cenomanian). This thickness variation was attributed by Homberg et al. (2009) to the development of an elongated E-W basin that deepens westward. According to these authors, the possible basin axis would be located in the Chouf area and its northern margin would be placed near the city of Tripoli where lower cretaceous deposits are represented by few meters of thickness (Homberg et al., 2009).

### **1.3. Geomorphology and structures of Lebanon**

Lebanon extends along the eastern margin of the Mediterranean Sea for about 210 km along the coast (Beydoun, 1977). It is bordered by Syria from the North and East and by Palestine to the South. Three basic mesostructures can be distinguished in Lebanon from west to east: Mount Lebanon, the Bekaa Valley, and Anti-Lebanon. These major geological structures have a characteristic directional trend to NNE-SSW (Walley, 1997). They consist of two anticlines (Mount and Anti-Mount Lebanon) separated by the syncline of the Bekaa valley which forms a high plain (Fig. 3).

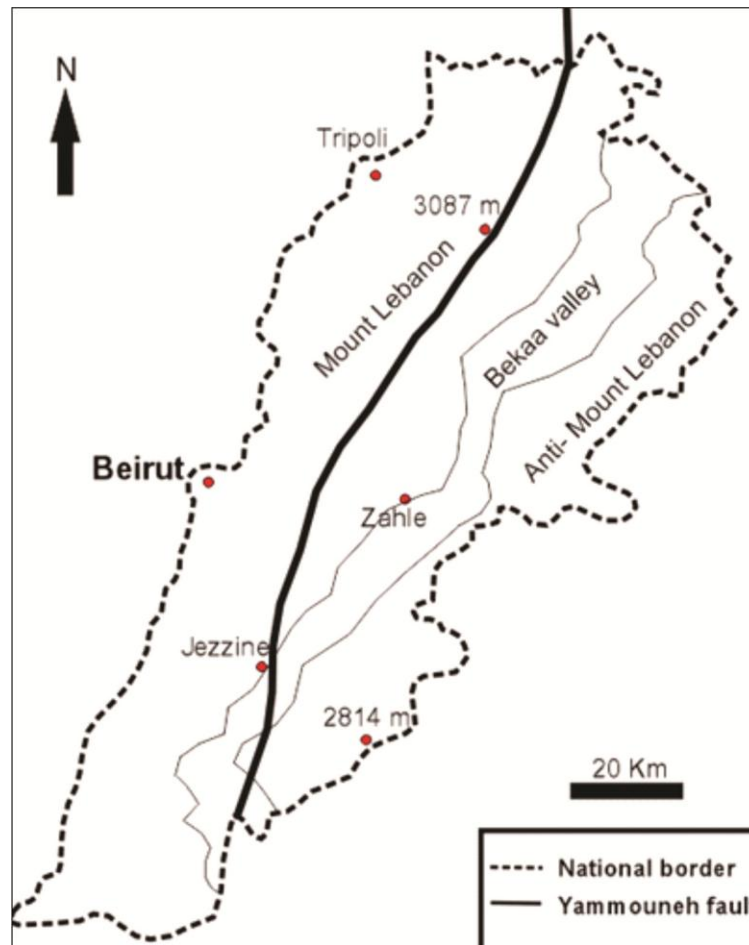


Figure 3: Simplified map of Lebanon showing main geostuctures (modified from Walley, 1997). Mount Hermon (2814 m) and Qornet es Saouda (3087 m) are shown.

Lebanon is characterized by a well exposed and thick sedimentary rock succession of different ages, from the oldest Jurassic to Quaternary. Two major stratigraphic gaps have been identified corresponding to the Early Cretaceous and Late Paleogene (Walley, 1997). The major fault in Lebanon is represented by the Yammouneh transform fault which displays a NNE-SSW trend. This fault connects and represents an extension of the Dead Sea fault system to the south and the Ghab fault system to the north. The complete Dead Sea/Yammouneh/Ghab fault system

separates the Levantine sub-plate of the African Plate from the Arabian Plate (Walley, 1997). The Yammouneh fault branches into several minor faults some of them are very active and responsible for many historical major earthquakes in the region (Fig. 4). These are the N-S Rourm fault, the NE-SW Rachaya, Serghaya and the Hasbaya faults (Walley, 1997; Buttler et al., 1998; Nemer et al., 2008). They display a combination of normal and left lateral motion (Dubertret, 1962; Mart et al., 2005).

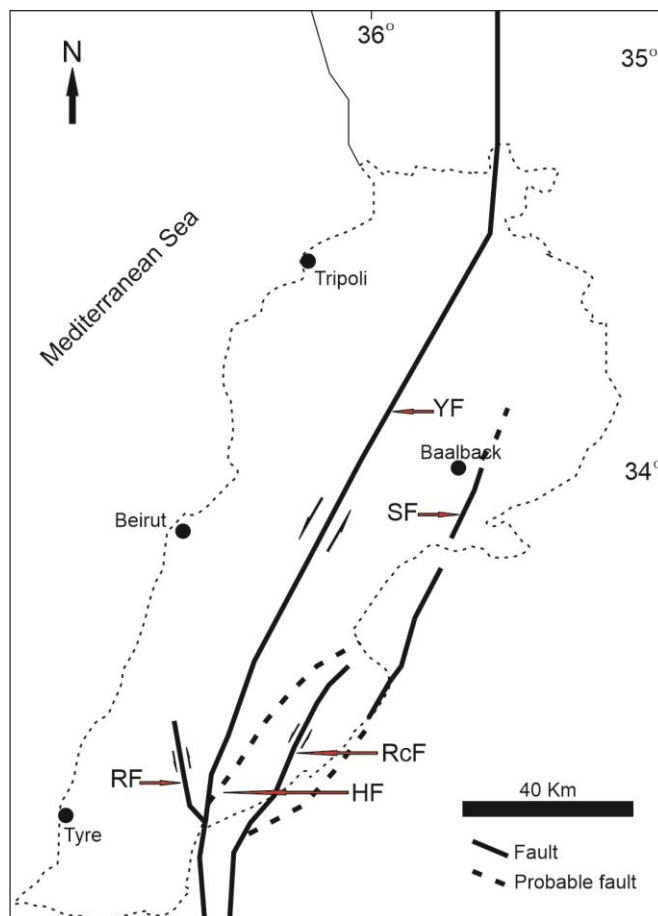


Figure 4: Simplified map showing the main faults in Lebanon. HF: Hasbaya fault; RcF: Rachaya fault; RF: Rourm fault; SF: Serghaya fault; YF: Yammouneh fault. Modified from Nemer et al., (2008).

#### **1.4. Stratigraphy of Lower Cretaceous units: Previous studies**

Lebanese geology is mainly composed of sedimentary rocks with minor volcanics (Renouard, 1955). A summary is provided here about the previous studies of the Lower Cretaceous non-marine and transitional rock formations in Lebanon i.e., Chouf and Abeih formations or “Grès de Base” which are the object of this study (Fig. 5).

The Cretaceous stratigraphic sequence overlies Jurassic rocks showing a clear unconformity in all Lebanon (Walley, 1997). The basal unit of the Lower Cretaceous is well exposed in many Lebanese localities especially in the Mount Lebanon area. It is represented by the Chouf Formation, followed by the Abeih Formation, and the Mdairej Formation representing an overall marine transgressive trend (Walley, 1997). However, the distinction between these different units is still debatable in terms of age and depositional environment.

The first studies of Lower Cretaceous sedimentary rocks were performed at the base of the nowadays known Chouf Formation by Douville (1910) and Zumoffen (1926). These authors reported that the Chouf Formation is composed of sandy and clayey beds with coal layers and wood remains. Dubertret (1955) noticed that the lithology of the Chouf Formation is gradually changing vertically from massive cross bedded brown sandstone to marly deposits rich in fossils. Kanaan (1966) reported that the Chouf Formation is composed of argillaceous sandstone, interbedded with clays, lignite, and shales except in the southwest, where it consists of marine facies composed of sandstones, marls, marly limestone, limestone,

dolomite, clay, and shale. Later, Searle (1974) and Shuayb (1974) demonstrated that the Chouf Formation contained several clay layers deposited as interbeds and not as continuous layers as previous authors reported.

Many authors reported that the Chouf Formation shows a characteristic lateral variation from east to west and from north to south including Dubertret et al. (1955), Searle (1974), Shuayb (1974), Beydoun (1977) and Walley (1997), Kanaan (1966), Wakim (1968) and Bellos (2008). The thickness of the Chouf Formation changes laterally from few meters in northern Lebanon i.e. 10 m in Sir el Daniyeh area to about 300 m near the Jezzine area i.e. type location at Jisr el Qadi. Kanaan (1966), Beydoun (1977) and Walley (1997) related this lateral change in thickness with the simultaneous deposition of the Chouf sand (sandstone after lithification) during block faulting in lower Cretaceous rather than basin development as stated by Ukla (1970) with depocenter in the Chouf-Jezzine area.

The primary structures abundant in the Chouf Formation include: cross-stratification mainly tabular type with rhythmic graded bedding reported by Kanaan (1966), Wakim (1968) and Bellos (2008).

The depositional context in which the Chouf Formation was formed has traditionally been considered as fluvio-deltaic environment (Kanaan, 1966; Masaad, 1976; Walley, 1997; Ferry et al., 2007). These authors reported that the Chouf Formation shows strong sedimentological similarities with other contemporaneous sandstone units from nearby countries such as the Rutbah Formation (Syria) and the Hathira Formation (Jordan). In addition, Kanaan (1966) noted that sandstone strata

of the Chouf Formation grades laterally into limestone beds towards the west. According to Kanaan (1966) and Wakim (1968) the Chouf Formation was probably affected by tides which interacted with the deltaic processes. After a more detailed sedimentological analysis of this rock formation at Jezzine (south Mount Lebanon), Tixier (1971-1972) concluded that these rocks were formed under a fluvio-deltaic depositional context without any eolian activity. In a more recent work, Bellos (2008) identified six microfacies within the Chouf Formation at Homsiyeh (Jezzine). He classified these facies as quartz arenites (most abundant) sometimes rich in muds, greywackes, clay, and limestone. He also divided the Chouf Formation into 3 parts (basal, middle and upper). According to this author, facies observed at the middle part of this lithologic unit can be related to an eolian depositional environment whereas the basal and upper parts of the rock formation was deposited under an aquatic flow regime (fluvial, overbank, alluvial and/ or turbidity currents, shallow marine).

The age of the Chouf Formation is still uncertain. Shirmon and Lang (1989) and Beydoun (1995) first proposed that this lithological unit was Hauterivian in age based on lateral correlations with sandstone units located in in the Middle East including the Helez Formation in Palestine, the Nubia Sandstone Formation in the Gulf of Suez and the Rutbah sandstones in Syria. According to Walley (1983), the lower boundary of the Chouf Formation is diachronous with the underlying Jurassic Salima Formation. The upper boundary of the Chouf Formation, in contact with the

lower Abeih Formation, is considered of Barremian in age (based on limited fauna of gastropods, bivalves and orbitolinid foraminifers) according to Walley (1983).

Little attempt were performed in order to study and characterize the overlying Abeih Formation. This lithological unit was defined as a transitional interval between the fluvio-deltaic sandstone of Chouf Formation and the marine limestone beds of the Mdairej Formation. The Abeih Formation is mainly composed of shales, sandstone, and fossiliferous calcareous deposits (Walley, 1997). It ranges in thickness between 80 and 170 m. Facies are mainly sandy in its lower parts, changing upwards into more calcareous deposits (Walley, 1983). The relative abundance of marls and sandstone intervals rich in marine mollusks marks the facies change between the Chouf and Abeih units. According to Walley (1983), the presence of a characteristic pisolitic horizon with high lateral extension marks the base of Abeih Formation. This lithologic unit shows a characteristic facies change from north to south. In central areas of Mount Lebanon, the Abeih Formation contains little amount of fossils (i.e. gastropods, bivalves) while in northern Lebanese outcrops it is composed of cross-bedded ferruginous sandy grainstones with green clays (Walley, 1997). The age of the Abeih Formation is considered as lower Aptian based on gastropods, orbitulina and bivalves (Dubertret, 1955; Walley, 1997; Nader, 2000). The depositional environment of the Abeih Formation was interpreted by Walley (1997) as lagoonal/estuarine and littoral environments.

The Mdairej Formation is stratigraphically located above the Abeih Formation (Dubertret, 1955). The deposits of the Mdairej Fm form an outstanding pale grey

cliff along the east and west sides of the Mount Lebanon traditionally known as *Falaise Blanche*. Mdairej Formation is composed of limestone beds related to shallow marine conditions (Walley, 1997). According to Blanche (1947), the Mdairej Formation consists of two main intervals i.e. an oolitic limestone bed at the base and a massive micritic limestone interval at the top. According to Heybroek (1942) and Dubertret (1947) the Mdairej Formation is also composed of reefal limestone. However, recent studies focused on this lithologic unit disproved the presence of reefs in the area of Jezzine (Maksoud et al., 2014). This lithologic unit has been dated as Aptian in age based on the macrofossil (rudist and echinoids) and microfossil (orbitolinids) assemblage (Dubertret, 1963). Saint-Marc (1970) precised the relative age of this formation as early Aptian based on benthic foraminifera and calcareous algae.

Recent data on the age of the Lower Cretaceous formations have been reported by Maksoud et al. (2014) and Maksoud et al. (2017). The Chouf and Abeih formations in the old sense of Walley (1983) consist one lithostratigraphic unit referred to as the “Grès de Base” or “Grès du Liban” (Maksoud et al., 2017). The upper part of the Abeih Fm. and the Mdairej Fm constitute a part of a single time unit that changes laterally known as the “Jezzinian Regional Stage”, JRS (Fig. 5). According to Maksoud et al. (2014), the Abeih and the Mdairej formations are genetically related sharing the same algal and foraminifera assemblage representing a transition zone between a shoal barrier and a protected lagoon. The lower boundary of the JRS is late Barremian in age and the upper boundary of the JRS is



early Bedoulian or lower Aptian in age (Maksoud et al., 2014). Maksoud et al. (2017) distinguished three units within the upper part of the “Grès de Base”. The lower unit is located below the pisolitic interval (possibly early Barremian in age or older). The middle unit is located between the pisolitic interval and the oolitic limestone interval known as Banc de Mrejatt. The latter unit is rich in charophytes, calcareous algae and benthic foraminifera. It is considered as early Barremian in age by Maksoud et al. (2017). The upper unit is located between the Banc de Mrejatt and the lower boundary of the JRS (late Barremian). The lithologic unit in this study is considered as the middle unit according to Maksoud et al. (2017).

Lower Cretaceous non-marine deposits in Lebanon are becoming known internationally thanks to recent paleontological works based on insect inclusions in amber from Mount Lebanon (Poinar & Milki, 2001; Deans et al., 2004; Azar & Ziadé, 2005; Azar, 2007). Around 180 different species of insects have been discovered in the Lebanese amber which helped in better understanding of some aspects regarding the paleoenvironment and paleoclimate that existed in the area during that time. Buffetaut et al. (2016) place Lebanon in the scientific media after their discovery of two dinosaur teeth related to sauropods at the top of the Chouf Formation near the Jezzine village.

On the other hand, few paleontological works have been performed on microfossils linked with facies such as charophytes and ostracods from the same deposits (Chouf and Aheih formations or “Grès de Base”). Grambast and Lorch (1968) first reported and described a charophyte assemblage in marly intervals

within the Chouf Formation near the village of Jezzine. These authors dated, for the first time, this formation as Lower Cretaceous (Aptian). Wakim (1968) reported the presence of ostracods in some shale layers. However, fossil ostracods from these deposits have never been described before. Recently, Granier et al. (2015) reported the presence of new fossiliferous outcrops near Jezzine rich in charophyte remains (gyrogonites, utricles and thalli). They improved some taxonomical aspects of the charophyte flora previously recovered by Grambast and Lorch (1968) and recovered new microfossils suggesting that the top of the Chouf Formation is Barremian in age. These authors have pointed out the interest of these microfossils in the local non-marine biostratigraphy, paleoecology and in future paleobiogeographic analysis.

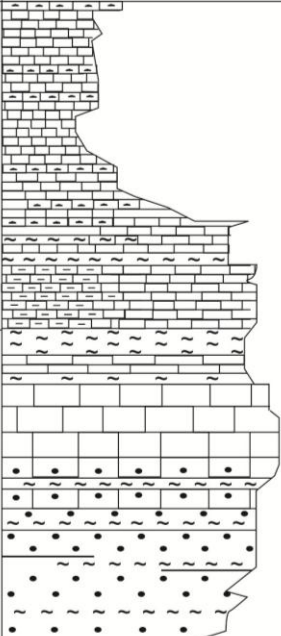
Period	Epoch	Profile	Stratigraphic Unit	
Cretaceous	Upper		Chekka Formation (C6) chalk, marly chalk, chert nodules	
			Maameltain Formation (C5) marl, marly limestone	
			Sannine Formation (C4) deep and shallow water limestone	
			Hammana Formation (C3) green marl, limestone	
	Lower		Mdairej Formation (C2b) limestone	Jezzinian Regional Stage
			Abeih Formation (C2a) sandy limestone, marls	Grés de Base
			Chouf Formation (C1) sandstone, marl, limestone, lignite	

Figure 5: Simplified lithostratigraphic section of Lebanon (modified after Walley, 1997 and new data from Maksoud et al., 2014). Studied lithologic unit is highlighted in red.

## **1.5. Micropaleontology**

A synthetic description of the dominant microfossils recovered from the studied lithologic unit (upper part of the Grès de Base) is here provided:

### **1.5.1. *Charophytes***

Charophytes (informally known as stoneworts) are a group of freshwater or brackish water aquatic plants which are considered the ancestors of mosses and vascular plant (Martín-Closas, 2000). The stems (thalli) and fructifications of these plants usually calcify (Martín-Closas, 2000). Hence, charophyte remains are frequently preserved in the fossil record through their incrustated stems and their biomineralised fructifications (i.e. gyrogonites and utricles). Charophytes grow forming dense meadows in the photic zone of waterbodies such as perennial or temporary lakes, ponds, estuaries and swamps (García & Chivas, 2006). Charophytes are essential for aquatic ecosystems providing food and habitat to many species of fish and other aquatic organisms. Charophyte plants grow attached to water body's floor and may attain different sizes ranging between few centimeters to few meters (Fig. 6).



Figure 6: Charophyte plant of *Lychnothamnus barbatus* (taken from Karol et al., 2017).

The vegetative structure of these plants is complex (Fig. 7A). The stem or thallus consists of a main internodal cell surrounded by cortical cells parallel or slightly coiled around the main internodal cell (Feist et al., 2005). The charophyte thallus is composed of alternating nodes and internodes (Fig. 7A). Each node consists of several small cells from which lateral branches arise. Very thin and colorless filaments called rhizoids arise from the branches on which the charophytes are fixed (Feist et al., 2005).

The reproductive organs of charophytes i.e. the antheridium (male) and the oogonium (female) develop from the nodes of the plant during the reproductive season (Fig. 7B & C) (Feist et al., 2005).

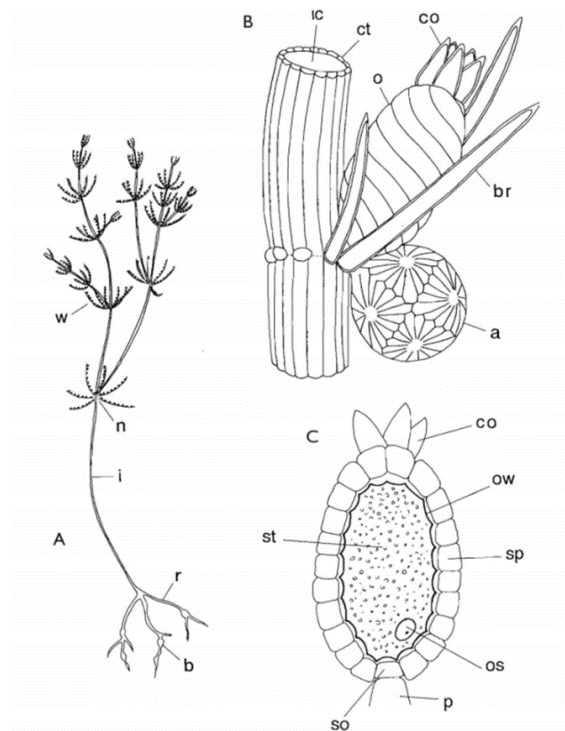


Figure 7: Vegetative and reproductive structure of extant Characeae. **A:** General structure of thallus. r, rhizoids; b, starch bulbils; i, internodes; n, nodes; w, whorls of branchlets. **B:** Structure of fructification of a monoecious species. ic, internodal cell; ct, cortical cell; co, coronula; o, oogonium; br, bract-cell; a, antheridium. **C:** Internal structure of the oogonium after fertilization. co, coronula; ow, oospore wall; sp, spiral cell (partly calcified); os, oospore nucleus; p, pedicel; so, sister cell of oospore; st, storage material (taken from Martín-Closas, 2000).

Soulié-Märsche and García (2014) explained the stages of the charophyte fertilization process. The oogonium is the unfertilized female gametangium. It is composed of an oosphere surrounded by five tubular vertical cells that start coiling in a clockwise direction to form spiral cells. The latter are joined at the apex surrounded by five coronular cells (Fig. 8, 1). After the fertilization process the oogonium is transformed into an oospore (Fig. 8, 1). The oospore is composed of 4 successive organic walls forming ridges between spiral cells. Frequently, above the

oospore wall an intracellular calcified layer can be formed (Fig. 8). This calcified structure is termed gyrogonite (Feist et al., 2005; Soulié-Märsche & García, 2014).

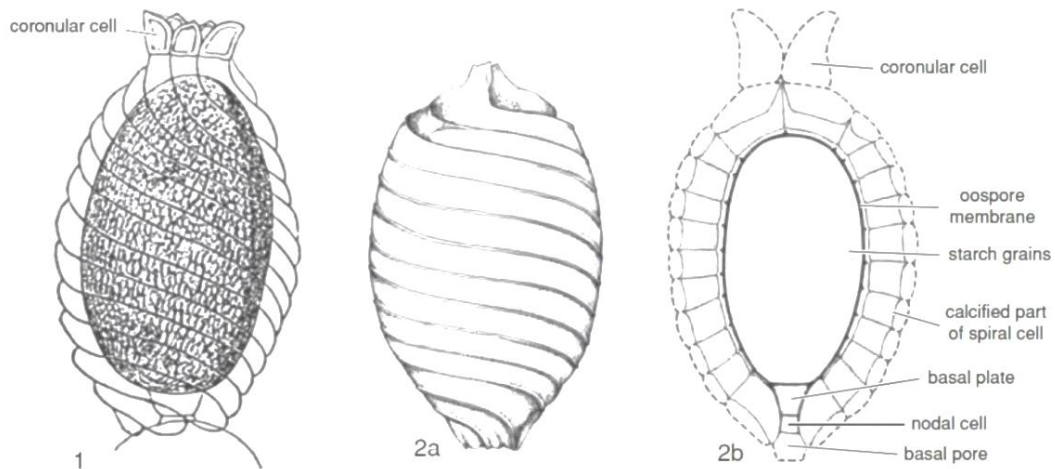


Figure 8: Female reproductive organs of a charophyte (40 X magnifications) 1) organic Oospore, 2a) Outer morphology of a calcified oospore (gyrogonite), 2b) Longitudinal section of a gyrogonite showing its internal structure; dotted lines represent the uncalcified parts of spiral and coronular cells that do not calcify (taken from Feist et al., 2005).

The gyrogonite (Fig. 8, 2a) is normally elliptical in shape ranging in size between 0.2 and 2 mm and it is composed of five spiral cells (Feist et al., 2005). In extinct Paleozoic and Mesozoic families the gyrogonite was covered by a protective calcified envelope known as the utricle (Fig. 9).

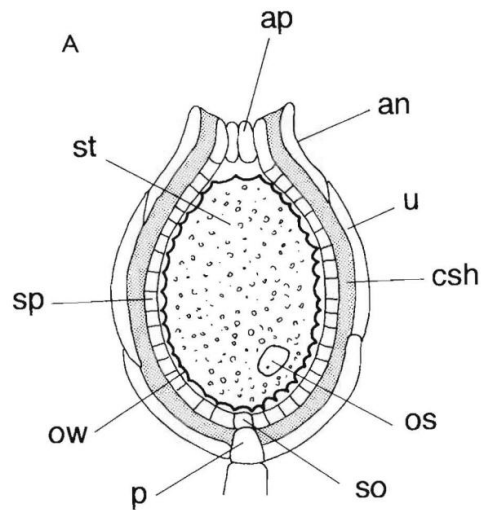


Figure 9: Draw of the longitudinal section of *Globator maillardii* fructification. This draw represents a reconstruction of the living fructification considering the organic and inorganic parts. ap, apical cells; an, apical neck; u, utricle; csh, calcitic shell; os, oospore nucleus; so, sister cell of oospore; p, pedicel; ow, oospore wall; sp, spiral cell; st, storage material. Note that only the calcitic shell (csh) is preserved in the fossil record (taken from Martín-Closas et al., 1999).

The size, morphology and ornamentation pattern of charophyte fructifications are very variable and genetically induced by the producing plants. This variability allowed the development of a parataxonomy used for the classification of fossil charophytes (Feist et al., 2005). On the one hand, the classification of gyrogonites is based on several parameters such as the general shape, number of convolutions, general dimensions (i.e. gyrogonite height and width), apical structure, basal structure (shape and type of basal pore and plate) and ornamentation of the spiral cells (Feist et al., 2005 and references herein). On the other hand, the classification of utricles is based on the size, apical and basal pore

structure, and the geometry and pattern of the branchlets impressions (Martín-Closas et al., 1999; Feist et al., 2005).

Fossil charophyte fructifications have been recovered in non-marine deposits as old as Silurian in age (Feist et al., 2005).

Fossil charophytes have numerous applications in paleontology. Their relatively high evolutionary rates and their wide paleobiogeographic distribution make them a very valuable microfossil for biostratigraphic purposes in non-marine sedimentary rocks (Soulié-Märsche & García, 2014). Local and regional charophyte biozonations have been developed during the last decades in many European and Asiatic basins (Anadón et al., 1992; Feist et al., 1995; Martín-Closas & Millán, 1998). Charophytes are sensitive to paleoenvironmental changes and many living taxa need specific habitat requirements (Gierlowski-Kordesch, 2010). Hence, fossil charophytes have been used as paleoecological proxies especially in Neogene and Holocene lacustrine deposits providing valuable information about paleosalinities, water level fluctuation and changes in trophic status of the ecosystems (García & Chivas, 2006; Martín-Closas et al., 2006; Soulié-Märsche et al., 2010; Sanjuan & Alqudah, 2018).

Recent studies involving experimental cultures have been developed with the aim to use geochemistry (trace-elements and oxygen isotopes) to reconstruct paleosalinities and paleotemperatures (Dux et al., 2015) and to find links between gyrogonite morphology and ecological parameters such as temperature and light irradiance (Sanjuan et al., 2017).



Moreover, species-specific paleoenvironmental constraints have been defined for Mesozoic and Cenozoic fossil charophytes based on sedimentological and taphonomical analyses (Villalba-Breva & Martín-Closas, 2011; Sanjuan & Martín-Closas, 2012; Vicente et al., 2016). The mineralogy of the charophyte remains i.e. Ca, Mg has been also used to determine the diagenetic and hydrologic changes of lacustrine deposits in the past (Anadón et al., 2000).

### **1.5.2. Ostracods**

Ostracods are small bivalve crustaceans known colloquially as seed shrimp. Their calcitic valves or carapaces range in size between 0.5 and 5 mm. However, some species of ostracods such as *Gigantocypris* can produce large shells up to 32 mm in length (Holmes & Chivas, 2002; Saraswati & Srinivasan, 2016). The ostracod record comprises more than 65000 living and fossil species which occur in nearly every type of aquatic environment from freshwater to marine, hypersaline, and even phreatic waters (Pokorný, 1978; Haq & Boersma, 1998; Holmes & Chivas, 2002). The fossil record of ostracods is based on their calcified valves that easily fossilize and occur abundantly in limestones, shales and marls as old as Ordovician in age (Moore & Pitrat, 1961). According to Moore and Pitrat (1961) the origin of this group during the Ordovician is related to marine environments. Then, after time, they progressively occupied coastal areas such as deltaic, lagoonal, and lacustrine environments by the Late Jurassic and Early Cretaceous (Saraswati & Srinivasan, 2016).

For the taxonomic classification of ostracods, micropaleontologists take into consideration the interior and the exterior features of the carapace. The carapace is composed of two valves united by a narrow hinge located in the dorsal margin and an adductor muscle (Pokorný, 1978; Haq & Boersma, 1998). The two valves overlap but usually differ in size and they are closed by the adductor muscle (Holmes & Chivas, 2002). Muscle scars could be quite complex and they are located at different positions of the inner shell (Fig. 10).

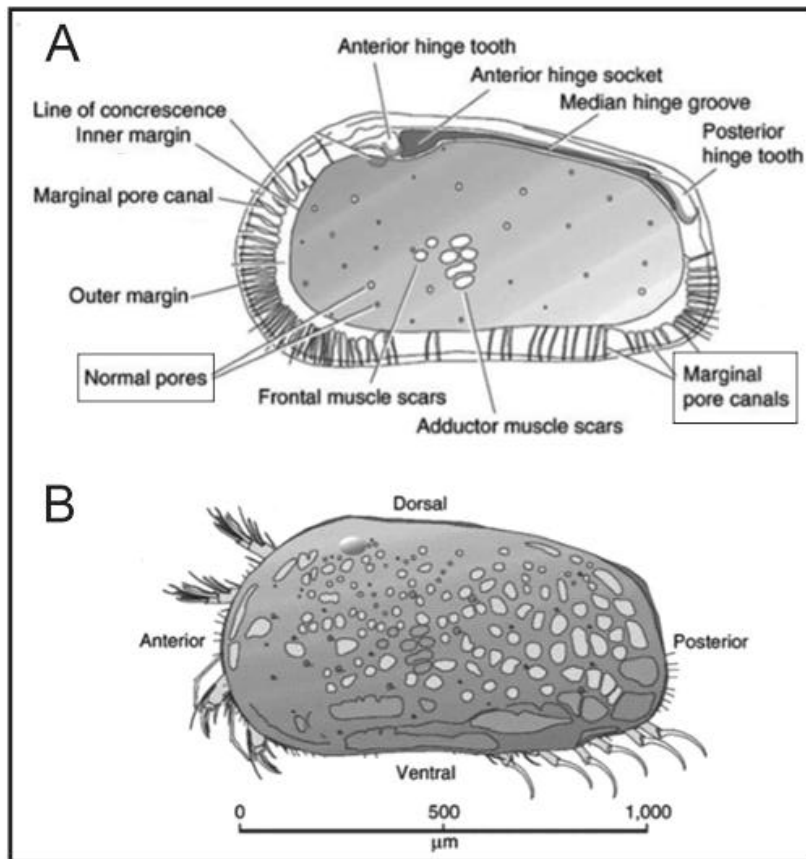


Figure 10: Morphology of an ostracod carapace (Cronin, 2009). A: Right empty valve/internal view, B: Left outer valve showing the appendices of the animal.

As other groups of crustaceans, ostracods change their carapaces (moulting) up to 9 times throughout their lifetime as they get older. Thus, a single ostracod can produce several shells. The growth stages of ostracod carapaces are known as instars. Adult carapaces and instars are easily preserved in sediments deposited in subaquatic conditions (Pokorný, 1978; Flügel, 2010; Saraswati & Srinivasan, 2016). The relative amount of instar vs. adult carapaces in a sample has been used as a taphonomic proxy (Pokorný, 1978). According to this author the presence of larval and adult carapaces together usually indicates quite environment conditions (lack of transport). In contrast, the absence of one of those two groups may indicate that some currents transported the shells.

The taxonomic classification of fossil ostracods is based on several carapace features (Figs. 10 & 11). These features include the shape of the carapace (bean-shaped, inflated, compressed, spheroidal and rectangular), ornamentation of the shell (ridges, spines, or nodes), pore density and morphology, muscle scars (adductor and mandibular muscles) and type of hinge (Flügel, 2010; Saraswati & Srinivasan, 2016). However, the carapace ornamentation should be taken with caution in the ostracod taxonomy since some groups change their ornamentation in function of the sex (sexual dimorphism) and environmental conditions such as salinity, temperature, and water depth (Saraswati & Srinivasan, 2016). Generally, female ostracods are higher in number than males in a population. Moreover, the length/height carapace ratio also is different between sexes.

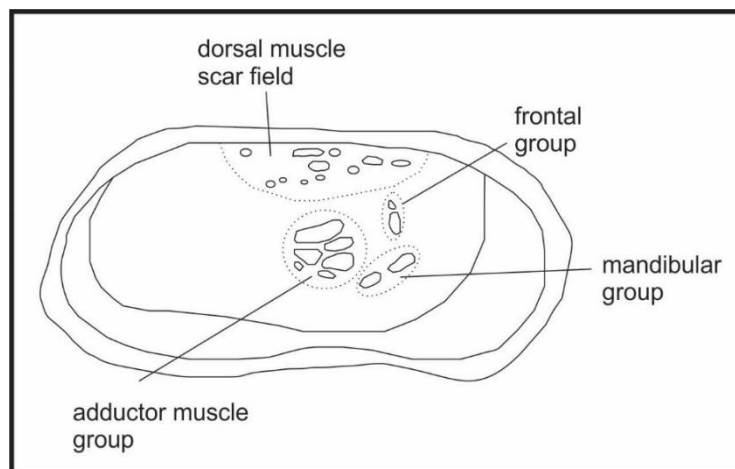


Figure 11: Sketch of the inner ostracod valve. Note the terminology of the different muscle scars (Haq & Boersma, 1998).

Because of their specific morphology and relatively high rates of evolution, ostracods are among the main biostratigraphic indicators of marine deposits (Rodriguez-Lazaro & Ruiz-Muñoz, 2012). Despite fossil non-marine ostracods have been little studied up to now in terms of biostratigraphy, their application in this field have been proved especially for Lower Cretaceous non-marine rock sequences from South Europe (Spain) by Schudack and Schudack (2009) and North Africa (Tunisia) by Trabelsi et al. (2015). Most of the biostratigraphic correlations proposed in their studies were based on species of the non-marine genus *Cypridea*. Schudack and Schudack (2009) established several ostracod associations for the Lower Cretaceous of Spain, characterizing different ages as well as paleoecologies. These authors established a local ostracod biozonation and correlated it with other microfossils biozonations such as the charophyte biozones.

Trabelsi et al. (2015) described a complete non-marine ostracod assemblage from the Lower Cretaceous Kebar Formation in Central Tunisian Atlas. Moreover,

these authors also correlated the ostracod assemblages with the charophyte biozones which allowed dating the lower member of the Kebar Formation as early Aptian. The ostracod assemblage reported in the Kebar Formation has also been reported in Lower Cretaceous non-marine sedimentary sequences from distant areas such as South America, West Africa and Western Europe (Trabelsi et al., 2015). This wide apparent distribution of ostracods demonstrates the usefulness of this group in non-marine biostratigraphy and regional chronostratigraphy.

Ostracods are especially sensitive to changes in water salinity and temperature. These two factors affect their distribution. Thanks to this sensitivity, fossil ostracods have been used in paleoecological and paleobiogeographical studies with the aim to characterize global Neogene paleoclimatic events such as sea-level changes and salinity crises. Moreover, the chemical composition of the carapaces has been considered as excellent paleoenvironmental indicators (Holmes, 2001; Frogley et al., 2002; Holmes & Chivas, 2002; Park & Smith, 2003). The shell chemistry of ostracods i.e.  $^{18}\text{O}/^{16}\text{O}$  in  $\text{CaCO}_3$  can indicate the salinity, water chemistry, sedimentation rate, and temperature of the lake system (Carbonel et al., 1988; Holmes & Chivas, 2002; Dettman et al., 2005).

### **1.5.3. Foraminifera**

Foraminifera are a well-diversified group of unicellular benthonic or planktonic marine organisms (protozoans with skeleton). Foraminifera live in all types of marine environments. They also thrive in brackish water but are absent in freshwater environments (Bellier et al., 2010; Saraswati & Srinivasan, 2016). The

size of a foraminifera commonly varies between 0.1 and 1 mm, however, some groups (also named macroforaminifers) can reach up to 10 cm. The basic structure of the shell is its divisions forming successive chambers. The chambers are separated from one another by partitions or septa (Bellier et al., 2010).

The basic classification of foraminifera is based on the shell type. Three main groups of foraminifers can be distinguished: agglutinated, calcareous, and microgranular (Haq & Boersma, 1998). Some foraminifera possess a shell made up of organic matter, however such groups are not preserved in the fossil record. Commonly, biomineralized shells (secreted or agglutinated mineral) are preserved in the fossil record (Haq & Boersma, 1998; Bellier et al., 2010).

Agglutinated foraminifera build their shells by secreting cement and agglutinating foreign particles (quartz grains, sponge spicules, calcite grains, etc.). Calcareous foraminifera have a calcium carbonate wall secreted by the animal. They can be either porcellaneous or hyaline. Porcellaneous foraminifera are characterized by a smooth and homogenous calcareous wall. However, hyaline foraminifera have a perforated wall (Bellier et al., 2010).

Foraminifera are of great importance in stratigraphy as well as paleoenvironmental studies since they inhabit in all environments and range in age from Early Cambrian to present (Bellier et al., 2010; Saraswati & Srinivasan, 2016). They are useful for biozonation of shallow and deep marine deposits and allow the reconstruction of depositional systems (Flügel, 2010). In addition, their shell chemistry allows the paleoclimate reconstruction by examining the stable isotope

ratios (i.e. oxygen and carbon) and trace element content (magnesium, lithium etc.) of the shell (Zachos et al., 2001; Misra & Froelich, 2012; Branson et al., 2013).

#### **1.5.4. *Dasycladales algae***

Dasyclads are benthic calcified unicellular green algae. They belong to the phylum Chlorophyta, class Chlorophyceae, and order Dasycladales (Flügel, 2010). They appeared in the Cambrian and were essential rock builders from Late Paleozoic until Early Cenozoic (Flügel, 2010).

The living dasycladales are small in size from few millimeters to few centimeters upright (Fig. 12). Most species are characterized by a large central stem (thallus) bearing one or smaller radiating branches or laterals (Wray, 1977; Flügel, 2010). These branches may be subdivided into one or more laterals. Dasycladales are preserved in the fossil record through calcified skeletal remains of thallus and laterals (Wray, 1977).

Most dasycladales have unbranched thalli exhibiting various shapes including rod-shaped (tube-like), spherical thalli, clavate thalli (pear-shaped forms) etc. (Flügel, 2010).

The classification of fossil dasycladales is based on several criteria: the growth form and shape of the thallus and the central stem, the arrangement, shape and the number of branching of laterals, and the position of reproductive organs (Flügel, 2010).

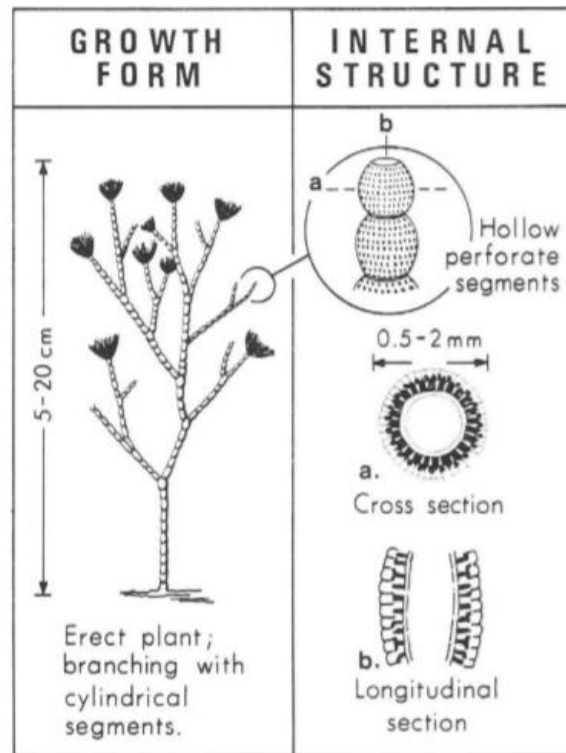


Figure 12: Growth form and internal structure of Dasycladaceae (taken from Wray, 1977, in Haq & Boersma, 1998).

Dasycladal assemblages are useful for regional biozonations (Bucur, 1999; Flügel, 2010). In addition, they allow differentiation of the paleoenvironments of various parts of platforms i.e. intertidal, supratidal, slope etc (Flügel, 2010).

### 1.6. Study area

The selected outcrops studied in this study are located (from north to south) near the villages of Qehmez, Ain Dara, Azzounyie, Barouk and Jezzine. All these localities are in central Mount Lebanon where the Lower Cretaceous rock formations are well exposed (Fig. 13).



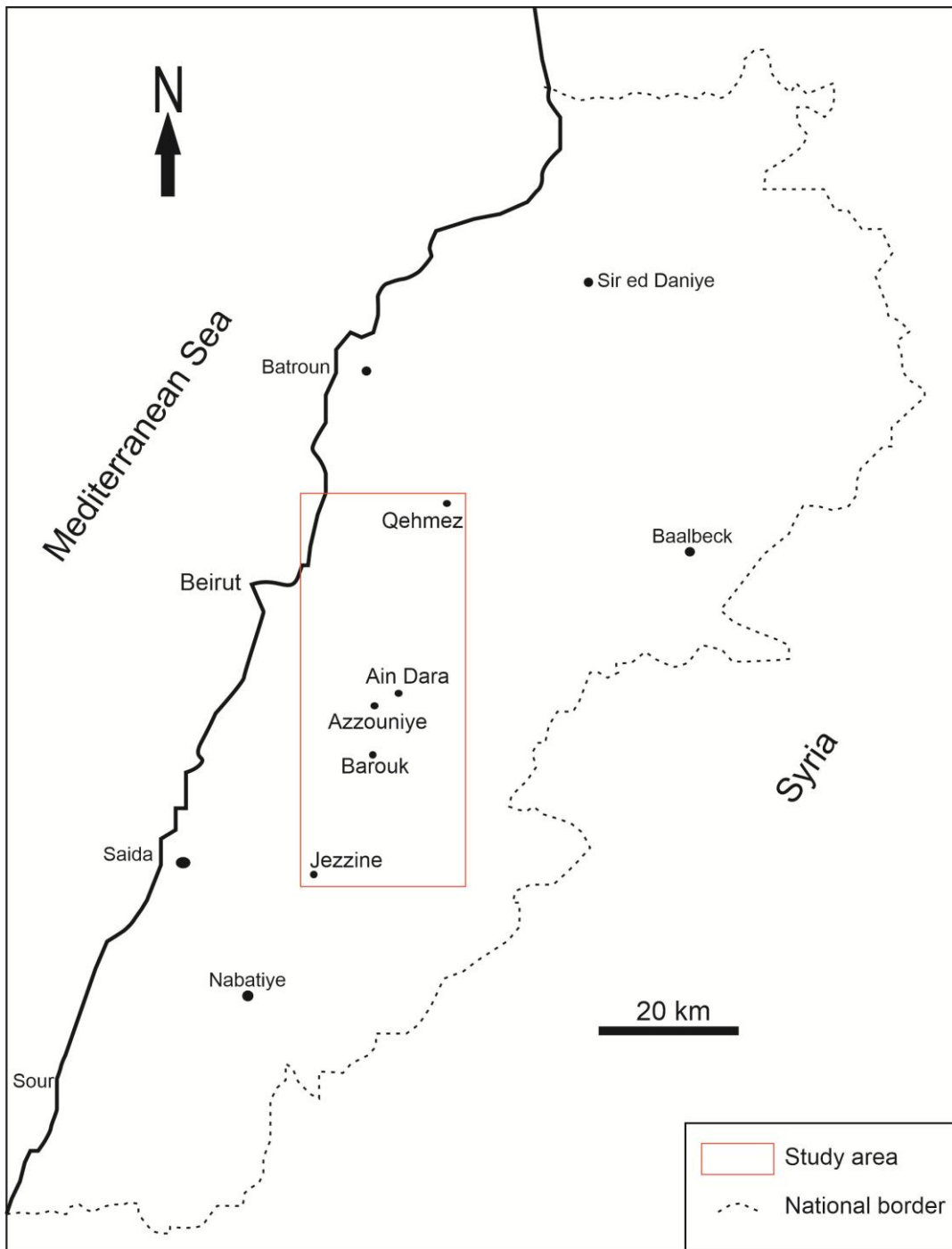


Figure 13: Geographic map of Lebanon showing the studied area in central Mount Lebanon. Studied outcrops are located near the villages of Qehmez, Ain Dara, Azzouniye, Barouk, and Jezzine.

## CHAPTER 2

### METHODOLOGY

#### **2.1. Field work**

##### **2.1.1. *Planning***

The first step considered for the fieldwork was the previous review of geologic maps and bibliography. Each fieldtrip performed in the Mount Lebanon was carefully planned several days before hand. Geologic and geographic maps were studied in order to find the best outcrops for the study. Previous scientific publications about lower Cretaceous rocks of the area were also consulted. Geological maps of Dubertret (1955) were used to choose the best localities where the the Chouf and Abeih formations outcrop. Geographic and geological maps of the selected localities were prepared (marking the boundaries between lithological units) in addition to the equipment required for field investigation i.e. Jacob staff, geological hammer, magnifying lens, Global Positioning Pystem (GPS), etc.

##### **2.1.2. *Field techniques and equipments***

A general sedimentological/stratigraphical approach at each outcrop/section was first performed with the aim to describe the facies. At the base of each section, GPS coordinates were recorded in order to better locate the outcrops on the maps. Stratigraphic logs were then constructed using the Jacob staff, a Brunton compass

and a meter with the aim to measure the thickness of the studied beds (Fig. 14). The stratigraphic sections were first drawn on a graphic paper (notebook) providing all the stratigraphic and sedimentary information (facies type, color, bed geometry and fossil content). Later the sections were digitized using CorelDRAW 2018 software.



Figure 14: Jacob staff used to measure the thickness of beds (Barouk section).

Sedimentological analysis was carried out during the field work taking notes and photos to each stratum. Detailed *in situ* analyses of each interval were performed using a magnifying lens. Thus, many parameters such as the composition, grain size, sorting, grain roundness, grain sphericity and presence of microfossils were considered and noted. Soft samples for microfossils were collected mainly from marl or silty marl beds. Two kilograms of sediments were collected in appropriately numbered plastic bags in order to obtain a representative number of microfossils (Fig. 15).



Figure 15: Field photo from the top of the Barouk section. About 2 kg of sediments were extracted for the sample B7.

Hard samples for thin sections were mainly extracted from hard intervals (limestone beds). During the extraction of these samples the stratigraphic position was considered in each sample marking an arrow on it. Each sample was labeled using the first letter of the locality followed by a number. For example, in the case of the stratigraphic section raised in Jezzine the abbreviations J1, J2, J3, etc, were (Fig. 16).

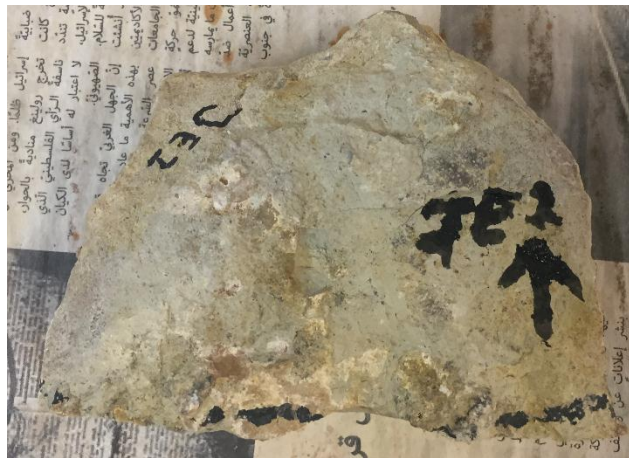


Figure 16: Hard limestone sample collected from Jezzine section 2.

## 2.2. Laboratory work

### 2.2.1. *Soft samples treatment*

A total of 33 soft rock samples were collected from the surveyed sections. The procedure used in this study follows the treatment explained by Feist et al. (2005). Each soft rock sample was first placed in a plastic container and mixed with water, 50 g of sodium carbonate ( $\text{Na}_2\text{CO}_3$ ) and 300 ml of 30 % hydrogen peroxide ( $\text{H}_2\text{O}_2$ ). The mixture was left for a period of time ranging between 2 and 5 days (Fig. 17). Samples were stirred several times a day to ensure a better disaggregation.



Figure 17: Sample preparation A: Chemicals used during the soft sample treatment (hydrogen peroxide and sodium carbonate), B: solution of the sample soaked with water and chemicals.

### 2.2.2. *Sieving process*

Disintegrated samples were later poured into a sieve column composed of 5 meshes with different mesh apertures i.e. 2 mm, 850  $\mu\text{m}$ , 600  $\mu\text{m}$ , 354  $\mu\text{m}$ , and 250  $\mu\text{m}$ . Using running tap water samples were washed (Fig. 18). In order to avoid fossil/grain contaminations between samples, the sieves were stained using a solution of water and methylene blue powder.

Each sample was washed thoroughly to eliminate the muddy material while the remaining sediment fractions (leavigates) in each sieve (i.e. quartz grains, microfossils, amber etc.) were left on a cupboard to dry. Once dried, the leavigates were stored in plastic boxes for the later microfossil extraction (picking process).



Figure 18: Sieving process of the soft rock samples for microfossil extraction. This process was performed in the thin section lab (Geology Department, AUB).

### ***2.2.3. Microfossil extraction***

The microfossil extraction process requires time as well as a high visual and handling precision. For each sample, a small fraction of the leavigate was sprinkled over a picking tray and examined thoroughly for several minutes using a binocular microscope. Any encountered microfossil was picked out using a wet fine brush and stored in labeled individual cells (Fig. 19). This process was repeated several times for each leavigate (minimum 3 times) and for each sample.





Figure 19: Binocular microscope, light, picking tray, brush, and microfossil cells used to store and study the microfossils.

#### ***2.2.4. Scanning electron microscope***

Well-preserved microfossils were selected for the Scanning Electronic Microscope (SEM) study. First, the selected microfossils were cleaned using an ultrasound machine. Then, they were mounted on a circular stub with double-sided adhesive tape (Fig. 20). Several shells were selected for each species in order to study all the 3D microfossil features. The mounted stubs were placed in a sputter coater machine Quorum Q150T (Fig. 21) located at the Central Research Science Laboratory (CRSL) to cover the microfossils with an electrically conductive material (gold, platinum, silver or carbon). In this study, we used platinum and gold with a coating thickness of 20 nm.

After the coating process, stubs were placed in the SEM MIRA 3LMU with OXFORD EDX detector by TESCAN located in the CRSL to study the

microfossils. The SEM provides high resolution images of the microfossil characters and detailed structures.

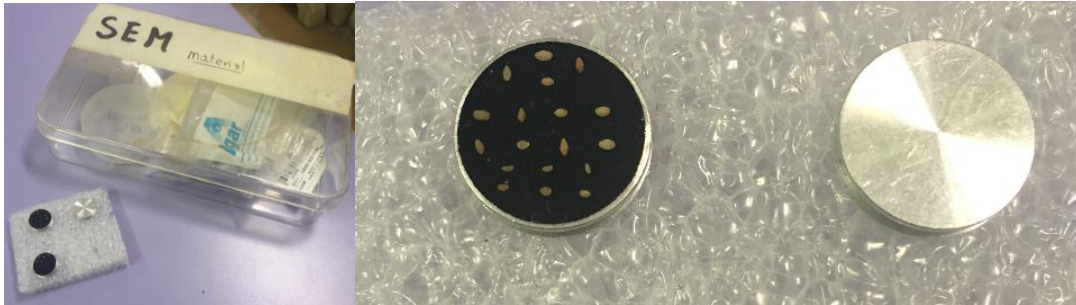


Figure 20: Material used during the SEM sessions (stubs and adhesive tape). Note the fossil ostracod shells orderly glued on the tape.



Figure 21: Sputter coater machine (Quorum Q150T).

Several images were taken for each specimen in order to study and measure its morphological parameters (Fig. 22). Afterwards, several digital plates were prepared in order to illustrate the recovered microfossils. These plates were created using the CorelDRAW 2018 software.





Figure 22: SEM MIRA 3LMU located in the Central Research Science Laboratory (CRSL) of AUB.

#### ***2.2.5. Thin sections preparation***

A total of 24 thin sections (representing 10 limestone rock samples) were prepared. Eleven samples were cut in the Barcelona University by Dr. Josep Sanjuan during the summer 2019. The remaining thin sections were prepared in the thin section lab of the department of Geology at AUB with guidance from Mr. Maroun Ijreiss, Dr. Joanna Doummar and Mr. Ahmad Azhari. The steps for the thin section preparation followed the processes of Doummar (2005).

The thin sections are later studied and photographed for microfacies analysis. Some photos were taken using stereomicroscope Motic BA310 with the integrated software Motic Images Plus 2.0 ML in the Barcelona University by Dr. Josep Sanjuan. Other images were taken using a ML 9000 Meiji Techno Co. Ltd in the Geology department at AUB.

## CHAPTER 3

### SEDIMENTOLOGY

Nine stratigraphic logs were raised in well exposed slopes in central Lebanon cutting the upper part of the Chouf and the complete Abeih formations. The studied sections are located in the following localities from north to south: Qehmez (Qehmez section 1 and Qehmez section 2), Ain Dara section, Azzouniye (Azzouniye section 1 and Azzouniye section 2), Barouk (Barouk section 1 and Barouk section 2) and Jezzine (Jezzine section 1 and Jezzine section 2).

Table 1: List showing the elevations above sea level (asl), GPS coordinates at the base and top and thicknesses of the studied sections.

Section	Elevation asl (m)		Coordinates				Thickness (m)
	Base	Top	Base		Top		
Qehmez 1	1500	1548	34°3'8.4''N	35°47'24'' E	34°3'1.7''N	35°47'27''E	50
Qehmez 2	1548	1560	34° 3'0.6''N	35°47'27''E	34° 2'57''N	35°47'28''E	15
Ain Dara	1270	1288	33°47'41''N	35°43'36''E	33°47'37''N	35°43'33''E	26
Azzouniye 1	1106	1126	33°46'13''N	35°42'16''E	33°46'17''N	35°42'12''E	24
Azzouniye 2	1120	1137	33°46'7''N	35°42'14''E	33°45'53''N	35°41'48''E	54
Barouk 1	1198	1250	33°44'3''N	35°42'25''E	33°44'5''N	35°42'19''E	115
Barouk 2	1255	1278	33°44'3''N	35°42'25''E	33°44'4''N	35°42'12''E	17
Jezzine 1	1090	1136	33°32'47''N	35°33'45''E	33°32'29''N	35°33'45''E	98
Jezzine 2	1045	1083	33°34'12''N	35°33'53''E	33°34'15''N	35°33'59''E	22

### 3.1. Qehmez section 1

Qehmez section 1 is located 1.8 km southwest of the Qehmez village in Kesrouane district (Fig. 23). The detailed stratigraphic log of Qehmez section 1 is shown in Figure 24 and its description is listed in Appendix A (Table 1).

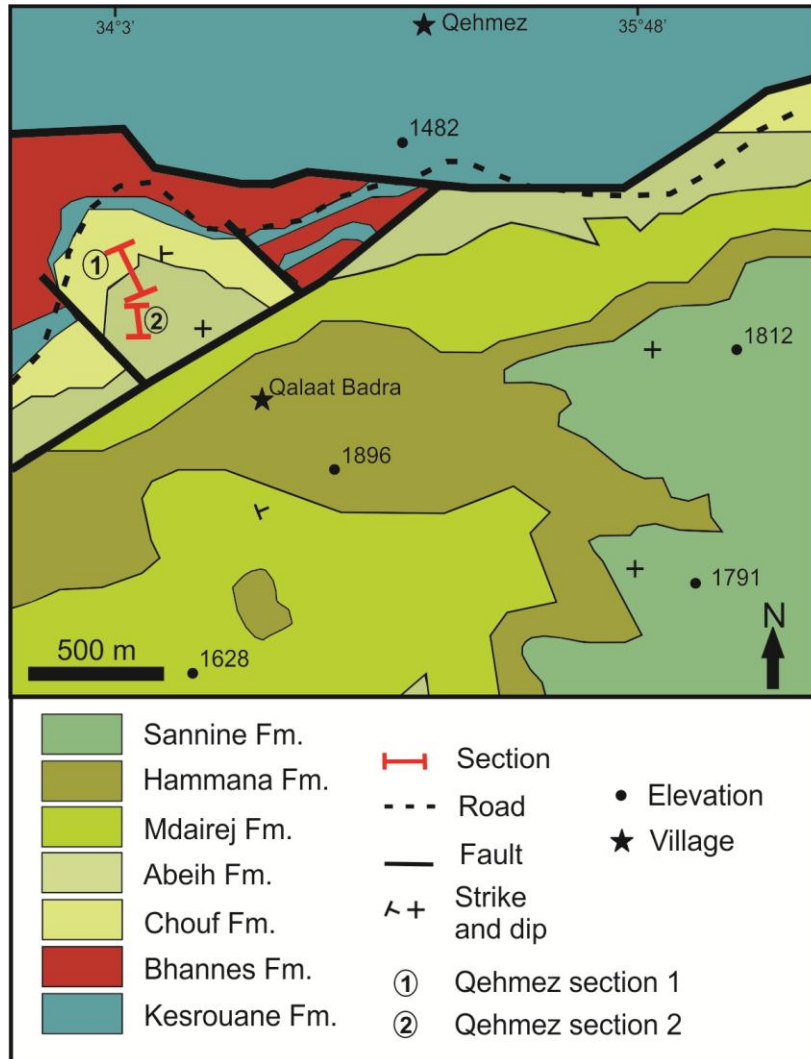


Figure 23: Geologic map of the Qehmez area showing the location of the two stratigraphic sections. Modified from Dubertret (1955).

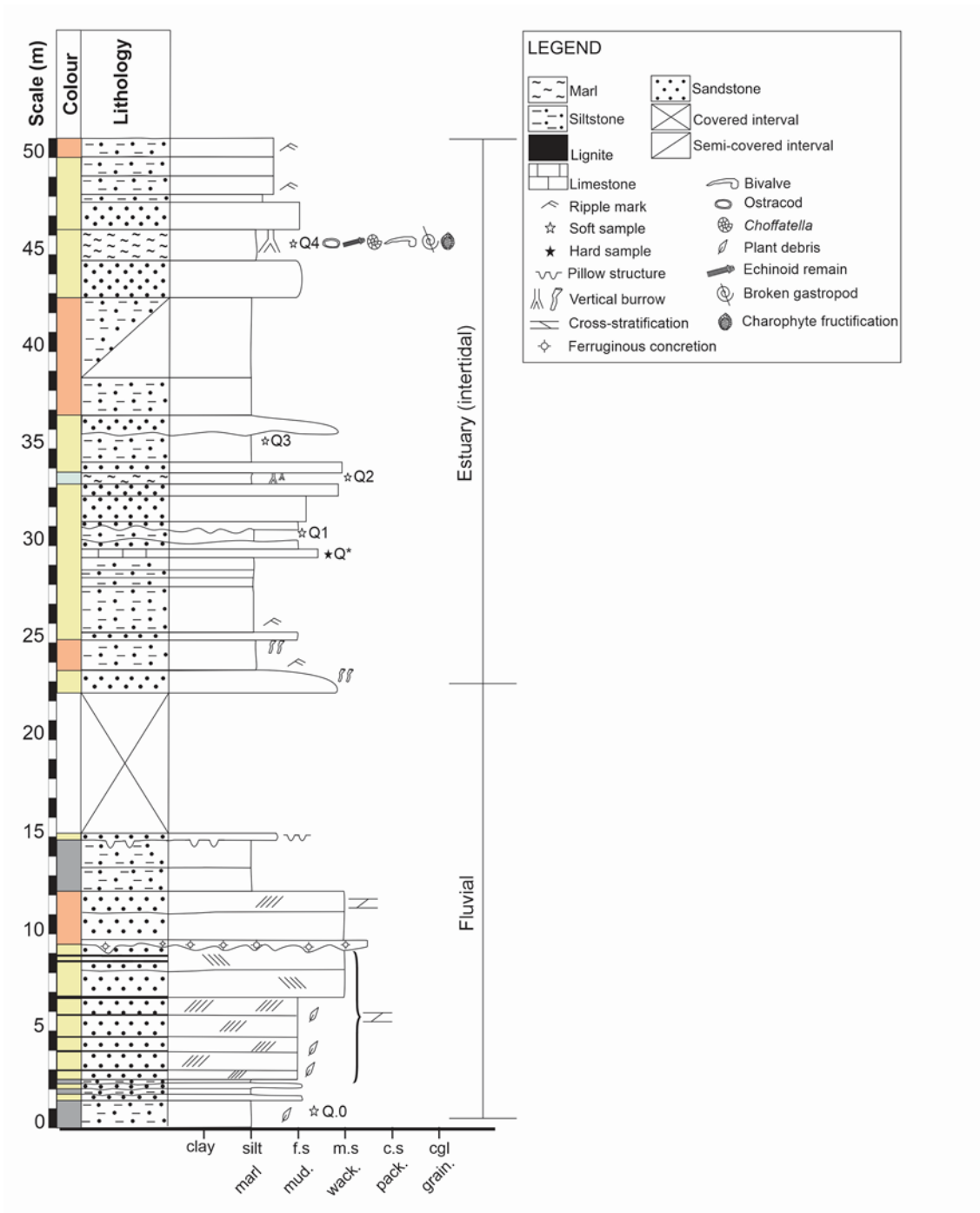


Figure 24: Stratigraphic log of the Qehmez section 1.

### 3.2. Qehmez section 2

The Qehmez section 2 represents the vertical continuation of Qehmez section 1 above a fault (Fig. 23). The detailed stratigraphic log of this section is shown in Figure 25 and its description is listed in Appendix A (Table 1).

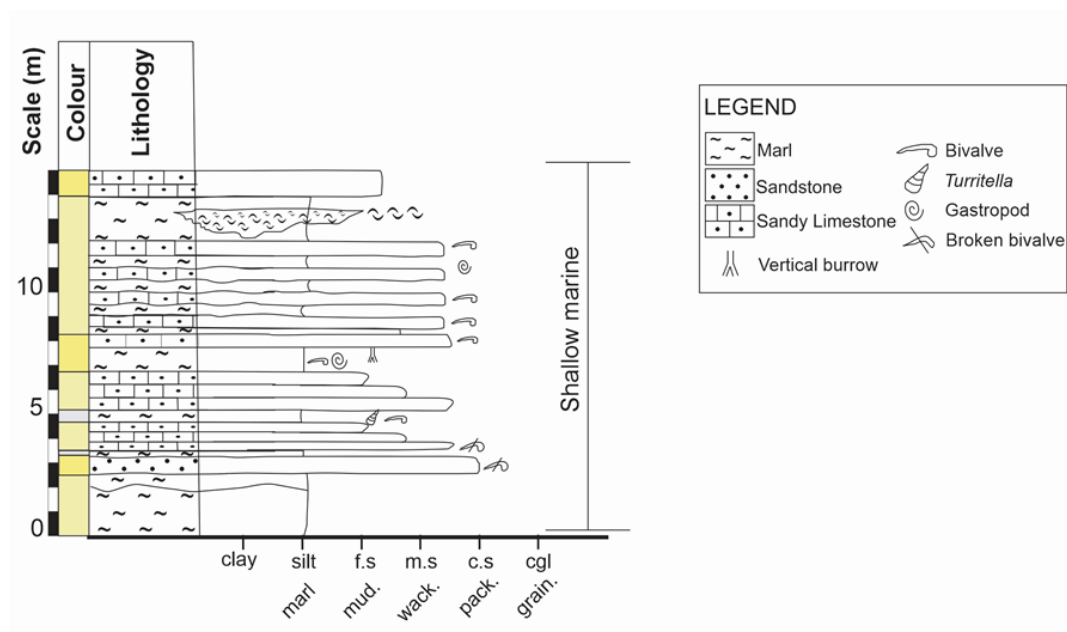


Figure 25: Stratigraphic log of the Qehmez section 2.

### 3.3. Ain Dara section

The Ain Dara section is located about 1.5 km north of the Ain Dara village in the Aley district (Fig. 26). The detailed stratigraphic log of Ain Dara section is shown in Figure 27 and its description is listed in Appendix A (Table 1).

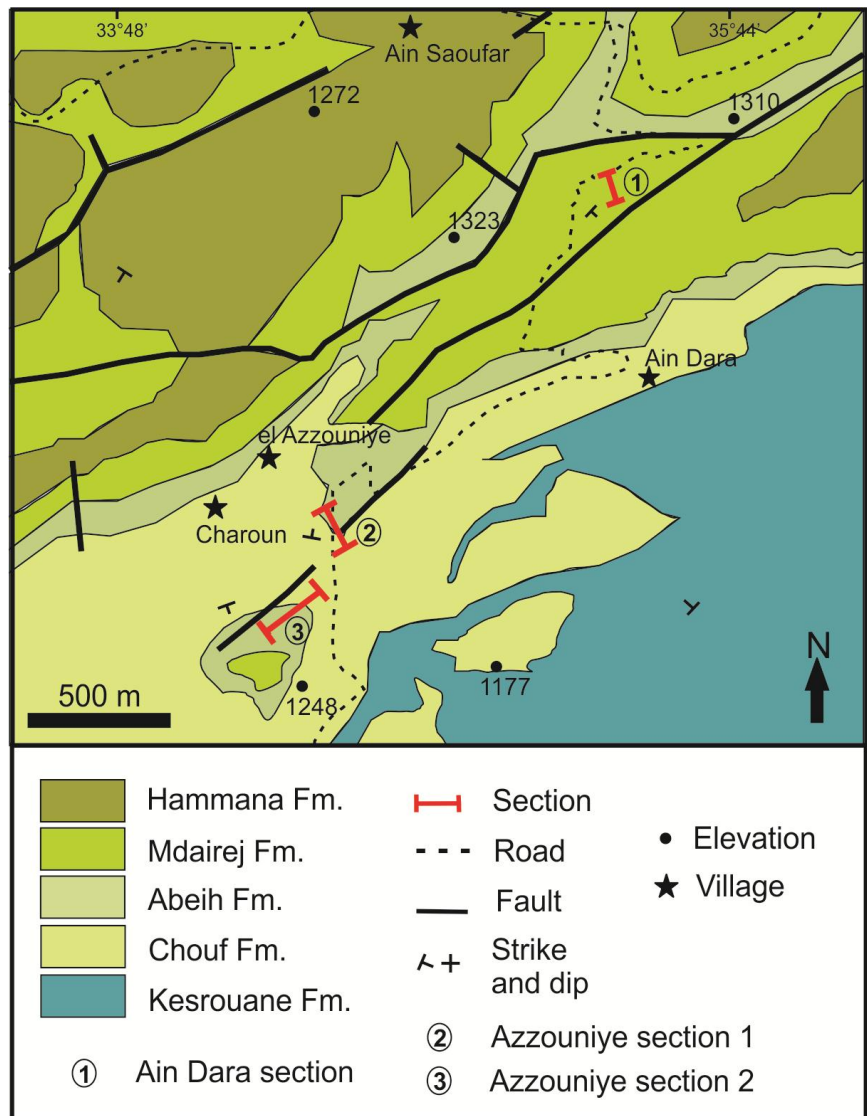


Figure 26: Geologic map of the areas of Ain Dara and Azzouniye showing the location of the three studied sections. Modified after Dubertret (1955).

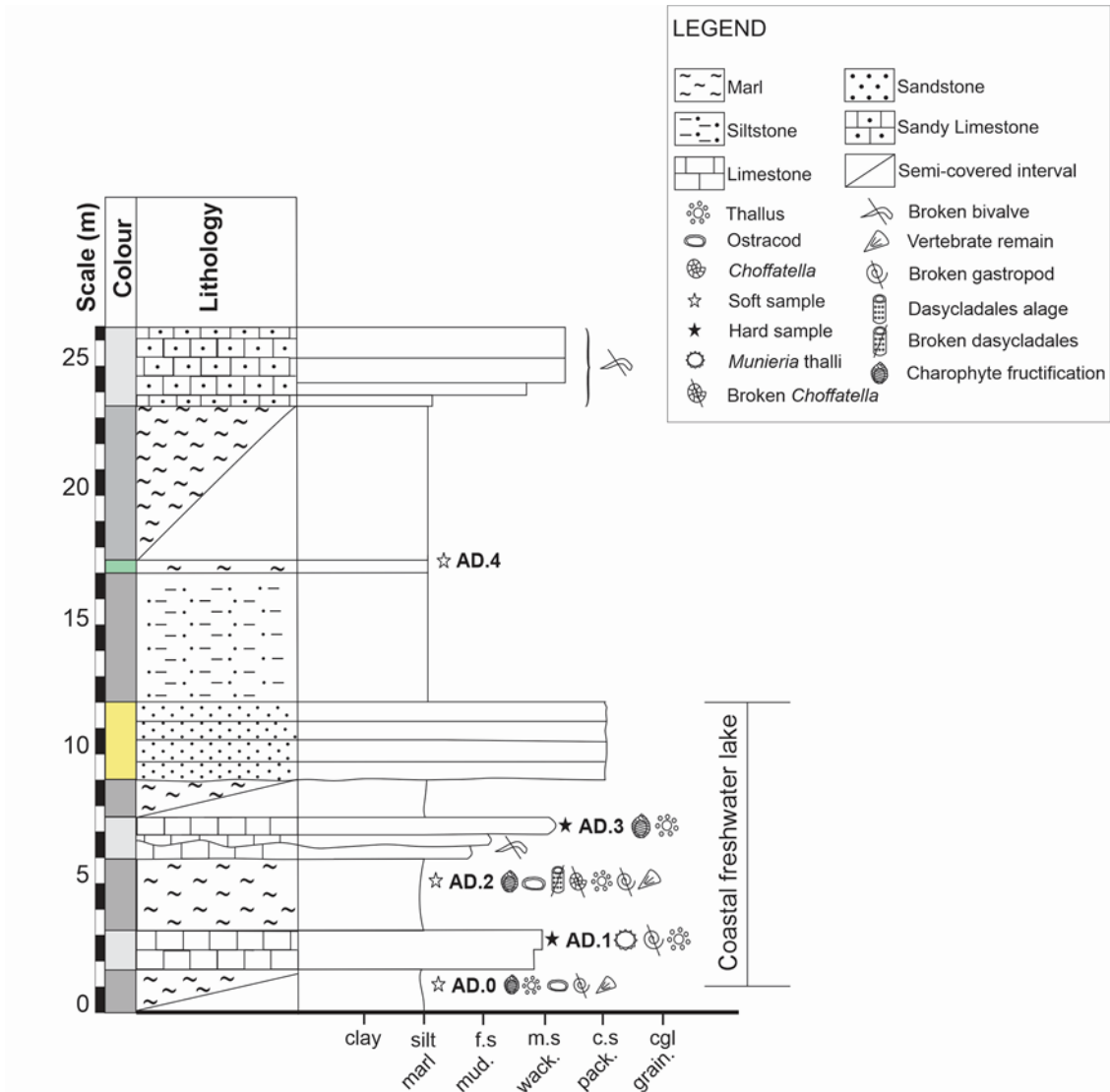


Figure 27: Stratigraphic log for Ain Dara section.

### 3.4. Azzouniye section 1

The Azzouniye section 1 is located about 0.3 km southwest of the Azzouniye village in Aley district (Fig. 26). The detailed stratigraphic log of Azzouniye section 1 is shown in Figure 28 and its description is listed in Appendix A (Table 1).

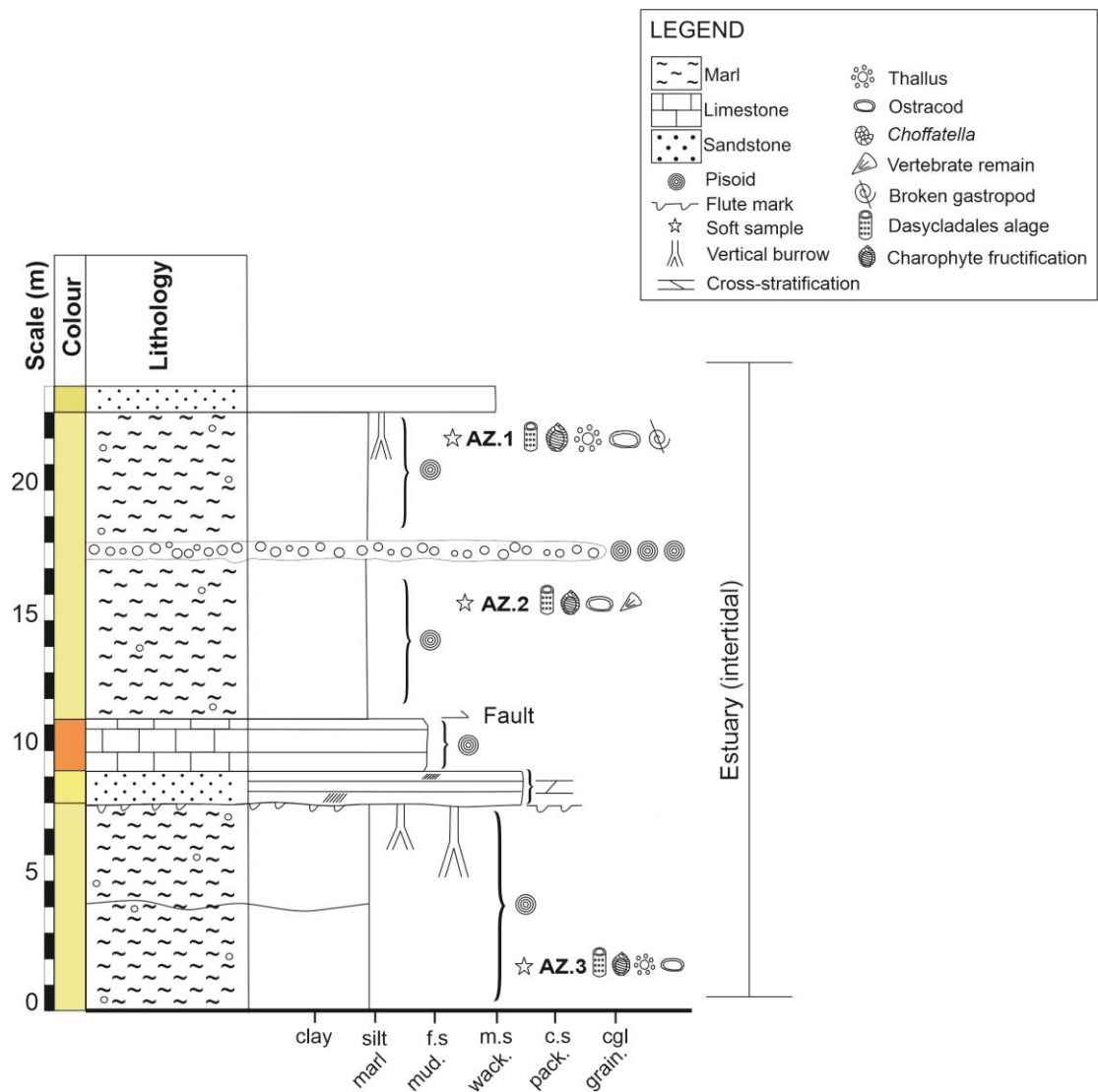


Figure 28: Stratigraphic log of the Azzouniye section 1.

### 3.5. Azzouniye section 2

The Azzouniye section 2 is located 0.3 km southwards and laterally equivalent to the previous section (Fig. 26). The detailed stratigraphic log of Azzouniye section 2 is shown in Figure 29 and its description is listed in Appendix A.



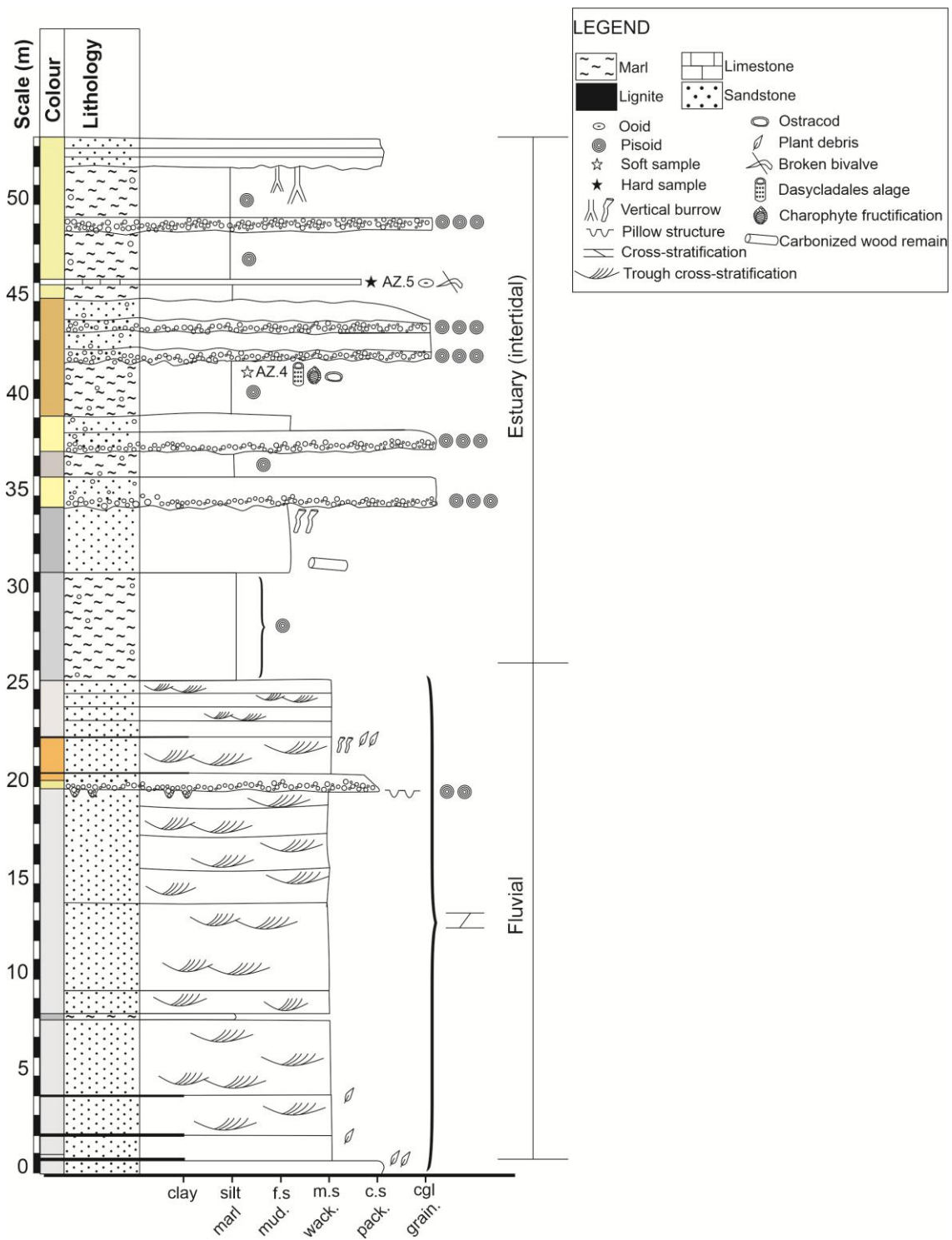


Figure 29: Stratigraphic log of the Azzouniye section 2.

### 3.6. Barouk section 1

Barouk section 1 is located at 1 km southeast of Ain Zhalta village near Barouk (Fig. 30). The detailed stratigraphic log of Barouk section 1 is shown in Figures 31 and 32 and its description is listed in Appendix A (Table 1).

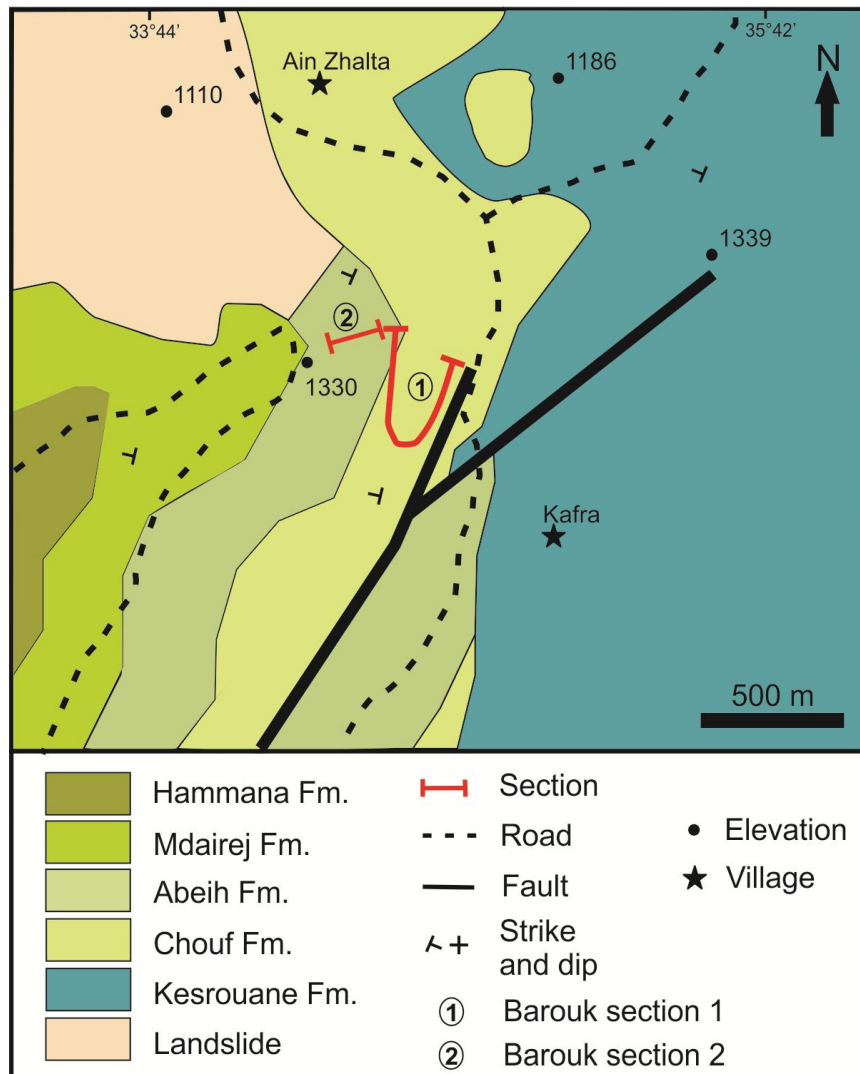


Figure 30: Geologic map of the area of Barouk showing the location of the two studied sections. Modified after Dubertret (1955).

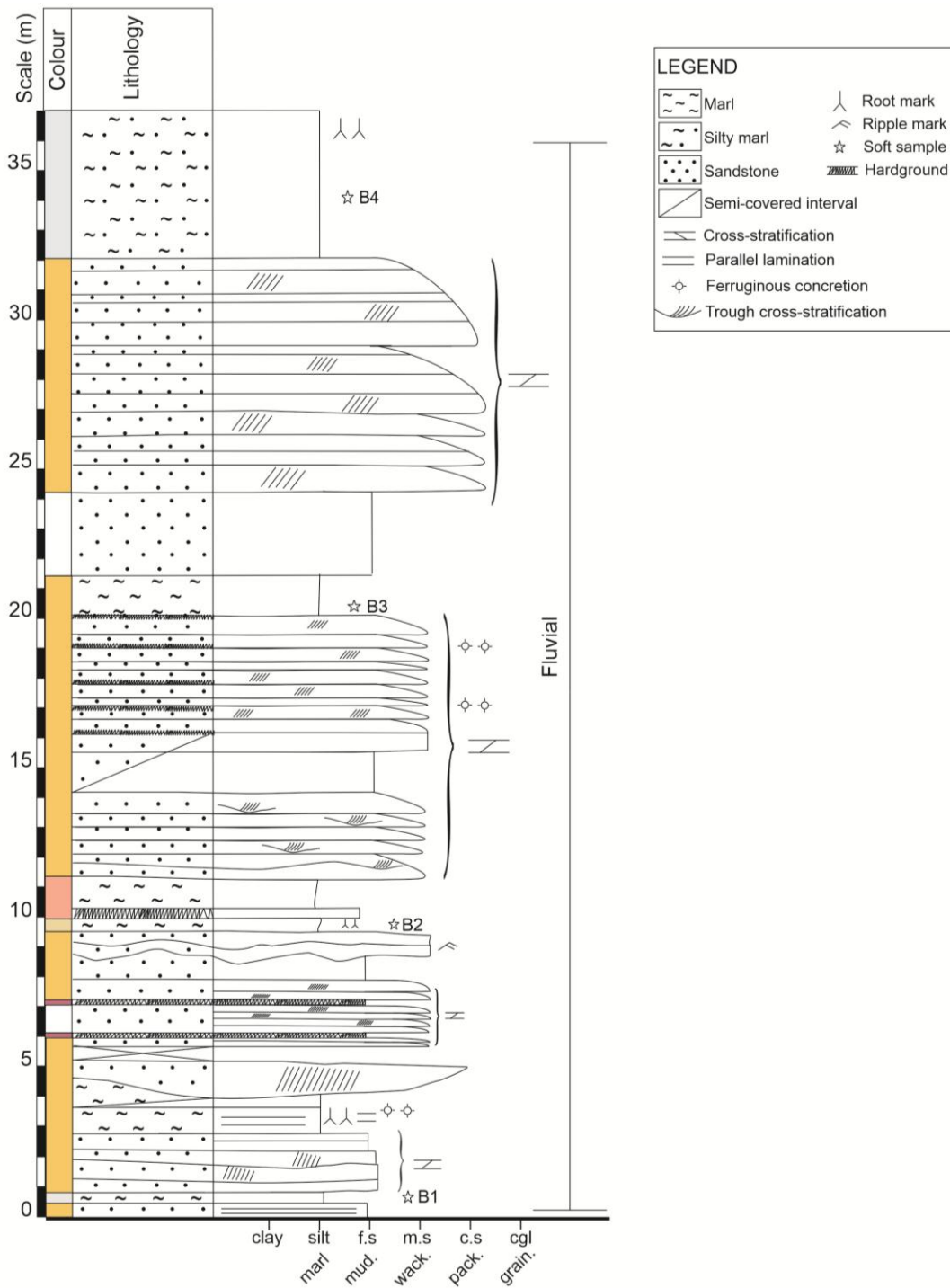


Figure 31: Stratigraphic log of the Barouk section 1 (base).

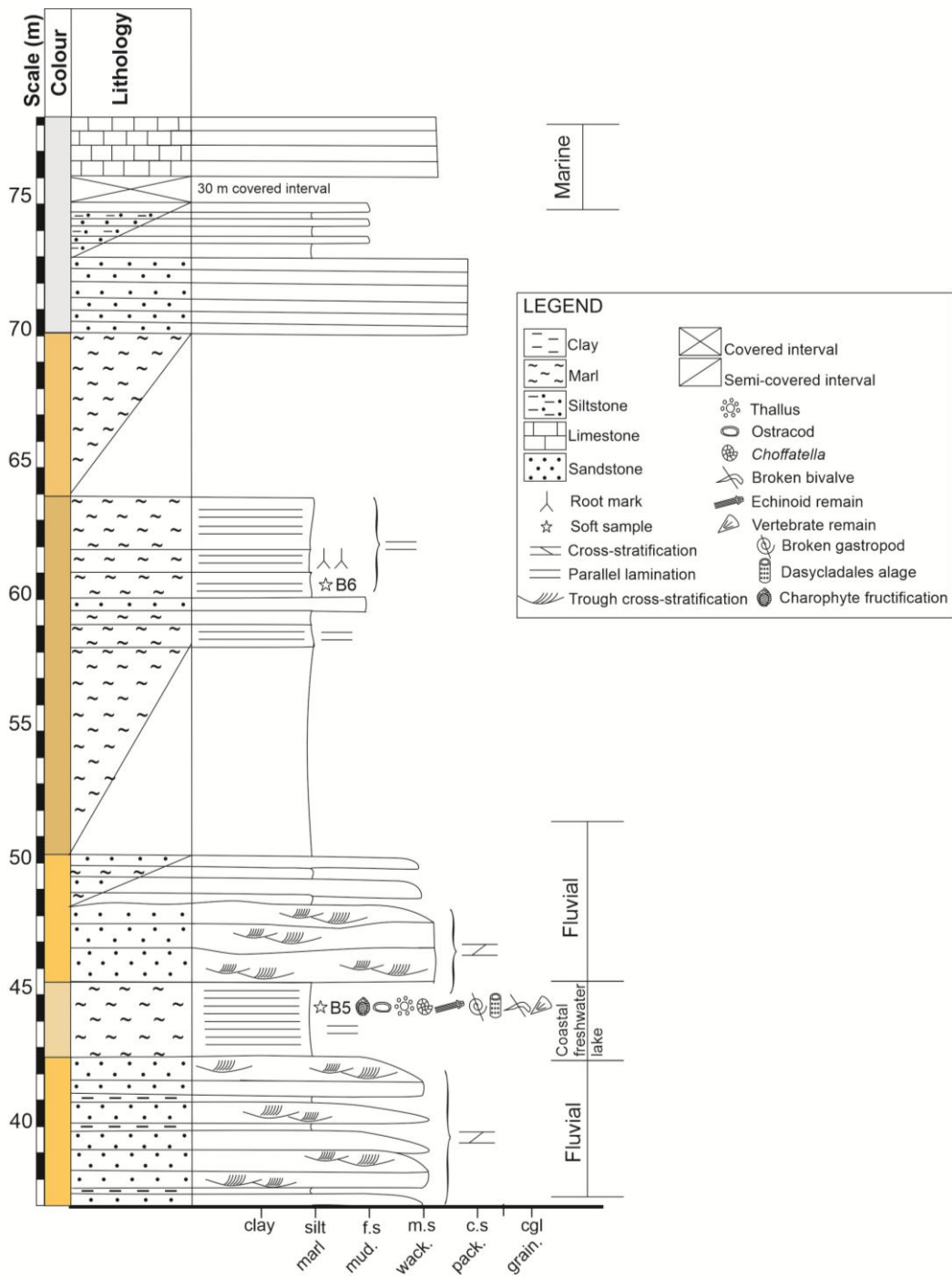


Figure 32: Stratigraphic log of Barouk section 1 (top).

### 3.7. Barouk section 2

This section is located about 1 km southeast of Ain Zhalta (Fig. 30). The detailed stratigraphic log of Barouk section 2 is shown in Figure 33 and its description is listed in Appendix A (Table 1).

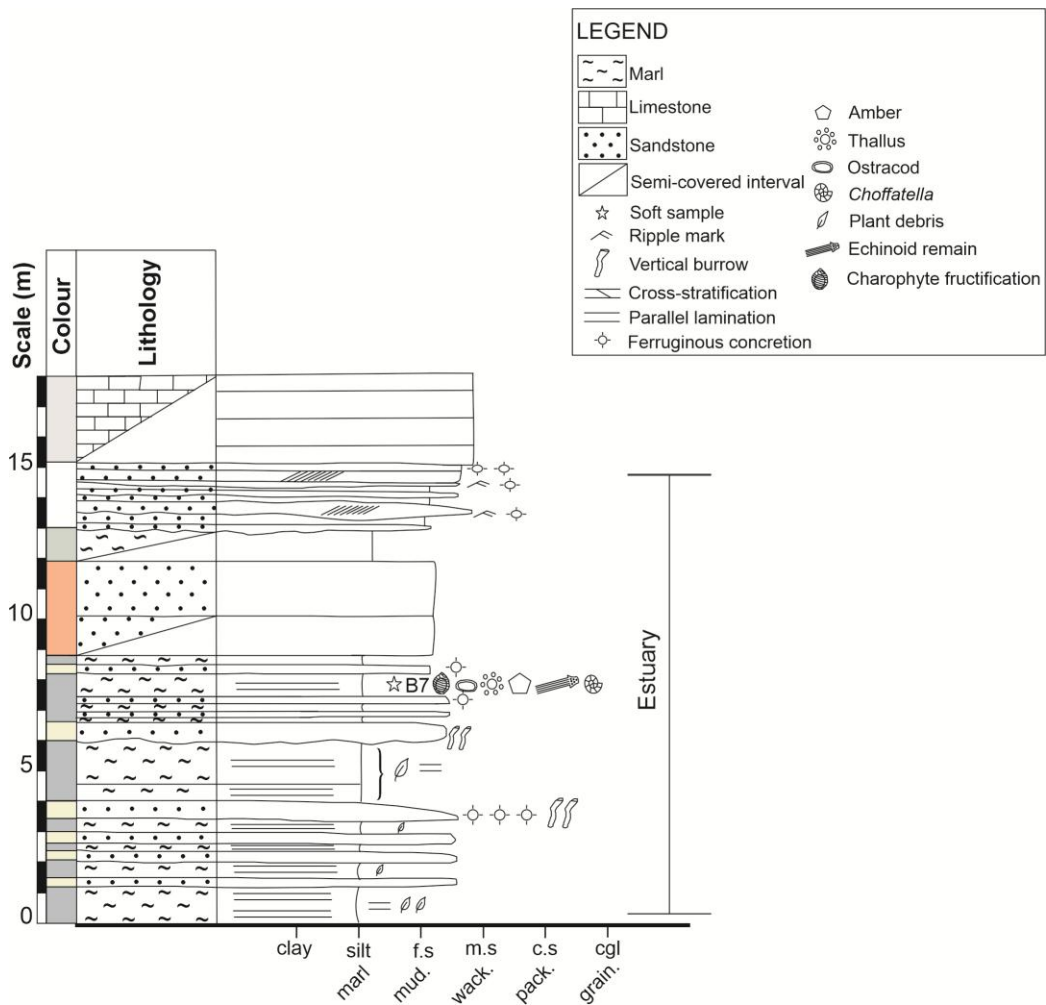


Figure 33: Stratigraphic log of Barouk section 2.

### 3.8. Jezzine section 1

Jezzine section 1 is located about 0.6 km east of Homsiyeh village (Fig. 34). The detailed stratigraphic log of Jezzine section 1 is shown in Figures 36 and 37 and its description is listed in Appendix A (Table 1).

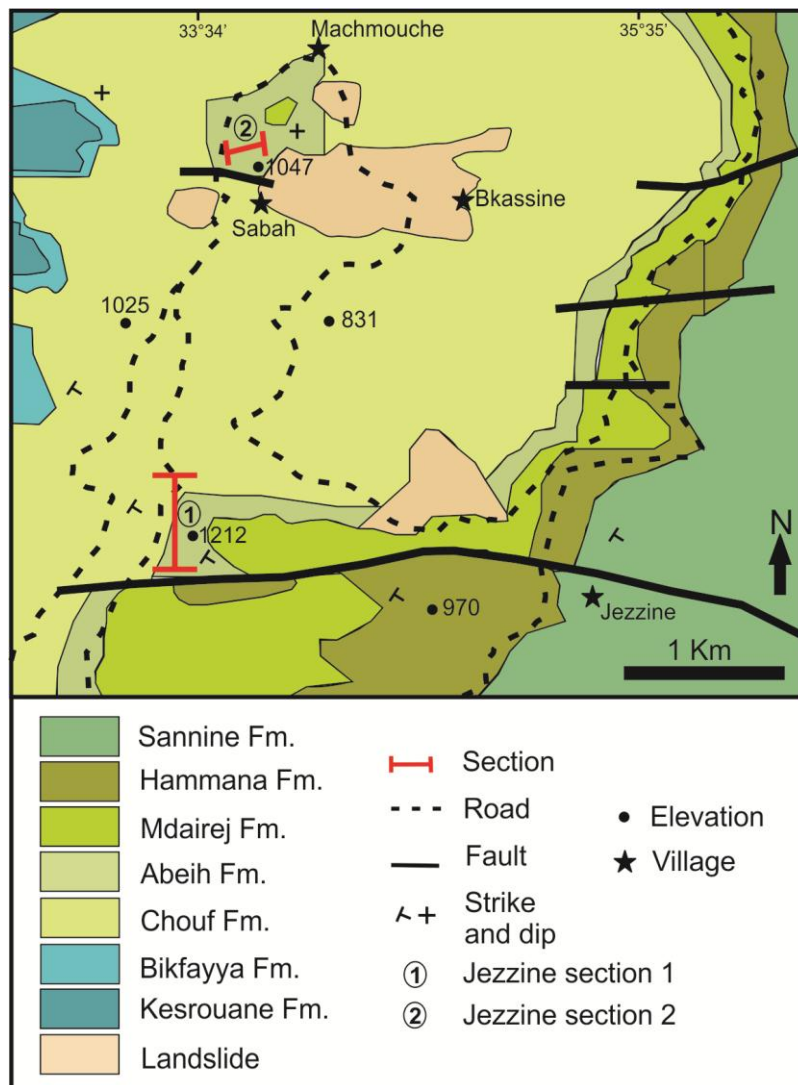


Figure 34: Geologic map of Jezzine area showing the location of the two stratigraphic sections. Modified from Dubertret (1955).

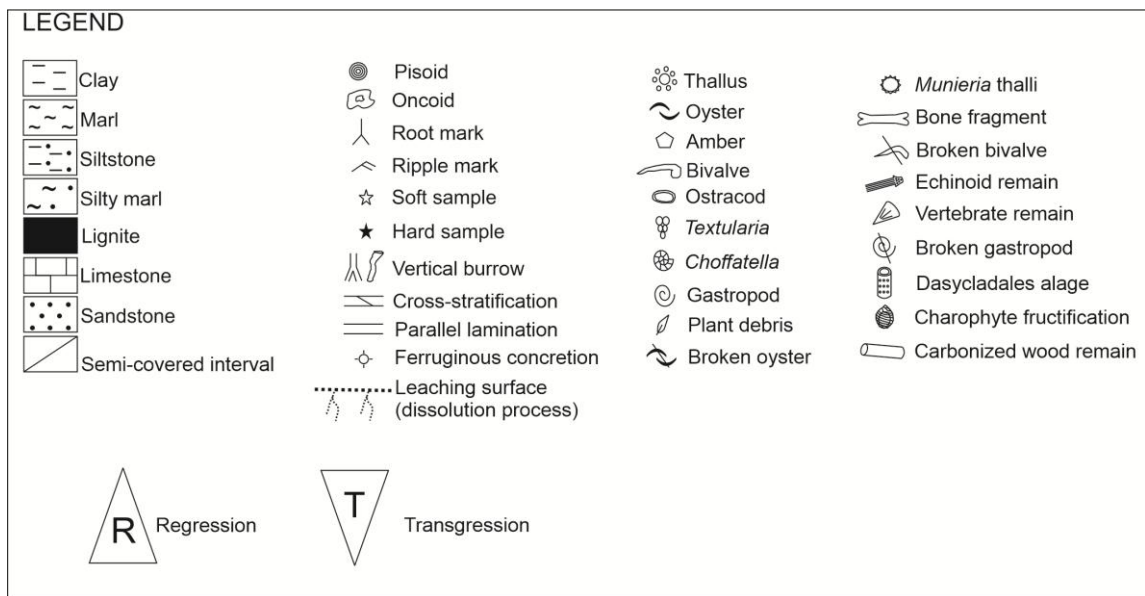


Figure 35: Legend for the Jezzine section 1 stratigraphic log.



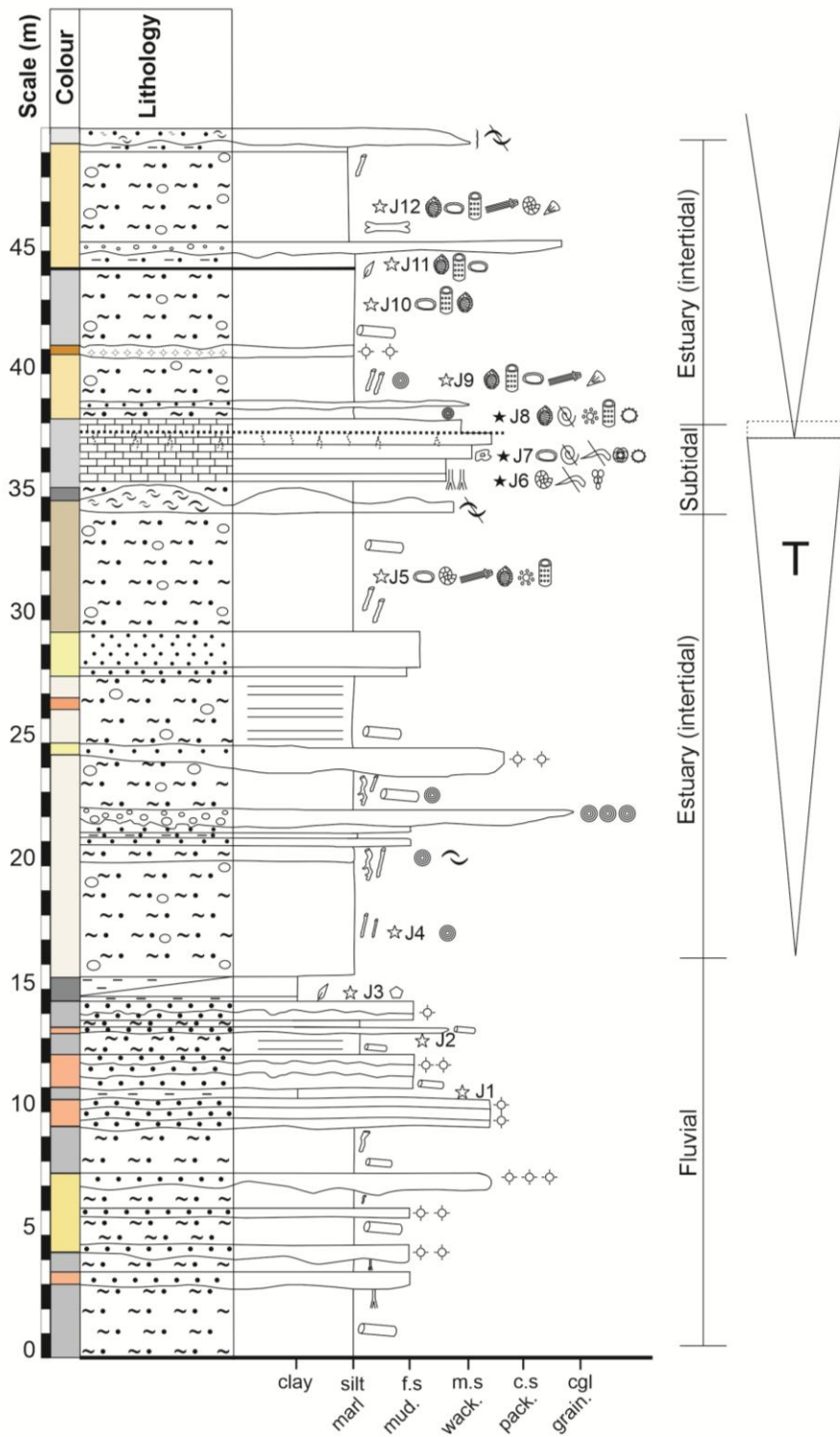


Figure 36: Stratigraphic log of Jezzine section 1 (base).



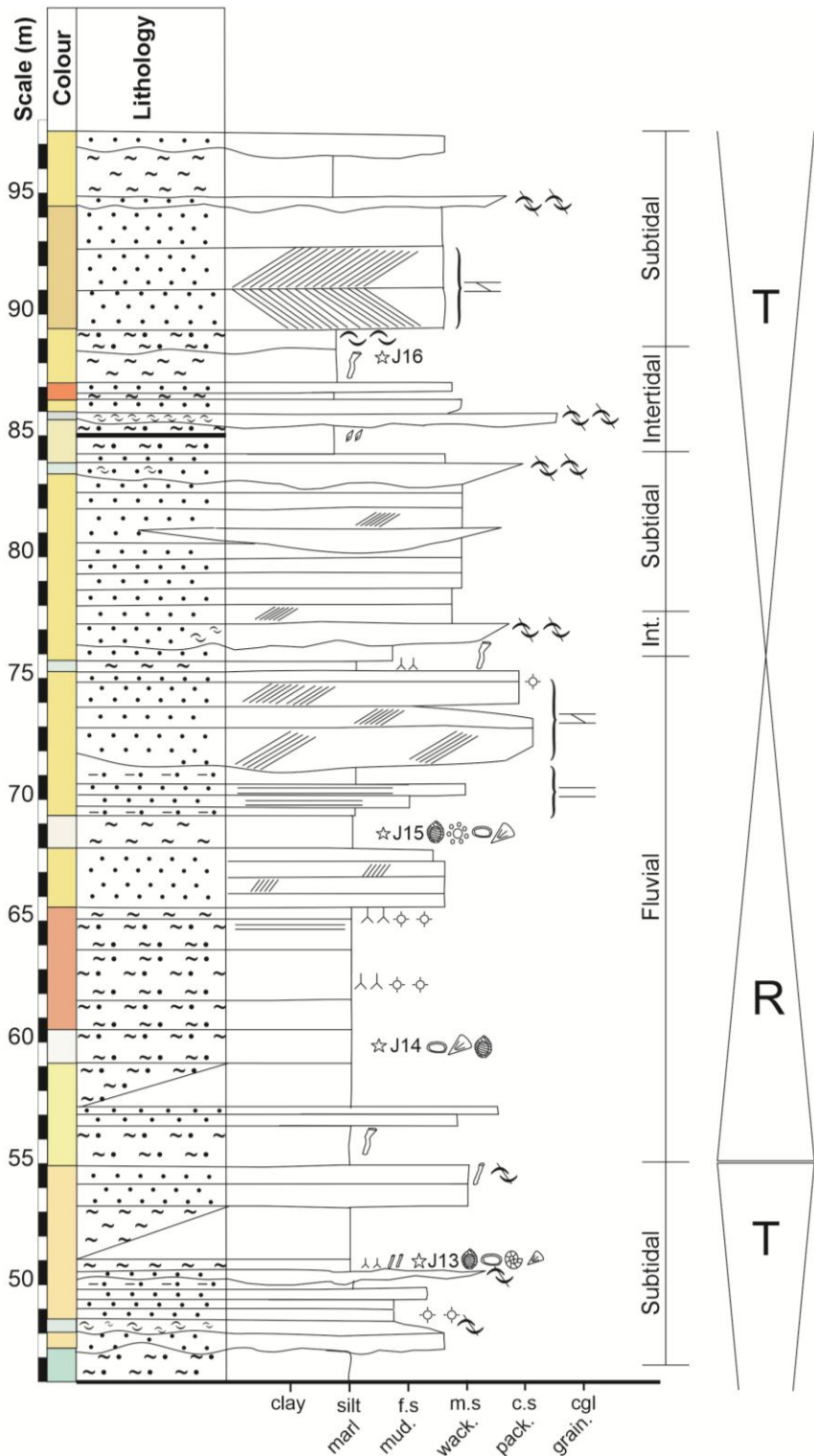


Figure 37: Stratigraphic log of Jezzine section 1 (top).

### 3.9. Jezzine section 2

The section is located 0.2 km North of Sabah Village, 0.5 km southeast Deir Machmouche (Fig. 34). The detailed stratigraphic log of Jezzine section 2 is shown in Figure 38 and its description is listed in Appendix A (Table 1).

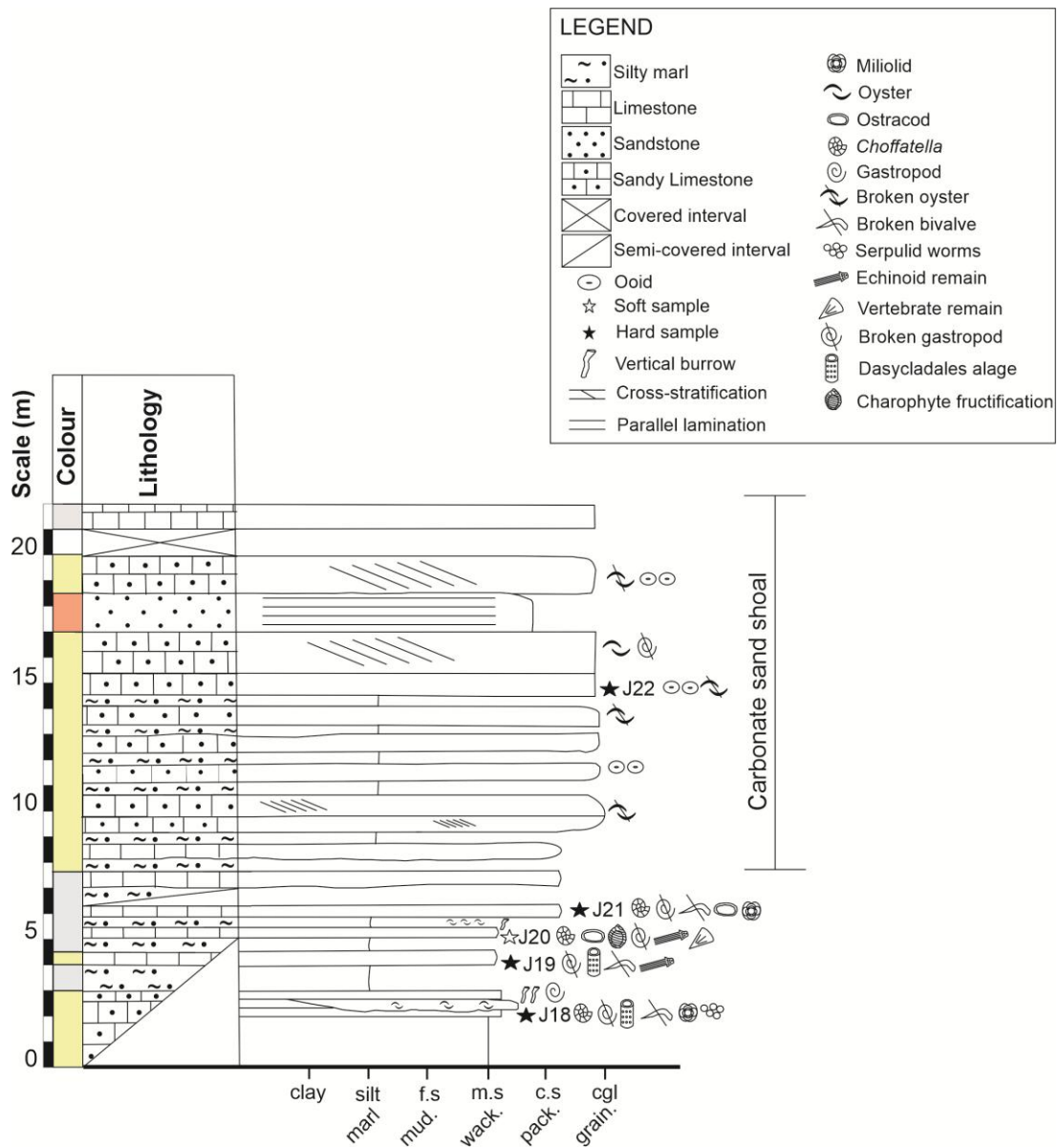


Figure 38: Stratigraphic log showing the Jezzine section 2.

## CHAPTER 4

### FACIES ASSEMBLAGES AND INTERPRETATION

#### 4.1. Fluvial

These facies assemblages are basically composed of poorly to moderately sorted cross-bedded quartz arenite beds alternated with reddish siltstone and clay intervals occurring mainly in the Barouk section 1, the base of the Qehmez section 1, the lower part of Azzouniye section 2 and upper part of Jezzine section 1 (meter 70-75). Two types of subenvironments can be identified (Table 2):

##### 4.1.1. *Channel fill*

This facies assemblage is characterized by the moderately sorted, coarse to medium quartz arenite beds showing cross bedding and low incision erosive bases. Quartz arenite beds generally display a fining upward grain size. These beds can be related to migration of subaquatic sandbars in a river channel. In Barouk section 1, sandstone strata display short lateral extension and marked erosive bases. The absence of gravel size particles and the low incision erosive bases of sandstone beds indicate that these deposits were formed under low flow regime conditions and far from the source area (Boggs, 2014). In the Qehmez and Azzouniye sections, quartz arenite beds occur intercalated with lignite lenses. Lignite lenses contain leave cuticles and carbonized wood remains. No edaphic features can be distinguished at

the base of these lenses suggesting that plant debris were transported and deposited filling the channels.

#### **4.1.2. Floodplain**

This assemblage is characterized by reddish claystone intervals with edaphic structures alternated with fine sandstone layers showing parallel lamination. Clay and silt deposits indicate sedimentation of the suspended load during periods of channel overflow (Flügel, 2010; Boggs, 2014). The presence of rizolites suggests that thin soils formed in the floodplain.

The vertical stacking of the fining upward quartz arenite successions separated by clays and paleosols indicates the shifting and migration of river channels. Most of fluvial deposits show a poor to moderate sorting. Commonly, they show a unidirectional paleocurrent direction (Boggs, 2014).

#### **4.2. Coastal freshwater lakes**

This facies assemblage is well represented in the Ain Dara section. Intervals related to coastal freshwater lakes can also be observed in the upper part of the Jezzine section 1 (meter 55-70) and Barouk section 1 (top). This facies assemblage is composed of marl/silty marl and limestone (wackestone/packstone) beds rich in charophyte remains (Table 2). Charophyte fructifications (utricles and gyrogonites) do not show any evidence of fragmentation or erosion and they occur in association with fragments of thalli. These taphonomical evidences suggest that fossils were

buried *in situ* or after short transport. The microfacies type and the presence of a diverse charophyte flora in both marl and limestone beds in Ain Dara indicate that relatively quiet, shallow, well-oxygenated and well-illuminated freshwater lakes prevailed in the area (Gierlowski-Kordesch, 2010). Marl and limestone deposits occur alternated with sandstone beds with erosive bases related to fluvial facies suggesting that these lakes were located adjacent to the river system. The coastal location of these lakes can be inferred based on other rare microfossils. Few bad preserved shells of foraminifera and dasycladal fragments also occur within the marl intervals indicating that they were subjected to occasional marine sediment inputs probably during storm events.

### **4.3. Estuary**

Estuary facies assemblages are the dominant type in most of the studied sections (Jezzine 1, upper part of Qehmez 1, Barouk 2, Azzouniye 1 and the upper part of the Azzouniye 2) (Table 2). These facies assemblages are very well represented in the Jezzine section 1 where 3 transgressive hemicycles and one regressive hemicycle can be detected based on the vertical succession of facies and microfossil content (Figs. 90 & 91).

#### **4.3.1. Intertidal zone**

The intertidal zone lies between mean high and low tide levels. This zone is subaerially exposed twice each day and it does not support significant vegetation.

Both bed load and suspension sedimentation take place in this zone (Boggs, 2014). Studied facies assemblages representing this zone in Jezzine comprise the pisolitic conglomerate beds, burrowed silty marl beds with pisoids, organic-matter rich marl horizons and oyster banks. These facies can be grouped in three main sub-environments i.e. intertidal channels, burrowed mudflats/lagoon and oyster reefs.

#### 4.3.1.1. Intertidal Channels

It is represented by the pisolitic conglomerate intervals. Pisoids form in subaqueous environments by the precipitation of calcium carbonate around nuclei in an energetic environment normally related to marginal environments (Gierlowski-Kordesch, 2010). The presence of pisoids suggests that warm water conditions, saturated in carbonate prevailed in the depositional environment. Esteban and Pray (1983) indicated that pisoids may be generated in shallow subtidal, intertidal to supratidal environments. Large pisoids from the Jezzine section 1 may display imbrication fabrics and erosive bases suggesting that they were accumulated filling low incised channels or coastal plains where they rolled back and forth due to the tidal or wave currents.

#### 4.3.1.2. Intertidal burrowed mud flats/lagoon

These facies are represented by burrowed silty marl beds showing dispersed pisoids alternated with few dark organic-matter rich clay horizons. The abundance of quartz grains in this facies indicates that the estuary was subjected to continuous

terrigenous sediment input. Extensive bioturbation structures characterize this facies, suggesting that original intertidal facies (lenticular stratification or flaser bedding) were obliterated by the organism activity mixing the coarser (sand and pisoids) and finer (marl and clay) sediment horizons. Otherwise, the absence of these structures can be related to the presence of permanently flooded restricted areas with little tidal effect. Bioturbation structures consist of large vertical burrow casts, sometimes branching downwards. Dominant burrow structures may be related to the *Psilonichnus* genus produced by crabs of the family Ocypodidae (Buatois & Mángano, 2012). This type of ichnotaxa has been traditionally linked to transitional environments with remarkable variations in energy, grain size, and salinity. Moreover, it is associated with subaerial exposure and periodic influx of freshwater (Buatois & Mangano, 2012). However, further studies should be performed in order to better classify this ichnotaxon. Rich microfossil assemblages composed of fresh/brackish water related organisms (charophytes and ostracods) and marine taxa (dasycladals, foraminifera and echinoids) were identified in this facies suggesting that salinity fluctuations prevailed in the permanently flooded areas of the estuary. The presence of large wood and bone fragments as well as abraded microfossils indicates that these remains were transported from their original thriving locations as a consequence of the current activity. Few organic-rich clay horizons containing vegetal debris were detected intercalated within the silty marl beds. Occasionally, thin lignite lenses can be observed. Wood fragments, amber pieces and leaf cuticles occur at the base and top of these lignite horizons. However, the absence of edaphic

structures underlying these horizons suggests that plant debris were transported and accumulated in restricted areas under prevailing anoxic conditions.

#### 4.3.1.3. Oyster Reefs

At least 7 oyster banks were detected in the Jezzine section 1. Oysters normally grow in very shallow brackish to marine environments often in intertidal and subtidal contexts (Flügel, 2010). Oyster banks from Jezzine display a characteristic vertical succession. Shells located at the base of each bank are fragmented showing imbrication structures. In contrast, shells at the upper part of bank are complete and arranged in “living position”. This vertical change of facies can be related to environmental variations with regards to water energy and depth. Hence, environmental conditions changed from agitated (tractive) currents probably related to tides to more flooded conditions which allowed oysters to grow *in situ* forming small reefs. Oyster reefs mark the change from the intertidal to subtidal zones.

#### 4.3.2. ***Subtidal zone***

The subtidal zone encompasses the part of the tidal area that normally lies below the low tide level. It is inundated with water most of the time and is normally subjected to the highest tidal current velocities (Boggs, 2014). Studied facies assemblages representing this zone have been observed at the top of the Jezzine section 1 (77-95 meter). This assemblage is composed of cross-bedded quartz



arenite and bioclastic sandstone beds showing fining upward grain size sequences and moderately incised erosive bases. Bi-directional dipping foresets related to herringbone structures can be observed in some intervals. Fragmented oyster shells showing imbrication fabrics are common in some beds indicating that these deposits were formed in subaquatic conditions under the mean low tide level. All these sedimentological characteristics suggest that sediments were subjected to tidal-current velocities transporting and depositing the bedload (mainly coarse to medium quartz grains and oyster shells) probably in tidal channels (Boggs, 2014).

#### **4.4. Shallow marine**

This environment is characterized by fossiliferous limestones beds (packstone and wackestone) located in Jezzine section 1 (between meters 35 and 38), and Qehmez section 2 (Table 2). Carbonate grains are dominated by bioclasts of mollusks, shells of agglutinated benthic foraminifera (*Choffatella* and *Textularia*) and dasycladal fragments. The wackestone/ packstone textures and the dominant carbonate grains suggest that sediments were deposited under a shallow, moderately energetic marine environment. This type of facies belongs to the Standard Microfacies Type 10 (SMF 10) i.e. *bioclastic packstones and grainstones with coated and abraded skeletal grains* of Flügel (2010). This type of microfacies indicates that dominant particles have been transported from high-energy to low-energy environments and there are characteristic of shelf lagoon with open circulation or open sea shelf (Flügel, 2010). The limestone strata in the Jezzine

section 1 contains few intervals rich in oncoids (rudstone of oncoids) suggesting a mix environment between shallow marine and subtidal.

#### **4.5. Carbonate sand shoal**

Carbonate sand shoals are formed by loose sand-size sediment in shallow warm water areas subjected to high energy. Carbonate grains are mainly ooids and shell fragments mixed with benthonic foraminifera which can be reworked by waves and tidal currents (Boggs, 2014). This type of facies has been detected at the top of the Jezzine section 2 where bioclastic packstone facies (containing benthic foraminifera, mollusk shell fragments and dasycladal thalli) occur alternated with oolitic grainstone beds showing low angle cross-bedding (Table 2). The microfacies assemblage and the sedimentary structures observed in the field indicate that these deposits were formed under waves or tide activity in shallow marine platform, banks and shelves. They form within the platform interiors and in inner and mid-ramps. This microfacies belongs to the Standard Microfacies Type 15 (SMF 15) i.e. *Oolite (commonly ooid grainstones but also oolitic wackestones)* of Flügel (2010).

Table 2: A summary of the facies description and their associated environment.

<b>Facies</b>	<b>Description</b>	<b>Sections</b>
Fluvial (Channel fill and floodplain)	<b>Lithology:</b> Poorly to moderately sorted quartz arenite beds alternated with reddish siltstone and clay intervals, paleosols. <b>Structures:</b> tabular and trough cross-bedding, edaphic structures, parallel lamination, fining-upward.	Barouk section 1, the base of the Qehmez section 1, the lower part of Azzouniye section 2 and upper part of Jezzine section 1 (70-75 meter)
Coastal freshwater lake	<b>Lithology:</b> Marl/silty marl and limestone (wackestone/packstone) beds rich in charophyte remains.	Ain Dara section, upper part of the Jezzine section 1 (55-70 meter) and Barouk section 1 (top)
Estuary:  Intertidal    Subtidal	<b>Lithology:</b> Pisolitic conglomerate beds, silty marl beds with pisoids, organic-matter rich marl horizons and oyster banks. <b>Structures:</b> Channels, large burrows.  <b>Lithology:</b> quartz arenite and bioclastic sandstone (fragmented oyster shells) beds showing fining upward grain size sequences and moderately incised erosive bases. <b>Structures:</b> Cross-bedding, Herringbone structures, channels.	Jezzine 1, upper part of Qehmez 1, Barouk 2, Azzouniye 1 and the upper part of the Azzouniye 2
Shallow marine	<b>Lithology:</b> Fossiliferous limestones beds (packstone and wackestone)	Jezzine section 1 (35-38 meter), and Qehmez section 2
Carbonate sand shoal	<b>Lithology:</b> Bioclastic packstone facies alternated with oolitic grainstone beds showing low angle cross-bedding.	Jezzine section 2

## CHAPTER 5

## MICROPALEONTOLOGY

A diverse microfossil assemblage has been recovered from 18 samples of the studied sections (Table 3). Dominant groups of microfossils include charophyte and ostracod remains.

Table 3: List of microfossils and their relative abundance based on semi-quantitative visual estimation. All samples were collected in soft rocks (marls and silty marls) from the Abeih Formation (Walley, 1983) or Grès de Base (Maksoud et al., 2014).

Locality	Sample	Species	Charophytes			Ostracods						Foraminifera	Dasycladales	Teeth	Gastropods	Bivalves	Echinoid remains	
			Clavatoraceae	Characeae	Charaxis	Cyprideidae	Cytherideidae		Cytheruridae									
Jezzine	J20	<i>Atopochara trivohis trivohis</i>	●				●			●	●	●	●		●	●		●
	J15	<i>Clavator ampullaceus</i>	●	●	●	●			●						●			
	J14	<i>Ascidella reticulata</i>			●			●	●	●					●			
	J13	<i>Sphaerochara asema</i>	●	●				●	●	●					●			
	J12	<i>Mesochara cf. harrissi</i>			●										●			
	J11	<i>Charaxis martinicosasi</i>						●							●			
	J10	<i>Charaxis sp.</i>													●			
	J9	<i>Cypridea tuberculata</i>	●	●			●								●			●
	J5	<i>Cypridea piedmonti</i>	●												●			●
Barouk	B7	<i>Cypridea sp.</i>					●							●				●
	B5	<i>Perissocytheridea sp.</i>	●	●	●	●	●	●	●	●				●	●	●	●	●
Ain Dara	AD.2	<i>Ovocytheridea sp.</i>	●	●	●	●	●	●	●					●	●	●		
	AD.0	<i>Dolococytheridea sp.</i>	●	●	●	●	●	●	●					●	●	●		
Azzouniye	AZ.1	<i>(Meta)cytheropteron sp.</i>	●	●	●	●	●							●		●		
	AZ.2	<i>Choffatella cf. decipiens</i>	●	●	●									●	●			
	AZ.3	<i>Salpingoporella dinarica</i>	●	●	●									●				
	AZ.4		●	●	●									●				
Qehmez	Q4		●						●			●	●		●	●	●	

Relative abundance: ● 1-10 specimens    ● 11-50 specimens    ● 51-100 specimens    ● >100 specimens

### 5.1. Charophytes

Five different species of charophyte fructifications (3 species of utricles belonging to the extinct Clavatoraceae family and 2 species of gyrogonites belonging to the modern Characeae family) and two species of charophyte thalli

were extracted from the studied sections. The identified Clavatoraceae species are *Atopochara trivolvis* var. *trivolvis* Peck 1938, *Clavator ampullaceus* Grambast and Lorch 1968 and *Ascidiella reticulata* Grambast and Lorch 1968. The two species of Characeae are *Sphaerochara asema* Grambast and Lorch 1968, and *Mesochara* cf. *harrissi* Mädler 1952. In addition, two species of charophyte thalli i.e. *Charaxis martinclosasi* Granier et al., 2015 and *Charaxis* sp. also occur in several samples. The charophyte systematics used in this study follows the taxonomical keys developed by Martín-Closas (1996).

Most of the charophyte species here described and illustrated have already been reported in other Lebanese localities by Grambast and Lorch (1968) and Granier et al. (2015). However, this study intends to perform a detailed description and morphometric study of each species also considering their biostratigraphical, paleoecological and paleobiogeographical aspects.

Division Charophyta Migula, 1897  
Class Charophyceae Smith, 1938 emend. Schudack, 1993  
Order Charales Lindley, 1836  
Family Clavatoraceae Pia, 1927  
Subfamily Atopocharoideae Grambast, 1968 emend. Martín-Closas. 1989  
ex Schudack, 1993  
Genus *Atopochara*

*Atopochara trivolvis* var. *trivolvis* Peck, 1938

Plate 1, A-D

1938 *Atopochra trivolvis* Peck n. sp. – Peck, p.173–176, fig.1, pl.28, figs 5–12.  
1968 *Atopochara trivolvis* subsp. *trivolvis* – Grambast, p.8, pl.3, fig.16.  
1994 *Atopochara trivolvis trivolvis* Grambast 1968 – Soulié-Märsche, p. 1146-1148, fig. 5.1-5.9.

2000 *Atopochara trivolis* var. *trivolis* Peck, 1938 – Martín-Closas, p.113–116, pl.9, figs 9–10.

**Material:** *Atopochara trivolis* var. *trivolis* has been only extracted from 2 samples located in Jezzine and Ain Dara respectively (Table 3). Utricles recovered from Ain Dara are generally well-preserved. In contrast, utricles extracted from J20 show evident signs of erosion (Plate 1, D). The description below is based on the measurements of four utricles.

**Description:** Utricles have an average width and height of 872  $\mu\text{m}$  and 888  $\mu\text{m}$  respectively. The average basal width of the utricle is 844  $\mu\text{m}$  and the basal pore is 132  $\mu\text{m}$  in diameter (Plate 1, B). The utricle shows a tri-radial symmetry. It consists of 2 superimposed branched units. The first branched unit of the utricle consists of 3 main branches. Each branch is subdivided into 3 almost equal bract cell impressions attached to the utricle base (Fig. 39). The outline of the utricle is more or less rounded. The utricle shows a second branching near the apex where the cells are helicoidally arranged in a clockwise direction. The rounded outline of the utricle, the elongated upper bract cells, and the reduced size of the antheridal marks distinguish the Lebanese morphotype i.e. *Atopochara trivolis* var. *trivolis* from the morphotype *A. trivolis* var. *triquetra* (pers. comm. Dr. Martín-Closas).



Figure 39: Structure of *Atopochara trivolvis* utricle opened out on a basal plane (Martín-Closas & Wang, 2008).

**Biostratigraphy:** *Atopochara trivolvis* var. *trivolvis* represents a characteristic species of the Lower Cretaceous. It characterizes the lower Aptian-middle Albian periods (Soulié-Märsche, 1994; Martín-Closas & Wang, 2008; Trabelsi et al., 2010). This species has been correlated with foraminifera (Orbitolinids) and ammonites. According to Grambast and Lorch (1968) this species was recovered in Lebanon from lower Aptian deposits in the upper part of the Chouf Formation. The *Atopochara trivolvis* var. *trivolvis* was also reported in Albian-Aptian deposits in Portugal (Rey & Ramalho, 1974), in Aptian rocks in China (Wang, 1981), early to middle Albian lacustrine sedimentary sequences in Spain (Martín-Closas, 1988) and Aptian deposits in the United States (Soulié-Märsche, 1994).

**Paleobiogeography:** The *Atopochara trivolvis* var. *trivolvis* belongs to a part of an evolutionary lineage defined by Martín-Closas and Wang (2008) originated during the lowermost Cretaceous (early Berriasian) in Western Europe. According to these authors *A. trivolvis* was restricted to non-marine environments



in the Central Tethyan domain. It reached Eastern European continent during the Valanginian and Asia during the Hauterivian. Later, the lineage expanded worldwide during the Barremian-Aptian, first into North Africa and South America (Martín-Closas & Wang, 2008). The variety of *A. trivolvis* recovered from Lebanon i.e. *A. trivolvis* var. *trivolvis* is a cosmopolitan species since it has been reported in Aptian and Albian non-marine sedimentary sequences in Europe, Africa, South America and North America (Rey & Ramalho, 1974; Wang, 1981; Martín-Closas, 1988; Martín-Closas & Wang, 2008 and references herein). The *Atopochara trivolvis* lineage became extinct during Late Cretaceous near the K/Pg boundary (Martín-Closas & Wang, 2008).

**Paleoecology:** According to Soulié-Märsche (1994) *Atopochara trivolvis* was a halophobous species growing in waterbodies with low levels of salinity (3-5 ‰). Furthermore, this species has been recovered in deposits related to perennial waterbodies (Soulié-Märsche, 1994). This author indicated that both the utricle and the gyrogonite possess an apical opening that made them very vulnerable to dissection. However, utricles of *A. trivolvis* have also been extracted from Barremian deposits related to brackish coastal environments (Martín-Closas, 1989; Mojon, 2002). These authors found this species associated with benthic foraminifera and dasycladales algae. Martín-Closas and Wang (2008) reported that the paleoecology of the *A. trivolvis* lineage changed over time. These authors stated that during the lowermost Cretaceous *A. trivolvis* mainly thrived in perennial freshwater lakes becoming more eurytopic and tolerant to certain salinity during the Barremian and Aptian. In agreement with this idea, the recovered utricles from sample J20

(Jezzine section 2) occur associated with marine fossils such as agglutinated foraminifera shells of *Choffatella* cf. *decipiens* and fragments of echinoid spines. However, utricles show evident signs of abrasion suggesting that they were transported from their thriving original areas. The absence of other charophyte species within the assemblage in sample J20 suggests that this species was tolerant to certain salinity.

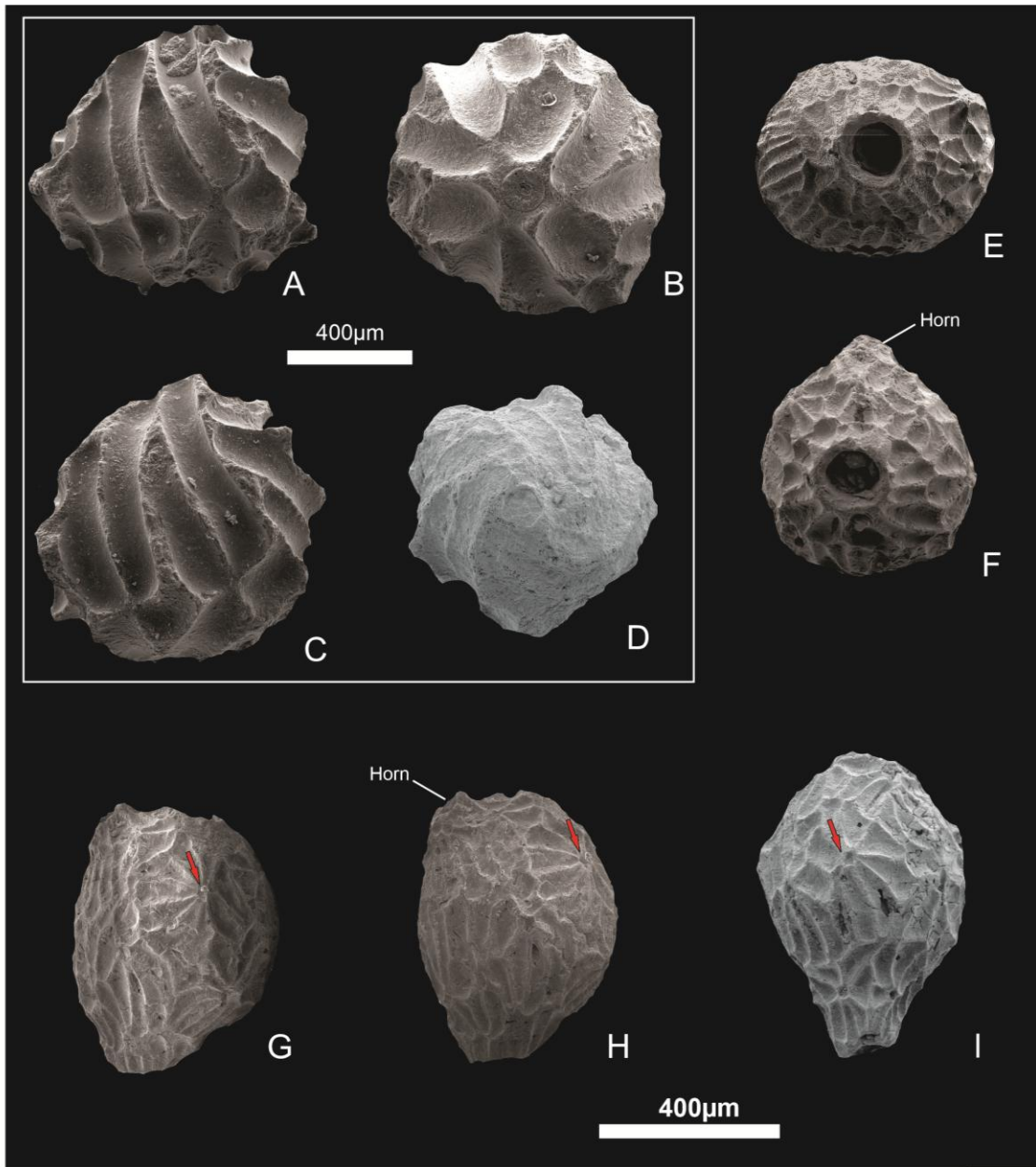


Plate 1: A & C (*Atopochara trivolvris trivolvris*, lateral view, AD.2), B (*Atopochara trivolvris trivolvris*, basal view, AD.2), D (*Atopochara trivolvris trivolvris*, apical view, J20), E (*Ascidiella reticulata*, basal view, AD.2), F (*Ascidiella reticulata*, apical view, J15), G & H (*Ascidiella reticulata*, lateral view, AD.2), I (*Ascidiella reticulata*, lateral view, B5). Red arrows in G-I point to the lateral pores.

Subfamily Clavatoroideae Pia, 1927  
Genus *Clavator* Peck, 1941

*Clavator ampullaceus* (Grambast & Lorch, 1968) Martín-Closas, 1996

Plates 2 & Plate 3, A-H

1968 *Lucernela ampullacea*– Grambast and Lorch, p.49, pl.1 and 2.

2015 *Clavator ampullaceus*– Granier et al., 2015, pl. 3A-E.

**Material:** This species occurs in almost all sections. However, it is especially conspicuous in Ain Dara, Azzouniye, and top of the Barouk section. They also occur in minor amount in 5 samples from Jezzine (Table 3). Fifty utricles were measured in this study.

**Description:** Large utricle, 960  $\mu\text{m}$  width (mean average) and 775  $\mu\text{m}$  height (mean average). In the lateral anterior view, the average width is 825  $\mu\text{m}$  and height is 780  $\mu\text{m}$ . In the lateral posterior view, the average width of the utricle is 827  $\mu\text{m}$  and height is 841  $\mu\text{m}$ . The utricle shows a characteristic bilateral symmetry and it is composed of elongated units (representing the impressions of the bract cells) which radiate from the base joining with furrows radiating from the two accessory pores (Plate 3, A). The furrow shown in the lateral posterior view (Plate 3, B) represents the insertion point where the utricle was attached to the charophyte stem. They display a rose shaped apical pore with two accessory pores at the shoulders of the apex (Plate 3, G-H). The average width of the apical pore is 161  $\mu\text{m}$ . The accessory pores are outlets for 2 internal canals originating at the utricle's base (Plate 2, G). The basal pore of the utricle is rounded with an average width of 194  $\mu\text{m}$ . Some utricles from the studied populations display a clear basal pore

showing the base of the inner gyrogonite. The basal plate of the gyrogonite is unicellular and has a pentagonal shape (Plate 2, G). Five tubular gyrogonite cells can be observed within the basal pore of the utricle (Plate 2, G).

Grambast and Lorch (1968) and Granier et al. (2015) differentiated two species of *Clavator* that haven't been distinguished here i.e. *Clavator delteus* and *Clavator ampullaceus*. According to these authors the main difference between both species is the utricle size being *C. ampullaceus* considerably larger than *C. delteus*. A morphometric analysis of a small population (20 *Clavator* utricles) from sample B5 (Barouk) has been performed in order to distinguish both species. The variation of the utricle width and height has been considered in this analysis (10 utricles in lateral view and 10 in lateral anterior view). Utricle size parameters are fit within the same cloud (Fig. 40). Hence, no clear difference was observed to distinguish the two species.

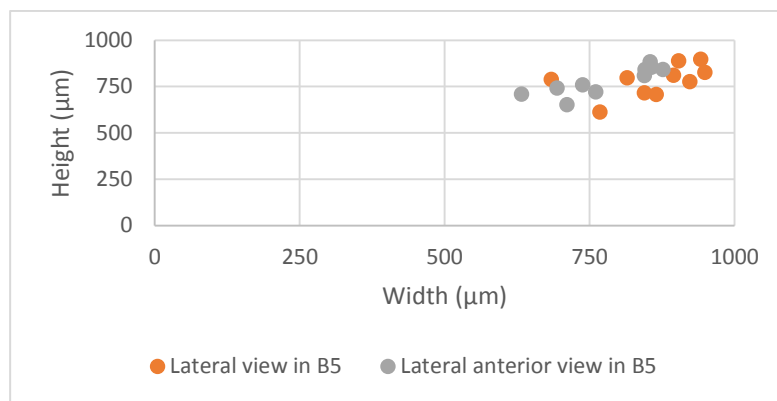


Figure 40: A graph showing the variation of Width vs. Height of *Clavator* utricles recovered from sample B5 (Barouk section 1) in lateral and lateral anterior view.

**Biostratigraphy:** This species has been reported in Lower Cretaceous (Barremian-lower Aptian) deposits in Lebanon, Palestine, and Somalia (Grambast & Lorch, 1968; Luger & Schudack, 2001). Recently, the revision of a charophyte collection housed in the Geology department of the Bucharest University (Romania) allowed distinguishing utricles of *C. ampullaceus*. These populations were extracted from Lower Cretaceous rocks in the Carpathian Mountain System (Romania). However, this population hasn't already been studied in detail (pers. comm. Dr. Josep Sanjuan).

**Paleobiogeography:** *C. ampullaceus* seems to display a very restricted paleogeography in the southern peri-Tethyan coastal basins (nowadays Lebanon, Palestine and North of Somalia). During the Barremian the Middle East and North of African regions were located in much lower latitudes than nowadays i.e. near the equator (Decourt et al., 1993). The presence of this species in Romania (Eastern Europe) indicates that *C. ampullaceus* had a wider distribution occurring also in northeastern peri-Tethyan archipelago.

**Paleoecology:** The genus *Clavator* has been related to non-marine (freshwater and brackish) deposits (Schudack, 1996; Luger & Schudack, 2001). In large number of soft samples, well-preserved utricles of *C. ampullaceus* occur associated with agglutinated foraminifera shells of *Choffatella* cf. *decipiens*, echinoid spines and dasycladales thalli of *Salpingoporella* (*Hensonella*) *dinarica* suggesting that this species was tolerant to certain degree of salinity. Utricles of this species can also be observed in hard limestone samples e.g. AD. 3 associated with charophyte thalli and gastropod shells related to freshwater lacustrine facies

(Appendix A, Fig. 63). The occurrence of utricles of this species in both freshwater and brackish water related facies indicates that *C. ampullaceus* was a euryhaline species able to thrive in a wide array of coastal waterbodies.

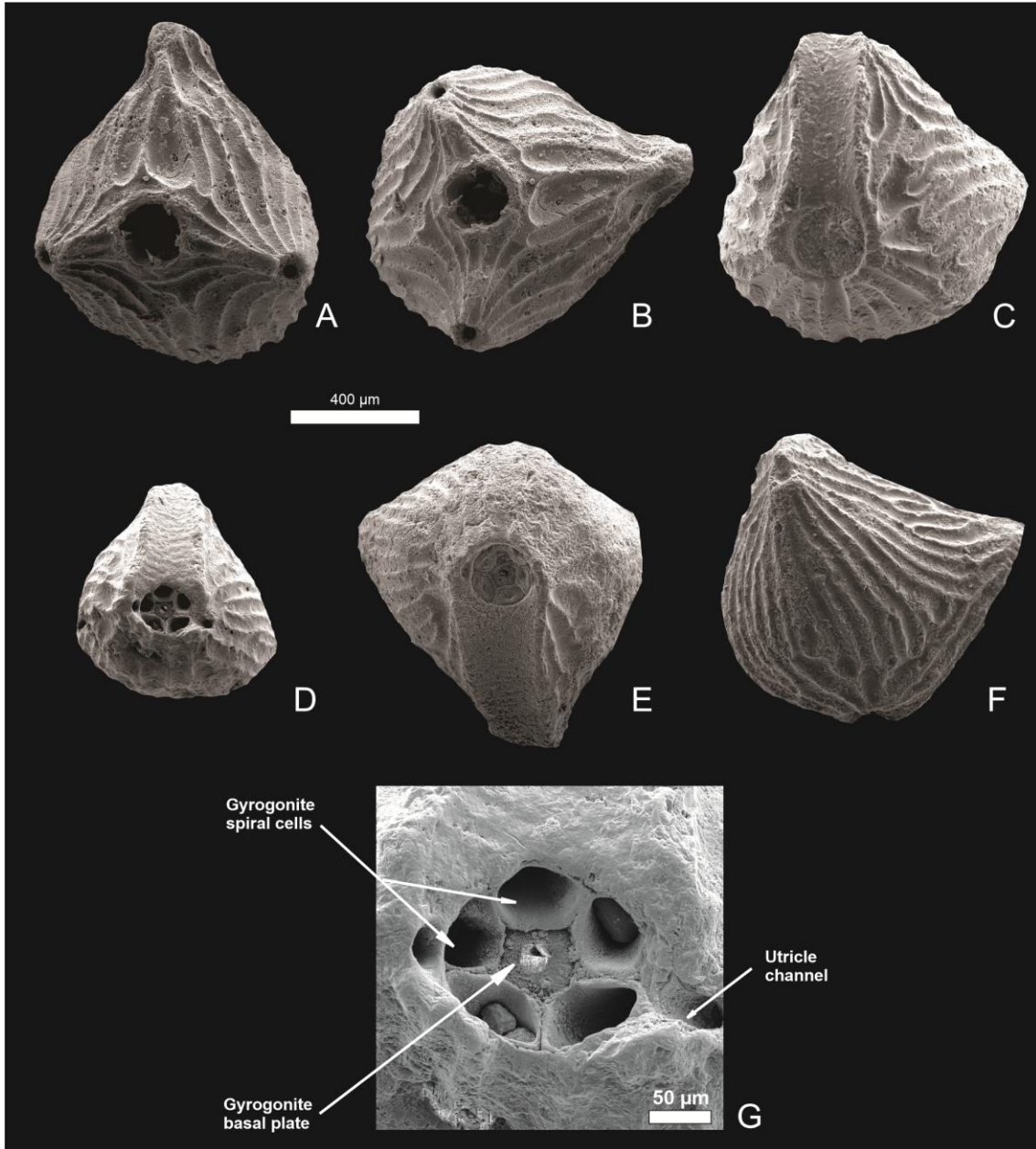


Plate 2: *Clavator ampullaceus*. A & B (apical view, AD.2), C (basal view, AD.2), D (basal view, J15), E (basal view, AD.2), F (lateral view, AD.2), G (detail of the utricle's basal pore in D, AD.2).

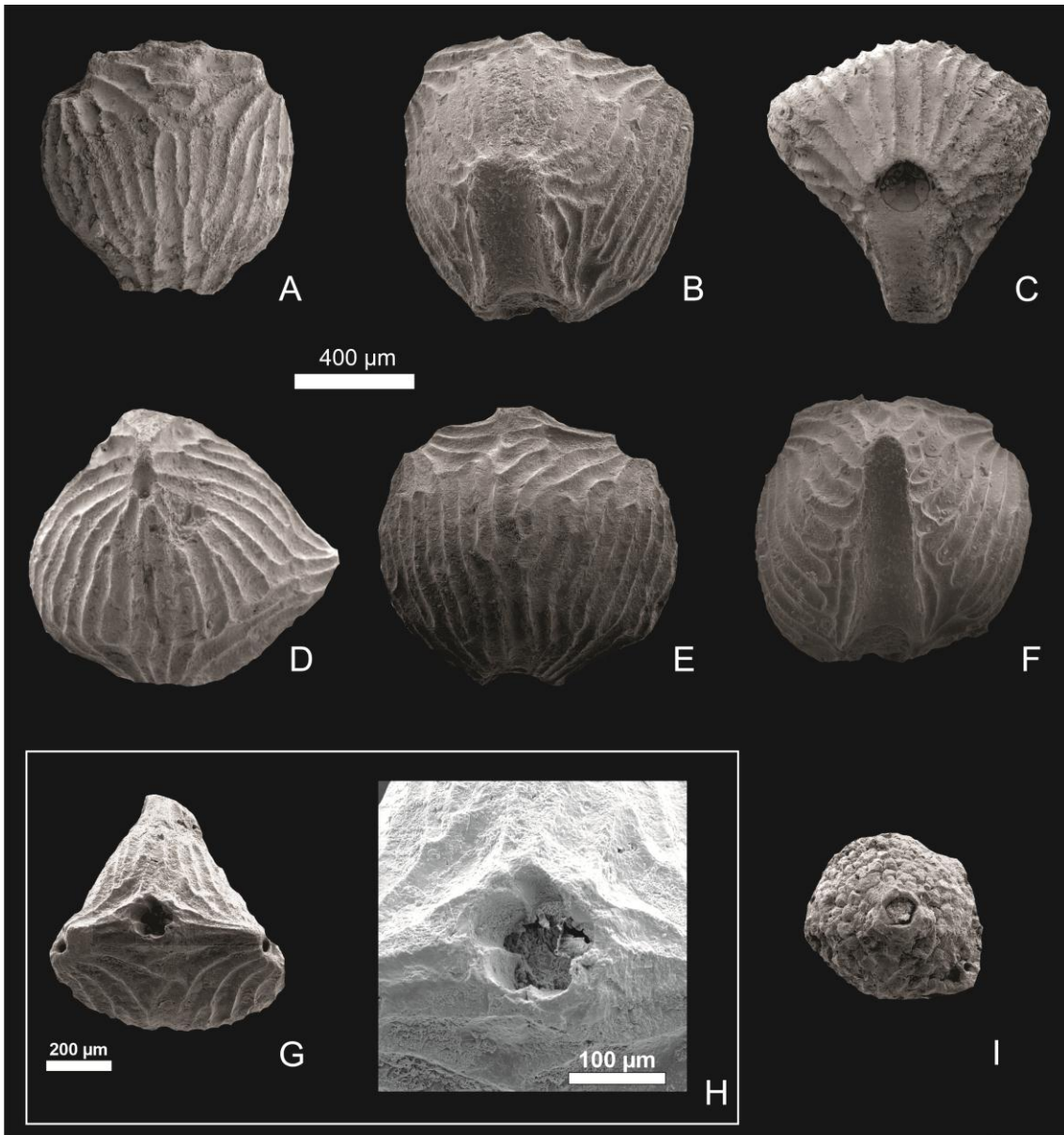


Plate 3: *Clavator ampullaceus*. A (lateral anterior view, AD.0), B (lateral posterior view, AD.2), C (basal view, AZ.3), D (lateral view, AD.0), E (lateral anterior view, J15), F (lateral posterior view, AD.2), G (apical view, J15), H (detail of the apical pore showing a flower-like shape, J15), I (*Ascidiella reticulata*, nodular layer covering the gyrogonite, apical view, J15).



Subfamily Clavatoroideae Pia, 1927  
Genus *Ascidiella* Grambast, 1966 emend. Martín-Closas ex Schudack, 1993

*Ascidiella reticulata* Grambast and Lorch, 1968

Plate 1, E-I & Plate 3, I

1968 *Ascidiella reticulata*- Grambast and Lorch, pl.4, figs. 1-11.

1986 *Ascidiella irregularis* nov. sp. - Grambast-Fessard, p. 256-260, pl.1, figs. 4-9, 11.

2001 *Ascidiella reticulata*- Luger and Schudack, Fig. 4 (10-14).

**Material:** This species is very common in sections Ain Dara and Barouk.

Few utricles were also extracted from Jezzine, Qehmez and Azzouniye sections (Table 3). Twelve utricles have been measured from different samples.

**Description:** Utricles of this species are medium in size, 617  $\mu\text{m}$  in length and 474  $\mu\text{m}$  in width (Plate 1, G-I). The diameter of the apical and basal pores are 95  $\mu\text{m}$  in average. The utricle shows a characteristic lateral horn near the apex with a pore opening at its end (Plate 1, F & H) very variable in size. Occasionally this horn is missing in some specimens. The utricle is made up of calcified impressions of three groups of short bract cells. Each bract cell group is attached to one node of the plant stem or phylloid. Twelve small lateral pores can be observed on the utricle's surface (Plate 1, G-I). These pores are outlets for internal canals. These calcified impressions and pores are absent in low calcified utricles which show a characteristic nodular texture covering the gyrogonite (Plate 3, I).

**Biostratigraphy:** *Ascidiella reticulata* have been recovered from Barremian-lower Aptian non-marine deposits of Lebanon, Palestine, and Somalia

(Grambast & Lorch, 1968; Luger & Schudack, 2001). Luger and Schudack (2001) synonymized this species with *Ascidiella irregularis* defined by Grambast-Fessard (1986) in Lower Cretaceous (upper Aptian) rocks from Portugal.

**Paleobiogeography:** *Ascidiella reticulata* displays a restricted paleogeography occurring abundantly in the southern peri-Tethyan coastal basins (nowadays Lebanon, Palestine and North of Somalia). However, the presence of this species in Portugal indicates that *A. reticulata* expanded in the northwestern peri-Tethyan islands (nowadays the Iberian Peninsula).

**Paleoecology:** The genus *Ascidiella* has been recovered from non-marine deposits related to freshwater environments (Luger & Schudack, 2001 and references therein). Utricles studied in this thesis frequently occur associated with shells of agglutinated foraminifera, fragments of echinoid and dasyclad algal thalli suggesting that *A. reticulata* was tolerant to a higher degree of salinity.

Order Charales Lindley, 1836  
Family Characeae (Richard ex C. Agardh, 1824) emend. Martín-Closas and  
Schudack, 1991  
Genus *Sphaerochara* (Mädler, 1952) emend. Soulié- Märsche, 1989

*Sphaerochara asema* Grambast and Lorch, 1968  
Plate 4, A-D

1968 *Peckisphaera asema* - Grambast and Lorch, pl. 3, figs. 7-12.

**Material:** This species occurs in Jezzine, Barouk, Ain Dara and Azzouniye sections (Table 3). Fifteen gyrogonites were measured.

**Description:** Gyrogonites are small (350  $\mu\text{m}$  height and 403  $\mu\text{m}$  width, mean average) and spheroidal in shape. Six to seven non-ornamented spiral convolutions can be observed in lateral view (Plate 4, C). The apex is rounded. Spiral cells don't show any periapical modification (Plate 4, D). The base is rounded showing a pentagonal-shaped basal pore with an average diameter of 150  $\mu\text{m}$  (Plate 4, A & B).

**Biostratigraphy:** This species has only been reported in Barremian/lower Aptian deposits from Lebanon and Palestine (Grambast & Lorch, 1968; Granier et al., 2015).

**Paleobiogeography:** From the paleobiogeographical viewpoint *S. asema* seems to have a very restricted distribution representing an endemic species of the southern peri-Tethyan Lebanese basin.

**Paleoecology:** Gyrogonites of *Sphaerochara asema* occur in many samples but it is especially abundant in two among them i.e. B5 and AD.2. Despite they are associated with some dasycladal stems and shells of agglutinated foraminifera, large number of gyrogonites show signs of abrasion and corrosion (Plate 4, A & C) indicating that they suffered some transport from its original growing area. The parautochthony of *S. asema* suggests that it thrived in freshwater lakes near the coastline.

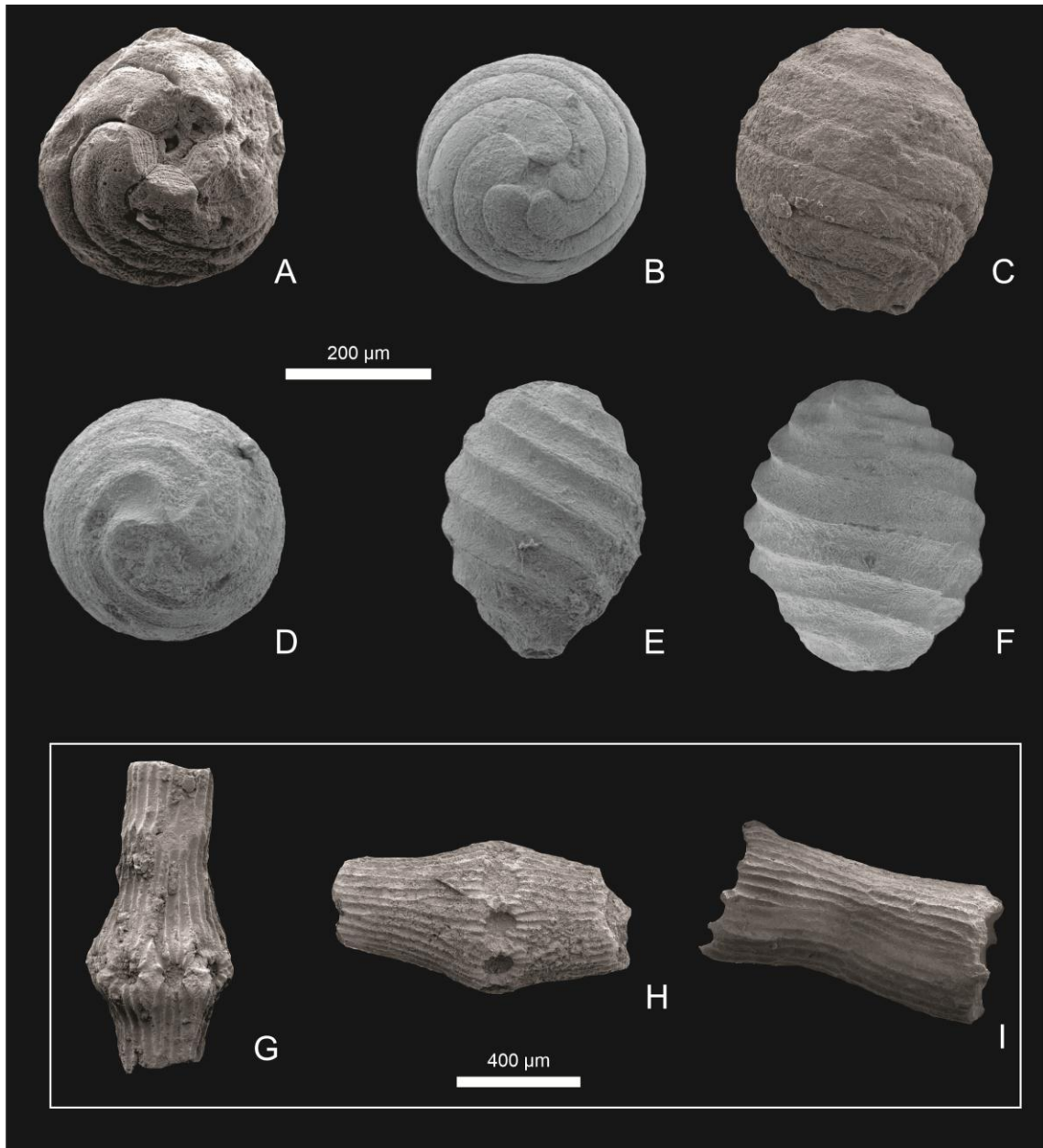


Plate 4: A (*Sphaerochara asema*, basal view, J15), B (*Sphaerochara asema*, basal view, B5), C (*Sphaerochara asema*, lateral view, AD.2), D (*Sphaerochara asema*, apical view, B5), E & F (*Mesochara cf. harrisii*, lateral view, B5), G (*Charaxis martinclousasi*, lateral view, AZ.3), H (*Charaxis martinclousasi*, lateral view, AD.0), I (*Charaxis martinclousasi*, internode, AD.0).

Family Characeae (Richard ex C. Agardh, 1824) emend. Martín-Closas and Schudack, 1991

Genus *Mesochara* Grambast, 1962

*Mesochara* cf. *harrissi* (Mädler, 1952) Shaikin, 1967

Plate 4, E-F

1952 *Tolypella harrissi* Mädler, pp. 31, 32, pl. B, figs. 31-35.

1967 *Mesochara harrissi* (Mädler) nov. comb.; Shaikin, p. 47.

**Material:** Few specimens of this species have been recovered from Barouk, Ain Dara, Azzouniye and Jezzine (Table 3). Two gyrogonites were measured.

**Description:** Gyrogonites are very small (390  $\mu\text{m}$  in height and 305  $\mu\text{m}$  in width). The gyrogonite is ellipsoidal in shape showing a rounded to slightly pointed apex (Plate 4, E). No periapical modification can be observed. Seven to eight convolutions can be observed in lateral view. Spiral cells are concave and devoid of ornamentation (Plate 4, E & F). The base is pointed showing a small pentagonal basal pore.

**Biostratigraphy:** This species has a very wide biostratigraphic range occurring in Upper Jurassic (Oxfordian) to Lower Cretaceous (Aptian) continental sedimentary rocks (Benoit et al., 2017 and references therein).

**Paleobiogeography:** This species has a cosmopolitan distribution occurring in Oxfordian (Upper Jurassic) to Aptian (Lower Cretaceous) rocks in Europe (Spain, France, and Germany), China and Japan (Benoit et al., 2017 and references herein). This study represents the first report of this species in the Middle East.

**Paleoecology:** The occurrence of this species has been related to temporary lakes in floodplain environments (Vicente & Martín-Closas, 2013). The presence of

this species associated with marine fauna suggests that it was a eurytopic charophyte able to tolerate certain degree of salinity.

Order Charales Lindley, 1836  
Organ-Genus *Charaxis* Harris, 1939  
*Charaxis martinclosasi* Granier et al., 2015

Plate 4, G-I

1968 Grambast and Lorch, p. 422, pl. IV, fig. 12  
2015 *Charaxis martinclosasi* Granier et al., Plate 4, Figs. G-I.

**Material:** This charophyte thalli species has been mainly extracted from the Barouk section. Several poorly preserved fragments have also been found in Jezzine, Ain Dara and Azzouniye sections (Table 3). Three fragments were measured.

**Description:** Remains of charophyte thalli (stems) consisting of nodes and internodes commonly broken in fragments. The description of this species fits perfectly to the original definition proposed by Granier et al. (2015). They are medium in size (972  $\mu\text{m}$  length and 473  $\mu\text{m}$  width). The individual fragments look like a double cone with 8 to 10 pores at the level of the nodes (Plate 4, G-H; Fig. 61A). The internodes are formed by one empty space corresponding to the internodal cell (observable in thin section) coated by 50 grooves which correspond to the impressions of the original cortical cells. Despite this charophyte thalli species has been included in the genus *Charaxis*, the structure and the morphological characteristics suggest that this species should be included in the genus *Munieria*.

**Paleobiogeography:** This species has only been reported in several Lebanese localities (Granier et al., 2015).

**Paleoecology:** *C. martinclosasi* occurs associated with charophyte utricles and gyrogonites forming wackestones of charophytes in some limestone intervals in the Ain Dara section. The absence of marine fossils in these hard rocks suggests that this species thrived in freshwater environments. Several specimens have also been extracted from soft rocks occurring associated with shells of marine fauna. However, they show a certain degree of abrasion particularly in the Jezzine section (sample J5) probably related to some kind of transport. Nevertheless, the tolerance of this species to a certain degree of salinity cannot be excluded.

Other rare charophyte remains have been recovered from sample J15. They are fragments of corticated thalli i.e. *Charaxis* sp. (Fig. 41).

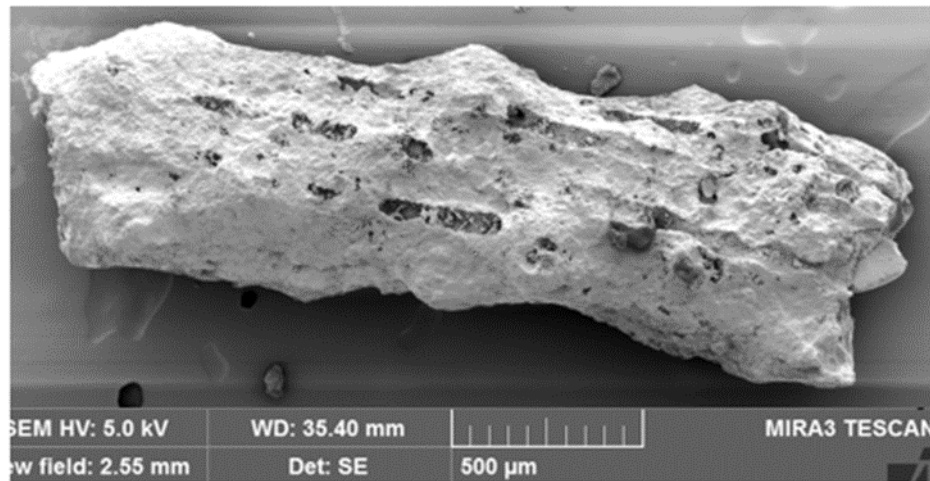


Figure 41: SEM photo of the *Charaxis* sp. recovered from J15.

## 5.2. Ostracods

Seven species of ostracods have been identified from the studied sections. Three species of freshwater *Cypridea* have been distinguished for the first time in Lebanon; 1) *C. tuberculata* Andesron, 1839, 2) *C. piedmonti* Roth 1933, and 3) a new species provisionally named *Cypridea libanii* nov. sp. *Cypridea* is a group of ostracods belonging to the family Cyprideidae Martin, 1940. During the late Tithonian to Early Cretaceous, this family reached a high diversity worldwide which make this group of ostracods excellent candidates for regional and supraregional biostratigraphy of Lower Cretaceous continental rocks (Wang et al., 2017). Figure 42 illustrates the morphological parameters present in *Cypridea* carapaces which have been considered in the following description.

Fossil carapaces of the species belonging to brackish water genus *Perissocytheridea* and marine water genus (*Meta*)*cytheropteron* have also been recovered. Moreover, shells of marine-related ostracods of the genus *Dolocytheridea* and *Ovocytheridea* occur in minor amount.

A basic preliminary description and biostratigraphical, paleoecological and paleobiogeographical implications are here reported for the dominant ostracod species.

Class Ostracoda Latreille, 1806  
Order Podocopida Müller, 1894  
Superfamily Cypridoidea Baird, 1845  
Family Cyprideidae Martin, 1940  
Genus *Cypridea* Bosquet, 1852

*Cypridea tuberculata* Andesron, 1839  
Plate 5



**Material:** This species is very abundant in the Barouk section (sample B5) where more than seventy carapaces have been recovered. *C. tuberculata* also occurs in minor amount in Jezzine, Ain Dara and Azzouniye (Table 3). Twelve carapaces have been measured.

**Description:** Carapaces are oval in shape. The length of carapaces ranges between 801 and 1035  $\mu\text{m}$ . The carapace height varies between 450-586  $\mu\text{m}$ . The right valve (RV) is smaller than the left valve (LV). The LV is overlapping the RV mainly around the ventral margin (Plate 5, B). The anterior margin is broadly rounded (Plate 5); the Anterior Cardinal Angle (ACA) is remarkable,  $135^\circ$  approx. The Posterior Cardinal Angle (PCA) is strongly rounded. The dorsal margin is straight and declined towards the posterior end. The ventral margin is straight or slightly convex. The Anteroventral Rostrum (AVR) is well developed and covered with small tubercles (Plate 5, E). The alveolar furrow is well marked and deep (Plate 5, A (1) & E). The alveolar notch is weak. A small cyathus can be observed (Fig. 43).

In lateral view, the position of greatest height is located within the anterior half of the shell. The surface of the carapace is punctuated showing rounded tubercles variable in size. More than 30 tubercles can be observed on both valves ranging in diameter between 40 to 100  $\mu\text{m}$ . The tubercles at the center of the carapace on both valves are notably larger than tubercles near the dorsal and ventral margins (Plate 5, A, D, & E).

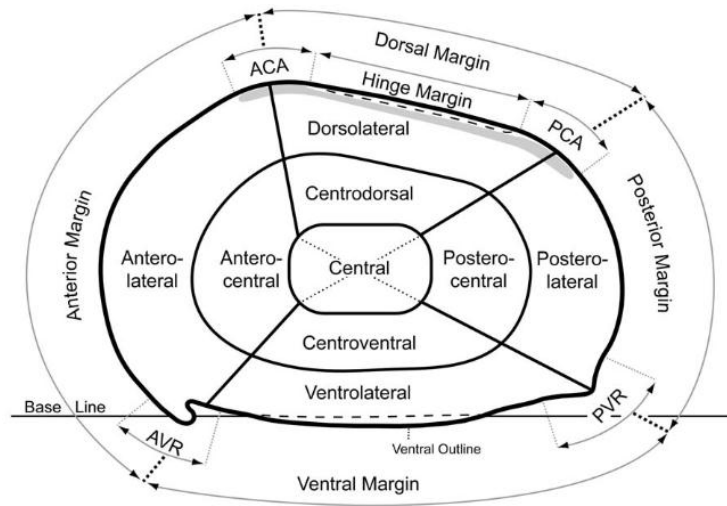


Figure 42: Illustration of the terminology used to describe the carapace of the genus *Cypridea*. ACA: Anterior Cardinal Angle. AVR: Anteroventral rostrum. PCA: Posterior Cardinal Angle. PVR: Posteroventral region (Sames, 2011).

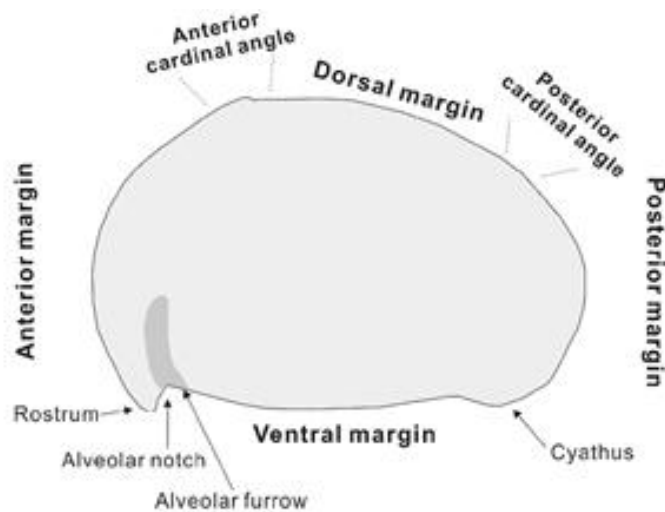


Figure 43: Illustration showing some external morphological terms used in the description of the *Cypridea* carapaces (Byung-Do et al., 2017).

**Stratigraphic range:** This species has been recovered from upper

Berriasian to Valanginian non-marine rocks in North America. On the other hand,

*C. tuberculata* has been extracted from upper Berriasian to lower/middle Barremian rocks in Western Europe (Hoedemaeker & Hengreen, 2003; Schudak & Schudack, 2009).

**Paleobiogeography:** Genus *Cypridea* has a worldwide distribution occurring in all continents except Australia and Antarctica (Sames, 2009 and references therein). *Cypridea tuberculata* represents a cosmopolitan species, reported in North America, Europe and China. Jones (1893) and Sames (2009) described *C. tuberculata* from the Bear River Formation near Cokeville/Wyoming (USA). This species has also been recovered from Louisiana and Arkansas as well as from several localities at the Atlantic Coastal regions in USA (Swartz & Swain, 1946; Swain & Brown, 1972). Li et al. (1988) reported this species in the Fuxin Basin (Liaoning Province, China). Schudack and Schudack (2009) reported *C. tuberculata* in eastern Spain. It has been found in the Purbeck Weald in the Lower Cretaceous in south England (Anderson, 1971).

**Paleoecology:** *Cypridea* species have traditionally been related to ephemeral or perennial deposits of fresh waterbodies (Horne, 2002; Sames, 2009). However, some species of this genus has been associated to brackish water paleoenvironments. According to Savelieva (2014), the abundance of the brackish/fresh water genus *Cypridea* indicates the closeness of the shoreline. *C. tuberculata* has been recovered from non-marine deposits related to freshwater permanent lakes (Schudack & Schudack, 2009). Well-preserved carapaces recovered in this study occur associated with marine microfossils such as

foraminifer shells (*Choffatella*) and dasycladales thalli (*Salpingoporella dinarica*) suggesting that this species was able to thrive in brackish water environments.

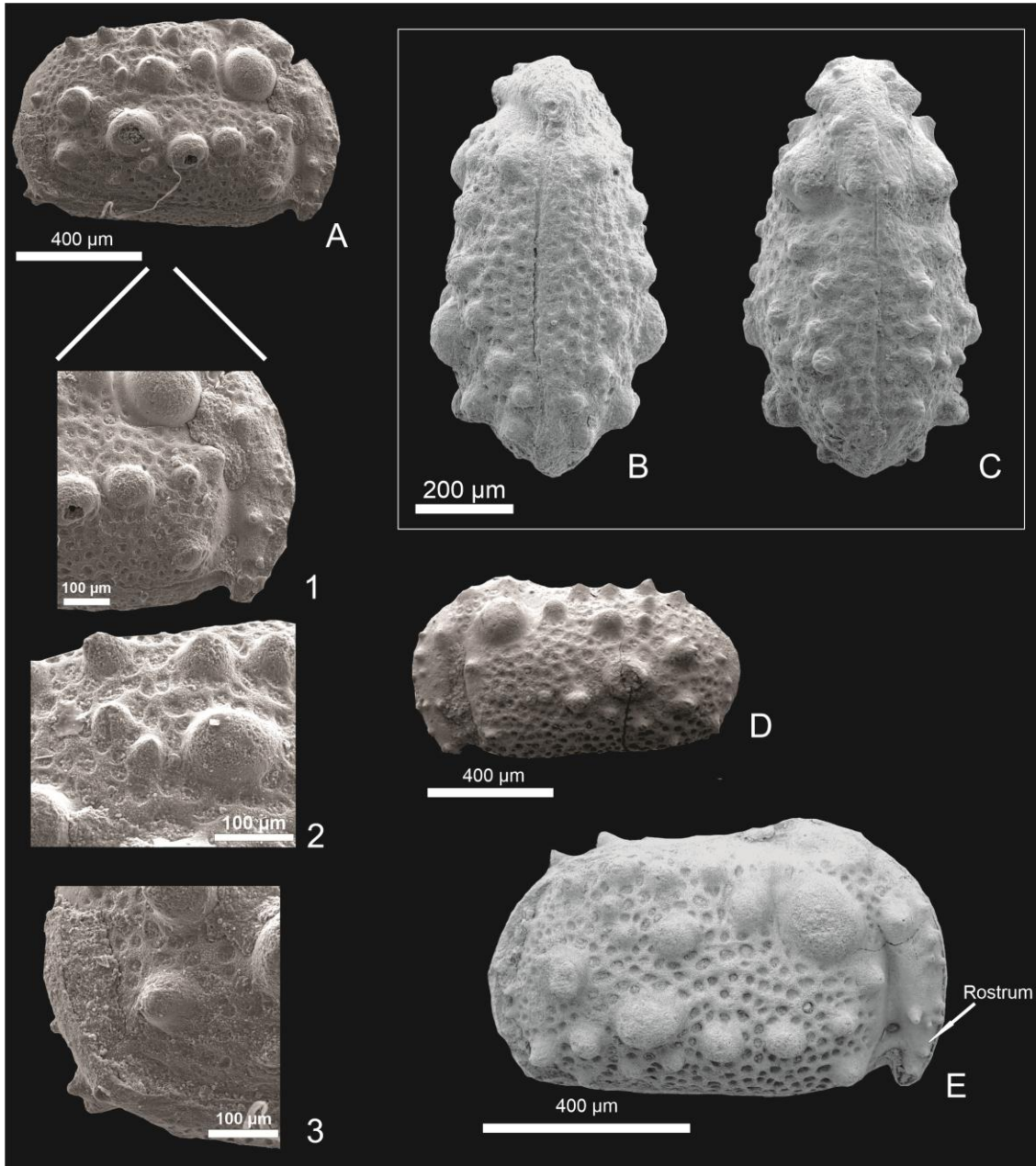


Plate 5: *Cypridea tuberculata*. A (lateral view, AD.2), 1 (detailed anterior view), 2 (detailed centrodosral view), 3 (detailed posterior view), B (ventral view, AZ.2), C (dorsal view, AZ.2), D (lateral view, AD.2), E (lateral view, B5).

*Cypridea piedmonti* (Roth 1933) syn. *C. (P.) Henrybelli* Sohn 1979, emend.  
Plate 6, A-I, K-L

**Material:** This species were extracted mainly from the Barouk section (sample B5). Few shells have also been recovered from Jezzine and Ain Dara sections (Table 3). Thirteen carapaces were measured.

**Description:** Carapaces are rounded to sub oblong in shape. The sizes of the carapace ranges between 682-1007  $\mu\text{m}$  in length, 350-627  $\mu\text{m}$  in height. The whole surface of the carapace is moderately punctuated (porous) and devoid of ornamentation. Some specimens may display a kind of reticulation. LV is overlapping the RV around all margins. (Plate 6, E, F & J). The rostrum is weakly developed and ornamented with small aligned tubercles. The anterior margin is broadly rounded. The ACA is weak,  $137^\circ$  approx. while the PCA is strongly rounded. The dorsal margin is slightly convex and declined towards the posterior end. The ventral margin is convex. The AVR is slightly developed and may be covered with small aligned tubercles (Plate 6, J). The alveolar notch and the alveolar furrow are almost absent. Carapaces of *C. piedmonti* show a reduced cyathus located in the PVR.

**Stratigraphic range:** In Western Europe this species has been reported in non-marine sedimentary rocks ranging in age from lower Valanginian to late Barremian (Schudack & Schudack, 2009). In North America *C. piedmonti* has also been found in Valanginian - Barremian rocks from South Dakota and Wyoming (Sohn, 1979; Sames, 2009).

**Paleobiogeography:** *C. piedmonti* is a cosmopolitan species (Swain, 1946; Sohn, 1979; Schudack & Schudack, 2009). It has been found in lacustrine deposits from several continents such as Western Europe (Iberian Chain, Spain), North America (South Dakota) and South America (Brazil).

**Paleoecology:** Carapaces of *C. piedmonti* has been related to lacustrine and fluviatile oligohaline environments (Sohn, 1979; Sames 2009). In Lebanon, well-preserved carapaces of this species occur associated with marine microfossils such as foraminifera shells (*Choffatella*) and dasycladales thalli (*Salpingoporella dinarica*). The association of this species with marine fossils suggests that *C. piedmonti* was tolerant to certain degree of salinity thriving in both freshwater and brackish water environments.

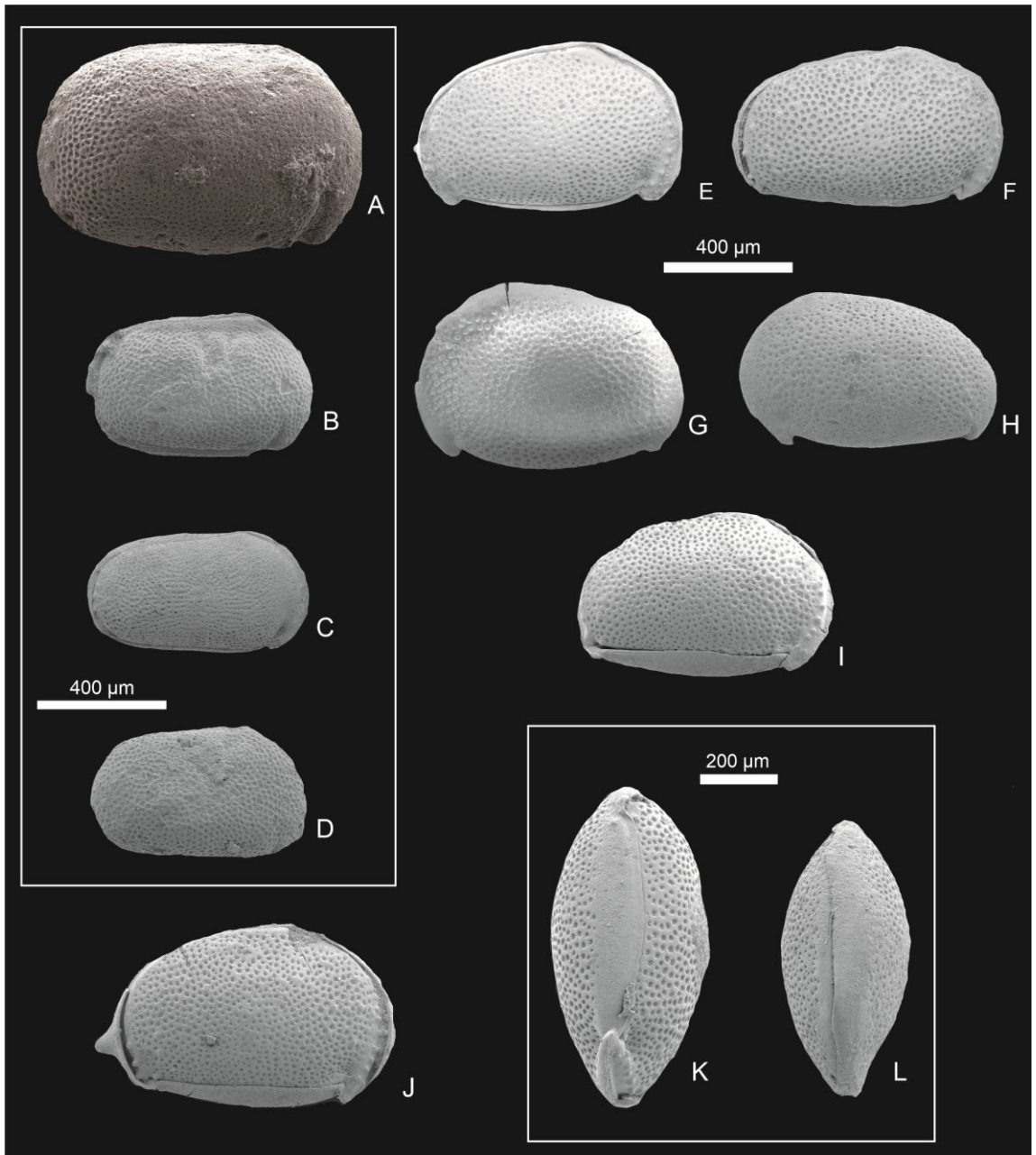


Plate 6: A (*Cypridea piedmonti* adult, right lateral view, AD.2), B (*Cypridea piedmonti* juvenile, right lateral view, AD.0), C (*Cypridea piedmonti*, right lateral view, B5), D (*Cypridea piedmonti*, right lateral view, J10), E, F, & I (*Cypridea piedmonti*, right lateral view, B5), G & H (*Cypridea piedmonti*, left lateral view, B5), J (*Cypridea* sp. 1, B5), K (*Cypridea piedmonti*, ventral view, B5), L (*Cypridea piedmonti*, dorsal view, B5).

*Cypridea* sp.  
(Plates 7, 8, & 9)

**Material:** Shells belonging to this new species of *Cypridea* are not very abundant (Table 3). They have mainly been recovered in the sample B5 from Barouk (twenty five valves). Ten carapaces have also been extracted from the Ain Dara section (sample AD.2).

**Dimensions:** Carapaces vary in length between 993- 1202  $\mu\text{m}$ , 491- 638  $\mu\text{m}$  in height, and 547 – 587  $\mu\text{m}$  in width (Fig. 44).

**Type locality:** Sample B5 (Barouk section 1). UTM location: 33° 43' 58.31" N, 35° 42' 18.92" E.

**Description:** Despite the low amount of carapaces extracted, they display clear distinctive parameters allowing us to define a new species of *Cypridea*. In a future scientific publication, the name *Cypridea libanii* nov. sp. will be proposed. This new species of *Cypridea* displays an oval shape. The left valve is bigger than the right valve (Plate 9). The LV is overlapping the RV around all margins. The position of greatest height is located at the center or slightly displaced towards the anterior half of the shell (Plate 8). The anterior margin is broadly rounded. The ACA is remarkable, 132° approx. while the PCA is strongly rounded. The dorsal margin is straight and declined towards the posterior end. The ventral margin is straight to slightly concave. The AVR is well developed and covered with small tubercles. The alveolar furrow and notch are deep. This species lacks a cyathus. The surface of the carapace is punctuated and bears several complex tubercles (11 to 14) varying in diameter between 50  $\mu\text{m}$  and 200  $\mu\text{m}$  (Plate 7, A & Plate 8). The



diameter of the tubercle diminishes towards the dorsal margin. Tubercles bear between 2 and 5 elongated horn-like structures displaying a characteristic flower-shaped margin (Plate 7, C & D). Each horn-like structure contains an internal channel connecting the exterior and the interior of the carapace.

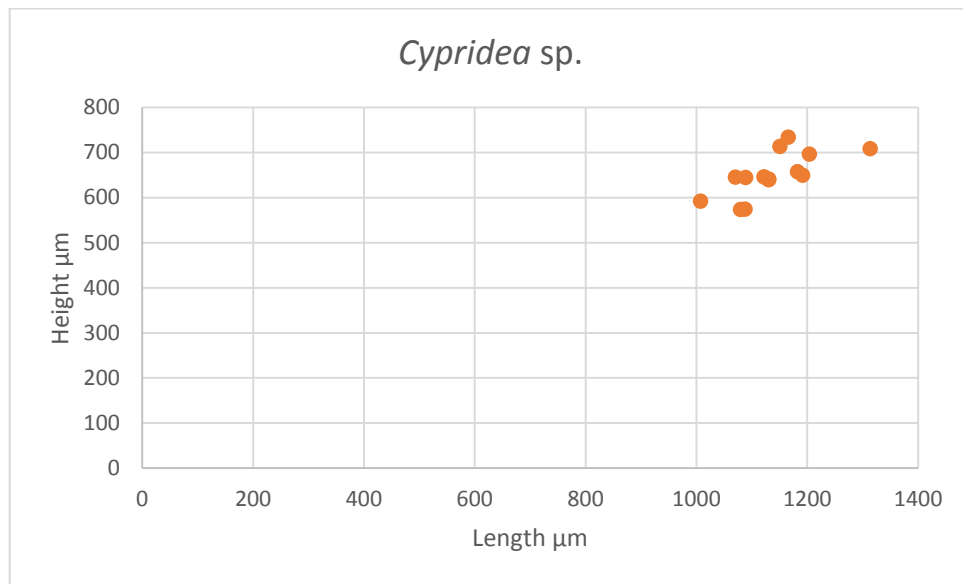


Figure 44: Dispersion graphic showing the relation between the carapace length and height in lateral view (n=14).

**Paleoecology:** The paleoecology of this species can be tentatively inferred considering the associated microfossils and the type of facies. This species is not very abundant and several carapaces occur fragmented or show evidences of abrasion. Moreover, most of the complete specimens consist of separated valves. About 25 specimens are well-preserved showing their delicate ornamentation intact (samples B5 and AD.2). Carapaces of this species appear associated with other shells related to brackish water ostracods (*Perissocytheridea* sp. and *Dolococytheridea* sp.), agglutinated foraminifera and dasycladales thalli suggesting that *Cypridea* sp.

probably was and euryhaline species able to tolerate a certain degree of salinity. However, larger populations and a deeper study are required to confirm this hypothesis.

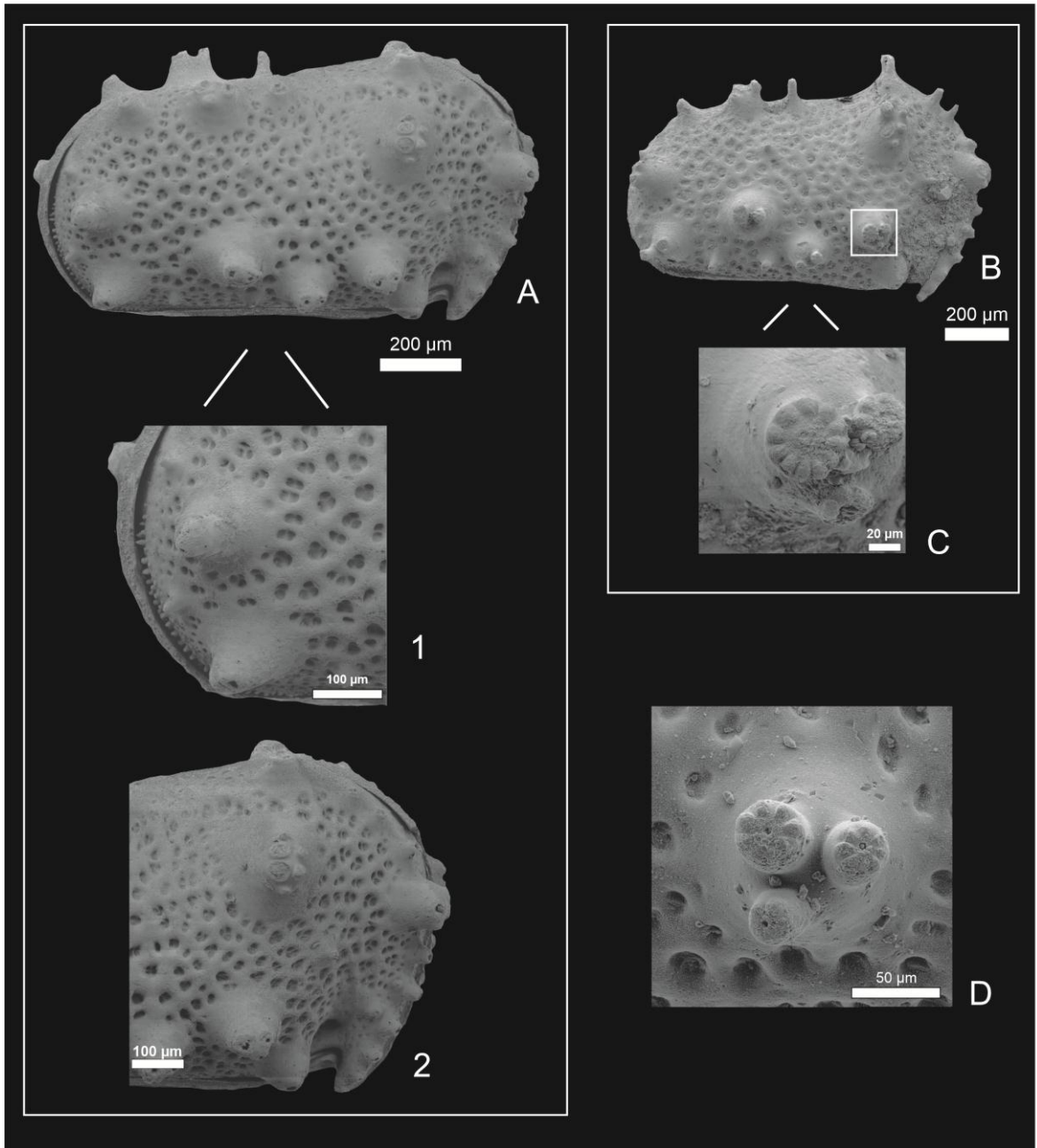


Plate 7: *Cypridea* sp. A (lateral view, B5), 1 (detailed anterior view), 2 (detailed posterior view), B (lateral view, B5), C & D (detailed ornamentation structures, B5).

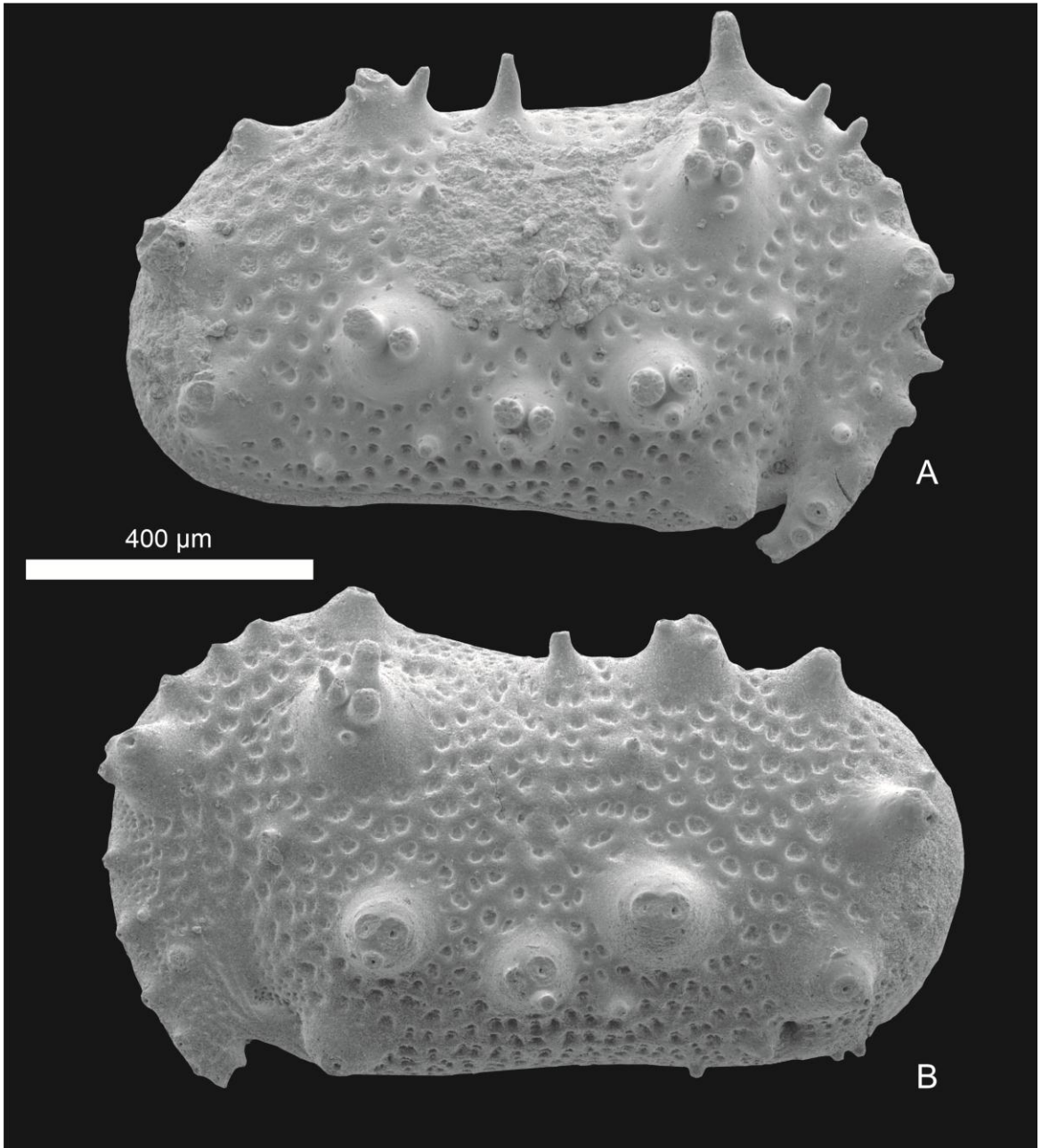


Plate 8: *Cypridea* sp. A (right lateral valve, B5), B (left lateral valve, B5).

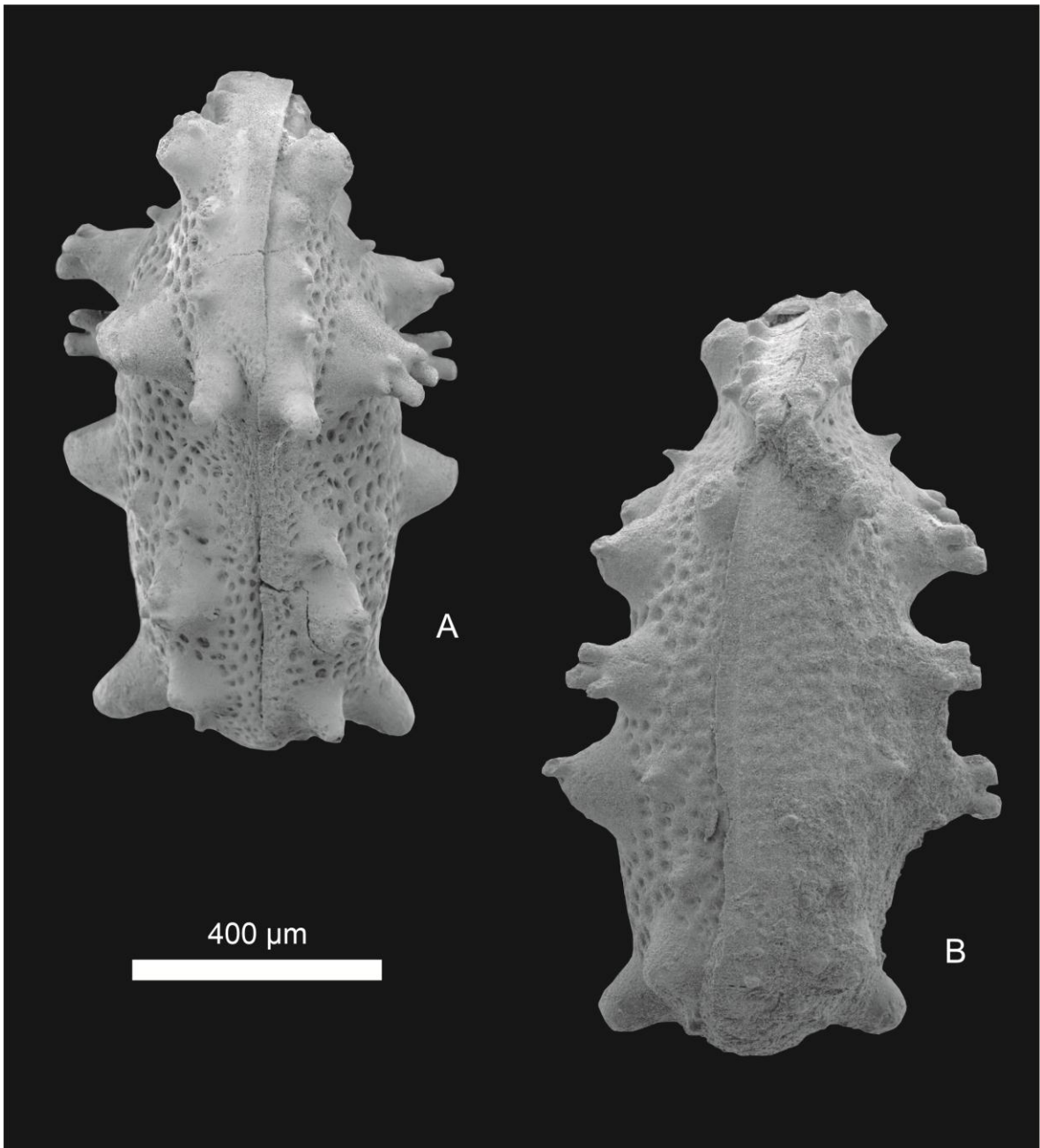


Plate 9: *Cypridea* sp. A (dorsal view, B5), B (ventral view, B5).

Class Ostracoda Latreille, 1806  
Order Podocopida Müller, 1894  
Superfamily Cytheroidea Braid, 1850  
Family Cytherideidae Sars, 1925  
Genus *Perissocytheridea* Stephenson, 1938

*Perissocytheridea* sp.  
Plate 10

**Material:** Few specimens have been recovered from Jezzine, Barouk and Qehmez sections (Table 3). The description below is based on the measurements of twenty carapaces from different samples.

**Description:** The carapaces are subovate in shape with sizes ranging between 605-1097  $\mu\text{m}$  in length, 378-648  $\mu\text{m}$  in height, and 480-503  $\mu\text{m}$  in width. The LV is overlapping the RV along the entire margin. The anterior margin and the dorsal margin are slightly infracuravte. The posterior cardinal angle is strongly rounded. The dorsal margin is straight and declined towards the posterior end moderately. Ventral margin is slightly convex. The surface of the carapace is reticulated forming ribs. Ribs display a triangular pattern in the central area of the carapace (Plate 10). The LV is larger than the RV. The anterior margin is narrower than the posterior margin.

**Stratigraphic range:** Fossil *Perissocytheridea* have been reported in Late Cretaceous deposits from Africa, Middle East, South America and southern Europe (Cusminsky et al., 2018). However, Trabelsi et al. (2015) reported *Perissocytheridea* in younger Lower Cretaceous deposits (lower Aptian) from the Central Tunisian Atlas. The stratigraphic range of the genus extends from Lower Cretaceous to Holocene (Swain & Brown, 1972).

**Paleoecology:** The genus *Perissocytheridea* has been related to lagoonal deposits and brackish water paleoenvironments (Swain & Brown, 1972; Grigg & Siddiqui, 1996; Trabesli et al., 2015). Their carapaces, however, are normally absent in fully marine facies (salinities higher than 30‰).

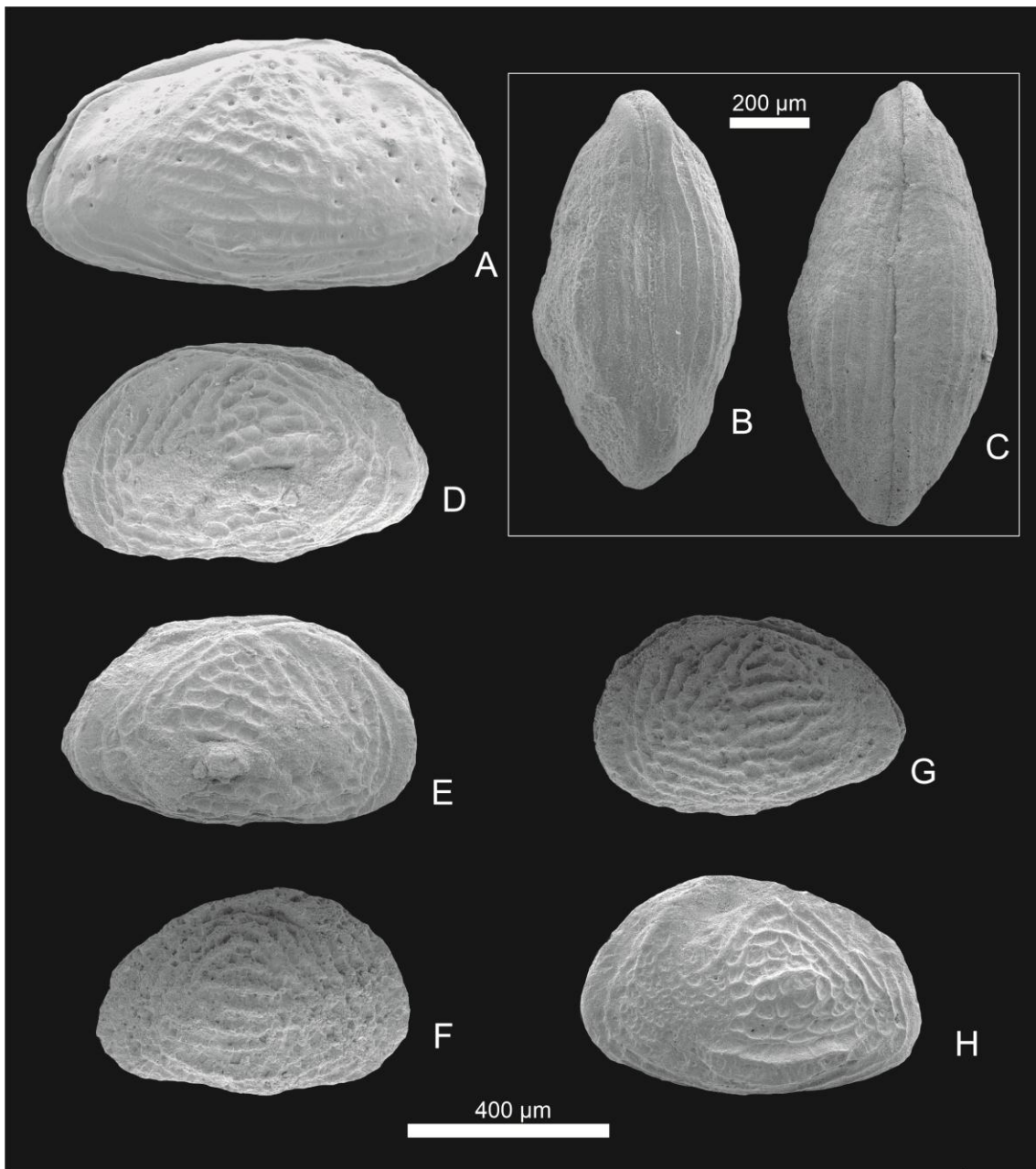


Plate 10: *Perissocytheridea* sp. A (right lateral view, J13), B (ventral view, J20), C (dorsal view, J20), D (lateral view, J20), E (lateral view, J20), F & G (lateral view, Q4), H (lateral view, J13).

Class Ostracoda Latreille, 1806  
Order Podocopida Müller, 1894  
Family Cytheruridae Müller, 1894  
Genus (*Meta*)*cytheropteron* Oertli, 1957

(*Meta*)*cytheropteron* sp.  
Plate 11

**Material:** Carapaces of this species have been found in only three samples (Table 3). Few carapaces have been recovered from Jezzine (samples J5 & J13) and more than one hundred carapaces have been extracted from Qehmez (sample Q4). Five valves have been measured.

**Description:** Carapaces are elongated in shape reminding the outline of an almond. The length of the carapaces is about 500 µm and their height is about 300 µm in average. The RV is overlapping the LV around the ventral margin. The ventral and dorsal margins are convex in shape. The anterior area is rounded in shape while the posterior area displays an elongated horn-like structure. The surface of the carapace is ornamented with longitudinal ridges.

**Stratigraphic range:** Middle Jurassic to Upper Cretaceous (Swain & Brown, 1972).

**Paleogeobiography and Paleoecology:** Species of this genus has been described in Egypt, Jordan, and Palestine in deposits related to shallow marine shelf environments. This genus has also been reported in marine rocks from Tunisia, Algeria, Saudi Arabia, Morocco and Portugal (Rosenfeld et al., 1988; Boukhary et al., 2009; Morsi & Wendler, 2010).



Few carapaces of other brackish to marine species have also been extracted from the studied sections. They have been provisionally attributed to *Ovocytheridea* sp. and *Doloccytheridea* sp. (Plate 12).

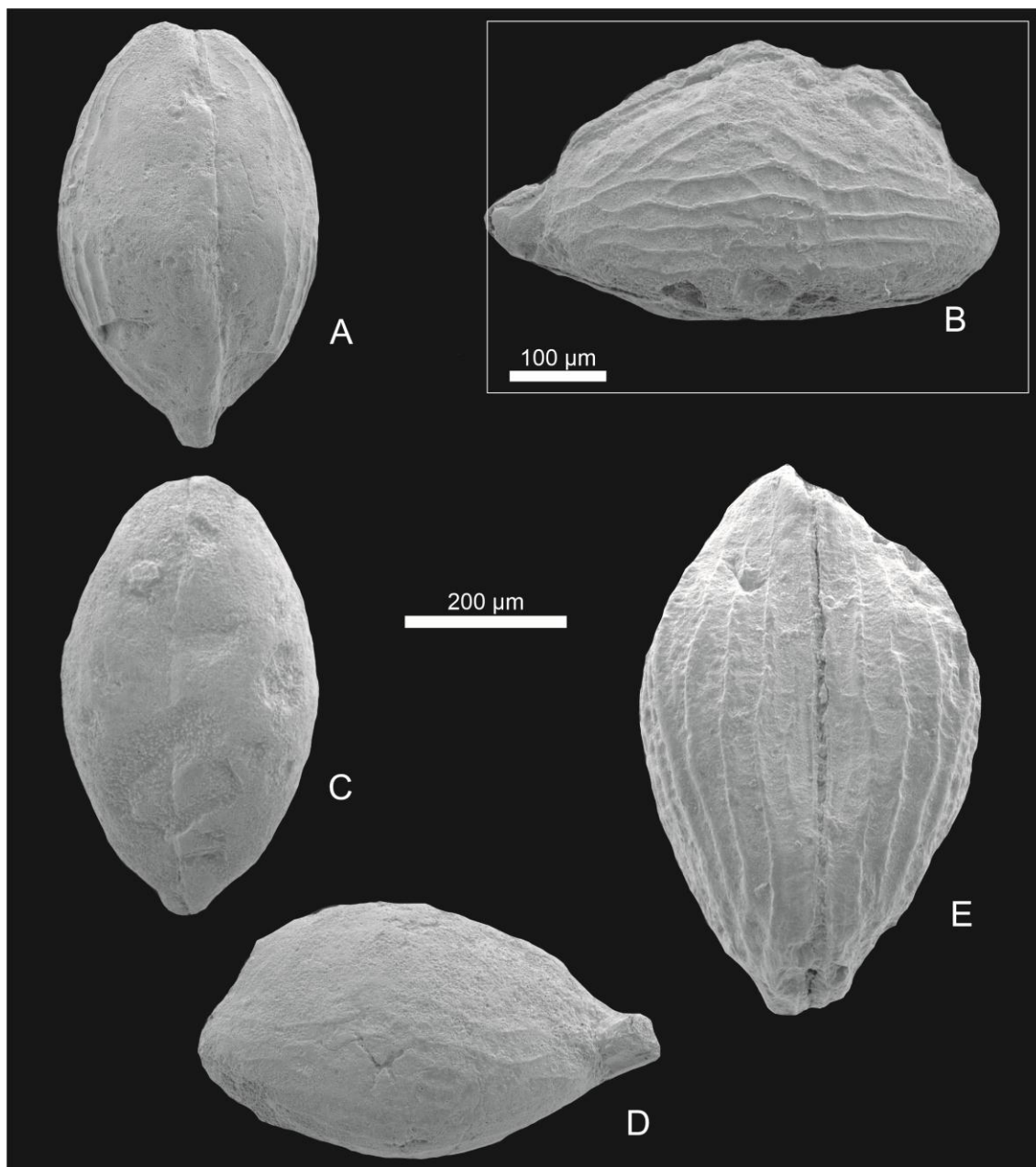


Plate 11: *(Meta)cytheropteron* sp. A & C (dorsal view, J5), B & D (lateral view, J5), E (ventral view, J13).

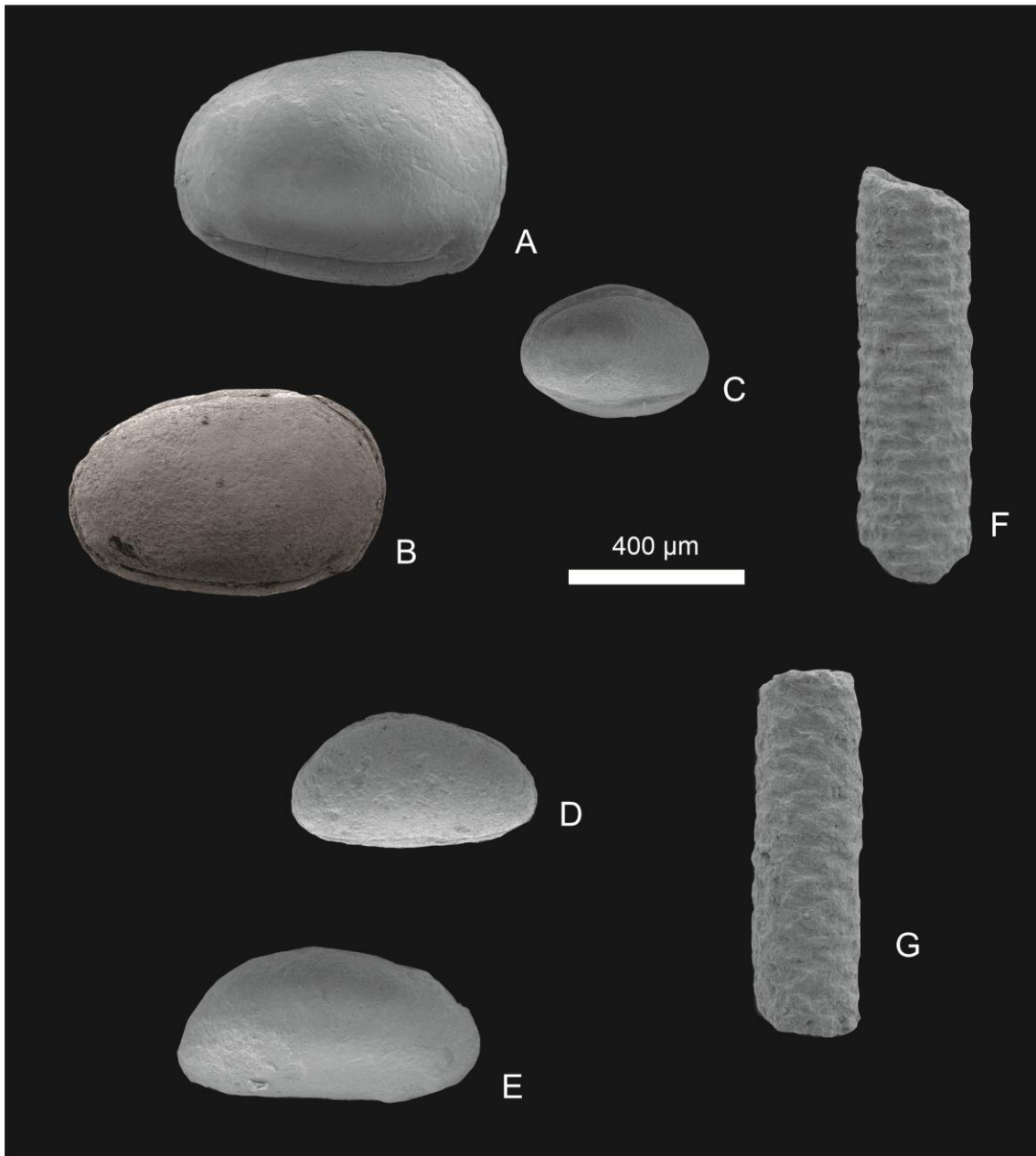


Plate 12: A (*Ovocytheridea* sp., right lateral valve, AZ.2), B (*Ovocytheridea* sp., right lateral valve, AZ.3), C (*Ovocytheridea* sp., right lateral valve, J5), D (*Dolocytheridea* sp., B5), E (*Dolocytheridea* sp., J20), F & G (*Salpingoporella dinarica*, AZ.2).

### 5.3. Foraminifera

Class Globothalamea Pawlowski et al., 2013  
Order Loftusiida Kaminski & Mikhalevich in Kaminski, 2004  
Family Spirocyclinidae (Munier-Chalmas, 1887) Maync, 1950  
Genus *Choffatella* Schlumberger, 1905

*Choffatella* cf. *decipiens* Schlumberger, 1905  
Plate 13, A-D

**Material:** Agglutinated shells of *C. decipiens* represent by far the dominant marine fossil in the studied sections. This species is also a common bioclast of the wackestone/packstone limestone beds in Jezzine. Several complete specimens have been extracted from soft samples (marls) in Jezzine, Qehmez, Barouk and Ain Dara sections (Table 3). Five specimens were measured.

**Description:** Type of agglutinated shell of benthic foraminifera. The shell is planispiral and compressed showing multiple chambers. Shells range in diameter between 540 µm and 750 µm. Several morphologies have been observed: rounded shells (Plate 13, A & D), and elongate shells where the last chambers are not planispiral (Plate 13, C). In addition, the type of the agglutinated particles varies from very fine (Plate 13, Fig. A) to coarse (Plate 13, B).

**Biostratigraphy:** According to Jaffrezo (1980), this species has a biostratigraphic range covering the complete Early Cretaceous time span i.e. Hauterivian to middle Aptian.

**Paleobiogeography:** *Choffatella decipiens* represents a cosmopolitan species that thrived mainly in shallow marine environments of the Tethys Ocean. It has been reported in lower Aptian deposits from Mexico (Omaña & Alencáster,

2009), lower Campanian, Barremian and Aptian rocks in north of Spain (Albrich et al., 2015; Flügel, 2010), Barremian to lower Aptian sedimentary sequences in SW of Iran (Hosseini et al., 2016), lower Aptian rocks in Romania (Neagu & Cîrnaru, 2004) and Aptian deposits in Lebanon (Saint-Marc, 1970; Maksoud et al., 2014).

**Paleoecology:** *Choffatella decipiens* has been extracted from marine rocks related to two different depositional environments; 1) high energy shallow-water associated with Dasycladales algae and orbitolinid foraminifera, and 2) deep water facies related to low energy associated with small benthic and planktonic foraminifera, pelagic echinoids and bivalve shells (Hosseini et al., 2016). Other authors indicated that this species mainly occurs forming packstone facies related to very shallow energetic conditions (Jaffrezo, 1980). Cusminsky et al. (2018) recently reinforced this idea indicating that *C. decipiens* may be related to restricted lagoonal environment. The high amount of well-preserved shells of *C. decipiens* in almost all the studied sections and their co-occurrence with charophyte remains in both marls and limestones also indicates that this species lived in very shallow coastal environments subjected to freshwater inputs.

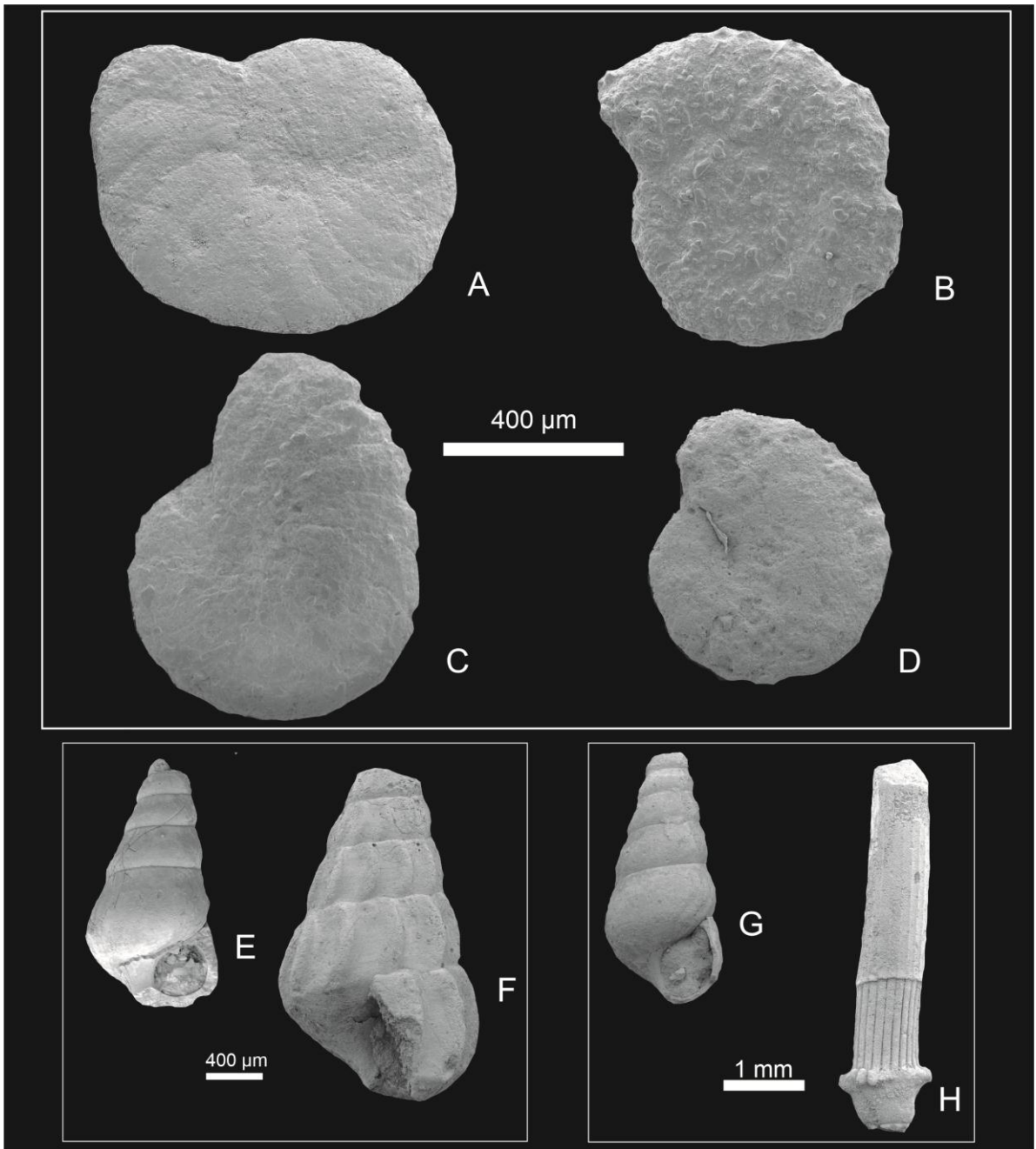


Plate 13: A, B, & C (*Choffatella* cf. *decipiens*, B5), D (*Choffatella* cf. *decipiens*, Q4), E (Potamididae, B5), F & G (Potamididae, AZ.1), H (basal part of an echinoid spine).

#### **5.4. Other micro and macrofossils**

Other fossils have been recovered from the studied sections. However, their occurrence is very low. A preliminary description and illustration is here provided.

##### **5.4.1. *Dasycladal thalli***

Fragments of dasycladal thalli have been recovered mainly from the Azzouniye section 1 and Jezzine section 1 (Plate 12, F & G). Few remains were also extracted from Barouk and Ain Dara (Table 3). Dasycladales are shallow marine calcareous green algae living in low energy shallow marine and brackish waters from tropical and subtropical areas (Huyghe et al., 2017 and references herein). The morphological characteristics and dimensions of the dasycladales thalli found in the studied section are fully consistent with the species *Salpingoporella (Hensonella) dinarica* Radoičić, 1959. This species has been previously reported in lower Cretaceous rocks from Lebanon by Granier et al. (2015). *S. dinarica* represents a common microfossil occurring in Early Cretaceous (Hauterivian-late Aptian) Tethyan marine sediments related to shallow water environments (Simmons et al., 1991). Fossils of this species recovered in Azzouniye and Ain Dara show signs of erosion and abrasion suggesting that they suffered some transport before their final burial. In contrast, fossils from the Jezzine section are well preserved. Different sections of these microfossils can be observed in limestone beds from Jezzine (Appendix A, Fig. 95B & C).

### **5.4.2. *Gastropods***

A reduced number of gastropod fragments have been found in the studied sections (Table 3). All recovered shells lack the apex and the aperture hindering their taxonomic classification. The absence of complete gastropod shells in the studied soft samples suggests that shells were transported away from their original thriving localities. The ornamentation pattern (elongated ribs) and shell angle (conical) observed in some specimens indicate that they may belong to the gastropod family Potamididae (Plate 13, E-G). This family of gastropods mainly thrives in brackish water environments such as mud flats and mangroves (Reid et al., 2008).

### **5.4.3. *Echinoid remains***

Few echinoid remains including sea urchin spines (Plate 13, H) were recovered in some samples from Jezzine, Barouk and Qehmez sections (Table 3). Sea urchins are fully marine fauna living in intertidal zones and downwards (Kroh, 2010). Spines extracted from Barouk and Jezzine sections display evident signs of abrasion. It suggests that these fossils are allochthonous.

### **5.4.4. *Vertebrate remains***

#### **5.4.4.1. Teeth**

Vertebrate remains (i.e. fish remains), mainly teeth fragments (crowns), have been extracted from Jezzine, Barouk, Ain Dara and Azzouniye sections (Table 3).

Recovered teeth fragments display different morphologies and sizes (Plate 14). The semi-oval crown shape of some teeth (Plate 14, E & F) could be related to fishes of the Batoidea family i.e. ray fishes (pers. comm. George Kachacha). The asymmetry and surface structure (elongated ridges) observed in some specimens (Plate 14, D) suggest that these teeth have a reptilian origin. Another larger reptilian tooth (crown) of 4.8 mm width and 4 mm high has been extracted from sample J12 (Fig. 45). It is characterized by a lanceolated shape, labiolingually compressed showing vertical wrinkles and a characteristic carina (crenulated edge) which can be tentatively related to crocodiles (pers. comm. Dr. Pedro Mocho). However, further studies must be performed to better classify these fossils.



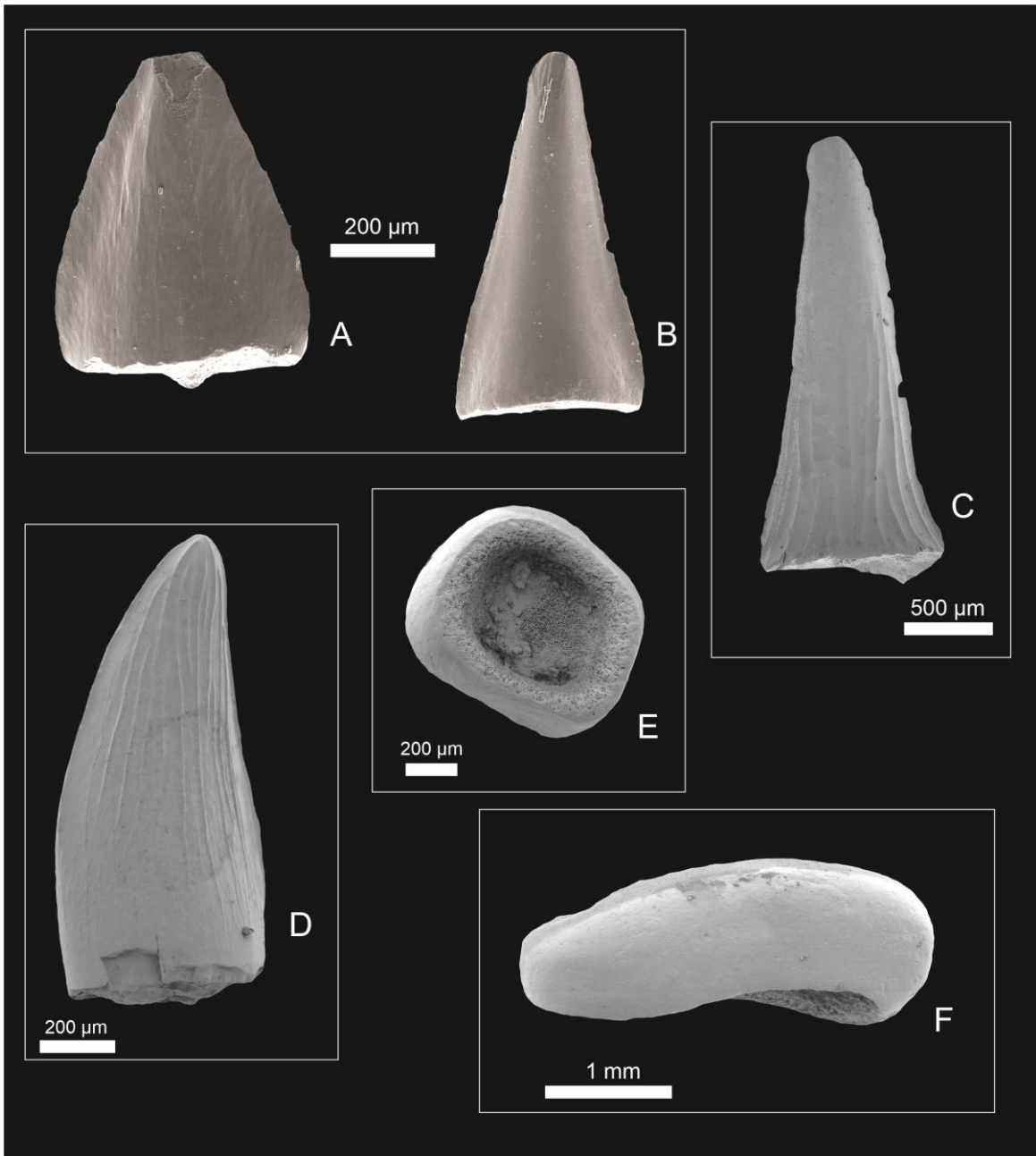


Plate 14: Assemblage of teeth. A & B (from AZ.2), C (from J12), D (from AD.0), E & F (from J15).



Figure 45: SEM photo of the reptilian tooth recovered from Jezzine section (J12).

#### 5.4.4.2. Bones

Few bone fragments have been extracted *in situ* from the Jezzine section (below sample J12). They are poorly preserved showing signs of abrasion. It suggests that they were transported before their final burial (Fig. 46). The dimensions and characteristics of these bones suggest that they would belong to dinosaur remains (pers. com. Dr. Pedro Mocho). However, further histological analyses (bone structure and texture) are required to classify these fragments.



Figure 46: Bone fragments recovered from the Jezzine section 1.

#### **5.4.5. *Vegetal remains***

Vegetal remains include wood fragments, amber and leaf cuticles which are particularly abundant in some marl intervals in Jezzine (Fig. 47). Wood fragments may be up to 30 cm in length and they may be carbonized. They have been related to conifers (pers. comm. Dr. Dany Azar) and occur dispersed in marl intervals (Fig. 48). Amber pieces and cuticles occur associated within organic rich layers occasionally forming lignite horizons. Lower Cretaceous Lebanese amber has been extensively studied with regards to its inclusions i.e. insects and palynomorphs (Kirejtshuk & Azar 2013). According to these authors, amber fragments were transported for short distances based on the exceptional preservation state of their inclusions. Nineteen insect orders such as Archeognatha, Blattodea, Coleoptera, Collembola, Dermaptera, Diptera, Ephemeroptera, Hemiptera, Hymenoptera, Isoptera, Lepidoptera, Mantodea, Neuroptera, Odonata, Orthoptera, Psocodea, Thysanoptera, Thysanura, and Trichoptera have been reported in the Lebanese amber (Kirejtshuk & Azar 2013 and references herein). These authors indicated that

most of the insect groups are related to a hot and humid climate with arboreal and litter habitats. This idea is in concordance with the palynological data obtained by Azar et al. (2001). The palynomorph assemblages from amber-bearing clays are dominated by high diversity of ferns, some conifers such as *Araucaria* and rare angiosperms suggesting that a dense, wet and hot tropical forest prevailed in the region during the Barremian-Aptian ages (Azar et al., 2001).

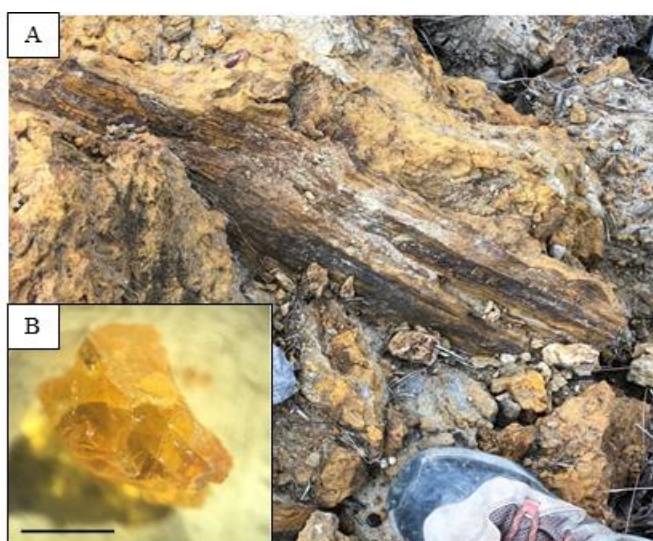


Figure 47: A) Field photo of a large conifer trunk located at the base of the Jezzine section 1. B) Amber fragment recovered from an organic-matter rich interval at the base of the Jezzine section 1, scale bar 1mm.



Figure 48: Detailed photo of a conifer wood fragment recovered at the base of the Jezzine section 1.

## CHAPTER 6

### DISCUSSION & CONCLUSION

#### 6.1. Microfossil taphonomy and paleoecology

The studied sedimentary sequences yielded a large and diverse number of microfossils (charophytes, ostracods, foraminifera, echinoids, mollusks, dasycladals and vertebrate remains) that display a characteristic vertical succession and facies association. This vertical succession helps in the characterization of the environmental evolution of the coastal area of Lebanon during the Lower Cretaceous marine transgression.

In general, three microfossil assemblages can be distinguished in agreement with the facies succession: 1) Coastal lake assemblage; 2) Estuary assemblage; 3) Shallow marine assemblage.

***Coastal lake assemblage.*** This assemblage occurs in the Ain Dara and top of Barouk section 1 and consists of 5 species of charophytes (*Atopochara trivolvis trivolvis*, *Clavator ampullaceus*, *Ascidiella reticulata*, *Sphaerochara asema*, *Mesochara harrissi* and *Clavatoraxis martinclusasi*) and 3 species of ostracods (*Cypridea tuberculata*, *C. piedmonti* and the new species *Cypridea* sp.). Charophytes fructifications (utricles and gyrogonites) represent by far the dominant group of microfossils. They are well preserved and occur associated with charophyte thalli in both marls and limestones. Ostracod carapaces occur normally

articulated (both valves attached) displaying their delicate ornamentation intact. These evidences suggest that the fossil assemblage was buried *in situ*. Other accessory abraded microfossils such as dasycladal thalli and agglutinated shells of foraminifera also occur within the marl beds. The sedimentological, micropaleontological and taphonomic analyses indicate that marls and limestones from Ain Dara and top of Barouk section 1 were deposited in shallow freshwater lakes near the coast (Fig. 49). The low abundance of abraded fossils of the endemic species *Sphaerochara asema* and *Cypridea* sp. as well as the cosmopolitan *Mesochara harrissi* in the other two assemblages indicate that they were exclusively freshwater groups.

***Estuary assemblage.*** This assemblage mainly occurs in the Jezzine section 1 and Azzouniye section 1. It consists of 1 species of dasycladal i.e. *Salpingoporella dinarica*, 2 species of charophytes (*Clavator ampullaceus* and *Ascidiella reticulata*) 5 species of ostracods (*Cypridea tuberculata*, *C. piedmonti*, *Perissocytheridea* sp., *Ovocytheridea* sp. and *Dolococytheridea* sp.), and 1 species of agglutinated foraminifera i.e. *Choffatella decipiens*. Well-preserved dasycladal thalli represent the dominant microfossil in this assemblage. Ostracod carapaces occur normally articulated (both valves attached). Ostracod shells and charophyte utricles are complete showing their external ornamentation intact indicating autochthony. Shells of *Choffatella* are also complete and well-preserved. Poorly preserved echinoid spines and vertebrate fragments (teeth and bones) also occur in minor amount suggesting that they were transported from marine and continental settings

respectively. The sedimentological, micropaleontological and taphonomic analyses indicate that burrowed silty marl beds from the Jezzine section 1 and Azzouniye section 1 were deposited in a restricted brackish water environment located in an estuary (Fig. 49). The occurrence of the charophyte species *C. ampullaceus* and *Asc. reticulata* and the ostracods *C. tuberculata* and *C. piedmonti* in both freshwater coastal lakes and estuaries indicate that these extinct taxa were euryhaline able to thrive in oligohaline and mesohaline conditions.

***Shallow marine assemblage.*** This assemblage mainly occurs in some intervals of the Jezzine section 1 and the complete Qehmez section 2. It is represented by fully marine microfossils such as indeterminate echinoid spines, shells of the foraminifera (*Choffatella decipiens*, *Textularia* sp. and miliolids), dasycladal thalli *Salpingoporella dinarica* and few shells of marine ostracod (*Dolocytheridea* sp., (*Meta*)*cytheropteron* sp., and *Ovocytheridea* sp.). Based on this information, marls and limestone beds from the Jezzine section 1 and Qehmez section 2 were formed under shallow marine conditions in a carbonate platform (Fig. 49). It worth mentioning that the presence of complete shells of the well-known Tethyan agglutinated foraminifera *C. decipiens* in both estuary and shallow marine facies indicates that it was an euryhaline species living in very shallow coastal environments and subjected to some freshwater inputs.



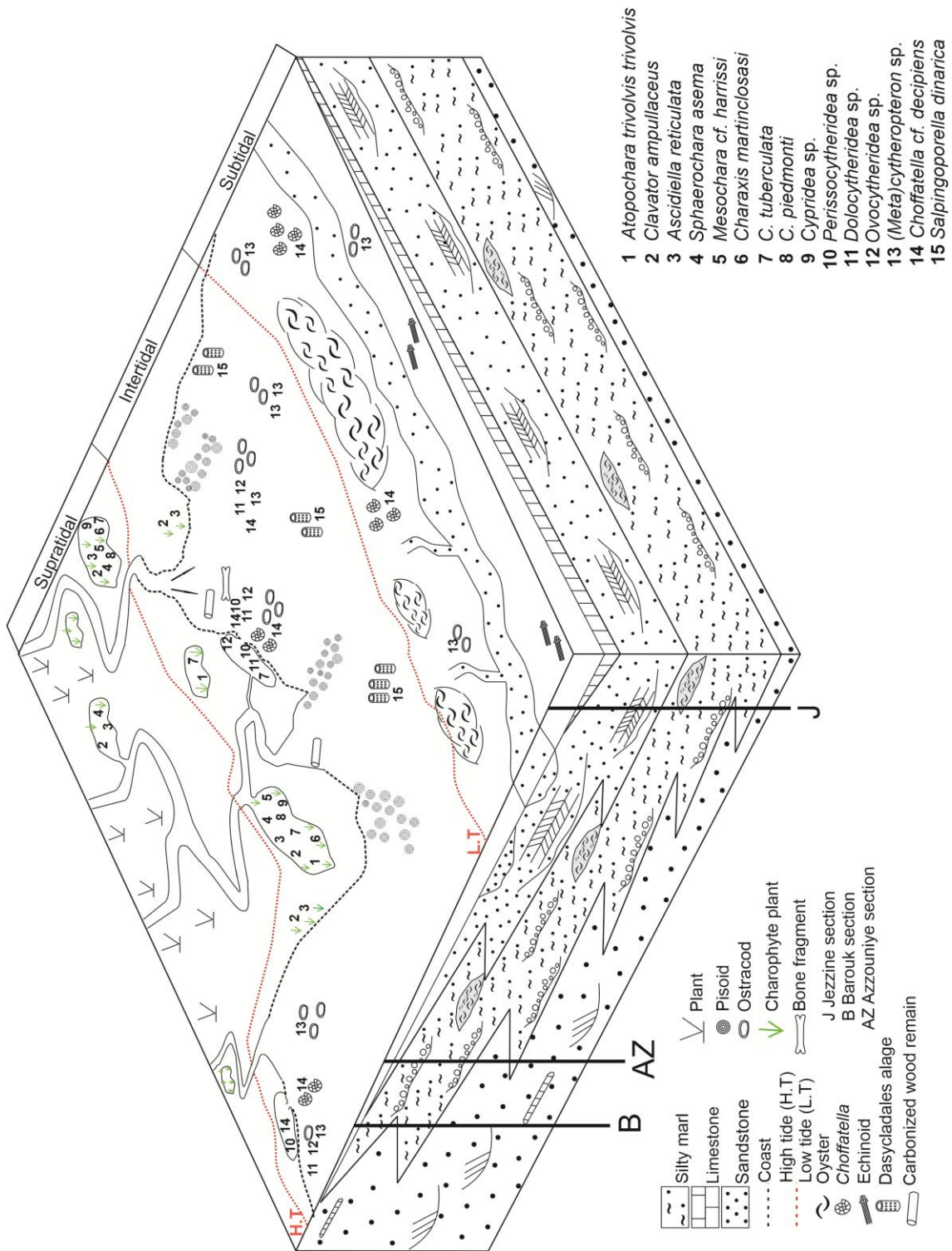


Figure 49: Paleoecological model showing a transgression hemicycle in the Abeih Fm at Jezzine (J), Azzouniye (Az) and Barouk (B). Note the distribution of facies belts as well as the microfossil assemblages.



## 6.2. Biostratigraphy

The microfossil assemblage extracted from the transitional Lower Cretaceous deposits in Lebanon is composed of several species with biostratigraphic interest. Among the charophyte species, only 3 i.e. *Atopochara trivolvis* var. *trivolvis*, *Clavator ampullaceus* and *Ascidiella reticulata* are significant. *A. trivolvis trivolvis* is a cosmopolitan and well accepted species characterizing the early Aptian-middle Albian periods (Martín-Closas, 2000). According to Grambast and Lorch (1968), *C. ampullaceus* and *Ascidiella reticulata* indicate older ages i.e. Barremian-lower Aptian. However, Riveline et al. (1996) stated that *Ascidiella reticulata* could be also found in late Aptian to middle Albian ages. The occurrence of *A. trivolvis* var. *trivolvis* and *Ascidiella reticulata* allows us to correlate the Abeih Formation/upper part of the “Grès de Base” with the European charophyte biozone named *Clavator grovesii lusitanicus* (Riveline et al., 1996) indicating late Aptian-middle Albian ages. However, this relative age can only be applied in the European basins since the position of Lebanon during the Early Cretaceous was much farther from Europe (equatorial latitude) than nowadays. Hence, the attribution of the relative age of the Abeih Fm or the “Grès de Base” based on this European biozonation should be taken with caution.

The recovered ostracod fauna suggests however, older ages than charophytes. Only two species i.e. *Cypridea tuberculata* and *Cypridea piedmonti* are biostratigraphically significant. *C. tuberculata* has been recorded in upper Berriasian to lower/middle Barremian rocks while *C. piedmonti* is early Valanginian to late Barremian in age (Fig. 50). The presence of both species

together with the well-known and cosmopolitan *A. trivolvis* var. *trivolvis* allows us to extend their stratigraphic ranges into the lower Aptian (dotted lines in Fig. 50). Marine microfossils extracted from the studied lithologic unit i.e. *Choffatella decipiens* and *Salpingoporella dinarica* are common in Tethyan rocks ranging in age from Hauterivian to upper Aptian (Fig. 50).

The proposed age of the upper boundary of the studied lithologic unit i.e. the upper part of the Abeif Fm or the uppermost part of the “Grès de Base” (below the Banc de Mrejatt) is late Barremian to early Aptian (between ~ 126-120 Ma) which disagree with the age reported by Maksoud et al. (2017).

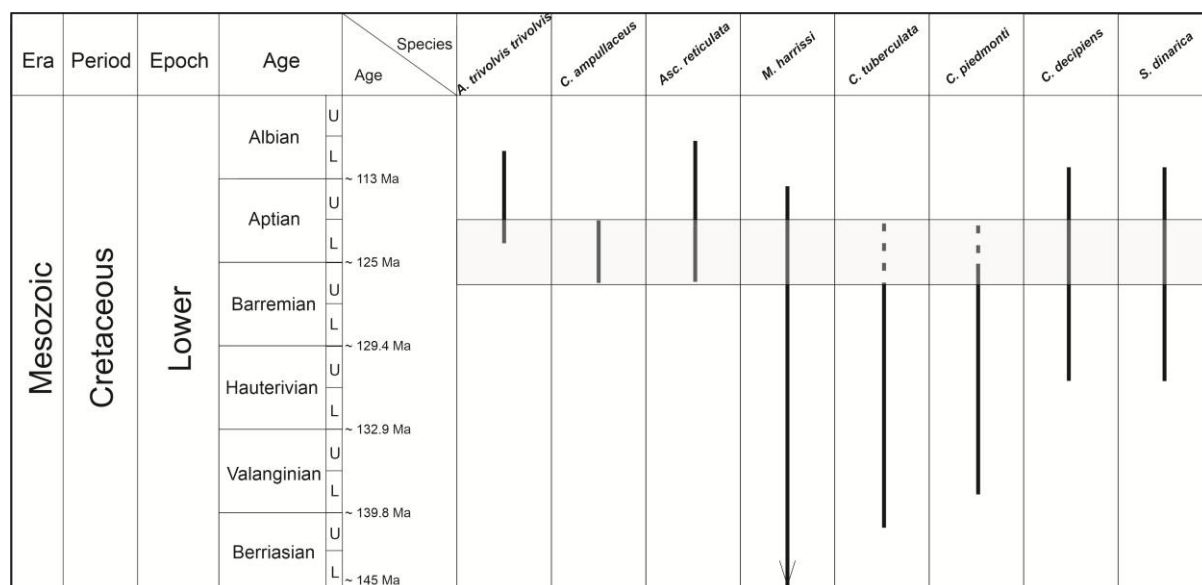


Figure 50: Lower Cretaceous chronostratigraphy. Suggested age of the upper boundary of the studied lithologic unit (shadow rectangle) according to the microfossil assemblage.

### 6.3. Paleobiogeography

This study provides significant data regarding the paleogeographic distribution of several Early Cretaceous freshwater microfossils within the

Mesogea. Because of its geographic position between Europe, Asia and Africa, Lebanon and the whole Middle East region represents a very interesting area for paleobiogeographical studies which may have important implications in the biostratigraphic correlation between distant non-marine basins.

### **6.3.1. Charophytes**

Several species of charophytes have been recovered within the Abeih Formation/upper part of the “Grès de Base”. Almost all species display a local or regional distribution within the southeast Tethys coastal regions (nowadays Lebanon, Palestine and Somalia). The species *Asciadiella reticulata* had a wider distribution occurring also in the western Tethys archipelago (Fig. 51).

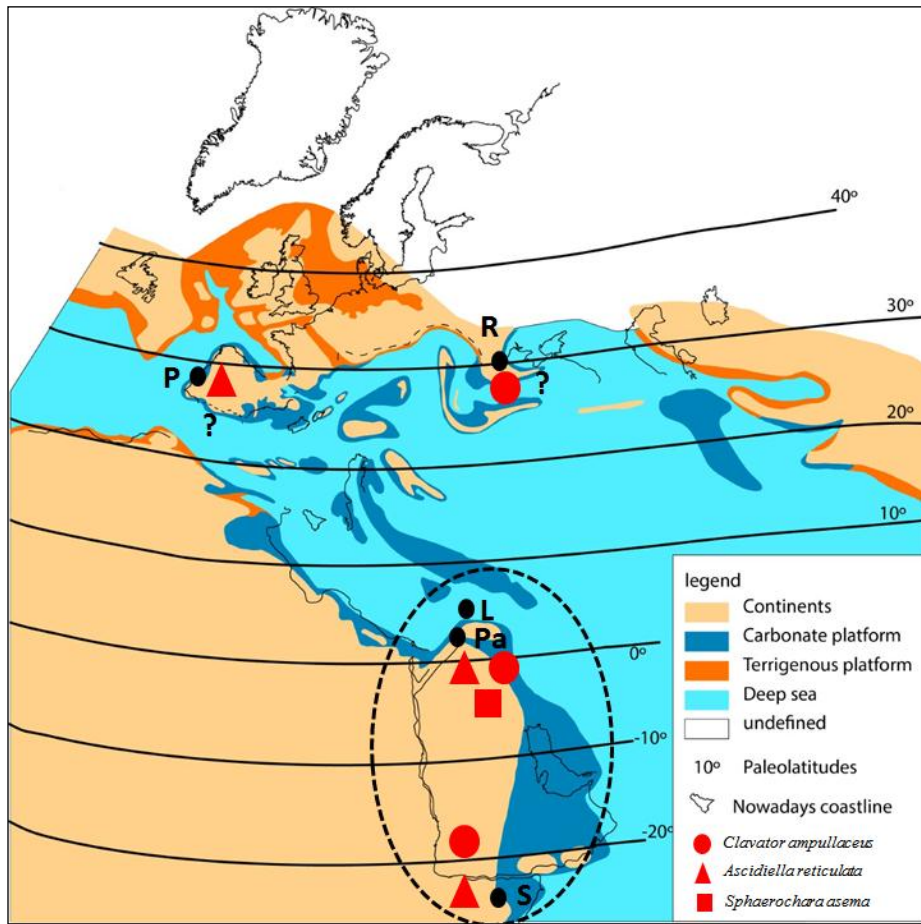


Figure 51: Paleogeographic map of mesogea during the Lower Cretaceous (Barremian-Aptian) showing the distribution of the dominant charophyte species recovered in the Abeih Fm./“Grès de Base”. *Clavator ampullaceus*, *Ascidiella reticulata* and *Sphaerochara asema*. Capital letters represent the position of the 5 main localities from where these species were found. The dashed ellipse indicates the possible bioprovince where this assemblage thrived. **S**= Somalia, **Pa**=Palestine, **L**=Lebanon, **P**= Portugal, **R**= Romania. Note the latitudinal position of Lebanon (in the Equator) during the Early Cretaceous. Paleogeographic map modified from Decourt et al. (1993).

Two species i.e. *Atopochara trivolvis* var. *trivolvis* and *Mesochara harrisi* had a worldwide distribution (Fig. 52). Only the species *Atopochara trivolvis* var. *trivolvis* has a biostratigraphic interest occurring in Aptian continental deposits

from south Europe, Middle East, Asia, North America, South America and North Africa (Martín-Closas & Wang, 2008).

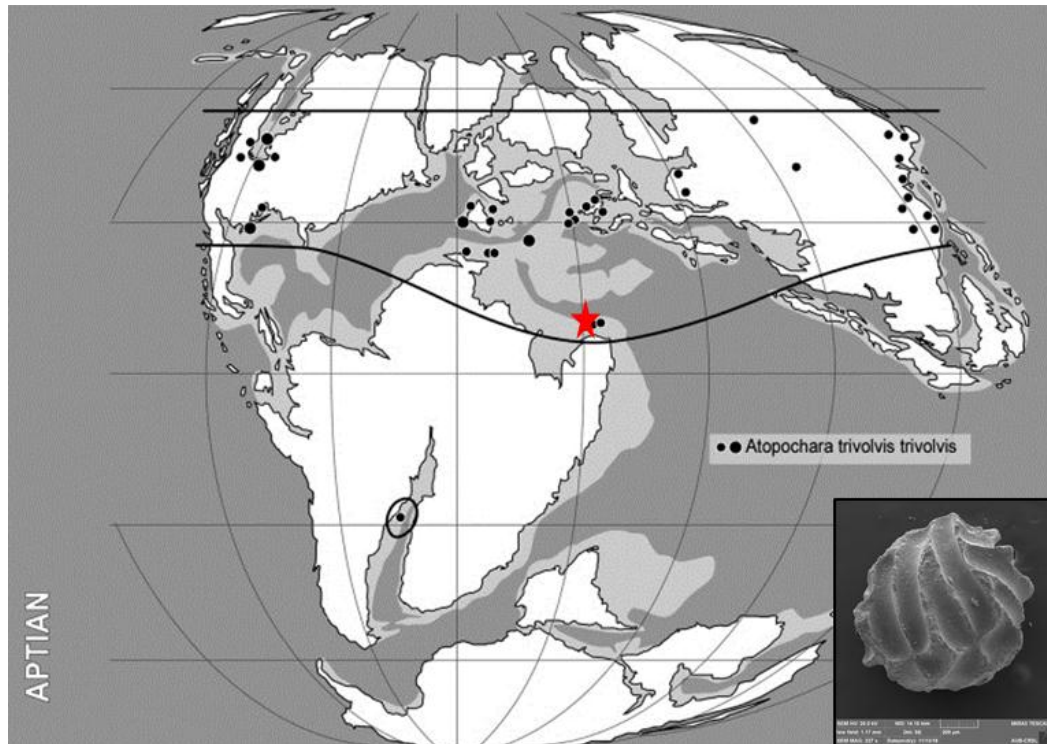


Figure 52: Biogeographic distribution of *Atopochara trivolis* var. *trivolis* on a paleogeographic map of the world at 120 Ma. Black dots represent the reported geographic location of this species in the Mesogea. The red star represents the occurrence of this species in Lebanon (extracted from Martín-Closas & Wang 2008).

In general, the charophyte diversity recovered from the Abeih Formation is low, which is in contrast with the high diversity in the coeval European and North African basins. Up to 20 species have been described in these peri-Tethyan basins (Martín-Closas and Serra-Kiel 1991).

The low diversity and the apparent regional distribution of Lebanese charophytes (restricted in the southeastern peri-Tethyan basins) allow defining a

separate bioprovince, different from the northern peri-Tethyan archipelago (Fig. 51). This distributional pattern could be related to differences in climatic conditions prevailing during the Lower Cretaceous in the Middle East and Northeast Africa. In fact, paleogeographic reconstructions indicate that the region of nowadays Lebanon was located at much lower latitudes than the present day (Decourt et al., 1993). The equatorial position of Lebanon during the Barremian-Aptian ages suggests that climatic conditions in the region were warmer than northern Tethys basins. This interpretation is in agreement with the paleoecological work of Azar et al. (2001) suggesting that dense, wet and hot tropical forests grew in the area.

### **6.3.2. Ostracods**

Two species of ostracods with biostratigraphic interest have been recovered within the Abeih Formation/upper part of the “Grès de Base” i.e. *Cypridea tuberculata* and *Cypridea piedmonti*. These findings represent the first report of these *Cypridea* in Lebanon and the whole Middle East. Both taxa display a cosmopolitan distribution occurring in North America and Europe and Middle East. In the Tethys realm, these species occur in both northwest and southeast margins (Fig. 53). The widespread distribution of these taxa in different coetaneous paleolatitudes would indicate that they were tolerant to a wide array of climatic conditions.

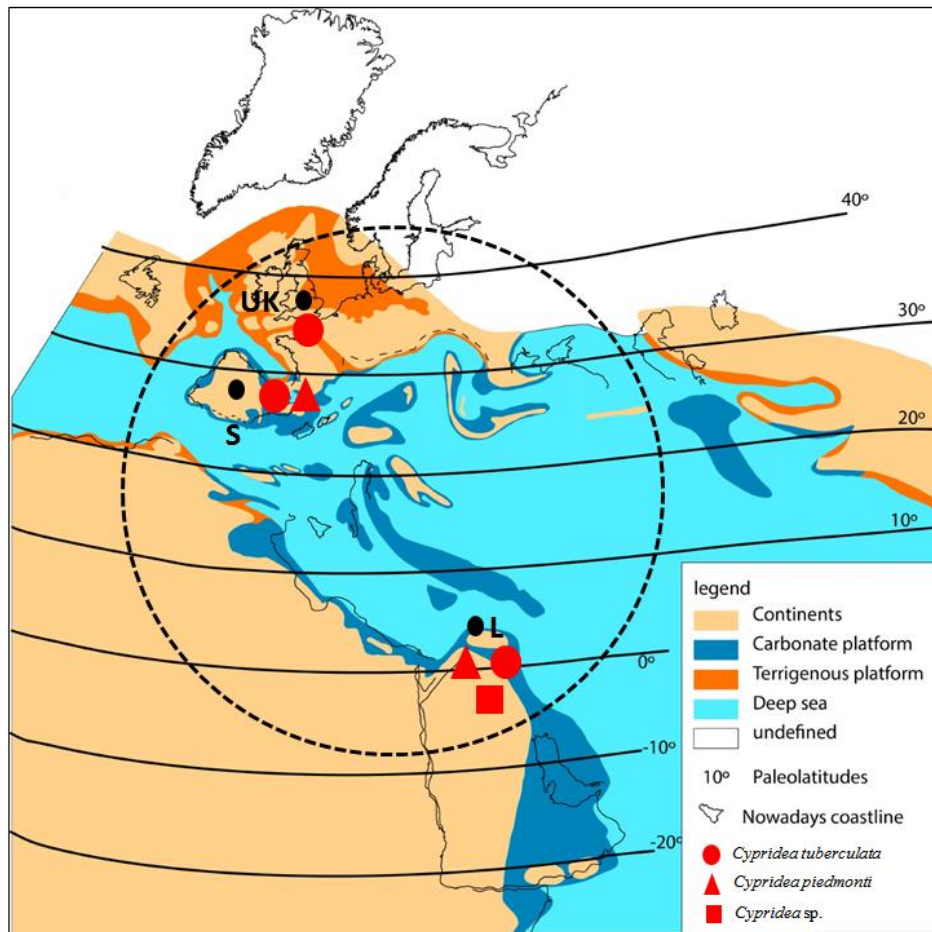


Figure 53: Paleogeographic map of Mesogea during the Lower Cretaceous (Barremian-Aptian) showing the distribution of the dominant *Cypridea* ostracod species recovered in the Abeih Fm./“Grès de Base”. Capital letters represent the position of the 3 main localities from where these species were found. The dotted circle indicates the possible bioprovince where this assemblage thrived in the Tethys realm. **UK**= United Kingdom, **S**=Spain and **L**=Lebanon. Paleogeographic map modified from Decourt et al. (1993).

#### 6.4. Conclusion

Transitional Lower Cretaceous deposits in central Mount Lebanon near the villages of Ain Dara, Azzouniye, Qehmez, Barouk and Jezzine have been analysed from the sedimentological and micropaleontological viewpoints. Studied rocks are stratigraphically located in the Chouf and Abeih formations in the sense of Walley

(1983) or the upper part of the “Grès de Base” in the sense of Maksoud et al.

(2014).

Facies analysis of the nine studied sections indicates that the Central Mount Lebanon was occupied by fluvial deposits changing laterally and vertically to estuary (intertidal, subtidal), shallow marine and carbonate sand shoal.

A rich microfossil assemblage is here described and illustrated considering the paleoecology, paleobiogeography and biostratigraphy. It is composed of 7 species of charophytes (*Atopochara trivolvis* var. *trivolvis*, *Clavator ampullaceus*, *Asciidiella reticulata*, *Sphaerochara asema*, *Mesochara harrissi*, *Charaxis martinclousasi* and *Charaxis* sp.), 7 species of freshwater, brackish water and marine ostracods (*Cypridea tuberculata*, *C. piedmonti*, *Cypridea* sp., *Perissocytheridea*, (*Meta*)*cytheropteron*, *Dolococytheridea* and *Ovocytheridea*), 1 species of agglutinated foraminifera *Choffatella decipiens*, 1 species of dasycladal algae *Salpingoporella dinarica*, mollusk fragments, echinoid remains and vertebrate teeth and bone fragments.

These fossils have been grouped in three distinct assemblages in concordance with with facies and taphonomy i.e. coastal lake; estuary and shallow marine.

The paleobiogeographical analysis of the charophyte and ostracod assemblage indicates an opposite distributional pattern within the Peri-Tethyan realm.

Ostracods occur in both northwest and southeast margins of the Tethys. Whereas, charophytes show a regional distributional pattern within the Middle East and northeastern Africa.



Based on the biostratigraphic range of some of the recovered microfossils, late Barremian to early Aptian age is proposed for the upper part of the Abeih Formation/upper part of the “Grès de Base”.

The results of this study are being disseminated in specific international congresses and will be published in scientific journals indexed in the Journal of Citation Reports (ISI) focused on micropaleontology and paleoecology.

## REFERENCES

- Agardh, C.A. (1824). *Systema Algarum*. Lund, Lundae Literis Berlingianis, 312 p.
- Albrich, S., Boix, C., & Caus, E. (2015). Selected agglutinated larger foraminifera from the Font de les Bagasses unit (Lower Campanian, southern Pyrenees). *Carnets de Geologie*, 15(18), 245-267.
- Anadón, P., Cabrera, L., Choi, S., Feist, M., Colombo, F., & Saez, A. (1992). Biozonación del Paleógeno continental de la zona oriental de la Cuenca del Ebro mediante carófitas: implicaciones en la Biozonación general de carófitas de Europa occidental. *Acta Geologica Hispanica* 27(1-2), 69-94.
- Anadón, P., Utrilla, R., & Vázquez, A. (2000). Use of charophyte carbonates as proxy indicators of subtle hydrological and chemical changes in marl lakes: Example from the Miocene Bicorn Basin, eastern Spain. *Sedimentary Geology*, 133(3-4), 325-347.
- Anderson, F.W. (1939). Wealden and Purbeck ostracoda. *Annals and Magazine of natural history*, 11(3), 291-310.
- Anderson, F.W. (1971): Part II. The ostracods. In: Anderson, F.W. & Bazley R.A.B. The Purbeck beds of the Weald. *Bulletin of the Geological Survey of Great Britain* (34), 1-173.
- Azar, D. (2007). Preservation and accumulation of biological inclusions in Lebanese amber and their significance. *Comptes Rendus Palevol*, 6, 151-156.
- Azar, D., Dejax, J., & Masure, E. (2001). Palynological Analysis of Amber-Bearing Clay from the Lower Cretaceous of Central Lebanon. *Acta Geologica Sinica* 85(4), 942-949.
- Azar, D., & Ziadé, K. (2005). *Xenopsychoda harbi* a new psychodoid fly from the Lower Cretaceous amber of Lebanon (Diptera, Psychodoidea). *Comptes Rendus Palevol*, 4, 25-30.
- Baird, W. (1845). Arrangement of the British Entomostraca, with a list of species, particularly noticing those which have as yet been discovered within the bounds of the club. *Transactions of the Berwickshire Naturalist's Club*, 2(13), 145-158.
- Baird, W. (1850). *The Natural History of the British Entomostraca*. Ray Society, London. 364 p.

- Bellier, J-P., Mathieu, P., & Granier, B. (2010). Short treatise on foraminiferology (Essential on modern and fossil Foraminifera). Carnets de Géologie - Notebooks on Geology, Brest, 104 p.
- Bellos, G.G. (2008). *Sedimentology and Diagenesis of Some Neocomian-Barremian Rocks (Chouf Formation), Southern Lebanon* (Unpublished master's thesis). American University of Beirut, 251 p.
- Benoit, R. A., Néraudeau, D., & Martín-Closas, C. (2017). A review of the Late Jurassic- Early Cretaceous charophytes from the northern Aquitaine Basin in south-west France. *Cretaceous Research*, 79, 199-213.
- Beydoun, Z.R. (1977). Petroleum Prospects of Lebanon: Reevaluation. *AAPG Bulletin*, 61(I), 43-64.
- Beydoun, Z. R. (1995). Productive Middle-East chiastic oil and gas reservoirs: Their depositional settings and origins of their hydrocarbons. *Special Publications of the International Association of Sedimentologists*, 23, 331-354.
- Beydoun, Z.R. (1997). The Levantine Countries: The Geology of Syria and Lebanon (Maritime Regions). In: Naim, A., Kanesh, W.K. & Stehli F.G. (Eds.), *The Ocean Basins and Margins*, 4A, 319-353.
- Blanche, C.I. (1947). Lettre du Liban. *Bulletin de la Societe Geologique de France*, 2(5), 12-17.
- Boggs, S. (2014). *Principles of Sedimentology and Stratigraphy*. Boston, Prentice Hall, 556 p.
- Bosquet, J. (1852). Description des Entomostracés Fossiles des Terrains Tertiaires de la France et de la Belgique. *Mémoires Couronnés et Mémoires des Savants Étrangers*, 24, 1-142.
- Boukhary, M., Morsi, A. M., Eissa, R., & Kerdany, M. (2009). Late Cenomanian ostracod faunas from the area south of Ain Sukhna, western side of the Gulf of Suez, Egypt. *Geologia Croatica*, 62(1), 19-30.
- Branson, O., Redfern, S., Tylliszczak, T., Sadekov, A., Langer, G., Kimoto, K., & Elderfield, H. (2013). The coordination of Mg in foraminiferal calcite. *Earth and Planetary Science Letters*. 383, 134-141.
- Brew, G., Barazangi, M., Al Maleh, A.K., & Sawaf, T. (2001). Tectonic map and geologic evolution of Syria. *GeoArabia*, 6, 573-616.
- Buatois, L., & Mangano, M.G. (2012). *Ichnology: Organism-Substrate Interactions in Space and Time*. Cambridge University Press, 358 p.

- Bucur, I.I. (1999). Stratigraphic significance of some skeletal algae (Dasycladales, Caulerpales) of the Phanerozoic. *Palaeopelagos Special Publication*, 2, 53-104.
- Buffetaut, E., Azar, D., Nel, A., Ziadé, K., & Acra, A. (2016). First nonavian dinosaur from Lebanon: a brachiosaurid sauropod from the Lower Cretaceous of the Jezzine District. *Naturwissenschaften*, 93, 440-443.
- Butler, R.W.H., Spencer, S., & Griffiths, H.M. (1998). The structural response to evolving plate tectonics during transpression: evolution of the Lebanese restraining bend of the Dead Sea Transform. In: Holdsworth R.E., Strachan, R.A. & Dewey J.F. (Eds.), *Continental Transpressional and Transtensional Tectonics*. Journal of the Geological Society 135, 81-106.
- Byung-Do, C., Munkhtsetseg, J., Min, H., & Khand, Y. (2017). Cretaceous non-marine ostracods from the Hampyeong Basin, southwestern Korean Peninsula. *Journal of the Geological Society of Korea*, 53, 631-643.
- Carbonel, P., Colin, J.P., Danielopol, D.L., Loeffler, H., & Neustrueva, I. (1988). Paleocology of limnic ostracodes: a review of some major topics. *Palaeogeography, Palaeoclimatology, Palaeoecology*, 62, 413-461.
- Cronin, T. M. (2009). Ostracodes. In: Gornitz, V. (Ed.), *Encyclopedia of paleoclimatology and ancient environments*. The Netherlands: Springer, 663-665.
- Cusminsky, G.C., Bernasconi, G., & Concheyro, G.A. (2018). *Advances in South American Micropaleontology: Selected Papers of the 11th Argentine Paleontological Congress*. Springer International Publishing, 78 p.
- Deans, A.R., Basibuyuk, H.H., Azar, D., & Nel, A. (2004). Descriptions of two new Early Cretaceous (Hauterivian) ensign wasp genera (Hymenoptera: Evaniidae) from Lebanese amber. *Cretaceous Research*, 25, 509-516.
- Dercourt, J., Ricou, L.E., & Vrielynck, B. (1993). Atlas Tethys, Palaeoenvironmental Maps, Gauthier-Villars. 260 p.
- Dettman, D.L., Palacios-Fest, M.R., Nkotagu, H.H., & Cohen, A.S. (2005). Paleolimnological investigations of anthropogenic environmental change in Lake Tanganyika: VII. Carbonate isotope geochemistry as a record of riverine runoff. *Journal of Paleolimnology*, 34, 93-105.
- Doummar, J.J. (2005). *Sedimentology and diagenesis of the Albian rock sequence (upper Hammana-lower Sannine formations), Northern Lebanon* (unpublished Master thesis). American University of Beirut, 199 p.

- Douvillé, H. (1910). Études sur les Rudistes du Liban. *Mémoire de la Société Géologique Française*, 41, 52-75.
- Druckman, Y. (1977). Differential subsidence during the deposition of the Lower Jurassic Ardon Formation in western Jordan, southern Israel and northern Sinai. *Israel Journal of Earth Sciences*, 26, 45-54.
- Dubertret, L. (1947). Sur la limite nord du plateau Syrien. *Société Géologique de France*, 107-108.
- Dubertret, L. (1955). *Notice explicative de la Carte géologique du Liban au 200.000ème*. Beirut: Ministère des Travaux Publics.
- Dubertret, L. (1962). Carte géologique *du Liban, Syrie, et bordure des pays voisins*. (Map). Paris: Museum National d'Histoire Naturelle.
- Dubertret, L. (1963). Liban, Syrie: chaîne des grands massifs contiers et confins à l'Est. In : Dubertret, L. (Ed.), *Lexique Stratigraphique Internationale*, 3, 9-153.
- Dubertret, L. (1975). Introduction a la carte Géologique à 1/ 50 000 du Liban. *Notes et Mémoires sur Le Moyen Orient*, 13, 345-402.
- Dubertret, L., Keller, A., Vautrin, H., Birembault, C., Heybroek, H.F., Canaple, G., Combaz, A.A., Mandersheid, G., & Renouard, G., (1955). Cartes Géologiques du Liban 1/ 200 000e. Avec notice explicative. [Map]. Beirut: Ministère des Travaux Publics.
- Dux, F.W., Chivas, A.R., & Garcia, A. (2015). Trace-element and stable-isotope chemistry of gyrogonites of the euryhaline charophyte *Lamprothamnium*. *Aquatic Botany*, 120, 51-59.
- Esteban, M., & Pray, L.C. (1983). Pisoids and pisolite facies (Permian), Guadalupe Mountains, New Mexico and west Texas. In: Peryt T.M. (Ed.), *Coated Grains*, Springer, Berlin, Heidelberg, 503-537.
- Feist, M., Lake, R. D., & Wood, C. J. (1995). Charophyte biostratigraphy of the Purbeck and Wealden of Southern England. *Paleontology*, 38, 407-442.
- Feist, M., Grambast-Fessard, N., Guerlesquin, M., Karol, K., Lu, H., McCourt, R.M., Wang, Q., & Shenzen, Z. (2005). Treatise on invertebrate paleontology. Part B, Protozoa 1. Volume 1: Charophyta. *The Geological Society of America*. 170 p.
- Ferry, S., Merran, Y., Grosheny, D., & Mroueh, M. (2007). The Cretaceous of Lebanon in the Middle East (Levant) context. In Bulot, L.G., Ferry, S. &

- Grosheny, D. (Eds.), *Relations entre les marges septentrionale et méridionale de la Téthys au Carnets de Géologie*, 38-42.
- Flügel, E. (2010). *Microfacies of Carbonate Rocks, Analysis, Interpretation and Application*. Springer, Verlag Berlin Heidelberg, 984 p.
- Frogley, M.R., Griffiths, H.I., & Martens, K. (2002). Modern and fossil ostracods from ancient lakes. In Holmes, J.A. & Chivas, A.R. (Eds.), *The Ostracoda: Applications in Quaternary Research*. American Geophysical Union 131, 167-184.
- García, A., & Chivas, A.R. (2006). Diversity and ecology of extant and Quaternary Australia charophytes (Charales). *Cryptogramie-Algologie*, 27, 323-340.
- Gardosh, M. (2002). The sequence Stratigraphy and Petroleum Systems of the Mesozoic, Southeastern Mediterranean Continental Margin. PhD thesis. Tel Aviv University, 159 p.
- Gardosh, M.A., Garfunkel, Z., Druckman, Y., & Buchbinder, B. (2010). Tethyan rifting in the Levant region and its role in the Early Mesozoic crustal evolution. In: Homberg, C. & Bachmann, M. (Eds.), *Evolution of the Levant Margin and Western Arabia Platform since the Mesozoic*. Geological Society, London, Special Publications (341), 9-36.
- Garfunkel, Z. (1989). Tectonic setting of Phanerozoic magmatism in Israel. *Israel Journal of Earth Sciences*, 38, 51-74.
- Garfunkel, Z. (1998). Constrains on the origin and history of the Eastern Mediterranean basin; collision-related processes in the Mediterranean region. *Tectonophysics*, 298, 5-35.
- Garfunkel, Z., & Derin, B. (1984). Permian-early Mesozoic tectonism and continental margin formation in Israel and its implications for the history of the Eastern Mediterranean. In: Dixon, R.J. & Robertson, A.H.F. *The Geological Evolution of the Eastern Mediterranean*. Geological Society of London, Special Publications, 17, 187-201.
- Ghalayini, R., Daniel, J.M., Homberg, C., Nader, F., & Comstock, J. (2014). Impact of Cenozoic strike-slip tectonics on the evolution of the northern Levant Basin (offshore Lebanon). *Tectonics*, 33, 2121-2142.
- Gierlowski-Kordesch, E.H. (2010). Lacustrine carbonates. In: Alonso-Zarza, A.M. & L. Tanner, H. (Eds.), *Carbonates in Continental Settings. Facies, Environments and Processes*. Developments in Sedimentology, 61, 1-101.

- Grambast, L. (1962). Classification de l'embranchement des Charophytes. *Naturalia Monspeliensis. Serie botanique abbreviation*, 14, 63-86
- Grambast, L. (1966). Structure de l'utricule et phylogénie chez les Clavatoracées. *Comptes Rendus des Séances de l'Academie des Sciences*, 262, 2207-2210.
- Grambast, L. (1968). Evolution of the utricle in the charophyta genera *Perimneste* Harris and *Atpochara* Peck. *Journal of the Linnean Society (Botany)*, 61(384), 5-11.
- Grambast-Fessard, N. (1986). Deux nouveaux représentants du genre *Ascidrella* (Clavatoraceae, Charophyta). *Geobios*, 19, 255-260.
- Grambast, L., & Lorch, J. (1968). Une flore de Charophytes de Crétacé inférieur du Proche Orient. *Naturalia Monspeliensis*, 19, 47-56.
- Granier, B., Azar, D., Maksoud, S., Geze, R., & Habchi, R. (2015). New fossiliferous sites with Barremian Charophyta in the "Grès du Liban" auct. (Lebanon), with a critical perspective regarding the nature of *Munieria* Deecke, 1883. *Carnets de Geologie*, 15, 199-229.
- Grigg, U.M., & Siddiqui, Q. (1996). *Perissocytheridea* Stephenson, 1938: a brackish water ostracod. 2nd European Ostracodologists Meeting, University of Glasgow, 23–27 July 1993. 257 p.
- Hancock, P.L., & Atiya, M.S. (1979.) Tectonic significance of mesofracture systems associated with the Lebanese segment of the Dead Sea transform fault. *Journal of Structural Geology*, 1(2), 143-153.
- Haq, B.U., & Boersma, A. (1998). *Introduction to marine micropaleontology*. Elsevier Science & Technology. 376 p.
- Harris, T.M. (1939). British Purbeck Charophyta. British Museum (Natural History), London, 83 p.
- Hawie, N., Gorini, C., Deschamps, R., Nader, F., Montadert, L., Granjeon, D., & Baudin, F. (2013). Tectono-stratigraphic evolution of the northern Levant Basin (offshore Lebanon). *Marine and Petroleum Geology*, 48, 392-410.
- Heybroek, M.F. (1942). La Géologie d'une partie du Liban Sud. *Leidsche Geologische Mededeelingen*, 12(2), 251-470.
- Hirsch, F., Bassoullet, J. P., Cariou, E., Conway, B., Feldman, H. R., Grossowitch, L., Honigstein, A., Owen, E. F., & Rosenfeld, A. (1998). The Jurassic of the southern Levant: biostratigraphy, paleogeography and cyclic event. In: Crasquin-Soleau, S.

- & Barrier, E. (Eds.), *Peri-tethys Memoir 4: Epicratonic Basin of Peri-tethyan Platforms 179*. Memoires du Museum National d'Histoire Naturelle, Paris, 213-235.
- Hoedemaeker, P.J., & Hergreen, G.F.W. (2003). Correlation of Tethyan and Boreal Berriasian - Barremian strata with emphasis on strata in the subsurface of the Netherlands. *Cretaceous Research*, 24, 253-275.
- Holmes, J.A. (2001). Ostracoda. In: Smol, J.P., Birks, H.J.B. & Last, W.M. (Eds.), *Tracing Environmental Change Using Lake Sediments*, Zoological Indicators Developments in Paleoenvironmental Research, 4, 125-151.
- Holmes, J.A., & Chivas, A.R. (2002). Ostracod shell chemistry-overview. In: Holmes, J.A. & Chivas A.R. (Eds.), *The Ostracoda: Applications in Quaternary Research*, American Geophysical Union, 131, 185-204.
- Homberg, C., Barrier, E., Mroueh, M., Hamdan, W., & Higazi, F. (2009). Basin tectonics during Early Cretaceous in the levant margin, Lebanon. *Journal of Geodynamics*, 47, 218-223.
- Horne, D.J. (2002). Ostracod biostratigraphy and palaeoecology of the Purbeck Limestone Group in southern England. *Special Papers in Palaeontology*, 68: 53-70.
- Hosseini, S., Conrad, M., Clavel, B., & Carras, N. (2016). Berriasian- Aptian Sallow water carbonates in the Zagros fold-thrust belt, SW Iran: integrated Sr-isotope dating and biostratigraphy. *Cretaceous Research*, 57, 257-288.
- Huyghe, D., Emmanuel, L., Renard, M., Lartaud, F., Génot, P., Riveline, J., & Merle, D. (2017). Significance of shallow-marine and non-marine algae stable isotope ( $\delta^{18}\text{O}$ ) compositions over long periods: Example from the Palaeogene of the Paris Basin. *Palaeogeography, Palaeoclimatology, Palaeoecology*, 485, 247-259.
- Jaffrezo, M. (1980). *Les formations carbonatées des Corbières (France) du Dogger à l'Aptien: micropaléontologie, stratigraphique, biozonation, paléoécologie. Extension des résultats a la Mésogée*. Unpublished Phd thesis, Université Pierre et Marie Curie, Paris, 615 p.
- Jaradat, R.A., Nusier, O.K., Awawdeh, M.M., Al-Qaryouti, M.Y., Fhjan, Y.M., & Al-Rawabdeh, A.M. (2008). Deaggregation of Probabilistic Ground Motions for Selected Jordanian Cities. *Jordan Journal of Civil Engineering*, 2, 172-196.
- Jones, T.R. (1893). On some fossil Ostracoda from S.-W. Wyoming, and from Utah, U.S.A. *Geological Magazine*, 10(9), 385-391.
- Kaminski, M.A. (2004). The year 2000 classification of the agglutinated foraminifera. In: Bubik, M. & Kaminski, M.A. (Eds.), *Proceedings of the fifth*



- international workshop on agglutinated Foraminifera*. Grzybowski Foundation Special Publication, 8, 237-255.
- Kanaan, F.M. (1966). *Sedimentary structures and thicknesses and facies variation in the Basal Cretaceous sandstones of Central Lebanon* (Master's Thesis). American University of Beirut, 182 p.
- Karol, K.G., Skawinski, P.M., McCourt, R.M., Nault, M.E., Evans, R., Barton, M.E., Berg, M.S., Perleberg, D.J., & Hall, J.D. (2017). First discovery of the charophycean green alga *Lychnothamnus barbatus* (Charophyceae) extant in the New World. *American journal of botany* 104(7), 1108-1116.
- Kirejtshuk, A.G., & Azar, D. (2013). Current knowledge of Coleoptera (Insecta) from the Lower Cretaceous Lebanese amber and taxonomical notes for some Mesozoic groups. *Terrestrial Arthropod Reviews* 6,103-134.
- Krenkel, E. (1924). Der Syrische Bogen. Zentralblatt für Mineralogie. *Geologie und Palaontologie*, 9, 274-281.
- Kroh, A. (2010). The phylogeny and classification of post-Paleozoic echinoids. *Journal of Systematic Palaeontology*, 8(2), 147-212.
- Latreille, P.A. (1806). *Cenera Crustaceorum et Insectorum, Tomus Primus*. A. Koenig, Paris, 302 p.
- Lindley, J. (1836). A natural system of botany. 2<sup>nd</sup> edition. Londres: Longman.
- Li, Y.G., Su, D.Y., & Zhang, L.J. (1988). The Cretaceous Ostracod Faunas from the Fuxin Basin, Liaoning Province. *Developments in Paleontology and Stratigraphy*, 11, 1173-1186.
- Luger, P., & Schudack, M. (2001). On Early Cretaceous (earliest Aptian) freshwater Charophyta and Ostracoda from Northern Somalia. *Neues Jahrbuch für Geologie und Paläontologie*, 220(2), 245-266.
- Mädler, K. (1952). Charophyten aus dem Nordwestdeutschen Kimmeridge. *Geologisches Jahrbuch*, 67, 1-46.
- Maksoud, S., Granier, B., Azar, D., Paicheler, J.C., & Moreno-Bedmar, J. (2014). Revision of "Falaise de Blanche" (Lower Cretaceous) in Lebanon, with the definition of a Jezzianian Regional Stage. *Carnets de Géologie*, 14(8), 401-27.
- Maksoud, S., Azar, D., Granier, B., & Gèze, R. (2017). New data on the age of the Lower Cretaceous amber outcrops of Lebanon. *Palaeoworld*, 26, 331-338.

- Mart, Y., Ryan, W.B.F., & Lunina, O.V. (2005). Review of the tectonics of the Levant Rift system: the structural significance of oblique continental breakup. *Tectonophysics*, 395, 209-232.
- Martin, G.P.R. (1940). Ostracoden des norddeutschen Purbeck und Wealden. *Senckenbergiana*, 22, 275-361
- Martín-Closas, C. (1988). Decouverte de la plaque basale chez les Clavatoraceae (Charophyta). Implications phylogenetiques. *Comptes Rendus de l'Académie des Science Paris*, 306(2), 1131-1136.
- Martín-Closas, C. (1989). Els caròfits del Cretaci inferior de les conques perifèriques del Bloc de l'Ebre. Barcelona (unpublisjhed PhD Thesis) Universitat de Barcelona, 581p.
- Martín-Closas, C. (1996). A phylogenic system of the Clavatoraceae (Charophyta). *Review of Paleobotany and Palynology*, 94, 259-293.
- Martín-Closas, C. (2000). Els caròfits del Juràssic superior i Cretaci inferior de la Península Ibèrica. Arxius de les seccions de ciències, institut d'estudis Catalans, 125, 1-304.
- Martín-Closas, C., & Millán, A. (1998). Estratigrafía y bioestratigrafía (charophyta) del Cretácico Inferior en el sector occidental de la Cuenca de Cameros (Cordillera Ibérica). *Revista de la Sociedad Geologica de España*, 11, 253-269.
- Martín-Closas, C., & Serra-Kiel, J. (1991). Evolutionary of Clavatoraceae (charophyta) in the mesogean basins analyzed according to environmental change during Malm and lower cretaceous. *Historical Biology*, 5, 291-307.
- Martín-Closas, C., & Schudack, M.E. (1991). Phylogenetic analysis and systematisation of post-palaeozoic charophytes. *Revue de la Société Botanique de France*, 138, 53-71.
- Martín-Closas, C., Bosch, R., & Serra-Kiel, J. (1999). Biomechanics and evolution of spiralization in charophyte fructifications. In: Kurmann, M.H. & Hemsley A.R. (Eds.), *The evolution of plant architecture*, London, Royal Botanic Gardens Kew, 399-421.
- Martín-Closas, C., Wojcicky, J.J., & Fonollà, L. (2006). Fossil charophytes and hydrophytic angiosperms as indicators of lacustrine trophic change. A case study in the Miocene of Catalonia (Spain). *Cryptogamie-Algologie*, 27, 357-379.

- Massaad, M. (1976). Origin and environment of deposition of the Lebanese Basal Sandstones. *Ecologiae Geologicae Helvetiae*, 69, 85-91.
- Maync, W. (1950). The foraminiferal genus *Choffatella* Schlumberger in the Lower Cretaceous (Urgonian) of the Caribbean region (Venezuela, Cuba, Mexico and Florida). *Ecologiae geologicae Helvetiae*, 42(2), 529-547.
- Migula, W. (1897). Die Characeen Deutschlands, Österreichs und der Schweiz. In X. Rabenhorst (Ed.), *Kryptogamic Flora* von Deutschland, Oesterreich und der Schweiz. E. Kummer, Leipzig, 772 p.
- Misra, S., & Froelich, P.N. (2012). Lithium Isotope History of Cenozoic Seawater: Changes in Silicate Weathering and Reverse Weathering. *Science*. 335(6070), 818-823.
- Mojon, P.O. (2002). Les Formations Mésozoïques à charophytes (Jurassique Moyen - Crétacé Inférieur) de la marge Téthysienne Nord-Occidentale (SE de la France, Suisse Occidentale, NE de l'Espagne) – Sédimentologie, micropaléontologie, biostratigraphie. *Géologie Alpine*, 41, 1-386.
- Moore, R.C., & Pitrat, C.W. (1961). *Treatise on Invertebrate Paleontology. Part Q, Arthropoda, 3. Crustacea. Ostracoda*. Geological Society of America and University of Kansas Press. Lawrence, Kansas, 442 p.
- Morsi, A.M., & Wendler, J. (2010). Biostratigraphy, palaeoecology, palaeogeography of the middle Cenomanian – early Turonian Levant Platform in Central Jordan based on ostracods. *Geological Society, London, Special Publications*, 341, 187-210.
- Müller, G.W. (1894). Die Ostracoden des Golfes von Neapel und der Angrenzenden Meeresabschnitte. *Fauna und Flora Golfes von Neapel*, 21, 1-404.
- Munier-Chalmas, E. (1887). Sur la Cyclolina et trois nouveaux genres de Spirocyclina. *Compte Rendu des Séances de la Société géologique de France*, 4 (7), 30-31. foraminifères des couches à rudistes: Cyclopsina, Dicyclina et Spirocyclina. *Compte Rendu des Séances de la Société géologique de France*, 4 (7), 30-31.
- Nader, F.H. (2000). *Petrographic and Geochemical characterization of the Jurassic Cretaceous Carbonate sequence of the Nahr Ibrahim region, Lebanon* (Master's Thesis). American University of Beirut, 227 p.
- Nader, F.H. (2011). The petroleum prospectivity of Lebanon: an overview. *Journal of Petroleum Geology*, 34(2), 135-156.

- Neagu, T., & Cîrnaru, P. (2004). Genus *Choffatella* (Schlumberger), 1904 (foraminifera) in the lower Aptian (Bedoulian) from southern Dobrogea and SE part of the Romanian plain. *Acta Palaeontologica Romaniaae*, 4, 269-275.
- Nemer, T., Meghraoui, M., & Khair, K. (2008). The Rachaya-Serghaya fault system (Lebanon): Evidence of coseismic ruptures, and the AD 1759 earthquake sequence, *Journal of Geophysical Research*, 113, 1-12.
- Oertli, H.J. (1957). Ostracodes du Jurassique superieur du Bassin de Paris (Sontage Vernon 1). *Rev. Inst. Français Petrole et Annales Combust. Liquides*, 12, 647-695.
- Omaña, L., & Alencáster, G. (2009). Lower Aptian shallow-water benthic foraminiferal assemblage from the Chilacachapa range in the Guerrero-Morelos Platform, south Mexico. *Revista Mexicana de Ciencias Geológicas*, 26(3), 575-586.
- Park, L.E., & Smith, A.J. (2003). Bridging the Gap. Trends in the Ostracode Biological and Geological Sciences. *Paleontological Society Papers*, 9, 290 p.
- Pawlowski, J., Holzmann, M., & Tyszka, J. (2013). New supraordinal classification of Foraminifera: Molecules meet morphology. *Marine Micropaleontology*, 100, 1-10.
- Peck, R.E. (1938). A new family of Charophyta from the Lower Cretaceous of Texas. *Journal of Paleontology*, 12(2), 173-176.
- Peck, R.E. (1941). Lower Cretaceous Rocky Mountain non marine microfossils. *Journal of Paleontology*, 15(3), 285-304.
- Pia, J. (1927). Charophyta. In: Hirmer, H. (Ed.), *Handbuch der Paläobotanik*. Munich-Berlin, 1, 88-93.
- Poinar, G., & Milky, R. (2001). *Lebanese amber: The oldest insect ecosystem in fossilized resin*. Corvallis: Oregon State University Press, 96 p.
- Pokorný, V. (1978). Ostracodes. In: Haq, B.U. & Boersma A. (Eds.), *Introduction to marine micropaleontology* New York: Elsevier, 109-149).
- Ponikarov, V. P. (1967). The geology of Syria: explanatory notes on the geologic map of Syria, scale 1:500000. Part 1, Stratigraphy, igneous rocks and tectonics. Ministry of Industry, Damascus, 230p.
- Radoičić, R. (1959). *Salpingoporella dinarica* n. sp. dans les sediments Crétacés inférieurs des Dinarides. *Geol. Glasnik*, 3, 33-42.
- Reid, D.G., Dyal, P., Lozouet, P., Glaubrecht, M., & Williams, S.T. (2008). Mudwhelks and mangroves: The evolutionary history of an ecological association 9Gasteropoda: Potamididae). *Molecular Phylogenics and Evolution*, 47(2), 680-699.

- Renouard, G. (1955). Oil prospects of Lebanon. *AAPG Bulletin*, 39(11), 2125-2169.
- Rey, J., & Ramalho, M. (1974). Le Crétacé inférieur de l'Algarve occidentale (Portugal). *Comunicacoes dos Servicos Geologicos de Portugal*, 57, 155-181.
- Riveline, J., Berger, J. P., Feist, M., Martin-Closas, C., Schudack, M., & Soulié-Märsche, I. (1996). European Mesozoic-Cenozoic Charophyte Zonation. *Bulletin de la Societe Geologique de France*. 167, 453-468.
- Roberts, G., & Peace, D. (2007). Hydrocarbon plays and prospectivity of the Levantine Basin, offshore Lebanon and Syria from modern seismic data. *GeoArabia*, 12, 99-124.
- Rodriguez-Lázaro, J., & Ruiz-Munoz, F. (2012). A general introduction to ostracods: morphology, distribution, fossil record and applications. In: Horne, D.J., Holmes, J.A., Rodriguez-Lazaro, A.J. & Viehberg, F.A. (Eds.), *Ostracoda as proxies for quaternary climate change*. Developments in Quaternary Science, 17, 1-14.
- Rosenfeld, A., Gerry, E., & Honiostein, A. (1988). Jurassic-Cretaceous non-marine ostracods from Israel and palaeoenvironmental implications. *Developments in Palaeontology and Stratigraphy*, 11, 659-669.
- Roth, R.I. (1933). Some Morrison Ostracoda. *Journal of Paleontology*, 7(4), 398-405.
- Saint Marc, P. (1970). Contribution à la connaissance du Crétacé Basal au Liban. *Revue de Micropaléontologie*, 12(4), 224-233.
- Saint-Marc, P. (1974). Etude stratigraphique en micropaléontologie de l'Albien, du Cenomanien et du Turonien du Liban. *Notes et Mémoires sur le Moyen Orient*, 8, 8-342.
- Sames, B. (2009). Revision of the genus *Cypridea* Bosquet (Ostracoda, Crustacea) and some of its species from the nonmarine Lower Cretaceous Lakota and Cedar Mountain formations of the U.S. Western Interior and the European 'Purbeck/Wealden'. In Taxonomy and systematics of nonmarine Late Jurassic and Early Cretaceous ostracods: their phylogeny and application to biostratigraphy with emphasis on the Early Cretaceous of the North American Western Interior foreland basin. (Thesis doctorat), 365 p.
- Sames, B. (2011). Early Cretaceous *Cypridea* Bosquet 1852 in North America and Europe. *Micropaleontology*, 57(4-5), 345-431.

- Sanjuan, J., & Alqudah, M. (2018). Charophyte flora from Miocene deposits of Zahle (Beeka Valley, Lebanon). Biostratigraphic, palaeoenvironmental and palaeobiogeographical implications. *Geodiversitas*, 40(10), 195-209.
- Sanjuan, J., & Martín-Closas, C. (2012). Charophyte palaeoecology in the Upper Eocene of the Eastern Ebro Basin (Catalonia, Spain). Biostratigraphic implications. *Palaeogeography, Palaeoclimatology, Palaeoecology*, 365-366, 247-262.
- Sanjuan, J., Vicente, A., Flor-Arnau, N., & Cambra, J. (2017). Effects of light and temperature on *Chara vulgaris* gyrogonite productivity and polymorphism-palaeoenvironmental implications. *Phycologia*, 56(2), 204-212.
- Sars, G.O., 1925. An account of the Crustacea of Norway with short descriptions and figures of all the species. *Ostracoda*, 9(3-10), 73-208.
- Saraswati, P.K., & Srinivasan, M.S. (2016). *Micropaleontology: Principles and applications* (1<sup>st</sup> ed.). Springer. 223 p.
- Savelieva, J.N. (2014). Palaeoecological analysis of Berriasian ostracods of the central Crimea. *Volumina Jurassica*, 12(1), 163-174.
- Schlumberger, C. (1905). Note sur le genre *Choffatella* n. g. *Comunicações da Comissão do Serviço Geológico de Portugal*, 6, 155-157.
- Schudack, M.E. (1993). *Die Charophyten im Oberjura und Unterkreide Westeuropas: Mit einer phylogenetischer Analyse der Gesamtgruppe*. Berliner Geowissenschaftliche Abhandlungen, Reihe A, Band 8, 209 p.
- Schudack, M. (1996). Die Charophyten des Niedersächsischen Beckens (Oberjura - Berriasium): Lokalzonierung, überregionale Korrelation und Palökologie. *Neues Jahrbuch für Geologie und Paläontologie*, 200, 27-52.
- Schudack, U., & Schudack, M. (2009). Ostracod biostratigraphy in the Lower Cretaceous of the Iberian chain (eastern Spain). *Iberian Journal of Geology*, 35(2), 139-166.
- Searle, T.R. (1974). *The geotechnical properties of Cretaceous clay shales in Lebanon* (Unpublished Ph.D. Thesis). University of Salford, 247 p.
- Shaikin, I.M. 1967. Fossil charophyta of upper Jurassic deposits of Dniepr-Donets depression. In: Fossil Algae of the USSR. Izdat Nauk SSSR, 43-47.
- Shirmon, A.E., & Lang, B. (1989). Cretaceous magmatism along the Southwestern flank of Mount Lebanon. *Israel Journal of Earth Sciences*, 38, 125-142.

- Shuayb, S. (1974). *Hydrology structures of the Aintoura-Tarshish and Qurnayel region, northern Metn, Mount Lebanon* (Unpublished Master's thesis). American University of Beirut, 137 p.
- Simmons, M.D., Emery, D., & Pickard, N.A.H. (1991). *Hensonella Dinarica*, an originally calcitic early Cretaceous dasycladacean alga. *Palaeontology*, 34(4), 955-961.
- Smith, G.M. (1938). *Botany: Vol 1: Algae and Fungi: Charophyceae*. Nova York: McGraw Hill. 127 p.
- Sohn, I.G. (1979). Nonmarine ostracodes in the Lakota Formation (Lower Cretaceous) from South Dakota and Wyoming. U.S. *Geological Survey Professional Paper*, 1069, 1-24.
- Soulié-Märsche, I. (1989). *Étude compare de gyrogonites de charophytes actuelles et fossiles et phylogénie des genres actuels*. Millau: Imprimerie des Tilleuls, 237 p.
- Soulié-Märsche, I. (1994). The paleoecological implications of the charophyte flora of the Trinity Division, Junction, Texas. *Journal of Paleontology*, 68(5), 1145-1157.
- Soulié-Märsche, I., Bieda, S., Lafond, R., Maley, J., Baitoudji, M., Vincent, P.M., & Faure, H. (2010). Charophytes as bio-indicators for lake level high stand at "Trou au Natron", Tibesti, Chad, during the Late Pleistocene. *Global and Planetary Change*, 72(4), 334-340.
- Soulié-Märsche, I., & García, A. (2014). Gyrogonites and oospores, complementary viewpoints to improve the study of the charophytes (Charales). *Aquatic Botany*, 120(A), 7-17.
- Stephenson, M.B. (1938). Miocene to Pliocene ostracoda of the genus *Cytheridea*. *Journal of paleontology* 12(2), 127-148.
- Swain, F. (1946). Middle Mesozoic Nonmarine Ostracoda from Brazil and New Mexico. *Journal of Paleontology*, 20(6), 543-555.
- Swain, F.M., & Brown, P.M. (1972). Lower Cretaceous, Jurassic (?), and Triassic Ostracoda from the Atlantic Coastal Region. *Geological Survey Professional Paper* 795, 72 p.

- Swartz, F.M., & Swain, F.M. (1946). Ostracoda from the upper Jurassic Cotton Valley Group of Louisiana and Arkansas. *Journal of Paleontology*, 2(4), 362-373.
- Tixier, B. (1971-72). Le “Grès de Base” Crétacé du Liban: Étude Stratigraphique et Sédimentologique. *Notes et Mémoires sur le Moyen Orient*, 12, 187-215.
- Trabelsi, K., Sames, B., Salmouna, A., Piovesan, E.K., Rouina, S.B., Houla, Y., Tourir, J., & Soussi, M. (2015). Ostracods from the marginal coastal lower Cretaceous (Aptian) of the central Tunisian Atlas (North Africa): Paleoenvironment, biostratigraphy and paleobiogeography. *Revue de Micropaléontologie*, 58(4), 309-331.
- Trabelsi, K., Tourir, J., Soulié-Märsche, I., Martín-Closas, C., Soussi, M., & Colin, J.P. (2010). Albian Charophytes discovered in the Kebar Formation (Central Tunisia): Palaeoecological and palaeobiogeographical implications. *Annales de Paléontologie*, 96, 117-133.
- Ukla, S.M. (1970). *Subsurface and well correlation in North and Central Lebanon* (unpublished Master's thesis). American University of Beirut. 249 p.
- Vicente, A., & Martín-Closas, C. (2012). Lower cretaceous charophytes from the Serrania de Cuenca, Iberian chain: taxonomy, biostratigraphy and palaeoecology. *Cretaceous research*, 40, 227-242.
- Vicente, A., Expósito, M., Sanjuan, J., & Martín-Closas, C. (2016). Small sized charophyte gyrogonites in the Maastrichtian of Coll de Nargó, Eastern Pyrenees: An adaptation to temporary floodplain ponds. *Cretaceous Research*, 57, 443-456.
- Villalba-Breva, S., & Martín-Closas, C. (2011). A Characean thallus with attached gyrogonites and associated fossil charophytes from the Maastrichtian of the eastern Pyrenees (Catalonia, Spain). *Journal of Phycology*, 47, 131-143.
- Wakim, S.B. (1968). *Petrography of the Basal Cretaceous Sandstones of Central Lebanon* (unpublished Master's thesis). American University of Beirut, 79.
- Walley, C.D. (1983). A revision of the lower Cretaceous lithostratigraphy of Lebanon. *Geologische Rundschau*, 72, 377-388.
- Walley, C.D. (1997). The Lithostratigraphy of Lebanon: A Review. *Lebanese Scientific Research Reports*, 10 (1), 81-108.



- Walley, C.D. (1998). Some outstanding issues in the geology of Lebanon and their importance in the tectonic evolution of the Levantine region. *Tectonophysics*, 298 (1), 37-62.
- Walley, C.D. (2001). The Lebanon passive margin and the evolution of the Levantine Neo-Tethys. In: Ziegler, P.A., Cavazza, W., Robertson, A.H. & Crasquin-Soleau, S.D. (Eds.), *Peri-Tethyan Rift–Wrench Basins and Passive Margins IGCP 369 Results* (Mem. 6). Mémoires du Musé National d’Histoire Naturelle, 186, 407-439.
- Wang, Z. (1981). Mesozoic charophytes from the Anhui and Zeijiang with its stratigraphic significance. *Acta Palaeontologica Sinica*, 20, 311-325.
- Wang, Y.Q., Yang, W.G., Pan, Y.H., & Liao, H.Y. (2017). Species of the genus *Cypridea* Bosquet, 1852 (Ostracoda) from the Lower Cretaceous Yixian and Jiufotang formations of western Liaoning, China. *Palaeoworld*, 26, 339-351.
- Wray, J. (1977). Calcareous algae. In: Haq, B.U. & Boersma, A. (Eds.), *Introduction to Marine Micropaleontology*, Elsevier, 171-187.
- Zachos, J.C., Pagani, M., Sloan, L., Thomas, E., & Billups, K. (2001). Trends, Rhythms, and Aberrations in Global Climate, 65 Ma to Present. *Science*, 292 (5517), 686-693.
- Zumoffen, G.S.J. (1926). *Géologie du Liban. Avec carte géologique 1/ 200 000e*. Paris: Henri Fascicule.

## APPENDIX A

### STRATIGRAPHIC LOGS DESCRIPTION

### **A.1. Description of Qehmez section 1**

- 1.5 m of dark grey marly siltstone rich in disarticulated plant remains such as cuticles. A soft sample Q0 was extracted from this interval for microfossils. However, no microfossils were recovered from this sample.
- 1 m of yellowish fine sandstone bed alternated with dark grey siltstone layers.
- 4 m yellowish fine cross-bedded sandstone beds sets (quartz arenite) intercalated with thin lignite bands (Fig. 54). Sandstone layers range in thickness between 0.2 and 1m. The quartz grains are sub-rounded and moderately sorted. These beds show tabular cross-stratification and normal grain size grading. Lignite layers are arranged parallel to the foreset lamination (Fig. 54B). No trace fossils neither edaphic structures have been observed in this interval suggesting that plant debris were transported from their original growing locality.

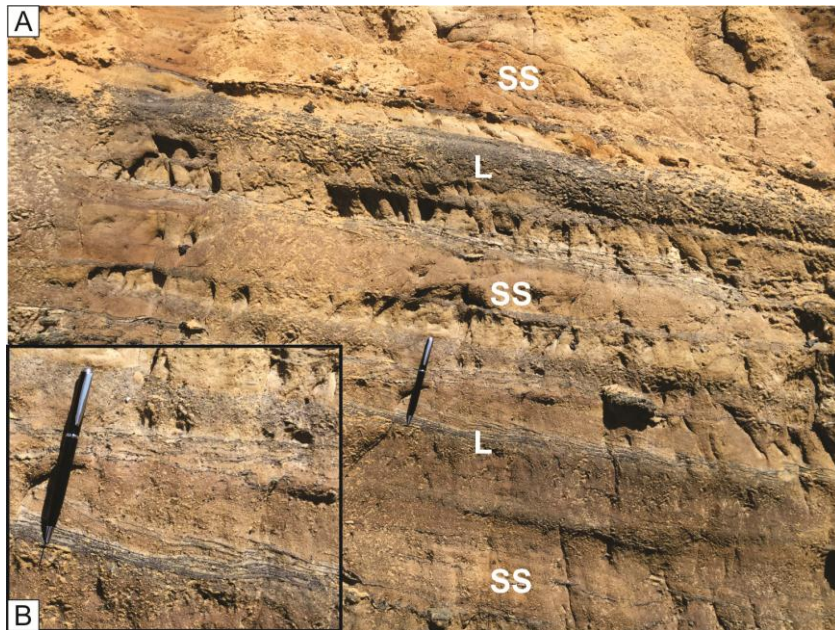


Figure 54: A: field photo showing the cross-bedded sandstone beds (SS) intercalated with thin lignite bands (L) at the base of Qehmez section 1, B: note the arrangement of lignite layers among the foresets.

- 2.5 m of yellowish medium sandstone bed intercalated with lignite bands with tabular cross-stratification.
- 20 cm reddish ferruginous concretions interval (Fig. 55).

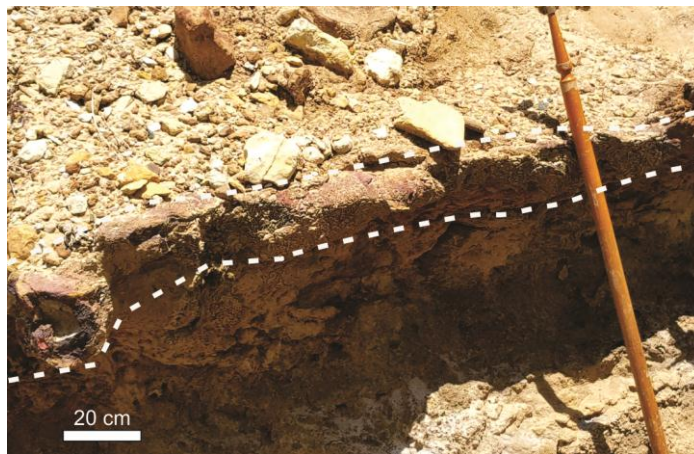


Figure 55: Field photo showing a reddish hard interval of ferruginous concretions (along the dotted white line) in Qehmez section 1.

- 2.5 m of reddish medium sandstone interval with tabular cross-stratification.
- 2.7 m of dark grey marly siltstone showing pillow structures at its top (Fig. 56).



Figure 56: Field photo showing the contact between silty marl and sandstone intervals showing balls and pillows structures, Qehmez section 1.

- 0.5 m yellowish sandstone bed (quartz arenite). Quartz grains are fine to medium in size moderately sorted and sub-rounded in shape.
- 7.5 m covered interval.
- 1 m of yellowish quartz arenite bed. Grains are medium in size and moderately sorted. Ripples can be observed at the top of this bed.



- 1.5 m of reddish siltstone interval with small vertical burrows at the top and base.
- 0.5 m hard sandstone bed with ripple marks.
- 4 m of beige monotonous siltstone bed.
- 0.5 m of limestone bed (mudstone rich in small quartz grains. No carbonate grains were distinguished in this facies (Fig. 57).

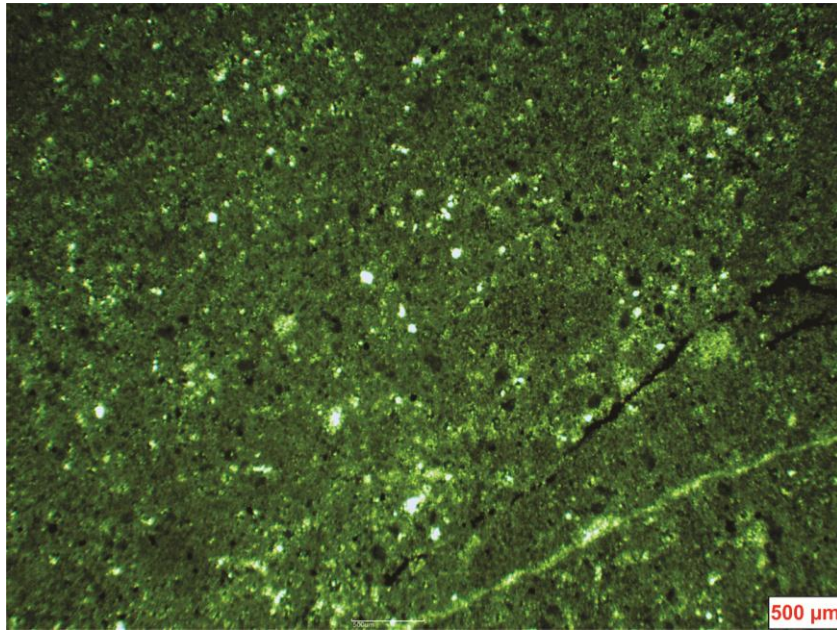


Figure 57: Thin section photo of the sample Q\* (mudstone rich in quartz grains).

- 0.5 m quartz arenite bed. Quartz grains are fine in size, moderately sorted and sub-rounded in shape.
- 80 cm siltstone interval displaying erosive base. A soft sample Q1 was collected from this interval. However, no fossils were recovered from this sample.

- 2 m of yellowish sandstone interval (quartz arenite) with erosive base. Quartz grains are grading upward from fine to medium in size. They are moderately sorted and sub-rounded in shape.
- 0.5 m of green marls with large vertical burrow casts. These burrows are up to 40 cm in length and up to 5 cm in diameter. A soft sample Q2 was extracted. However, no microfossils were recovered.
- 0.5 m of fine to medium yellowish, poorly to moderately sorted sandstone bed.
- 1.5 m of beige siltstone interval. A soft sample Q3 was extracted with no fossil content.
- 60 cm of yellowish poorly sorted medium-coarse quartz arenite bed with erosive base.
- 2 m of structureless reddish siltstone interval.
- 4.5 m semi-covered interval of siltstone.
- 1.5 m of yellowish fine quartz arenite bed. Grains are moderately sorted and sub-rounded in shape.
- 1.5 m of beige silty marl interval crossed by large vertical branching burrow casts. A soft sample Q4 was extracted from this interval (Fig. 58). Microfossils recovered from this sample include marine ostracods (*Meta*)*cytheropteron* sp. and brackish species *Perissocytheridea* sp., echinoid spines, shells of agglutinated foraminifera *Choffatella* cf.

*decipiens*, , broken mollusk shells, and few eroded charophyte utricles of *Asciidiella reticulata*.



Figure 58: Detailed photo of the upper part of the beige silty marl interval showing vertical branching burrows. The sample Q4 has been extracted from this interval.

- 1.5 m of yellowish medium to fine quartz arenite strata. Quartz grains are moderately sorted and sub-rounded in shape.
- 3.5 m of yellowish siltstone beds showing ripple marks.
- 1 m of reddish siltstone bed with ripple marks.

The top of the Qehmez section 1 is limited by a fault.

## A.2. Description of Qehmez section 2

- 2.5 m of beige marls interval with abundant poorly sorted quartz grains.



- 1 m of yellowish medium-grained quartz arenite strata showing dispersed broken bivalve shells.
- 25 cm of light grey marl layer with no clear sedimentary structures.
- 75 cm limestone bed rich in broken bivalve shells. Facies shows a vertical change from packstone of mollusks (mainly bivalves) to wackestone-mudstone at the top.
- 0.5 m of light grey marl interval rich in marine mollusk shells such as gastropods (*Turritella*) and bivalve fragments. Occasionally these shells are highly concentrated forming coquinas (Fig. 59).



Figure 59: Detailed photo of the fossil-rich marl interval (coquina).

- 1.5 m of limestone interval grading upwards from packstone/wackestone to mudstone.

- 60 cm of yellowish marl bed showing burrows and large marine mollusk shells.
- 4 m of limestone interval rich in mollusks (bioclastic wackestone/packstone of bivalves and gastropods) alternating with marls (Fig. 60). Limestone intervals display low incised erosive bases.

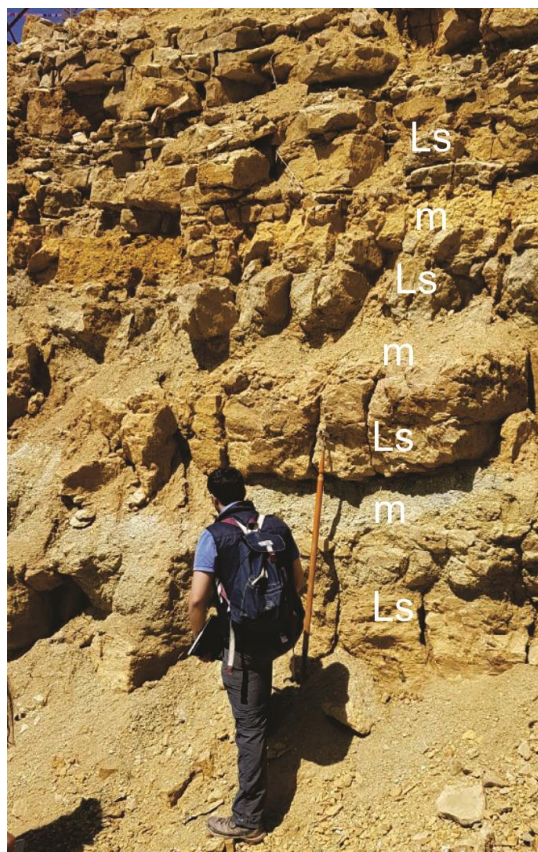


Figure 60: Field photo showing the alternating succession of bioclastic limestone and marl intervals.

- 2 m thick yellowish marl interval rich in marine shells and quartz grains.

- 40 cm limestone bed composed exclusively by oyster shells. They are arranged randomly and many shells are fragmented. This interval displays a short lateral extension showing a clear channel shape. Oyster shells display a characteristic arrangement decreasing in size upwards
- 1 m of yellowish sandy limestone interval.

### **A.3. Description of Ain Dara section**

- 1.5 m of semi-covered dark grey marls interval. A soft sample AD.0 was extracted from this interval. A diverse microfossil assemblage was recovered containing charophyte utricle and gyrogonites (*Clavator ampullaceus*, *Asciadiella reticulata*, *Sphaerochara asema* and *Mesochara* cf. *harrissi*), well-preserved charophyte thalli of *Charaxis martinclousasi*, several species of freshwater ostracod shells (*Cypridea tuberculata* and *Cypridea piedmonti*). Other rare microfossils include, broken gastropod shells, and one reptilian tooth (Plate 14, D).
- 1.5 m of light grey limestone bed. A hard sample AD.1 was extracted at the top of this interval. AD.1 represents a wackestone rich in charophyte thalli (*Charaxis martinclousasi* and *Munieria*) and gastropods (Fig. 61). No marine microfossils have been detected within this limestone bed.

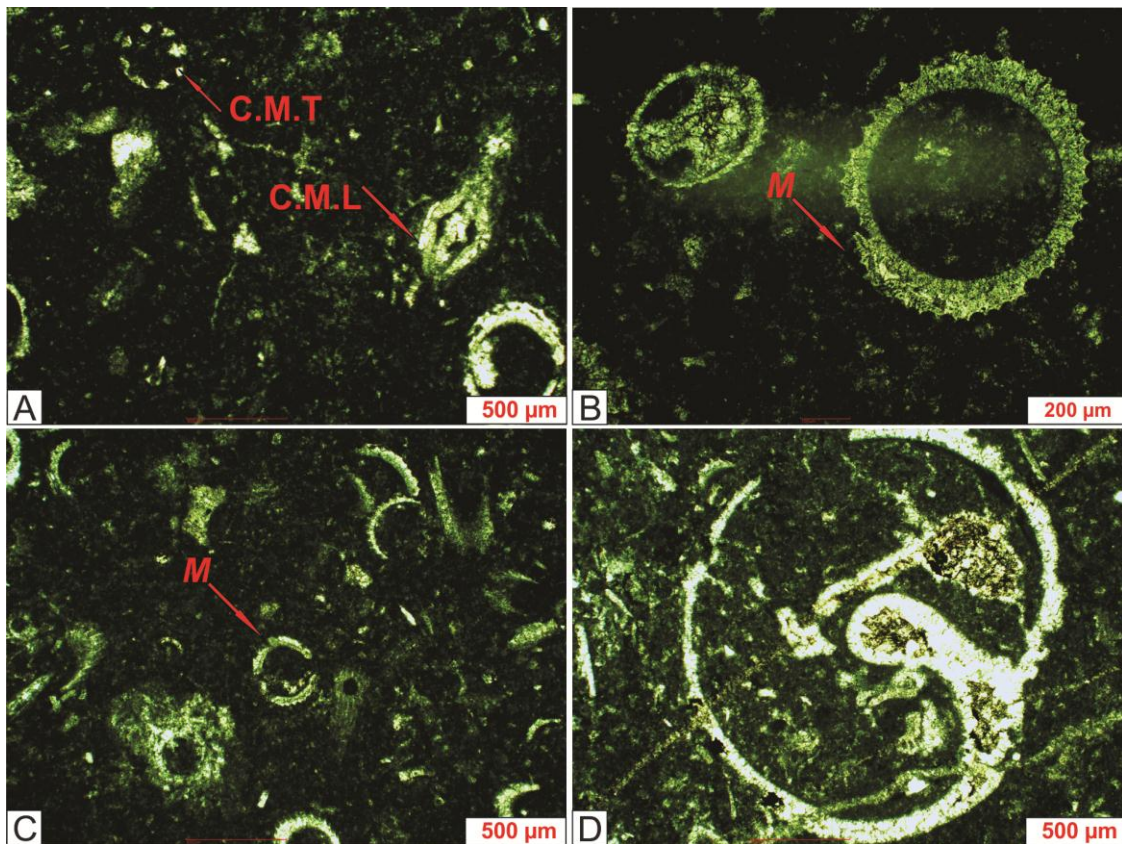


Figure 61: Microfacies of sample AD.1. A, B & C: wackestone of charophyte thalli. Note the several sections of *Charaxis martinclosasi* (C.M.T= transverse section; C.M.L = longitudinal section) and *Munieria* (M). Note that the C.M.T. is located at the node where 8 nodal cells can be counted. D: wackestone showing a transverse section of a gastropod shell.

- 3 m of dark grey monotonous marl bed. A soft sample AD.2 was collected from the top of this bed (Fig. 62) yielding well preserved charophyte utricles (*Clavator ampullaceus* and *Ascidiella reticulata*), gyrogonites (*Sphaerochara asema* and *Mesochara cf. harrissi*) and thalli (*Charaxis martinclosasi*), few broken gastropods and many well preserved ostracod carapaces of the freshwater genus *Cypridea* (*C. tuberculata*, *C. piedmonti*, and *Cypridea* sp.). Other rare microfossils include abraded shells of



foraminifera shells of *Choffatella cf. decipiens* and few fragments of bad-preserved dasycladal thalli (*Salpingoporella dinarica*) as well as few fish teeth.



Figure 62: Field photo showing the location of samples AD.2 (dark grey marl) and AD.3 (grey limestone).

- 1.5 m of light grey limestone interval (wackestone/packstone) containing abundant broken shells of bivalves and charophyte remains. This interval can be subdivided in 3 beds. A hard sample AD.3 was extracted from the upper part of the third interval (Fig. 62). Microfacies reveal a wackestone/packstone exclusively composed of charophyte remains (utricles, thalli and bract cells). No marine microfossils were detected in this microfacies (Fig. 63).

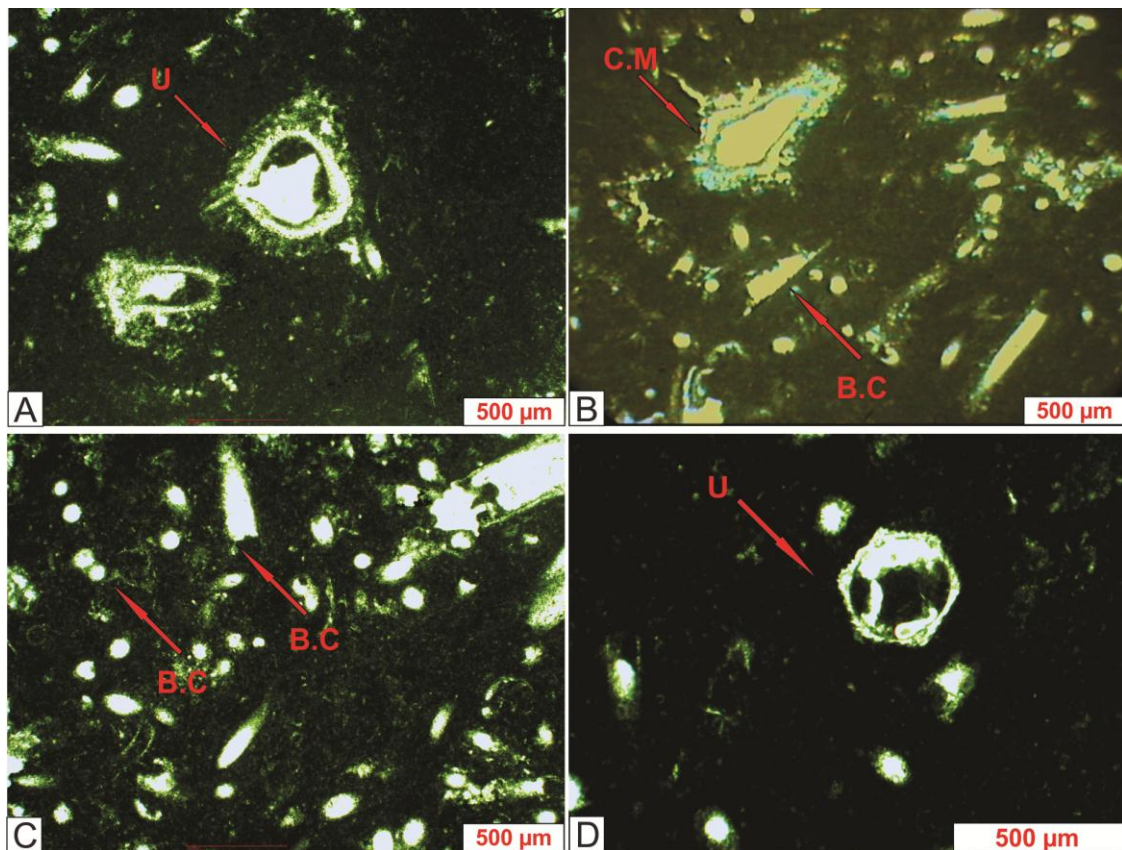


Figure 63: Microfacies (wackestone/packstone of charophytes) obtained from the sample AD.3. A: tangential section of a utricle (U) probably *Clavator ampullaceus*. B & C: several sections of charophyte thalli *Charaxis martinicosasi* (C.M) and charophyte bract cells (B.C). D: detail of an equatorial section of a utricle (U).

- 1.5 m of semi-covered dark grey marl interval.
- 3 m of yellowish quartz arenite bed. Quartz grains are well sorted and moderately rounded ranging in size between medium to coarse.
- 4.5 m of a grey monotonous siltstone interval.
- 0.5 m of green marl bed. A soft sample AD.4 was collected from this interval. However, no fossils were recovered from it.

- 6 m of semi-covered dark grey marly interval.
- 3 m of light grey sandy limestone bed. It contains broken bivalve shells and form a small cliff below the *Falaise Blanche* (Mdairej Formation or upper part of the Jezzianian regional stage).

#### **A.4. Description of Azzouniye section 1**

- 8 m thick interval composed of burrowed beige marls rich in pisoids and quartz grains. Pisoids vary in diameter from 1 to 3 cm (occasionally 4 cm). A soft sample AZ.3 was collected for microfossils at the base of this interval. This sample provides moderately preserved charophyte gyrogonites (*Sphaerochara asema*), utricles (*Clavator ampullaceus* and *Ascidiella reticulata*), and thalli as well as few ostracods carapaces of *Ovocysteridea* sp., and poorly preserved dasycladid remains related to *Salpingoporella dinarica*. The upper part of the interval is completely burrowed showing large vertical branching trace fossils. These branching burrows may reach 7 cm in diameter and are up to 1 m long (Fig. 64).



Figure 64: Detail field photo showing a vertical trace fossil in a silty marl interval located at the base of Azzouniye 1 section.

- 1.5 m of yellowish quartz arenite bed showing tabular cross-stratification. Grains are coarse, moderately sorted and subrounded in shape. Flute marks can be observed at its base.
- 2 m of brownish claystone with dispersed pisoids. Pisoids are smaller in size than previous intervals displaying a diameter ranging between 0.5 and 2 cm. This interval is intersected by a fault.
- Above the fault, a 5.5 m of pisolithic beige silty marls interval occurs. A soft sample AZ.2 was collected from this interval (Fig. 65). This sample yielded few microfossils i.e. poorly preserved charophyte utricles (*Clavator ampullaceus* and *Ascidiella reticulata*), gyrogonites (*Sphaerochara asema*), ostracods shells of *Cypridea tuberculata*, dasycladal thalli of *Salpingoporella dinarica* and few fish teeth.



- 20 cm thick pisolitic conglomerate bed (Fig. 65). This stratum shows low incised erosive base and continuous lateral extension. Pisoids are very large ranging in size between 1 and 5 cm in diameter.



Figure 65: Field photo showing the position of the sample AZ.2 and the pisolitic conglomerate interval (marked between dotted lines) located at the top of the Azzouniye section 1.

- 5 m of beige silty marl bed containing dispersed pisoids and vertical burrows. These trace fossils occur at the top of this interval (Fig. 66). They are very large and can reach a length of up to 2 m and a diameter of up to 10 cm. A soft sample AZ.1 was extracted from this interval. Several microfossils were recovered i.e. moderately preserved charophyte utricles (*Clavator ampullaceus* and *Asciidiella reticulata*), gyrogonites (*Sphaerochara asema*) and thalli (*Charaxis martinclousasi*), ostracod shells of *Cypridea tuberculata*, broken gastropods shells related to the

Potamididea family, and few abraded dasycladal thalli related to *Salpingoporella dinarica*.

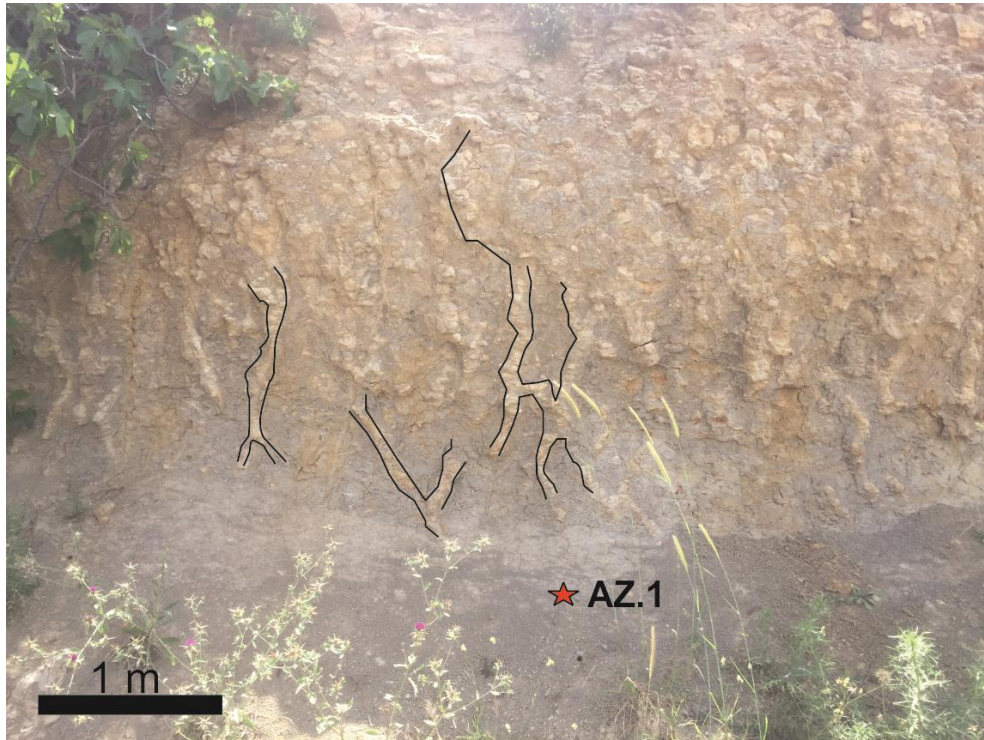


Figure 66: Field photo of the marl interval with pisoids and microfossils burrowed by large vertical bioturbations at the top of Azzouniye section 1.

- 1 m of yellowish coarse sandstone bed (quartz arenite).

#### A.5. Description of Azzouniye section 2

- 70 cm of light grey poorly sorted interval of quartz arenite. Grains are sub-rounded and medium in size.
- 7 m of light grey medium quartz arenite intercalated with several lignite bands or lenses ranging in thickness between 0.5 cm and 3 cm (Fig. 67). Lignite bands display high lateral continuity. No edaphic structures were

observed at the base of these lignite bands. Quartz grains are poorly sorted and sub-rounded in shape.



Figure 67: Detailed field photo showing the basal quartz arenite alternated with lignite lenses.

- 15 cm of grey marl interval.
- 12 m of light grey quartz arenite. Quartz grains are medium in size, poorly sorted and sub-rounded in shape. This interval displays consecutive beds showing of through-cross stratification (Fig. 68). Grains of each cross lamina show normal grading from coarse sand (occasionally gravel) to fine sand (Fig. 69). Deformation sedimentary structures such as pillows can be observed at the top of some beds.





Figure 68: Detailed field photo showing quartz arenite interval with trough cross-stratification.



Figure 69: Detailed field photo showing the normal grading.

- 30 cm of a pisolitic conglomerate interval showing erosive base. Pisoids range in diameter between 1 and 4 cm (Fig. 70).



Figure 70: Detailed field photo of the pisolitic conglomerate. Note the large size of some pisoids.

- 2 m of orange coarse quartz arenite with trough cross-stratification. Several lignite lenses can be observed between the cross-lamination (Fig. 71).



Figure 71: Detailed field photo showing the quartz arenite with lignite lenses.

- 3 meters of light grey medium sandstone interval with trough cross-stratification. Quartz grains are sub-rounded and poorly sorted in general.
- 5 meters of dark grey marls with dispersed pisoids and fine-medium quartz grains.
- 3.5 m of grey fine to medium sandstone bed containing dispersed carbonized wood remains and vertical burrows at its top (Fig. 72).





Figure 72: Detailed field photo showing carbonized wood remains.

- 0.5 m of pisolitic conglomerate bed showing erosive base. Pisoids range in diameter between 1 cm and 4 cm becoming smaller at the top of the interval.
- 1 m of coarse-grained quartz arenite with dispersed pisoids.
- 1.5 m of grey silty marl interval with dispersed pisoids.
- 0.5 m pisolitic conglomerate bed showing erosive base. Pisoids decrease in diameter upward from 6 cm at the base to 1 cm at the top (Fig. 73).
- 0.5 m of medium sandstone interval (quartz arenite) with dispersed pisoids (about 1 cm in diameter) showing normal grading.



Figure 73: Detailed photo showing the pisolitic conglomerate interval. Note the decreasing size of pisoids upwards.

- 3 m of dark grey marl interval. It contains dispersed pisoids and coarse quartz grains. A soft sample AZ.4 was extracted from this interval providing bad preserved charophytes utricles and gyrogonites (*Clavator ampullaceus*, *Asciidiella reticulata*, and *Sphaerochara asema*), broken ostracod shells (*Cypridea tuberculata* and *Cypridea piedmonti*), and few bad-preserved fragments of dasycladal thalli (*Salpingoporella dinarica*).
- 0.5 m pisolitic conglomerate bed showing erosive base. Pisoids decrease in diameter upward (following the same pattern as the previous conglomerate interval).



- 1.5 m of light grey coarse sandstone stratum (quartz arenite) with dispersed pisoids.
- 0.5 m pisolitic conglomerate with erosive base. Pisoids decrease in diameter upward (from 5 cm to 1 cm). Moreover, pisoids occur very concentrated (clast supported) at the base of the interval and become more dispersed (matrix supported) at its top (Fig. 74).



Figure 74: Detailed field photo of the pisolitic conglomerate. Pisoids are more concentrated (clast supported) at the base of the interval becoming more dispersed (matrix supported) at its top.

- 1.5 m of light grey coarse quartz arenite sandstone interval.
- 1.5 m of grey marl bed with small dispersed pisoids.
- 10 cm of light brown limestone bed. A hard sample AZ.5 was extracted for microfacies analysis (Fig. 75). It represents a grainstone of micritized ooids, intraclasts, quartz grains, and few broken mollusk shells (Fig. 76).

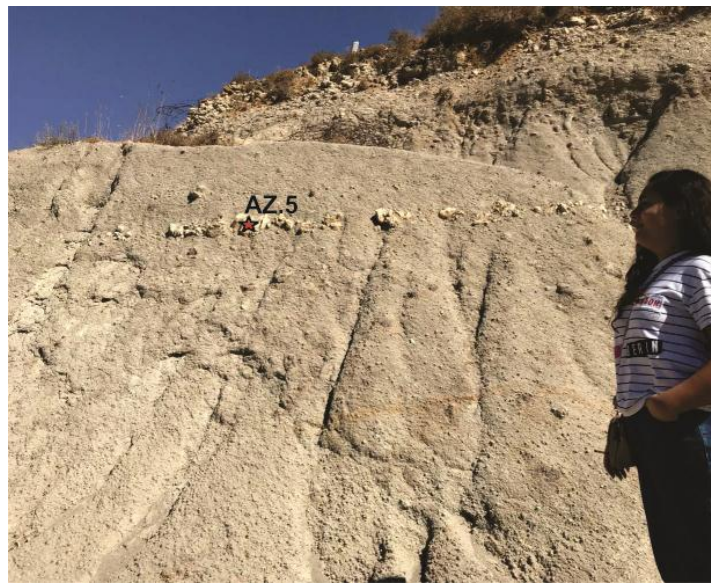


Figure 75: General field photo of silty marl intervals rich in pisoids and the thin limestone layer studied for microfacies (sample AZ.5).

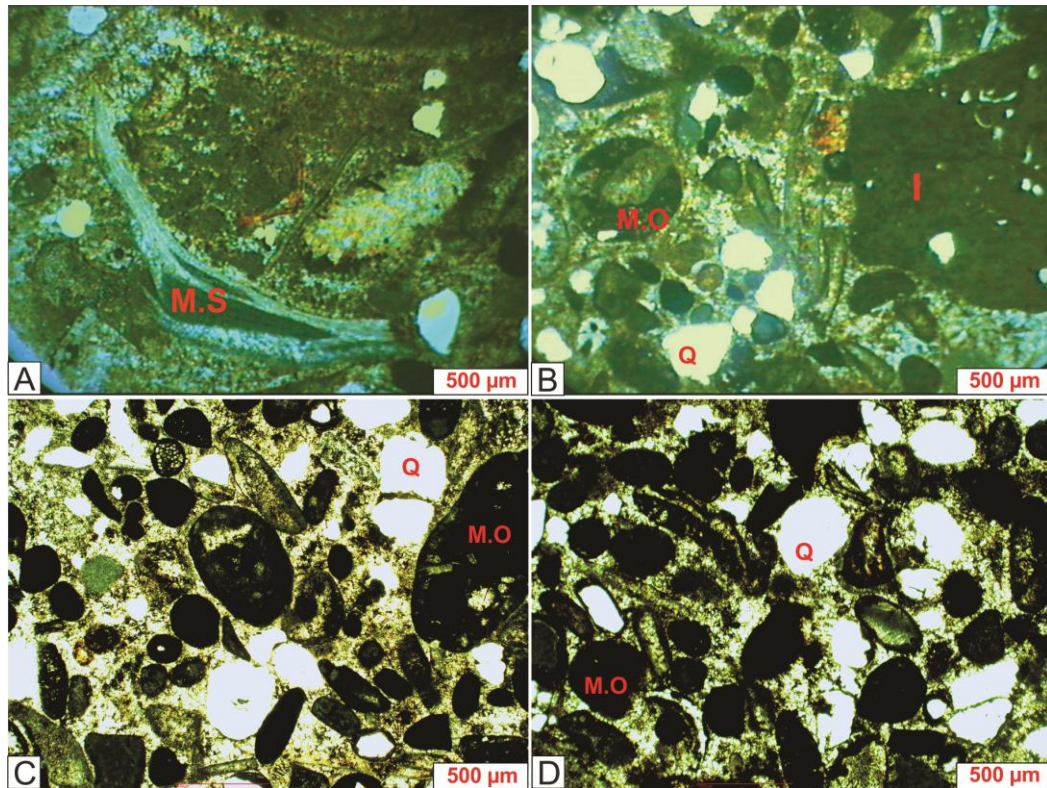


Figure 76: Microfacies from the sample AZ. 5. Grainstone of micritized ooids and intraclasts. (M.S=mollusk shell, I=intraclast, M.O=micritized ooid, Q=quartz).

- 2.5 m beige marl interval containing dispersed pisoids. Pisoids are ranging in diameter between 0.5 cm and 3 cm.
- 30 cm pisolitic conglomerate bed interval with erosive base.
- 2.5 m interval of beige burrowed marls with dispersed pisoids ranging in diameter between 0.5 cm and 3 cm. The burrows are vertical and reach more than 30 cm in length and 5 cm in diameter.
- 1.5 m of beige medium sandstone bed partially covered.

## A.6. Description of Barouk section 1

### **Base:**

- 30 cm of yellowish orange moderately sorted fine sandstone bed with parallel lamination.
- 30 cm of grey marl interval. A soft sample B1 has been extracted with no fossil content.
- 2 m of yellowish fine to medium moderately sorted quartz arenite bed with tabular cross- stratification.
- 2 m of grey marls showing parallel lamination. Root marks and iron concretions can be observed at the top of this interval. The upper part of this interval is partially covered.
- 0.5 m coarse quartz arenite bed with tabular cross-stratification and short lateral extension showing an erosive base.
- 0.5 m covered interval.
- 2.5 m of medium sandstone bed (quartz arenite) showing clear tabular cross-stratification. Internal foresets have a thickness ranging between 5 and 10 cm showing normal grading. Two indurated intervals of 10 cm can be identified within this sandstone interval (Fig. 77).





Figure 77: General field photo showing the sandstone intervals at the base of the Barouk section. Red arrows indicate the presence of two indurated beds.

- 1 m of yellowish fine sandstone interval (quartz arenite).
- 0.5 m orange yellowish medium to coarse sandstone bed with erosive base and ripple marks at its top.
- 0.5 m of beige marls with edaphic structures. A soft sample B2 collected for microfossils. However, no fossils were recovered from it.
- 40 cm of reddish claystone interval forming a hard ground. Ripple marks can be observed at the top of this interval.
- 1 m of reddish silty marl bed.
- 3 m of yellowish quartz arenite (medium) with trough cross-stratification. Internal foresets are 20 cm thick with normal grading.

- 2 m of semi-covered sandstone interval.
- 4 consecutive coarse quartz arenite beds of 1 to 1.5 m thick (Fig. 78). They are orange in color and display low angular planar cross-bedding. The forests range in thickness between 5 and 10 cm showing normal grading.

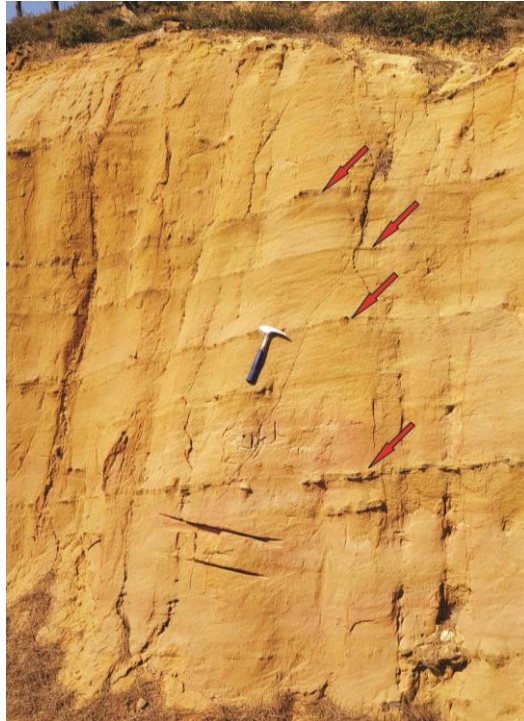


Figure 78: Field photo showing the quartz arenite beds with tabular cross-bedding. Red arrows mark the location of the hard concretions.

- 1.5 m of yellowish marl interval. A soft sample B3 was collected. However, no fossils were extracted from it.
- 3 m of whitish massive fine quartz arenite stratum.
- 10 consecutive medium-coarse quartz arenite beds ranging in thickness between 0.3 and 1 m. They are yellowish in color and show tabular cross-

bedding. Forests show normal grading from coarse to fine sandstone (Fig. 79).



Figure 79: Detailed photo of a sandstone bed showing tabular cross-bedding.

- 5 m of light grey silty marl interval with root marks at its top. A soft sample B4 was collected with no fossil content.

**Top:**

- 6 m of yellowish coarse to medium quartz arenite bedset showing trough cross-stratification intercalated with clay intervals.
- 3 m of beige marly interval. A soft sample B5 was collected at its base yielding a rich microfossil assemblage. Well preserved charophyte remains such as utricles (*Clavator ampullaceus* and *Asciidiella reticulata*), gyrogonites (*Sphaerochara asema* and *Mesochara cf. harrissi*), and thalli (*Charaxis martinclusasi*) and ostracod shells dominated by freshwater *Cypridea* (*C. tuberculata*, *C. piedmonti* and *C. pridea* sp.). Ostracod shells show their delicate structure preserved and the valves are anatomically

connected. Few bad-preserved ostracod valves of the species

*Perissocytheridea* sp. and *Dolocytheridea* sp. also occur in the assemblage.

Other microfossils recovered from the sample B5 includes agglutinated shells of the foraminifera species *Choffatella* cf. *decipiens*, dasycladal thalli of *Salpingoporella dinarica*, few echinoid spines and gastropod fragments.

- 3 m of yellowish coarse quartz arenite showing a normal grading. It shows trough cross-bedding.
- 2 m of semi-covered interval of intercalated marls and fining upward sandstone.
- 10 m of semi-covered marl interval.
- 1.5 m marly interval with parallel laminations.
- 0.5 m of fine sandstone interval.
- 1 m of marls with parallel laminations. A soft sample B6 was collected from this interval. No fossils were recovered from it.
- 3 m of brownish marl bed with root marks and parallel laminations.
- 6 m of semi-covered marls.
- 3 m of light grey coarse laminated sandstone bed. Each lamina displays normal grading.
- 3 m of semi-covered interval of marls intercalated with fine sandstone layers.
- 30 m covered interval. This interval is completely reworked by human activity (croplands).



- 10 m of light grey high weathered limestone interval. This interval is composed of mudstone/wackestone beds ranging in thickness between 0.2 and 2 m. Despite no samples were extracted for microfacies analysis, several marine microfossils such as foraminifera shells were identified *in situ*. This interval belongs to the fully marine Mdairej Formation according to the geologic maps of Dubertret (1955).

#### **A.7. Description of Barouk section 2**

- 1 m of dark grey marls with parallel laminations containing plant remains i.e. cuticle fragments.
- 2 m of marls intercalated with fine sandstone layers. Marls show parallel laminations and contain plant debris.
- 0.5 m of grey fine sandstone interval with ferruginous nodules and vertical burrows.
- 2 m of dark grey marl bed with parallel lamination rich in fragmented plant remains.
- 0.5 m grey fine sandstone strata showing erosive base and vertical burrows.
- 0.5 m of marls intercalated with fine sandstone layers with iron nodules at its top.
- 1 m of dark grey marly interval. A soft sample B7 was collected which provided few microfossils (Fig. 80). The assemblage is composed of a reduced number of bad preserved charophyte utricles (*Clavator ampullaceus*

and *Asciidiella reticulata*), gyrogonites (*Sphaerochara asema*), and thalli (*Charaxis martinclousasi*), few ostracod shells of *Cypridea tuberculata*, agglutinated shells of foraminifera (*Choffatella cf. decipiens*), echinoid fragments and small fragments of amber.



Figure 80: Field photo of the grey marl interval from which sample B7 was collected.

- 0.5 m of fine sandstone bed with ferruginous nodules.
- 0.3 m of dark grey marl interval.
- 3 m of orange massive fine sandstone (quartz arenite).
- 1 m of semi-covered interval.
- 1.5 m of silty marl interval showing ferruginous concretions.
- 1.5 m of beige medium/coarse sandstone (quartz arenite) bedsets showing low angle cross-bedding, erosive base and short lateral extension (Fig. 81).

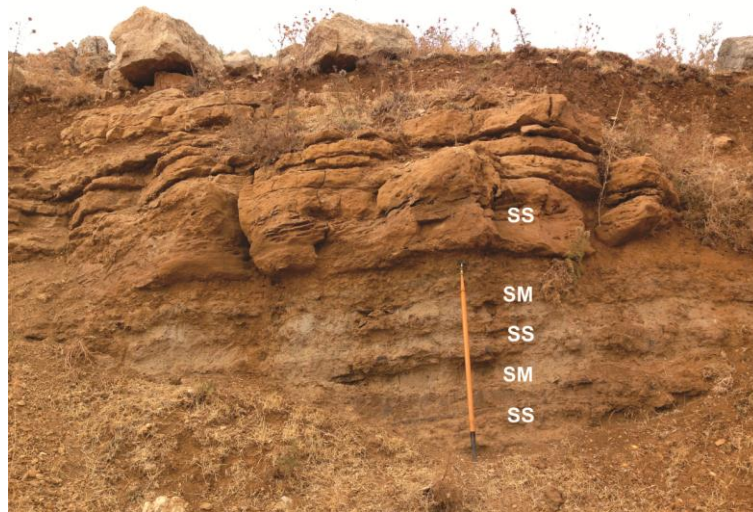


Figure 81: Field image showing the alteration of silty marl (SM) and sandstone (SS) beds at the top of the Barouk section 2.

- 3 m of semi-covered light grey limestone bed provably related to the marine Mdairej Formation according to Dubertret (1955).

#### **A.8. Description of Jezzine section 1**

##### **Base:**

- 3 m of dark grey sandy marl interval with dispersed carbonized wood remains. Sand grains are medium in size, sub-rounded and moderately sorted. Large vertical burrows can be observed at the top of this interval.
  - 0.5 m of reddish fine sandstone bed.
  - 70 cm of dark grey burrowed sandy marl.
  - 2.5 m of yellowish fine sandstone bed intercalated with sandy marls.
- Ferruginous concretions can be observed forming indurated and outstanding

layers. Marl intervals show vertical burrows. Sandstone strata display erosive bases.

- 0.5 m of yellowish coarse sandstone bed with erosive base and dispersed ferruginous nodules.
- 2 m of dark grey sandy marl interval with dispersed carbonized wood remains and vertical burrows at the upper part. Wood fragments may be up to 10 cm in length.
- 1 m of reddish medium to coarse quartz arenite showing ferruginous concretions.
- 0.5 m of dark grey clay bed with fine quartz grains. A soft sample J1 was extracted. However, no fossils have been recovered (Fig. 82). The quartz grains are sub-rounded to moderately-rounded.

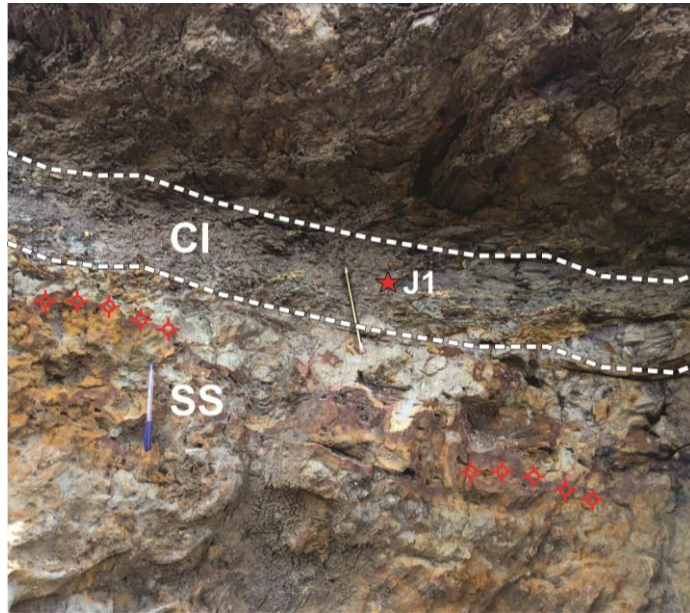


Figure 82: Field photo showing the ferruginous sandstone bed (SS) with iron nodules (red) topped with grey clays (Cl) from which J1 is extracted.

- 1.5 m of reddish fine sandstone interval with large transported carbonized wood remains (5 cm length). Wood remains are concentrated at its base (Fig. 83). This interval is divided into three strata each one about 0.5 m in thickness separated by erosive bases.



Figure 83: Detailed photo of a large carbonized wood located at the base of sandstone interval.

- 1 m of dark grey sandy marl interval with parallel lamination and wood remains at its base. A soft sample J2 was extracted with no fossil content.
- 40 cm of reddish medium sub-rounded and moderately sorted sandstone bed with erosive base and small wood remains.
- 10 cm dark grey clay interval.
- 30 cm dark grey sandy marl strata.
- 0.5 m of dark grey fine sandstone bed with erosive base and ferruginous concretions.
- 30 cm of dark grey clays rich in amber and plant remains (i.e. fragmented leave cuticles). A soft sample J3 was extracted with no fossil content (Fig. 84).



Figure 84: Detailed photo of the dark grey clays rich in plant debris and amber.

- 1.5 m of semi-covered dark grey clay bed.
- 4.8 m of light grey silty marls interval with dispersed pisoids and quartz grains. Vertical burrows can be observed at the top of this interval (Fig. 85). Pisoids range in diameter between 0.5 and 3 cm. Dispersed small fragments of carbonized woods can be observed within this interval. A soft sample J4 was extracted from the middle part of this interval. However, no microfossils were recovered from it.





Figure 85: Detailed photo of the silty marl interval with vertical burrows (outlined with dotted lines).

- 30 cm of light grey quartz arenite bed showing a normal grading from medium to silt grain sizes.
- 50 cm of light grey fine structure less sandstone interval.
- 50 cm of pisolitic conglomerate strata showing erosive base (Figs. 86 & 87).

Pisoids are up to 3 cm in diameter and they show some degree of imbrication. According to Dubertret (1955) this interval represents the boundary between the Chouf and the Abeih formations.





Figure 86: Field image of the pisolitic conglomerate interval.



Figure 87: Detailed photo showing a cross-section of a pisoid.

- 2 m of light grey silty marl bed rich in organic debris and dispersed pisoids ranging in diameter between 0.5 and 3 cm (Fig. 88). Several carbonized wood remains can be observed. Vertical burrows occur especially at the top of the interval.

- 50 cm of light yellow medium to coarse sandstone strata. It shows erosive base (Fig. 88). Irregular ferruginous nodules outstand within this stratum. Dispersed carbonized wood fragments can be observed within it.

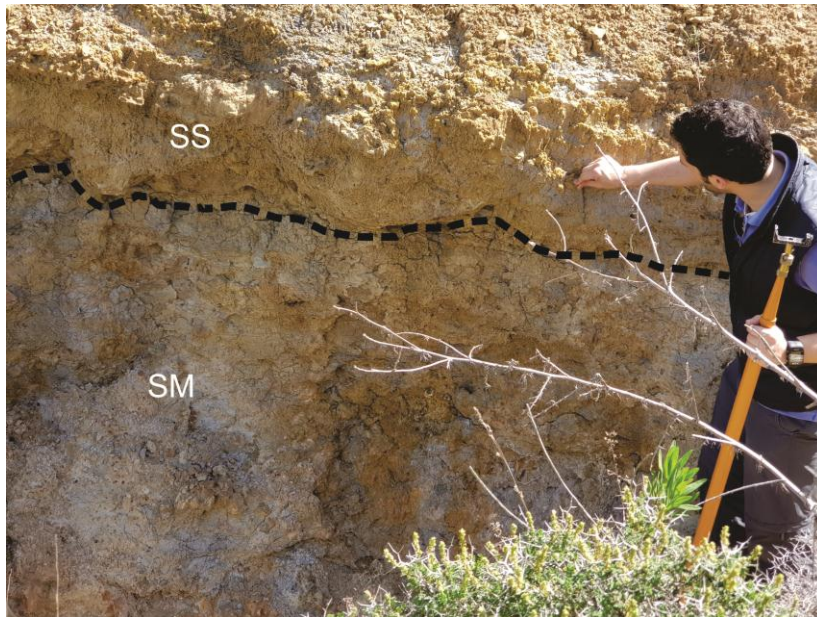


Figure 88: Field image showing the silty marl (SM) interval topped by a medium to coarse sandstone (SS) bed displaying an erosive base (marked with a dotted line).

- 2.7 m of silty marls interval. It contains wood remains at its base. Parallel lamination can be observed at its upper part.
- 2.5 m of yellowish fine to medium sandstone (quartz arenite) interval.
- 5 m of dark grey silty marl interval with dispersed pisoids and wood fragments. Vertical burrows can be observed at the base of this interval. A soft sample J5 was extracted at the middle part of this interval. Several microfossils were recovered from this sample i.e. charophyte utricle of *Clavator ampullaceus*, shells of agglutinated foraminifera *Choffatella* cf.

*decipiens*, marine ostracods valves related to *Doloccytheridea* sp., *Ovocytheridea* sp., and *(Meta)cytheropteron* sp., few fragments of echinoid shells, and dasycladal stems of *Salpingoporella dinarica*. Charophyte utricles display a certain degree of abrasion. In contrast, foraminifera and marine ostracod shells are well preserved. Ostracod carapaces occur in anatomical connection (fused valves) suggesting that these organisms grew *in situ*.

- 0.5 m of an oyster bank. It shows short lateral extension. At the base of the interval shells do not show any preferred orientation and many of them appear broken. In contrast, shells at the upper part of the interval occur complete and in living position forming a small reef (Fig. 89).





Figure 89: Field photo showing the upper part of the oyster bank. Note that oyster shells are arranged in living position forming a reef.

- 2.7 m fossiliferous limestone interval. Its base is mainly composed of highly burrowed marly limestone changing upwards to an indurated limestone bed (wackestone/packstone) rich in bivalves and gastropod shells, casts and molds (Fig. 91). Mollusk shells and vertical burrows can be distinguished within this interval. Few oncolid layers occur at the top of the second interval. Oncoids display irregular shapes and are in between 5 mm to 1 cm in diameter (Fig. 92). Three hard samples were collected at the base, middle and upper part of the bed i.e. J6, J7, and J8 respectively (Fig. 90). The

sample J6 is composed of mudstone/wackestone microfacies containing agglutinated foraminifera shells of *Choffatella* and *Textularia* and broken mollusk shells. In addition, fine to medium sub-rounded quartz grains can also be observed (Fig. 93).



Figure 90: Field image of the burrowed marly limestone (ML) interval. Note the vertical change of facies from soft marls (M) at the base of the section to hard limestone (L) at its top. Note also the presence of vertical burrows cutting the horizontal strata (dotted red line). Samples J6, J7, and J8 were collected respectively from the base, middle, and upper part. B: Detailed photo of a vertical burrow cast.



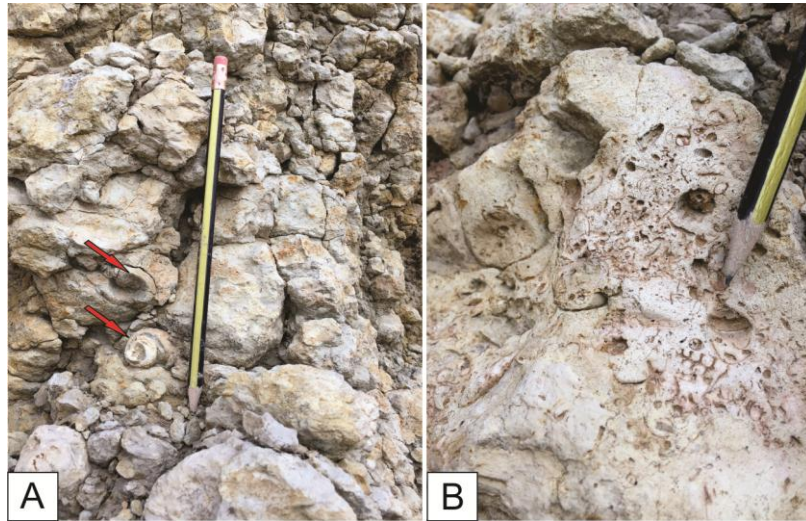


Figure 91: Detail images of the facies located at the top of the marly limestone interval. A: Gastropod casts; B: Weathered surface of the limestone interval (wackestone/packstone facies) with mollusk shells.



Figure 92: Detail images of the facies (rudstone of oncoids) located at the top of hard limestone interval (L).

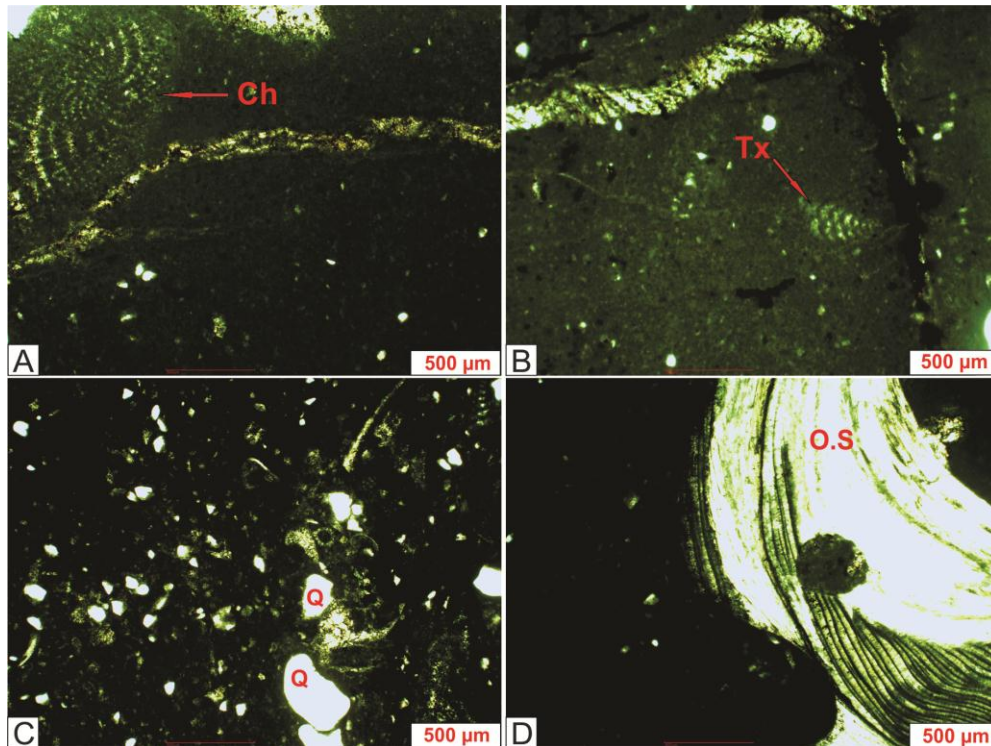


Figure 93: Wackestone microfacies from sample J6. A: oblique equatorial section of foraminifera (*Choffatella*) shell (Ch); B: oblique axial section of a foraminifera (*Textularia*) shell (Tx); C: rounded quartz grains (Q) of different sizes; D: oyster shell (O.S) showing its internal structure or lamellae.

Microfacies in sample J7 are characterized by wackestone/packstone.

The dominant clast type is represented by mollusk shell fragments (gastropods and bivalves). Other bioclasts include ostracod carapaces and agglutinated foraminifera shells. Quartz grains and fecal pellets also occur in this sample (Fig. 94).



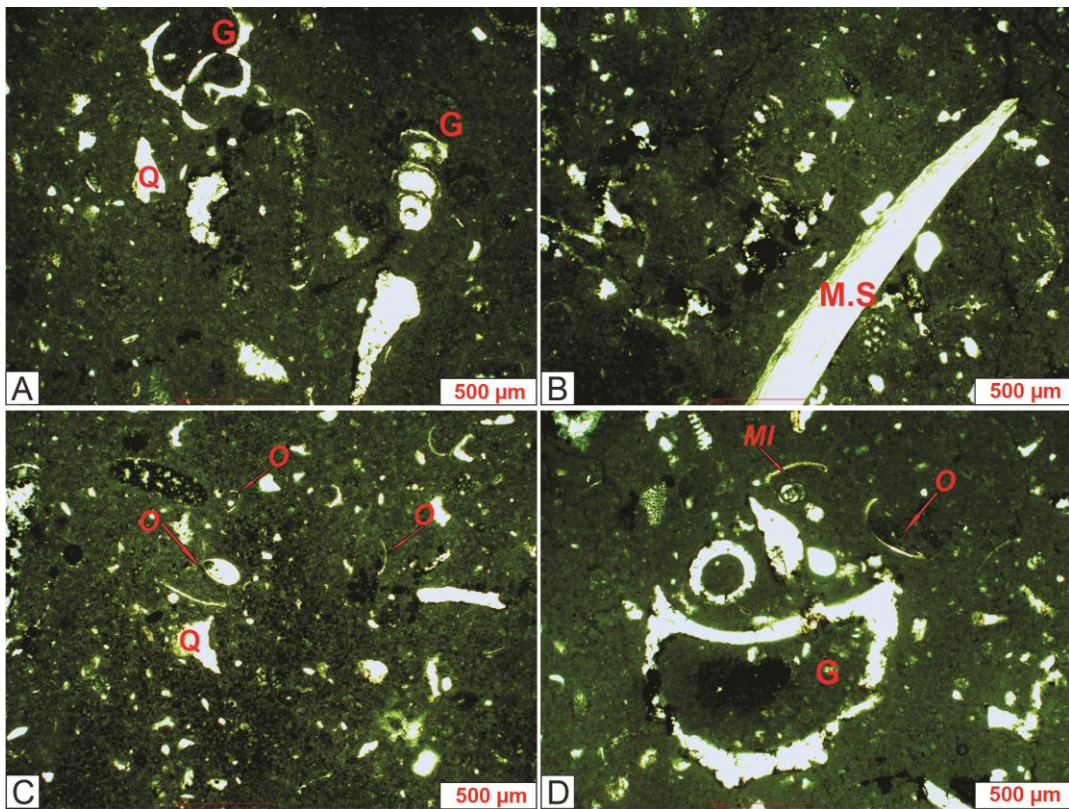


Figure 94: Wackestone/packstone microfacies from sample J7. Note the abundance of gastropod shell fragments (G), quartz grains (Q), and ostracod shells (O). Few miliolid shell (MI), and mollusk shells (M.S) are also observed.

Wackestone/packstone microfacies can be observed in sample J8.

Several grain types can be distinguished i.e. fragmented charophyte utricles and charophyte thalli related to *Charaxis martinclousasi*, thalli of the dasycladales species *Salpingoporella dinarica*, tiny quartz grains, broken indeterminate mollusk shells, and very rare foraminifera (Fig. 95).



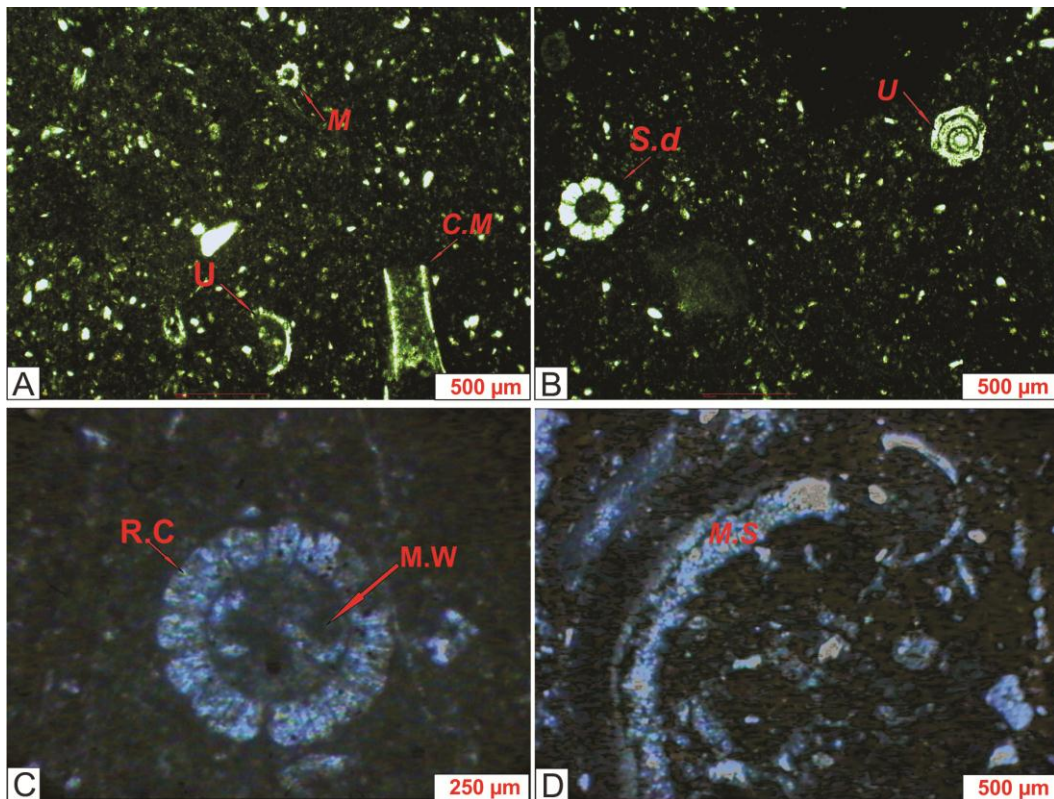


Figure 95: Wackestone/packstone microfacies from sample J8. (*Munieria*=M; *Charaxis martinicosasi*=C.M; Charophyte utricle=U; *Salpingoporella dinarica*=S.d; Mollusk shell=M.S). Note the transverse section in C showing the inner micritic wall (M.W) and the radial calcitic structure (R.C) of *Salpingoporella dinarica*.

- 0.5 m of beige silty marl interval with dispersed pisoids.
- 20 cm of quartz arenite bed. Quartz grains are medium in size and well sorted.
- 2 m of beige silty marl with dispersed pisoids and vertical burrows. A soft sample J9 was extracted from this interval for microfossils. The microfossil assemblage is composed of well-preserved charophyte utricles of *Clavator ampullaceus* and *Ascidiella reticulata*, some gyrogonites of *Mesochara* cf. *harrissi*, fragments of dasycladal thalli *Salpingoporella dinarica*, few

ostracod carapaces of *Cypridea tuberculata*, broken echinoid spines, and fish teeth. A ferruginous crust at the top of this interval outstands (Fig. 96).



Figure 96: Detailed field photo of the ferruginous crust.

- 3 m of light grey silty marls bed with pisoids, carbonized wood fragments and lignite lenses (Figs. 97 & 98). Pisoids occur dispersed within the marls and are more concentrated at the upper 50 (Fig. 97). They range in diameter between 1 and 3 cm. In contrast carbonized wood fragments occur dispersed mainly at its base. A lignite band (5 cm thick) can be observed at the top of this interval. A soft sample J10 was extracted for microfossils. An assemblage composed of ostracod carapaces (*Cypridea piedmonti* and *Perissocytheridea* sp.) and charophytes utricles (*Clavator ampullaceus* and *Ascidiella reticulata*), gyrogonites (*Sphaerochara asema*) and dasycladal thalli probably (*Salpingoporella dinarica*) was recovered at the base of this interval. Charophyte remains display signs of abrasion and ostracod shells appear broken.



Figure 97: Detailed field photo showing the upper part of the marl interval. Note the increase of pisoids concentrated on top.



Figure 98: Detailed image of the facies at the base of the marl interval from where the sample J10 was recovered. Note the presence of carbonized wood fragments.



- 0.5 m of beige silty marl bed. A soft sample J11 provided several microfossils i.e. abraded charophyte utricles (*Clavator ampullaceus* and *Asciidiella reticulata*) and dasycladal thalli, broken ostracod carapaces of *Cypridea piedmonti* and fish teeth.
- 10 cm of pisolitic conglomerate strata showing erosive base and imbrication fabric. Pisoids range in diameter between 0.5 and 2 cm (Fig. 99).

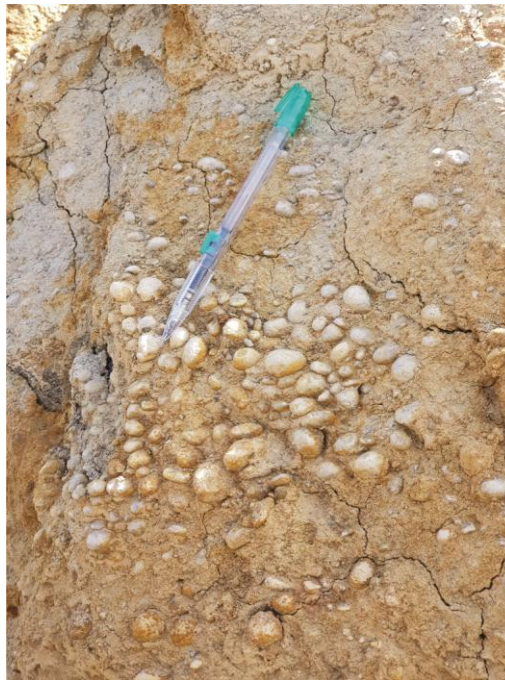


Figure 99: Detailed facies showing imbricated pisoids.

- 3.5 m of beige silty marl interval with dispersed pisoids. Bone fragments were found at the base of this interval probably related to dinosaurs (Fig. 100). A soft sample J12 extracted at the middle part of this interval provided few microfossils including dasycladal thalli probably *Salpingoporella dinarica*, utricles (*Clavator ampullaceus* and *Asciidiella reticulata*),

gyrogonites of *Sphaerochara asema*, ostracods (i.e. *Cypridea piedmonti* and *Perissocytheridea* sp.), shells of the foraminifera *Choffatella* cf. *decipiens*, fragmented echinoid spines, and fish teeth. Almost all microfossils show signs of abrasion suggesting that they were transported from their original thriving localities. However, *Choffatella* shells are well preserved.

- 0.6 m siltstone bed with horizontal burrows (Fig. 101).

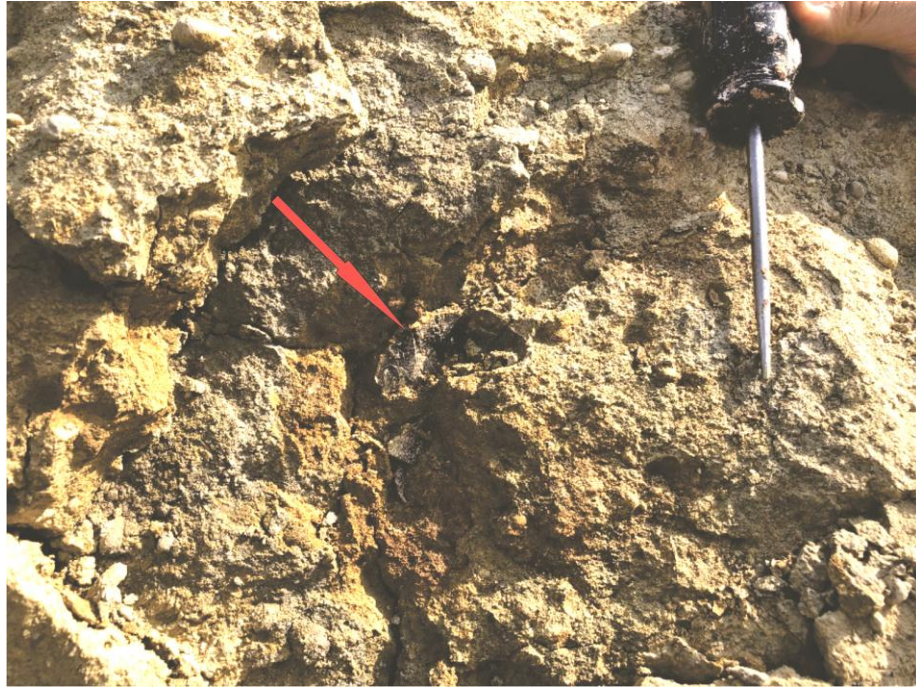


Figure 100: Field photo of a bone fragment in silty marl interval (below J12).



Figure 101: Detailed facies photo of the burrowed siltstone bed with horizontal burrows.

- 1.2 m of light grey medium sandstone interval rich in oyster shells. Many shells appear broken and with no apparent organization. Shells decrease in size from base to top of this interval.
- 1 m of beige silty marls.
- 1.5 m medium to coarse sandstone bed with erosive base. Broken shells can be observed at the base of this interval.
- 50 cm sandstone strata with high concentration of oyster shells forming a coquina. They are chaotically organized.
- 1.5 m interval of fine to medium bad sorted sandstone (quartz arenite) alternated with siltstone.
- 0.5 m medium sandstone interval rich in oyster shells. It displays an erosive base.



- 30 cm of silty marl bed with apparent edaphic structures and vertical burrows. A soft sample J13 was extracted for microfossils. Remains of charophytes utricles (*Clavator ampullaceus* and *Asciella reticulata*), ostracods (i.e. *Cypridea tuberculata*, *Cypridea piedmonti*, *Cypridea* sp., *Perissocytheridea* sp., *Dolococytheridea* sp., and *(Meta)cytheropteron* sp.) and fish teeth have been recovered from this sample. Fossils are in general well-preserved.
- 2 m of semi-covered marl interval.
- 1.5 m of medium sandstone (quartz arenite) strata with small vertical burrows and broken oyster shells (Fig. 102). The oyster shells show no preferred orientation.



Figure 102: Detailed image of a sandstone bed with broken oyster and gastropod shells.

**Top:**

- 1.5 m of yellowish silty marl interval with vertical burrows.
- 80 cm of yellowish fine to medium sandstone (quartz arenite) bed. Quartz grains are sub-angular in shape and moderately sorted.
- 2 m of semi-covered silty marl interval.
- 1.5 m of white silty marls strata with poorly sorted, sub-angular quartz grains. A soft sample J14 was extracted from this interval (Fig. 103). The microfossil assemblage is composed of poorly preserved charophyte gyrogonites of *Sphaerochara asema* and broken ostracod carapaces (*Cypridea tuberculata*, *C. piedmonti*, and *Perissocytheridea* sp.). Few broken fish teeth have also been extracted.



Figure 103: Field image of the white silty marl interval from which sample J14 was extracted.



- 5 m of reddish to purple silty marl interval with iron nodules and root marks. Parallel laminations can be observed at the top of this interval.
- 0.5 m reddish marl bed with root marks.
- 2.5 m of yellowish medium sandstone strata (quartz arenite) showing tabular cross-stratification.
- 0.5 m of bluish marl interval. A soft sample J15 was extracted from it. A large number of microfossils were recovered from this sample. The assemblage is composed of well-preserved charophyte thalli (*Charaxis martinclousasi*), gyrogonites (*Sphaerochara asema* and *Mesochara cf. harrissi*) and utricles (*Clavator ampullaceus* and *Asciidiella reticulata*) and few fragmented ostracod carapaces of *Cypridea* sp.
- 0.5 m siltstone interval.
- 1 m sandstone (quartz arenite) bed showing inverse grading upward (fine to medium grain size).
- 0.5 m of siltstone bed.
- 2.5 m of yellowish medium to coarse sandstone (quartz arenite) interval with erosive base showing tabular cross-bedding (Fig. 104). Foresets show normal grading (Fig. 105). Quartz grains are well sorted and sub-rounded in shape.



Figure 104: Field photo of the sandstone interval with tabular cross-bedding.



Figure 105: Detailed photo of the foresets showing normal grading.

- 1 m medium to coarse sandstone interval showing ferruginous concretions at its top.
- 40 cm of yellowish medium sandstone bed with tabular cross-stratification.
- 40 cm bluish marl interval showing root marks at its top.
- 50 cm fine sandstone bed with vertical burrows.
- 1 m of coarse bad-sorted sandstone bed containing abundant oyster shells. Oyster shells may appear broken and they tend to decrease in size towards the upper part of the interval. This bed show short lateral extension and erosive base.
- 4 m of medium sandstone bed with normal grading and tabular cross-bedding.
- 0.5 m coarse sandstone interval (quartz arenite) showing clear erosive base and short lateral extension.
- 3 m of medium sandstone interval with normal grading showing tabular cross-bedding.
- 0.5 m of yellowish coarse sandstone with erosive base and abundant broken oyster shells.
- 0.5 m of greyish silty marl interval.
- 1.5 m organic-rich silty marls with lignite lenses. The lignite contains fragmented leaf cuticles.

- 0.5 m whitish silty marl interval with oyster coquinas. This interval shows erosive base and short lateral extension. Oyster shells show no preferred orientation and many specimens appear broken.
- 0.5 m of yellowish medium-coarse sandstone interval composed of quartz grains and broken oyster shells.
- 10 cm of beige marly interval.
- 0.5 m of yellowish structure less medium sandstone interval.
- 1.5 m marl interval with burrows. A soft sample J16 was extracted from this interval. However, no fossil have been recovered from it.
- 0.5 m of beige silty marl interval with oyster coquinas. This interval shows erosive base and high lateral extension (Fig. 106).





Figure 106: General field photo of the facies located at the top of the section Jezzine 1. Note the vertical succession of deposits; M=marl; SM=Silty marl; SS=sandstone. The silty marl interval is rich in oysters in between the dotted line.

- 5 m of brown medium sandstone (quartz arenite) beds showing low angle cross-bedding. Grains are moderately sorted and sub-rounded. Opposite foreset dipping directions can be observed in successive beds (Fig. 107).

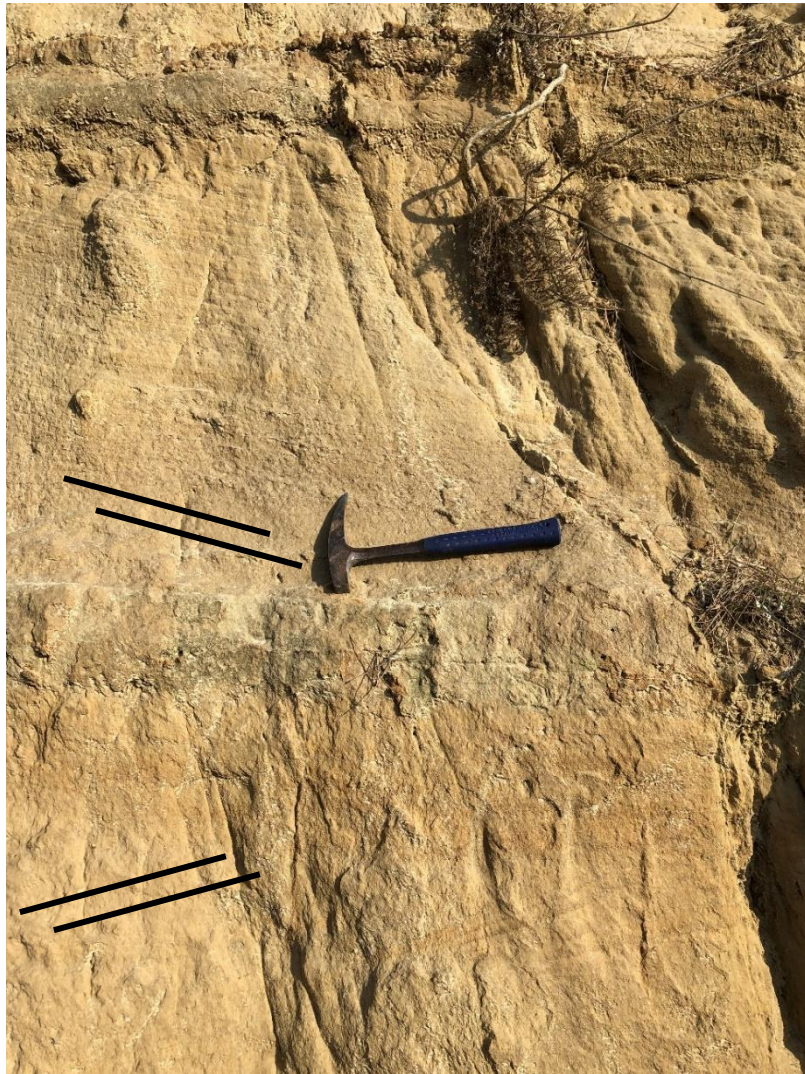


Figure 107: Detailed field photo of the contact between two sandstone intervals showing the opposite foreset dipping directions related to herringbone structures. Black lines represent the dipping direction of the foresets.

- 0.5 m of yellowish sandstone bed with erosive base rich in coarse quartz grains and oyster shell fragments.
- 2 m of beige marl interval.
- 0.5 m of yellowish medium sandstone bed with erosive base.



### A.9. Description of Jezzine section 2

- 2.5 m of yellowish sandy limestone interval. A hard sample J18 was collected for microfacies analysis. Microfacies is represented by a bioclastic packstone. Bioclasts are represented by *Choffatella* shells, indeterminate foraminifera shells, shells of serpulid worms, fragments of mollusk shells and dasycladal thalli (Fig. 108).

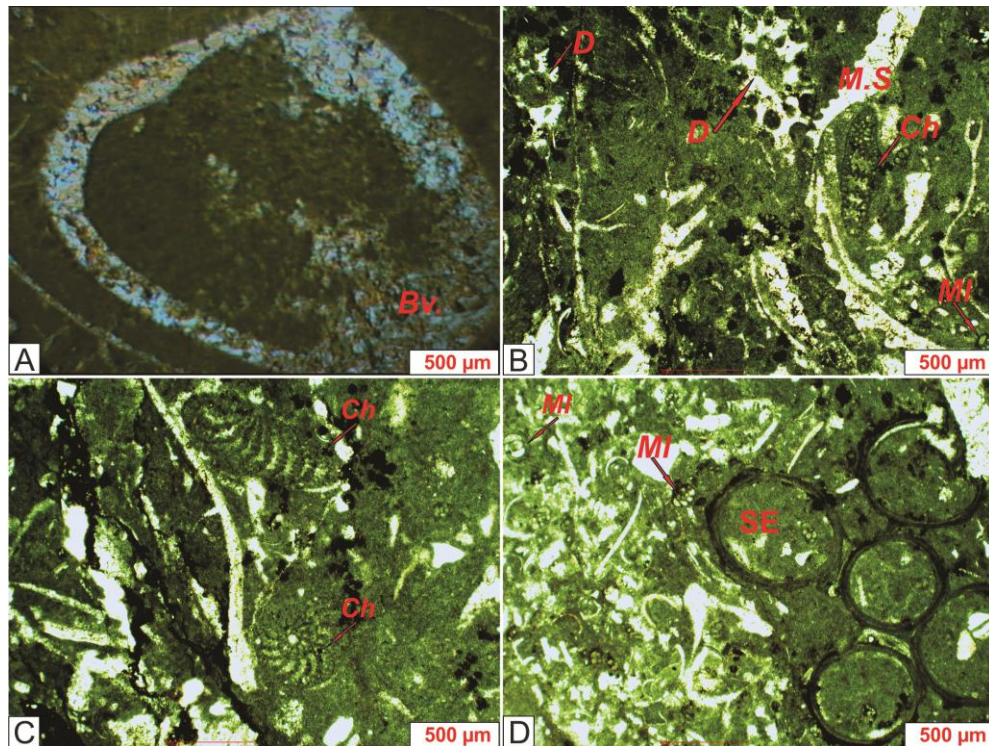


Figure 108: Bioclastic packstone microfacies of sample J18. Note: A) zoom of a bivalve shell (Bv.); B) several sections of bioclasts (D=dasycladal oblique view; Ch=subaxial view of a *Choffatella* shell, M.S=Mollusk shell, Miliolid shells=MI; C) Equatorial and subaxial view of a *Choffatella* shell. Note the location of the proloculus in the equatorial section; D) several bioclasts. Note the transverse cross-section of skeletal tubular structures related to serpulid worm tubes (SE).

- 25 cm sandy limestone interval rich in well preserved oyster shells.

- 25 cm sandy limestone with preserved gastropods and vertical burrows.
- 1 m of light grey silty marls interval.
- 0.5 m of beige limestone bed. A hard sample J19 was collected for microfacies analysis. This sample is composed of a packstone/grainstone of bioclasts (broken gastropod shells, fragments of dasycladales thalli, echinoid remains, and fragments of bivalve shells (Fig. 109).

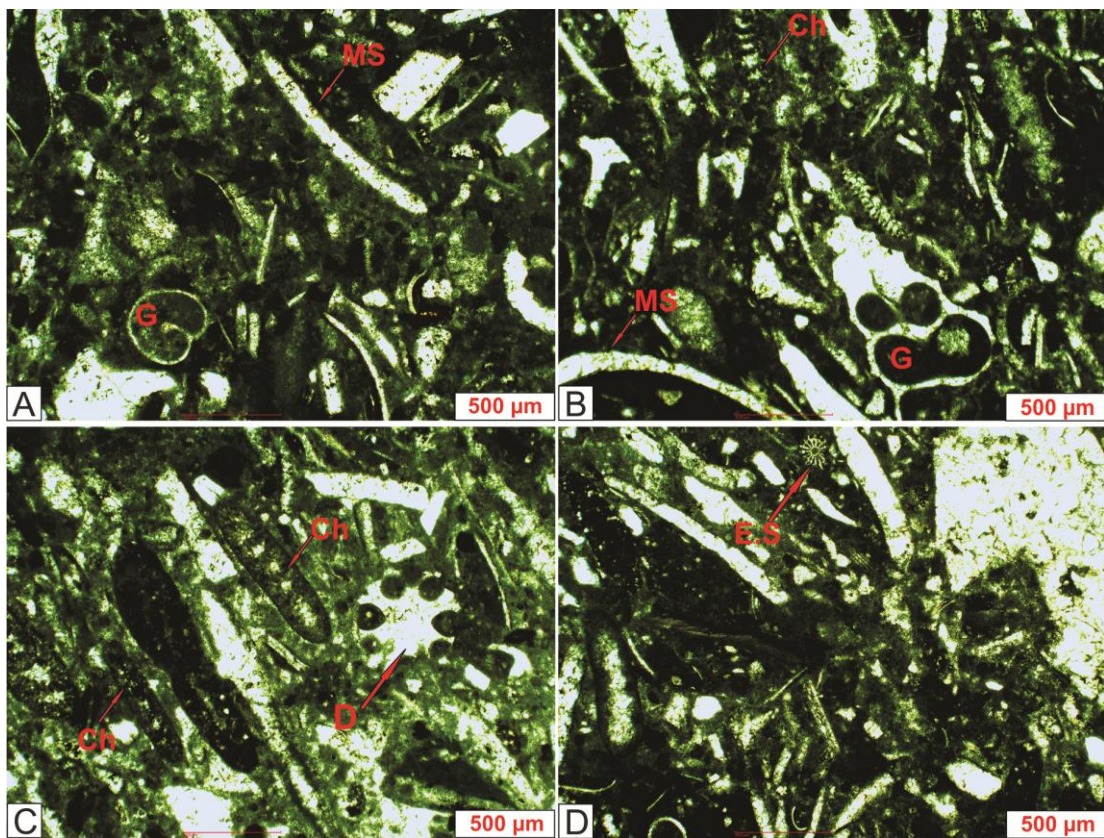


Figure 109: Packstone microfacies from sample J19. Note the abundance of mollusk shell fragments. A) Several bioclasts (Gastropod = G and Mollusk shell = M.S). B) Packstone of mollusk shells, gastropod shell (G), and *Choffatella* (Ch) in subaxial view. C) *Choffatella* in subaxial view and Dasycladal thalli (D) in equatorial view. D) Fragments of mollusk shells and echinoid spine (E.S).

- 0.5 m of light grey silty marl interval. A soft sample J20 has been extracted from this interval. Shells of the foraminifera *Choffatella* cf. *decipiens*



represent the dominant microfossil. Few well-preserved charophytes utricles of the species *Atopochara trivolvis*, several ostracod carapaces (*Cypridea tuberculata* and *Perissocytheridea* sp.) and few echinoid spines, fish teeth and broken gastropods shells were also recovered from this sample.

Ostracod carapaces show their external ornamentation complete and frequently occur connected with their coeval right or left valve.

- 25 cm light grey limestone (wackestone) interval.
- 25 cm light grey silty marl bed with well-preserved oyster shells and vertical burrows.
- 0.5 m light grey limestone strata. A hard sample J21 was collected for a microfacies analysis. Wackestone/packstone microfacies can be distinguished containing bioclasts such as *Choffatella* and other foraminifera shells, broken mollusk shells and ostracod carapaces (Fig. 110). Some bioclasts display signs of micritization.

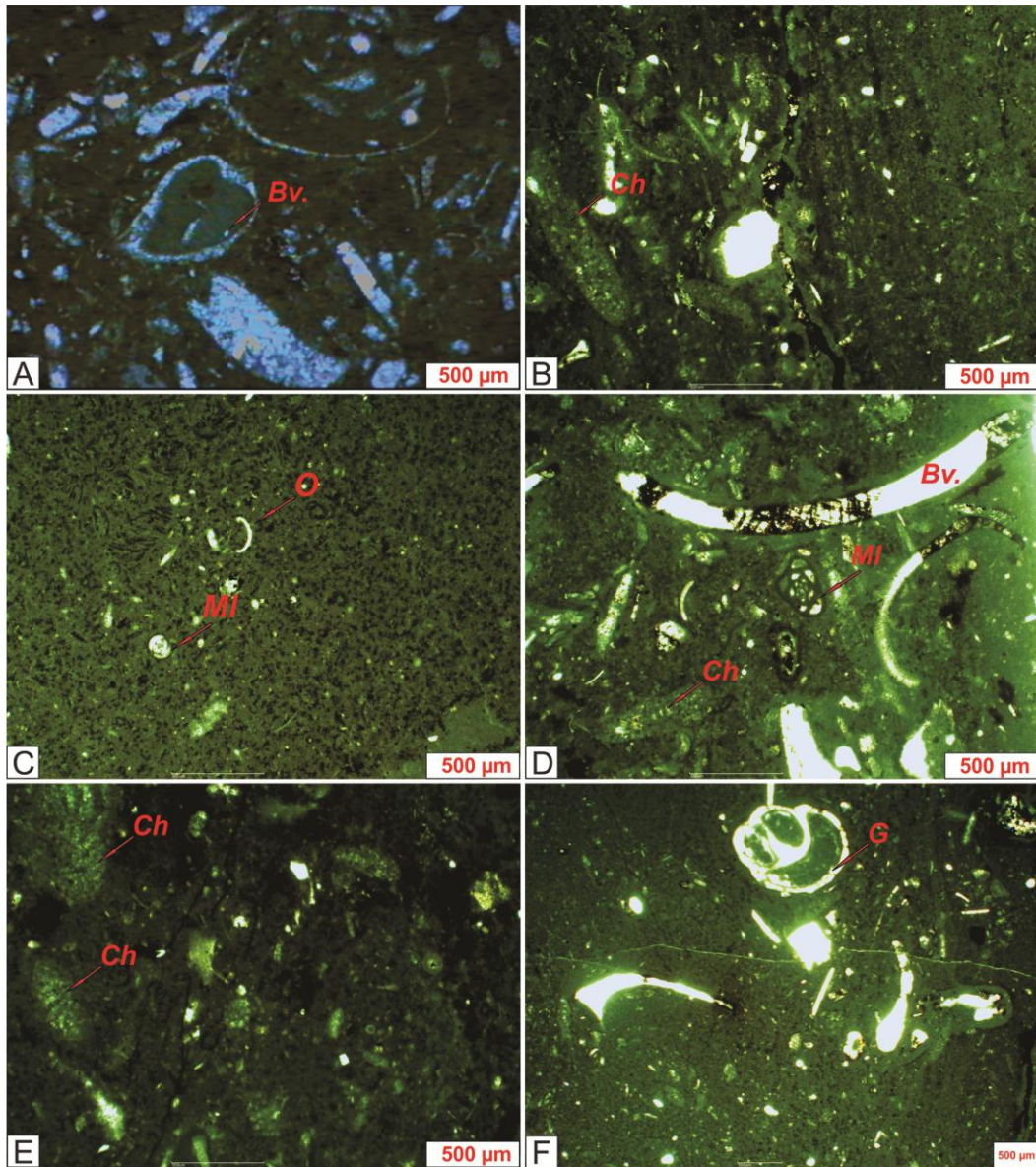


Figure 110: Wackestone/packstone microfacies from sample J21. A) Abundance of bivalve shells (Bv.) and mollusk fragments; B & E) *Choffatella* in subaxial view; C) ostracod shells (O) and miliolid shells (MI); D) Several bioclast (*Choffatella* and micritized bivalve fragments); F) Few gastropod shells (G).

- 1 m semi-covered silty marl interval.
- 0.5 m light grey limestone (wackestone/packstone) rich in bioclasts such as broken oyster shells.

- 2 m of alternating silty marl intervals (25 cm) and wackestone/packstone limestone beds (0.5 m) with dispersed broken bivalve shells.
- 1.5 m of grey oolitic limestone bed showing low angle cross bedding rich in bioclasts such as broken oyster shells. A hard sample J22 was collected from the base of this bed. Grainstone microfacies are dominant in this sample. Carbonate grains are mainly represented by ooids, intraclasts and bioclasts (Fig. 111). Carbonate grains display a certain degree of micritization.

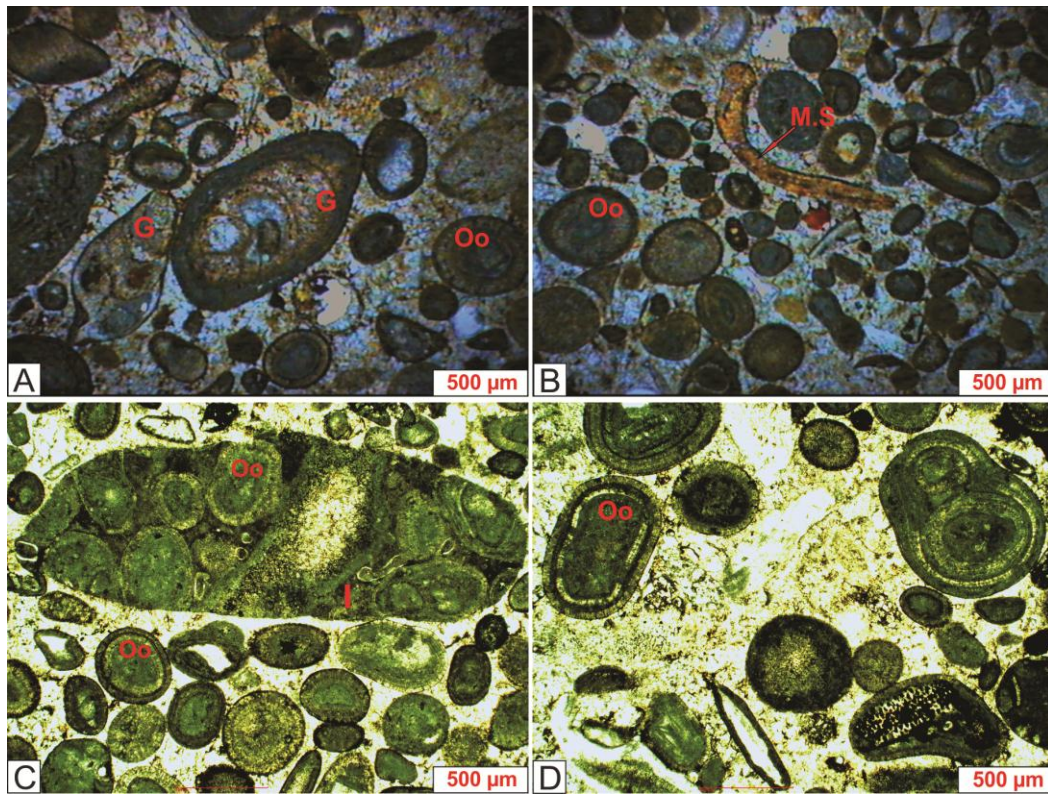


Figure 111: Grainstone microfacies of sample J22. A) The nucleus of the some ooids is composed of gastropod shells; B) Ooids and few bioclasts (mollusk shells); C & D) Ooids with large intraclast. (Ooid = Oo, Intraclast = I, Gastropod shell = G, Mollusk shell = M.S).

- 2 m of reddish medium sandstone bed with parallel lamination.

- 1.5 m limestone interval (grainstone) composed of ooids and bioclasts.
- 1 m covered interval.
- 1 m light grey limestone with no fossils identified.